Recombinant Expression and Analysis of Tetraspanin Extracellular-2 Domains

A thesis submitted for the degree of Doctor of Philosophy

John Samuel Palmer

September 2015

Department of Molecular Biology and Biotechnology

University of Sheffield

Acknowledgments

I would like to start by thanking my supervisors, Dr Lynda Partridge and Dr Pete Monk, for their guidance on all things tetraspanin and continuous support throughout my PhD. A great deal of help has also come from lab members both past and present, for which I am deeply grateful. Thanks to Rachel for keeping me chipper at work (for the most part), Marzieh and Kathryn for teaching me how to science, plus Fawwaz, Atiga, Ahmed, Ibrahim and Shamaa for helping with experiments (and my grasp of the Arabic language), and Dan "Coz-ed" Cozens, Jenny and Tom for their friendship and help with experiments. Special thanks go to ~~Dr~~ Mr Andrew O'Leary for going out of his way to help during challenging times and whose words of encouragement were invaluable. I'm grateful for the help from several members of other labs from whom I was able to sponge knowledge and lab equipment, with particular gratitude towards Shuo Jiang, Luke Johnson and Pete Davis for sharing their protein knowledge! The help and guidance offered by BioServe UK Ltd during the early years of my project was particularly helpful and I would like to express my gratitude towards Simon Smith and the other members of the BioServe team.

This work could not have been completed without help outside of academia, from all those family and friends who kept my chin up when experiments were not behaving (more often than not). Thanks to Bin-ed, Kate, Charlotte, Sam, Simon and Jack for making my time in Sheffield as enjoyable as possible and taking care of me on visits back there! Thanks to the lovely Lowry family for keeping the larders stocked and the house as warm as it could be. More importantly, thank you for making the effort to come round for a catch-up and a cuppa and cooking an amazing Sunday dinner!

I would especially like to thank Jude for the sagely advice during times of frustration (have you tried it slower, quicker, colder etc.) and Dad for the working lunches that kept things in perspective and organised my thoughts. I would also like to thank the siblings: Mike, Em and Soph, for making sure that home visits and holidays were always something to look forward to, I couldn't have coped without the Palmer clan!

Last but certainly not least I would like to thank Rebecca. Not only has she helped me (both academically and emotionally) through my PhD and put up with me during the write up, but without her motivation during countless late night/early morning revision session at undergrad I would not be where I am today. More importantly her love and support has kept me happy – Thank you!

Abstract

Tetraspanins are a superfamily of membrane proteins which span the membrane four times; they are found predominantly at the cell surface but are also located on intracellular vesicles. Tetraspanins (with a few exceptions) do not have conventional receptor ligand functionality and instead form lateral associations with other molecules within the membrane. Binding partners include, but are not limited to, MHC proteins, integrins, signalling proteins and other members of the tetraspanin superfamily. This large network of interactions has led to the idea of tetraspanin enriched microdomains (TEMs) or the tetraspanin web, in which tetraspanins function by bringing together proteins to form functional clusters which allow processes (such as signal transduction or adhesion) to take place more efficiently. Due to the numerous diverse binding partners, tetraspanins have been implicated in a number of cellular and pathological processes.

Despite tetraspanins being involved in fundamental physiological processes, relatively little is known about the function of individual members. Difficulties arise as only a few monoclonal antibodies are available to the native proteins and mouse knock outs often show only a mild phenotypic change. Our group and others have used recombinant human EC2 domains in the form of GST fusion proteins to assess tetraspanin involvement in several processes. This region is thought to attribute specificity to individual tetraspanin members and when recombinant versions are added to cells exogenously, they have been shown to modulate different cellular events including adhesion, migration and fusion.

Due to a number of inherent drawbacks associated with bacterially expressed recombinant EC2 domains (such as LPS contamination and inferior folding), the initial aim of this work was to express the recombinant proteins in a mammalian host. Despite multiple attempts to express the proteins in mammalian or insect cells using different vector systems, this was not successful, although it was demonstrated that DNA was integrated into the host genome and that EC2 encoding mRNA was expressed. Following this, it was decided to focus on bacterial expression and use the EC2 domains generated to further our understanding of tetraspanin involvement in IgE mediated degranulation this is a critical first step in Type I Hypersensitivity and although several tetraspanin family members have been implicated in this pathway, their exact involvement is not yet clear. Here, recombinant EC2 domains of tetraspanins CD9, CD63, CD81 and CD151 were used for the first time in conjunction with RBL-2H3 cells (a cell line commonly used as a model for mast cell degranulation) to examine tetraspanin involvement in IgE mediated degranulation. These particular tetraspanins were selected because past studies

have implicated these members in mast cell activation, but dispite an anti-CD63 antibody being able to down regulate degranulation, in this instance the EC2 domains did not exhibit any modulating effect on this form of degranulation in RBL-2H3 cells. The activity of these particular recombinant proteins was demonstrated in two other functional assays; bacterial adhesion to endothelial cells and bacterial induced giant cell formation.

Later work sought to characterise the EC2 proteins in terms of their secondary structure, LPS content and their ability to bind to cells, with the hope of elucidating their mechanism of action. The binding of each EC2 domains to two cell lines was examined: RBL-2H3 where EC2 domains show no effect on degranulation, and HEC-1B cells, where EC2 domains were previously shown exhibit biological activity by reducing bacterial adhesion. At highest concentrations utilised, the EC2 domains were shown to bind to both cell lines significantly more than the GST control protein, but attempts to examine the specificity of the EC2 interaction with the cells by competitive inhibition gave inconclusive results. Whilst this may have been due to technical issues it is tempting to speculate that this indicates cellular interactions that do not follow conventional binding mechanisms. The LPS content of the EC2 domains was shown not to correlate with their ability to modulate bacterial-induced cell fusion. Finally, to facilitate structural and future functional studies, attempts were made to optimise the removal of the GST tag from the fusion proteins. CD spectroscopy was then performed and attributed the EC2 domains of CD9 and CD81 with 50% and 52% α-helical structure, respectively, as expected for these proteins.

Although initial aims of producing mammalian EC2 domains were not fulfilled, they were successfully produced in bacteria and used in RBL degranulation assays. later work indicated that LPS contamination was not the causative component of EC2 preparations and confirmed some level of secondary structure. Furthermore, the apparent lack of effect of recombinant EC2 domains in RBL-2H3 activation may shed light on tetraspanin interaction with the high affinity IgE receptor.

Table of Contents:

List of Tables

Appendix

List of figures

Chapter 4

Chapter 5

Chapter 6

Appendix

Table of abbreviations

Abbreviation	Meaning
AMPs	Antimicrobial peptides
ANOVA	Analysis of variance
BGH	Bovine growth hormone
BMMC	Bone marrow derived mast cell
bp	Base pairs
BSA	Bovine serum albumin
CD	Cluster of differentiation
CD spectroscopy	Circular dichroism spectroscopy
CDS	Cell dissociation solution
CHO	Chinese hamster ovarian
CMV	Cytomegalovirus
Da	Daltons
DMEM	Dulbecco's modified eagles medium
DMSO	Dimethyl sulphoxide
DNP	2,4-dinitro-phenol
DOL	Degree of labelling
EC1	Extracellular domain 1
EC2	Extracellular domain 2
ECL	Enhanced chemiluminescence
ECM	Extra-cellular matrix
ELISA	Enzyme-linked immunosorbent assay
EMEM	Eagle's minimum essential medium
ER	Endoplasmic reticulum
F	Faraday
Fab	Fragment antigen binding
FACS	Fluorescence activated cell sorting
Fc	Fragment crystallisable
FCS	Fetal calf serum

FITC	Fluorescein Isothiocyanate
FRT	Flp recombinase target
g	Gravity
GPCR	G protein-coupled receptor
GST	Glutathione S-transferase
HBSS	Hank's balanced salt solution
HEC	Human endometrial carcinoma
HEK	Human embryonic kidney
HRP	Horseradish peroxidase
HSA	Human serum albumin
ICAM	Intercellular adhesion molecule
Ig	Immunoglobulin
IPTG	Isopropyl β-D-1-thiogalactopyranoside
LAL	*Limulus* Amebocyte Lysate
LB	Lysogeny Broth
LPS	Lipopolysaccharide
LS	Leader sequence
mAb	Monoclonal antibody
MFI	Median fluorescence intensity
MHC	Major histocompatibility complex
MMP	Matrix metalloproteinase
MNGC	Multi nucleated giant cell
MOI	Multiplicity of infection
NK cells	Natural killer cells
NMR	Nuclear magnetic resonance
OD	Optical density
P/S	Penicillin streptomycin solution
PAGE	Polyacryladmide gel electrophoresis
PAMPs	Pathogen associated molecular patterns
PBS	Phosphate buffered saline

PBST	Phospate buffered saline TWEEN20
PCR	Polymerase chain reaction
PFA	Paraformaldehyde
PSG17	Pregnancy specific glycoprotein 17
RBL	Rat Basophil Leukaemia
RBL	Rat basophilic leukaemia
RFI	Relative fluorescence intensity
RPM	Revolutions per minute
RT	Reverse transcriptase
SCF	Stem cell factor
SDS	Sodium dodecyl sulphate
SRB	sulforhodamine B
TBS	Tris buffered saline
TEM	Tetraspanin enriched microdomain
Tm	Melting temperature
TMB	3,3’,5,5’-Tetramethylbenzidine
UPEC	Uropathogenic *E. coli*
V	Volts
VCAM	Vascular cell adhesion molecule
VLA	Very late antigen

Chapter 1: Introduction

1.1 The Tetraspanin superfamily

1.1.1 The history, evolution and distribution of tetraspanins

Tetraspanins are a superfamily of membrane proteins which span the membrane four times and the main focus of this project was to express recombinant proteins corresponding to specific extracellular sections of tetraspanin proteins, with the aim of using these proteins to find out more about how tetraspanins function. This is important because despite tetraspanins being involved in many fundamental processes, relatively few functions have been ascribed to individual tetraspanin members. The superfamily first came to light in 1990 when similarities were discovered between TAPA-1 (CD81), CD37, the melanoma antigen ME491 (CD63) and Sm23 (Oren et al., 1990; Wright et al., 1990). Since then, tetraspanins have been identified in all metazoan, fungi (although not unicellular fungi), plants and protozoa; to date 33 human members have been identified (Table 1.1) along with 20 in *Caenorhabditis. elegans* and 36 in *Drosophila. melanogaster* (Huang et al., 2005). In addition to the four membrane spanning alpha helices true tetraspanins also contain a number of key defining features including short intracellular N and C terminal domains, a short extracellular loop (EC1), a large extracellular loop (EC2) and specific conserved residues within the EC2 (Section 1.1.2) (Hemler, 2008; Wright et al., 2000) Conservation of tetraspanins across such a diverse range of species indicates an ancient evolutionary origin, and their expression in early multicellular eukaryotes along with amoeba has led to speculation of involvement in initial cell-cell interactions (Huang et al., 2010). In addition, conservation of the gene structure itself lead to the suggestion of evolution from a common ancestor by duplication (Boucheix and Rubinstein, 2001).

Tetraspanins are mainly thought to play an organisational role in which they interact laterally with one another and other partner proteins within cell membranes which enables clustering of functionally related proteins. Tetraspanins are found on all human cells both on intracellular membranes and the plasma membrane, with the majority of tetraspanins found predominantly at the cell surface, with the exception of CD63 which is mainly localised to the surface of intracellular vesicles (Boucheix and Rubinstein, 2001; Charrin et al., 2009; Hemler, 2003). Different family members exhibit different patterns of expression, for example some members are widely distributed such as CD9, CD63 and CD81, whilst others show more restricted levels of tissue distribution, for instance Tspan25 and 26 which are found solely on immune cells (van Spriel and Figdor, 2010). Furthermore, there are more specialised

tetraspanins, such as RDS/peripherin and ROM1 and the uroplakins UP1a and UP1b which are expressed exclusively in the retina and bladder epithelium respectively (Wu et al., 1995, 2009).

The breadth of tetraspanin expression and diversity in the proteins which they associate with has led to them being implicated in a range of cellular and pathological processes, some of which have been discussed later (Section 1.1.3).

Tetraspanin name/ alternate name	Protein accession	Size (amino acids)	Known Functions and additional information
TSPAN1 / NET-1, TM4-C	O60635	241	Increased expression in several cancers suggests a role in tumour progression (Scholz et al., 2009)
TSPAN2 / NET-3	O60636	221	
TSPAN3 / TM4-A	O60637	253	
TSPAN4 / NAG-2	O14817	238	
TSPAN5 / NET-4	P62079	232	RNAi suggest positive regulatory role in osteoclsatogenesis (Iwai et al., 2007). Member of the TspanC8 family which Regulates trafficking and activity of ADAM10 (Dornier et al., 2012)
TSPAN6 / T245, A15 homologue, TM4-D	O43657	245	Regulates retinoic acid-inducible gene I-like receptors (Wang et al., 2012)
TSPAN7 / A15, TALLA-1, CD231	P41732	249	Highly expressed in areas of the brain, mutation leads to mental retardation (Zemni et al., 2000)
TSPAN8 / CO-029	P19075	237	Regulated cancer progression (Charrin et al., 2014)
TSPAN9 / NET-5	O75954	239	May regulate platelet function (Protty et al., 2009)
TSPAN10 / Oculospanin	Q9H1Z9	355	Largest tetraspanin. Member of the TspanC8 family which Regulates trafficking and activity of ADAM10 (Dornier et al., 2012)
TSPAN11	A1L157	253	
TSPAN12 / NET-2	O95859	305	Mutation may be linked to exudative vitreoretinopathy (Junge et al., 2009)
TSPAN13 / NET-6	O95857	204	RNAi suggests a negative regulatory role in osteoclastogensis (Iwai et al., 2007). Smallest tetraspanin
TSPAN14 / DC-TM4F2	Q8NG11	270	Member of the TspanC8 family which Regulates trafficking and activity of ADAM10 (Dornier et al., 2012)
TSPAN15 / NET-7	O95858	294	Member of the TspanC8 family which Regulates trafficking and activity of ADAM10 (Dornier et al., 2012)
TSPAN16 / TM4-B	Q9UKR8	245	
TSPAN17 / F-box only protein 23, SB134	Q96FV3	270	Member of the TspanC8 family which Regulates trafficking and activity of ADAM10 (Dornier et al., 2012)
TSPAN18	Q96SJ8	248	

TSPAN19	P0C672	248	
TSPAN20 / UP1b	O75841	260	In complex with Tspan21 and two non-tetraspanin proteins this tetraspanins help establish a permeability barrier in the bladder (Min et al., 2002)
TSPAN21 / UP1a	O00322	258	In complex with Tspan20 and two non-tetraspanin proteins this tetraspanins help establish a permeability barrier in the bladder (Min et al., 2002)
TSPAN22 / PRPH2, RDS	P23942	346	Required for photoreceptor morphology and function, mutation leads to retinal dystrophy (Clarke et al., 2000).
TSPAN23 / ROSP1, ROM-1	Q03395	351	Required for photoreceptor morphology and function (Clarke et al., 2000)
TSPAN24 / CD151	P48509	253	Mutation leads to skin blistering and kidney disease (Crew et al., 2004). Mutation led to reduced adhesion strengthening in vitro (Lammerding et al., 2003).
TSPAN25 / CD53	P19397	219	Regulation of TNFα production May promote cell survival (Beckwith et al., 2015)
TSPAN26 / CD37	P11049	281	Involved in B-cell function and B-cell T-cell interaction (Hemler, 2001). Target of therapeutic antibody for NHL treatment(Pagel et al., 2014)
TSPAN27 / CD82	P27701	267	Potential suppressor of metastasis (Ono et al., 1999)
TSPAN28 / CD81, TAPA-1	P60033	236	Required for surface expression and function of CD19 on B cells and complete B cell function (Hemler, 2001). Co-receptor for HCV entry (Moseley, 2005). Mutation led to reduced adhesion strengthening in vitro (Feigelson et al., 2003)
TSPAN29 / CD9, H59, MIC2, MRP-1, P24	P21926	228	Required for sperm egg fusion (Le Naour et al., 2000; Zhu et al., 2002)
TSPAN30 / CD63, MLA1	P08962	238	Selectively Incorporates into HIV virions (von Lindern et al., 2003). Marker for granulocyte and platelet activation
TSPAN31 / SAS	Q12999	210	Amplified from a subset of human sarcomas (Jankowski et al., 1994)
TSPAN32 / PHEMX, TSSC6	Q96QS1	320	
TSPAN33 / Penumbra	Q86UF1	283	Member of the TspanC8 family which Regulates trafficking and activity of ADAM10 (Dornier et al., 2012)

Table 1.1 Alternate name, accession number and function of all 33 human tetraspanins. Accession number alternate names and amino acid size were sourced from Uniprot http://www.uniprot.org/

1.1.2 Tetraspanin Structure

Tetraspanins range in size from 204-355 amino acids (Boucheix and Rubinstein, 2001) and consist of four membrane spanning helices separated by a short extracellular loop (EC1), an intracellular loop and a large extracellular loop (EC2) with short intracellular N- and C- terminal regions (Figure 1.1a). To be classed as a *bona fide* tetraspanin, four-span membrane proteins must also contain a number of conserved residues within transmembrane helix two, the intracellular loop and transmembrane helix three (Seigneuret et al., 2001) and must also contain four to eight conserved cysteine residues within the EC2 domain, one of which resides in the absolutely conserved CCG motif (Seigneuret et al., 2001; Wright et al., 2000). The only available tetraspanin crystal structure is of the CD81 large extracellular domain (Figure 1.1b) (discussed in section 1.1.2.4), however, CD spectroscopy has also been employed to analyse full length CD81 and attributed it with a predominantly (77.1%) α-helical content (Jamshad et al., 2008). Cryo-electron microscopy (EM) studies on the specialised uroplakin tetraspanins have also aided our understanding of how tetraspanins function (1.1.3.1) (Min et al., 2006). Here the four different regions of the tetraspanin protein will be considered (namely the intracellular regions, membrane spanning region, EC1 and EC2) with respect their structure and function. An alignment has been generated to demonstrate the level of conservation between the 33 different mammalian members. It is also clear from this figure that the level of conservation varies depending on which region of the tetraspanin is considered for instance the TM domains show a high degree of similarity whilst the EC2 domains of more varied.

1.1.2.1 Intracellular regions

The cytoplasmic portion of tetraspanin proteins consist of short N- and C- termini which are generally under 20 amino acids long and a small linker region between transmembrane helices two and three (Charrin et al., 2009). Relatively few functions have been assigned to the tetraspanin amino terminal sequence, although Lineberry *et al.* (2008) have demonstrated that in CD151 this region is the target of ubiquitination which leads to its degradation at the proteasome. It has also been demonstrated that the amino terminal region of CD81 is required for efficient *N*-linked glycosylation of its partner molecule CD19 (Shoham et al., 2006)

The C-terminus on the other hand, has been implicated in a number of tetraspanin properties and associated processes. For instance, the C-terminal tail of CD63 contains a tyrosine based lysosomal targeting motif (GYEVM) (Berditchevski and Odintsova, 2007) and interacts with the adaptor protein AP-3 to enable CD63 lysosomal targeting (Rous et al., 2002). This sorting motif is not unique to CD63 as twelve other members have been shown to have a similar sequence; however, in these members the sorting motifs proximity to the transmembrane region may

preclude interaction with AP-3 (Berditchevski and Odintsova, 2007). Another signalling motif in the C-terminal tail of CD151 (YXXϕ, where ϕ is an amino acid with a bulky side chain) is responsible not only for CD151 trafficking to intracellular vesicles, but trafficking of CD151 integrin partner proteins also (Liu et al., 2007). Mutation of this motif did not alter CD151-integrin association but did have an effect on cell motility, adhesion and spreading (Zhang et al., 2002). Similarly mutation of the EMV residues in the CD9 C-terminal region also led to reduced spreading and had the added effect of abolishing CD9-dependent microvilli formation (Wang et al., 2011). The C-terminus may also be involved in tetraspanin interaction with other membrane protein, as this region in CD63 and CD81 interacts with PDZ domains in syntenin-1, Sap97 and EPB-50; it is yet to be determined if this type of interaction is responsible for other protein-protein interactions within tetraspanin microdomains however (Latysheva et al., 2006; Pan et al., 2007). The C-terminus may also provide a link between tetraspanins and the actin cytoskeleton, as the CD81 C-terminal tail has been shown to interact with Rac GTPase, and EZRIN which are suggested to enable interaction with the actin cytoskeleton through ERM proteins (Charrin et al., 2014; Sala-Valdés et al., 2006; Tejera et al., 2013). Deletion of the C-terminus in CD151 also implicated this region in partner protein signalling as it led to reduced α6β1 dependent cell spreading and impaired adhesion strengthening to laminin-1 (Lammerding et al., 2003; Zhang et al., 2002)

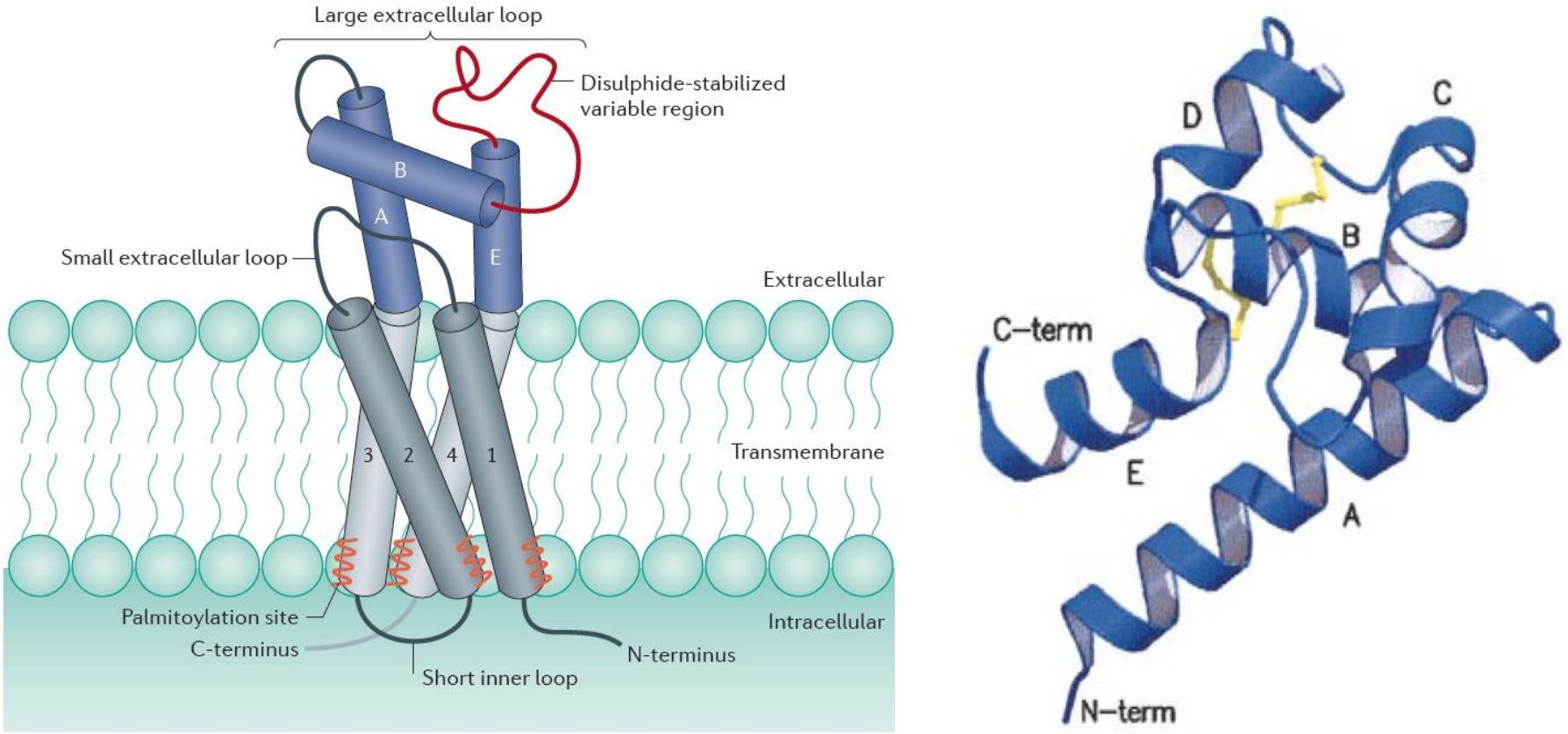

Figure 1.1: **(a) Diagrammatic representation of a tetraspanin showing key structural features**. Transmembrane helices 1-4 form a coiled coil structure within the membrane. The large extracellular region consisting of helices A, B and E and the more variable region (shown in red) is stabilised by disulphide bonds between conserved cysteine residues which vary in number depending on the tetraspanin member (4-8). Intracellular membrane proximal palmatoylation is thought to enable interaction with other membrane proteins (Taken from (Hemler, 2013)). **(b) Crystal structure of the human CD81 EC2 domain.** This crystal structure represents helices A, B and E of Figure 1.1a and shows an additional 2 helices (C and D) which may not be a conserved feature across the entire tetraspanin family. The stalk region is comprised of helices A and E whilst the head domain is made up of helices B, C and D. Disulphide bridges are depicted in yellow (modified from (Kitadokoro et al., 2001)).

BAD AVG GOOD - strength of residue alignment

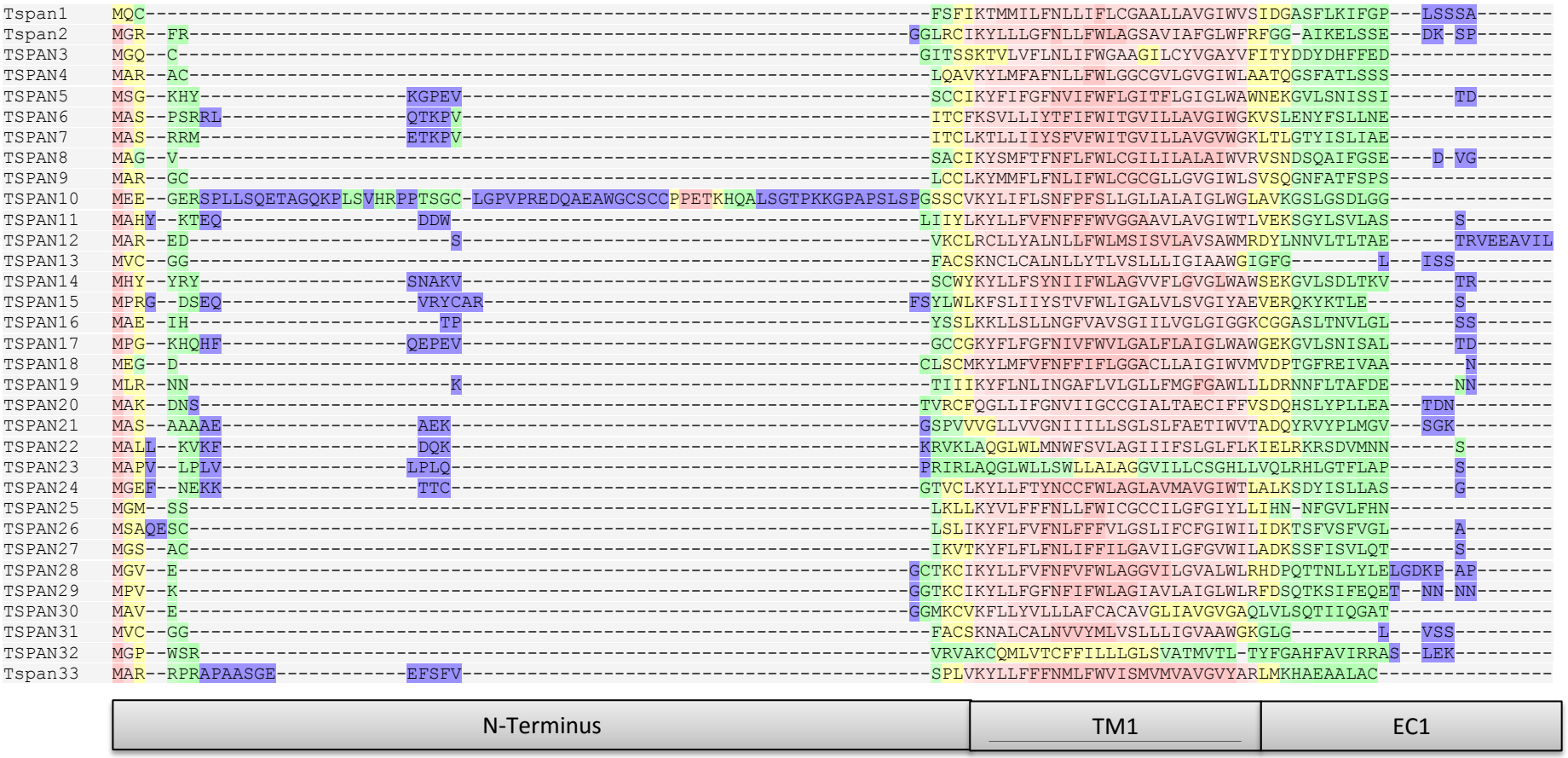

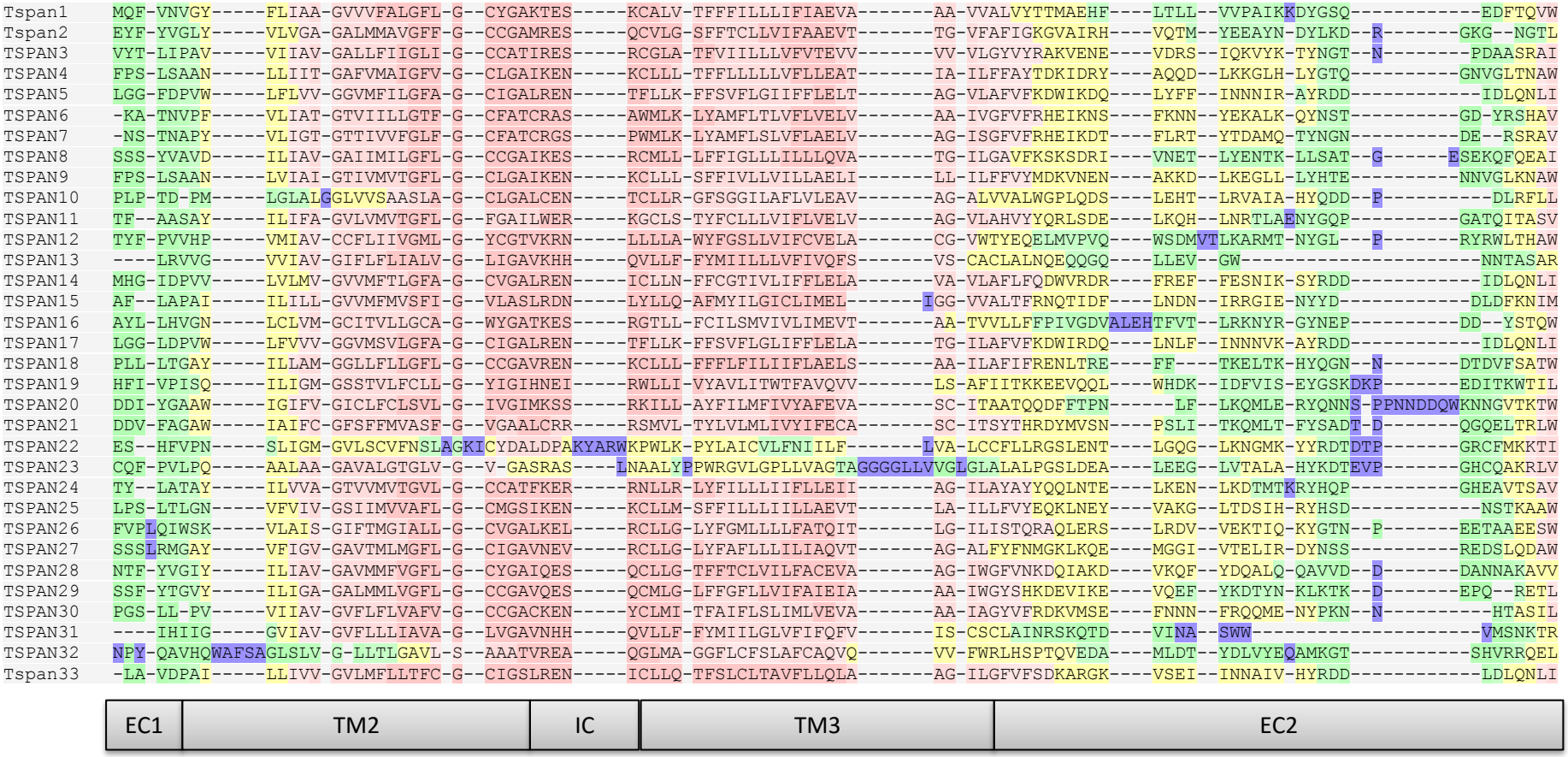
Tspan1 MQF-VNVGY-----FLIAA-GVVVFALGFL-G--CYGAKTES-----KCALV-TFFFILLLIFIAEVA-------AA-VVALVYTTMAEHF----LTLL--VVPAIKKDYGSQ----------EDFTQVW
Tspan2 EYF-YVGLY-----VLVGA-GALMMAVGFF-G--CCGAMRES-----QCVLG-SFFTCLLVIFAAEVT-------TG-VFAFIGKGVAIRH----VQTM--YEEAYN-DYLKD--R-------GKG--NGTL
TSPAN3 VYT-LIPAV-----VIIAV-GALLFIIGLI-G--CCATIRES-----RCGLA-TFVIILLLVFVTEVV-------VV-VLGYVYRAKVENE----VDRS--IQKVYK-TYNGT--N--------PDAASRAI
TSPAN4 FPS-LSAAN-----LLIIT-GAFVMAIGFV-G--CLGAIKEN-----KCLLL-TFFLLLLLVFLLEAT-------IA-ILFFAYTDKIDRY----AQQD--LKKGLH-LYGTQ----------GNVGLTNAW
TSPAN5 LGG-FDPVW-----LFLVV-GGVMFILGFA-G--CIGALREN-----TFLLK-FFSVFLGIIFFLELT-------AG-VLAFVFKDWIKDQ----LYFF--INNNIR-AYRDD----------IDLQNLI
TSPAN6 -KA-TNVPF-----VLIAT-GTVIILLGTF-G--CFATCRAS-----AWMLK-LYAMFLTLVFLVELV-------AA-IVGFVFRHEIKNS----FKNN--YEKALK-QYNST----------GD-YRSHAV
TSPAN7 -NS-TNAPY-----VLIGT-GTTIVVFGLF-G--CFATCRGS-----PWMLK-LYAMFLSLVFLAELV-------AG-ISGFVFRHEIKDT----FLRT--YTDAMQ-TYNGN----------DE--RSRAV
TSPAN8 SSS-YVAVD-----ILIAV-GAIIMILGFL-G--CCGAIKES-----RCMLL-LFFIGLLLILLLQVA-------TG-ILGAVFKSKSDRI----VNET--LYENTK-LLSAT--G------ESEKQFQEAI
TSPAN9 FPS-LSAAN-----LVIAI-GTIVMVTGFL-G--CLGAIKEN-----KCLLL-SFFIVLLVILLAELI-------LL-ILFFVYMDKVNEN----AKKD--LKEGLL-LYHTE----------NNVGLKNAW
TSPAN10 PLP-TD-PM-----LGLALGGLVVSAASLA-G--CLGALCEN-----TCLLR-GFSGGILAFLVLEAV-------AG-ALVVALWGPLQDS----LEHT--LRVAIA-HYQDD--P----------DLRFLL
TSPAN11 TF--AASAY-----ILIFA-GVLVMVTGFL-G--FGAILWER-----KGCLS-TYFCLLLVIFLVELV-------AG-VLAHVYYQRLSDE----LKQH--LNRTLAENYGQP----------GATQITASV
TSPAN12 TYF-PVVHP-----VMIAV-CCFLIIVGML-G--YCGTVKRN-----LLLLA-WYFGSLLVIFCVELA-------CG-VWTYEQELMVPVQ----WSDMVTLKARMT-NYGL---P-------RYRWLTHAW
TSPAN13 ----LRVVG-----VVIAV-GIFLFLIALV-G--LIGAVKHH-----QVLLF-FYMIILLLVFIVQFS-------VS-CACLALNQEQQGQ----LLEV--GW----------------------NNTASAR
TSPAN14 MHG-IDPVV-----LVLMV-GVVMFTLGFA-G--CVGALREN-----ICLLN-FFCGTIVLIFFLELA-------VA-VLAFLFQDWVRDR----FREF--FESNIK-SYRDD----------IDLQNLI
TSPAN15 AF--LAPAI-----ILILL-GVVMFMVSFI-G--VLASLRDN-----LYLLQ-AFMYILGICLIMEL-------IGG-VVALTFRNQTIDF----LNDN--IRRGIE-NYYD----------DLDFKNIM
TSPAN16 AYL-LHVGN-----LCLVM-GCITVLLGCA-G--WYGATKES-----RGTLL-FCILSMVIVLIMEVT-------AA-TVVLLFFPIVGDVALEHTFVT--LRKNYR-GYNEP----------DD--YSTQW
TSPAN17 LGG-LDPVW-----LFVVV-GGVMSVLGFA-G--CIGALREN-----TFLLK-FFSVFLGLIFFLELA-------TG-ILAFVFKDWIRDQ----LNLF--INNNVK-AYRDD----------IDLQNLI
TSPAN18 PLL-LTGAY-----ILLAM-GGLLFLLGFL-G--CCGAVREN-----KCLLL-FFFLFILIIFLAELS-------AA-ILAFIFRENLTRE----FF----TKELTK-HYQGN--N-------DTDVFSATW
TSPAN19 HFI-VPISQ-----ILIGM-GSSTVLFCLL-G--YIGIHNEI-----RWLLI-VYAVLITWTFAVQVV-------LS-AFIITKKEEVQQL----WHDK--IDFVIS-EYGSKDKP-------EDITKWTIL
TSPAN20 DDI-YGAAW-----IGIFV-GICLFCLSVL-G--IVGIMKSS-----RKILL-AYFILMFIVYAFEVA-------SC-ITAATQQDFFTPN------LF--LKQMLE-RYQNNS-PPNNDDQWKNNGVTKTW
TSPAN21 DDV-FAGAW-----IAIFC-GFSFFMVASF-G--VGAALCRR-----RSMVL-TYLVLMLIVYIFECA-------SC-ITSYTHRDYMVSN----PSLI--TKQMLT-FYSADT-D-------QGQELTRLW
TSPAN22 ES--HFVPN-----SLIGM-GVLSCVFNSLAGKICYDALDPAKYARWKPWLK-PYLAICVLFNIILF-------LVA-LCCFLLRGSLENT----LGQG--LKNGMK-YYRDTDTP-------GRCFMKKTI
TSPAN23 CQF-PVLPQ-----AALAA-GAVALGTGLV-G--V-GASRAS-----LNAALYPPWRGVLGPLLVAGTAGGGGLLVGLGLALALPGSLDEA----LEEG--LVTALA-HYKDTEVP-------GHCQAKRLV
TSPAN24 TY--LATAY-----ILVVA-GTVVMVTGVL-G--CCATFKER-----RNLLR-LYFILLLIIFLLEII-------AG-ILAYAYYQQLNTE----LKEN--LKDTMTKRYHQP----------GHEAVTSAV
TSPAN25 LPS-LTLGN-----VFVIV-GSIIMVVAFL-G--CMGSIKEN-----KCLLM-SFFILLLIILLAEVT-------LA-ILLFVYEQKLNEY----VAKG--LTDSIH-RYHSD----------NSTKAAW
TSPAN26 FVPLQIWSK-----VLAIS-GIFTMGIALL-G--CVGALKEL-----RCLLG-LYFGMLLLLFATQIT-------LG-ILISTQRAQLERS----LRDV--VEKTIQ-KYGTN--P-------EETAAEESW
TSPAN27 SSSLRMGAY-----VFIGV-GAVTMLMGFL-G--CIGAVNEV-----RCLLG-LYFAFLLLILIAQVT-------AG-ALFYFNMGKLKQE----MGGI--VTELIR-DYNSS----------REDSLQDAW
TSPAN28 NTF-YVGIY-----ILIAV-GAVMMFVGFL-G--CYGAIQES-----QCLLG-TFFTCLVILFACEVA-------AG-IWGFVNKDQIAKD----VKQF--YDQALQ-QAVVD--D-------DANNAKAVV
TSPAN29 SSF-YTGVY-----ILIGA-GALMMLVGFL-G--CCGAVQES-----QCMLG-LFFGFLLVIFAIEIA-------AA-IWGYSHKDEVIKE----VQEF--YKDTYN-KLKTK--D-------EPQ--RETL
TSPAN30 PGS-LL-PV-----VIIAV-GVFLFLVAFV-G--CCGACKEN-----YCLMI-TFAIFLSLIMLVEVA-------AA-IAGYVFRDKVMSE----FNNN--FRQQME-NYPKN--N----------HTASIL
TSPAN31 ----IHIIG-----GVIAV-GVFLLLIAVA-G--LVGAVNHH-----QVLLF-FYMIILGLVFIFQFV-------IS-CSCLAINRSKQTD----VINA--SWW----------------------VMSNKTR
TSPAN32 NPY-QAVHQWAFSAGLSLV-G-LLTLGAVL-S--AAATVREA-----QGLMA-GGFLCFSLAFCAQVQ-------VV-FWRLHSPTQVEDA----MLDT--YDLVYEQAMKGT----------SHVRRQEL
Tspan33 -LA-VDPAI-----LLIVV-GVLMFLLTFC-G--CIGSLREN-----ICLLQ-TFSLCLTAVFLLQLA-------AG-ILGFVFSDKARGK----VSEI--INNAIV-HYRDD----------LDLQNLI
EC1
TM2
IC
TM3
EC2

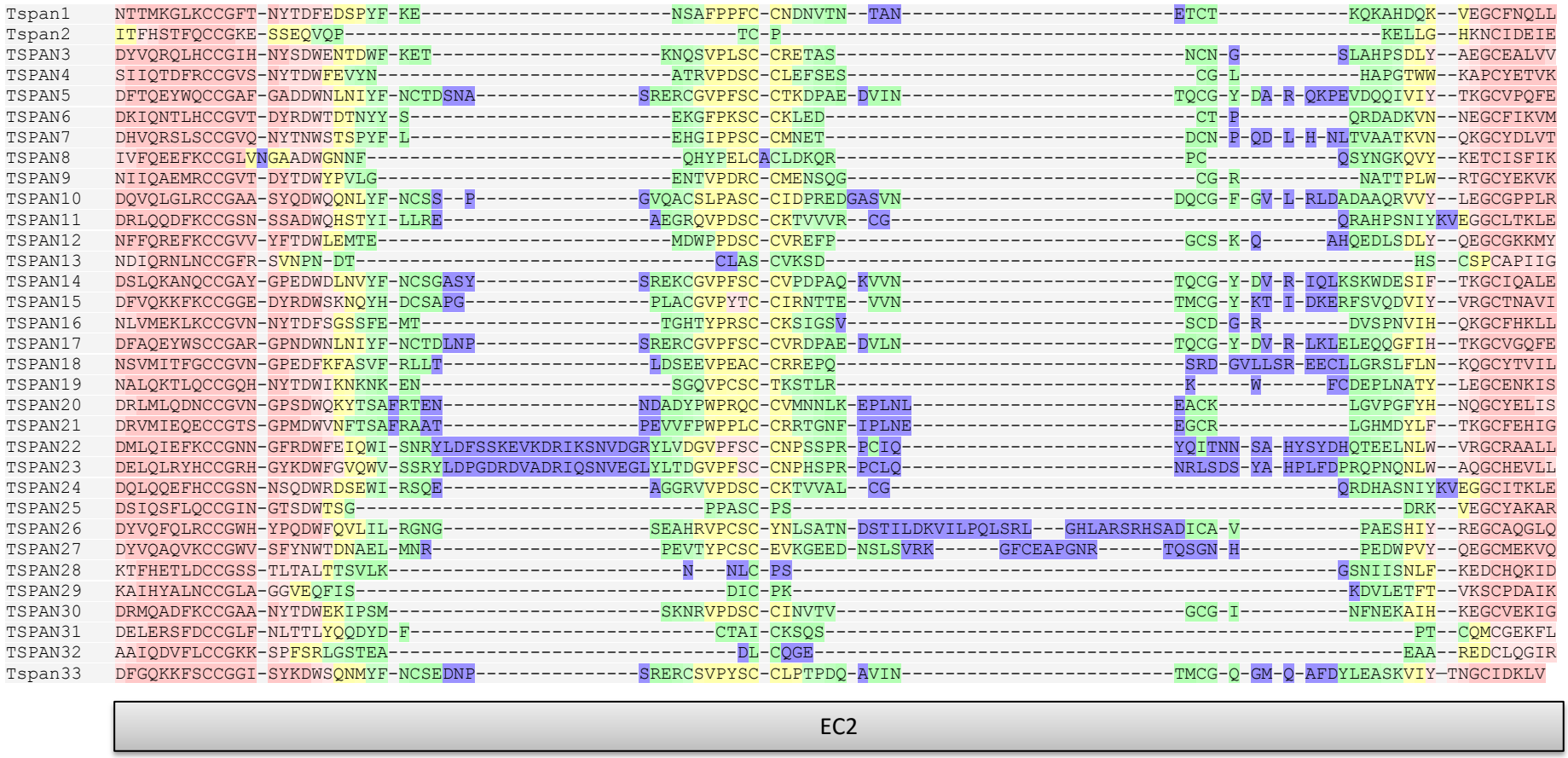
Tspan1 NTTMKGLKCCGFT-NYTDFEDSPYF-KE----------NSAFPPFC-CNDNVTN--TAN----------ETCT----------KQKAHDQK--VEGCFNQLL
Tspan2 ITFHSTFQCCGKE-SSEQVQP----------TC-P----------KELLG--HKNCIDEIE
TSPAN3 DYVQRQLHCCGIH-NYSDWENTDWF-KET----------KNQSVPLSC-CRETAS----------NCN-G----------SLAHPSDLY--AEGCEALVV
TSPAN4 SIIQTDFRCCGVS-NYTDWFEVYN----------ATRVPDSC-CLEFSES----------CG-L----------HAPGTWW--KAPCYETVK
TSPAN5 DFTQEYWQCCGAF-GADDWNLNIYF-NCTDSNA----------SRERCGVPFSC-CTKDPAE-DVIN----------TQCG-Y-DA-R-QKPEVDQQIVIY--TKGCVPQFE
TSPAN6 DKIQNTLHCCGVT-DYRDWTDTNYY-S----------EKGFPKSC-CKLED----------CT-P----------QRDADKVN--NEGCFIKVM
TSPAN7 DHVQRSLSCCGVQ-NYTNWSTSPYF-L----------EHGIPPSC-CMNET----------DCN-F-QD-L-H-NLTVAATKVN--QKGCYDLVT
TSPAN8 IVFQEEFKCCGLVNGAADWGNNF----------QHYPELCACLDKQR----------PC----------QSYNGKQVY--KETCISFIK
TSPAN9 NIIQAEMRCCGVT-DYTDWYPVLG----------ENTVPDRC-CMENSQG----------CG-R----------NATTPLW--RTGCYEKVK
TSPAN10 DQVQLGLRCCGAA-SYQDWQQNLYF-NCSS--P----------GVQACSLPASC-CIDPREDGASVN----------DQCG-F-GV-L-RLDADAAQRVVY--LEGCGPPLR
TSPAN11 DRLQQDFKCCGSN-SSADWQHSTYI-LLRE----------AEGRQVPDSC-CKTVVVR--CG----------QRAHPSNIYKVEGGCLTKLE
TSPAN12 NFFQREFKCCGVV-YFTDWLEMTE----------MDWPPDSC-CVREFP----------GCS-K-Q------AHQEDLSDLY--QEGCGKKMY
TSPAN13 NDIQRNLNCCGFR-SVNPN-DT----------CLAS-CVKSD----------HS--CSPCAPIIG
TSPAN14 DSLQKANQCCGAY-GPEDWDLNVYF-NCSGASY----------SREKCGVPFSC-CVPDPAQ-KVVN----------TQCG-Y-DV-R-IQLKSKWDESIF--TKGCIQALE
TSPAN15 DFVQKKFKCCGGE-DYRDWSKNQYH-DCSAPG----------PLACGVPYTC-CIRNTTE--VVN----------TMCG-Y-KT-I-DKERFSVQDVIY--VRGCTNAVI
TSPAN16 NLVMEKLKCCGVN-NYTDFSGSSFE-MT----------TGHTYPRSC-CKSIGSV----------SCD-G-R--------DVSPNVIH--QKGCFHKLL
TSPAN17 DFAQEYWSCCGAR-GPNDWNLNIYF-NCTDLNP----------SRERCGVPFSC-CVRDPAE-DVLN----------TQCG-Y-DV-R-LKLELEQQGFIH--TKGCVGQFE
TSPAN18 NSVMITFGCCGVN-GPEDFKFASVF-RLLT----------LDSEEVPEAC-CRREPQ----------SRD-GVLLSR-EECLLGRSLFLN--KQGCYTVIL
TSPAN19 NALQKTLQCCGQH-NYTDWIKNKNK-EN----------SGQVPCSC-TKSTLR----------K-----W------FCDEPLNATY--LEGCENKIS
TSPAN20 DRLMLQDNCCGVN-GPSDWQKYTSAFRTEN----------NDADYPWPRQC-CVMNNLK-EPLNL----------EACK----------LGVPGFYH--NQGCYELIS
TSPAN21 DRVMIEQECCGTS-GPMDWVNFTSAFRAAT----------PEVVFPWPPLC-CRRTGNF-IPLNE----------EGCR----------LGHMDYLF--TKGCFEHIG
TSPAN22 DMLQIEFKCCGNN-GFRDWFEIQWI-SNRYLDFSSKEVKDRIKSNVDGRYLVDGVPFSC-CNPSSPR-PCIQ----------YQITNN-SA-HYSYDHQTEELNLW--VRGCRAALL
TSPAN23 DELQLRYHCCGRH-GYKDWFGVQWV-SSRYLDPGDRDVADRIQSNVEGLYLTDGVPFSC-CNPHSPR-PCLQ----------NRLSDS-YA-HPLFDPRQPNQNLW--AQGCHEVLL
TSPAN24 DQLQQEFHCCGSN-NSQDWRDSEWI-RSQE----------AGGRVVPDSC-CKTVVAL--CG----------QRDHASNIYKVEGGCITKLE
TSPAN25 DSIQSFLQCCGIN-GTSDWTSG----------PPASC-PS----------DRK--VEGCYAKAR
TSPAN26 DYVQFQLRCCGWH-YPQDWFQVLIL-RGNG----------SEAHRVPCSC-YNLSATN-DSTILDKVILPQLSRL---GHLARSRHSADICA-V----------PAESHIY--REGCAQGLQ
TSPAN27 DYVQAQVKCCGWV-SFYNWTDNAEL-MNR----------PEVTYPCSC-EVKGEED-NSLSVRK------GFCEAPGNR------TQSGN-H----------PEDWPVY--QEGCMEKVQ
TSPAN28 KTFHETLDCCGSS-TLTALTTSVLK----------N---NLC-PS----------GSNIISNLF--KEDCHQKID
TSPAN29 KAIHYALNCCGLA-GGVEQFIS----------DIC-PK----------KDVLETFT--VKSCPDAIK
TSPAN30 DRMQADFKCCGAA-NYTDWEKIPSM----------SKNRVPDSC-CINVTV----------GCG-I----------NFNEKAIH--KEGCVEKIG
TSPAN31 DELERSFDCCGLF-NLTTLYQQDYD-F----------CTAI-CKSQS----------PT--CQMCGEKFL
TSPAN32 AAIQDVFLCCGKK-SPFSRLGSTEA----------DL-CQGE----------EAA--REDCLQGIR
Tspan33 DFGQKKFSCCGGI-SYKDWSQNMYF-NCSEDNP----------SRERCSVPYSC-CLPTPDQ-AVIN----------TMCG-Q-GM-Q-AFDYLEASKVIY-TNGCIDKLV
EC2

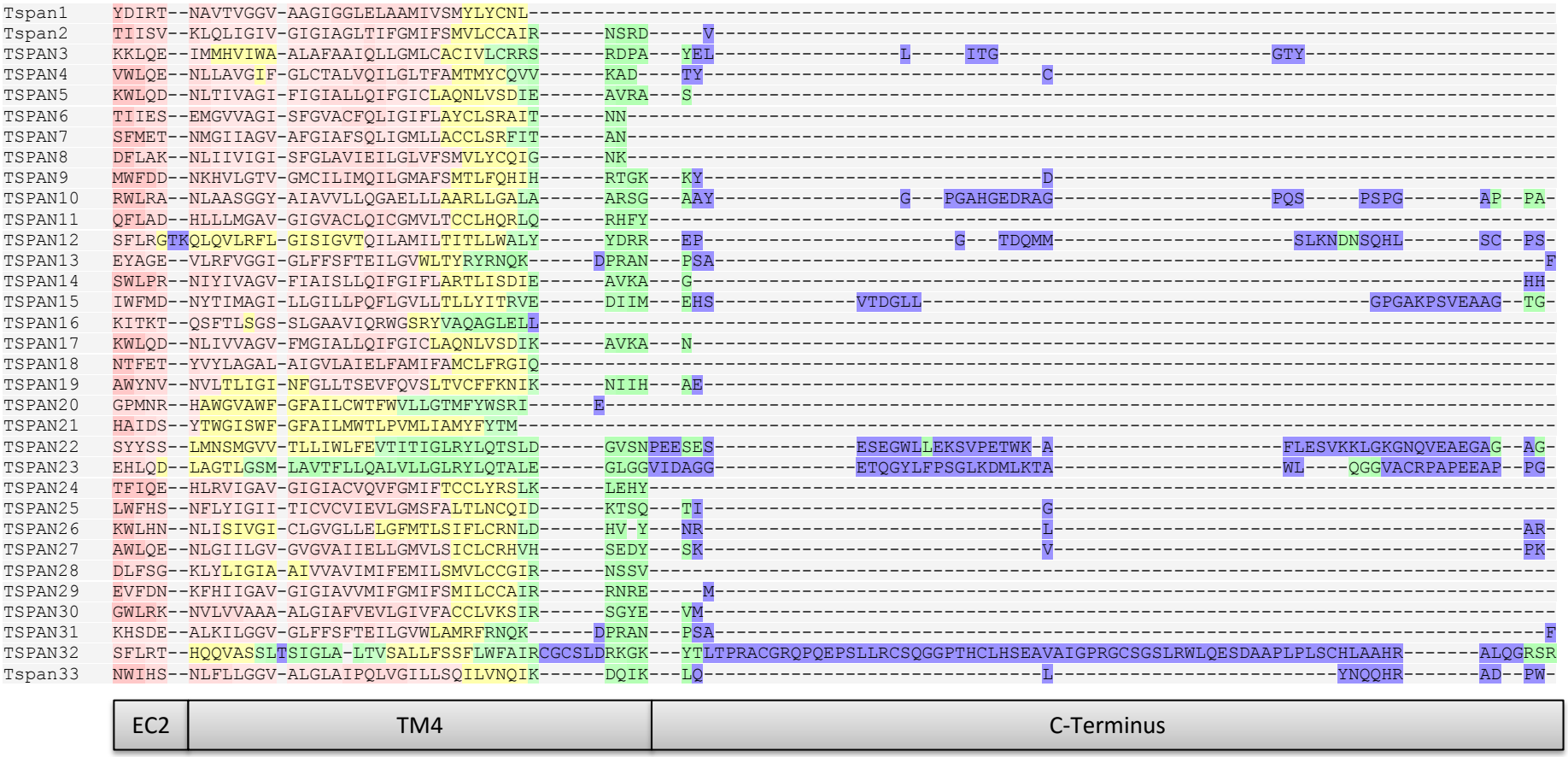
Tspan1
Tspan2
TSPAN3
TSPAN4
TSPAN5
TSPAN6
TSPAN7
TSPAN8
TSPAN9
TSPAN10
TSPAN11
TSPAN12
TSPAN13
TSPAN14
TSPAN15
TSPAN16
TSPAN17
TSPAN18
TSPAN19
TSPAN20
TSPAN21
TSPAN22
TSPAN23
TSPAN24
TSPAN25
TSPAN26
TSPAN27
TSPAN28
TSPAN29
TSPAN30
TSPAN31
TSPAN32
Tspan33
EC2
TM4
C-Terminus

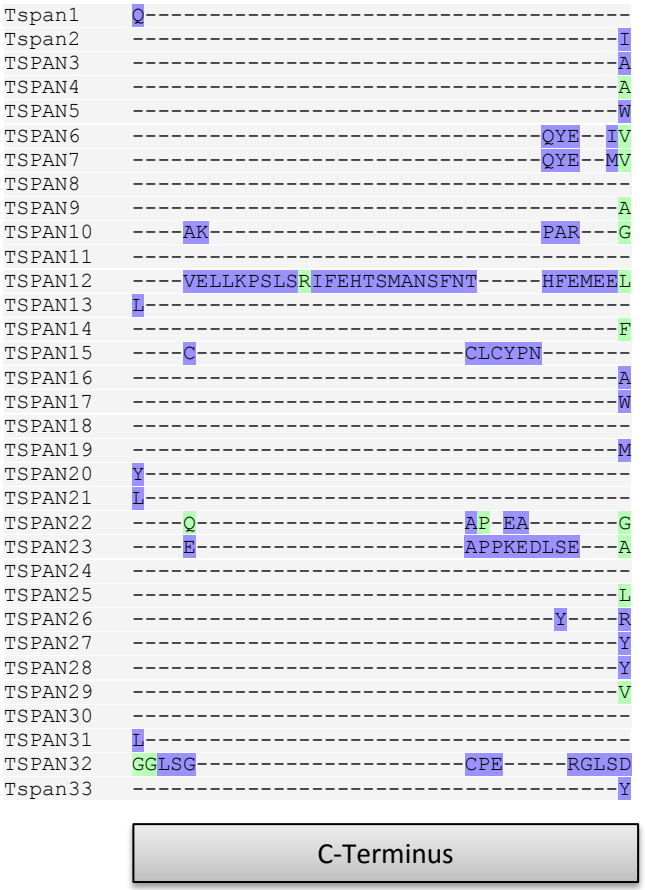

Figure 1.2. Alignment of the primary amino acid sequence of all 33 human tetraspanins. Full length tetraspanin amino acid sequences were attained from www.uniprot.org and aligned using the online software T-coffee simple multiple sequence alignment http://tcoffee.crg.cat/. Tetraspanin names are labelled using the Tspan nomenclature but alternate name can be found in Table 1.1

1.1.2.2 Transmembrane domains

The four transmembrane domains range in size from 21-25 amino acids (Kovalenko et al., 2005) and are the areas of highest homology between the superfamily members (Stipp et al., 2003). Alignment and analysis of multiple tetraspanin transmembrane sequences by Kovalenko *et al.* (2005) revealed a conserved heptad repeat motif in TMs one to three indicative of a coiled coil structure found in many membrane proteins. In the same study, a model was proposed in which TM1 and TM2 are able form intermolecular associations via packing of bulky hydrophobic residues; this is suggested to result in tetraspanin dimerization (Kovalenko et al., 2005). The authors also identify a second potential intermolecular interface between TM3 and TM4 which may enable the formation of higher order structures. Unusually, there are a number of polar residues within membrane spanning helices one, three and four, which have also been suggested as possible areas of interaction between tetraspanins (Stipp et al., 2003). More recently it has been suggested that they are involved in intramolecular interactions between the transmembrane domains which help maintain the conformation stability of tetraspanin CD81 within the membrane, enabling its interaction with CD9 and CD151 (Bari et al., 2009)

Transmembrane regions are not only required for packing of separate tetraspanin molecules, but for efficient expression of tetraspanins at the cell surface too. CD82 lacking the initial transmembrane region was retained within the endoplasmic reticulum (ER) but its expression was restored by separate co-expression of the missing TM1 region (Cannon and Cresswell, 2001). CD82 lacking the TM1 region was not recognised by an anti-CD81 mAb indicating incorrect EC2 folding. This led the authors to suggest that retention at the ER is a means of quality control imposed by the cell to ensure that only fully formed, correctly folded tetraspanins are transported to the surface. Berditchevski *et al.* (2001) also found that deletion of any of the initial three transmembrane domains of CD151 resulted in its distribution to intracellular vesicles, indicating a requirement of the four-span structure for efficient surface expression. Work by Shoham *et al.* (2006) suggested a role for transmembrane domains in partner protein interactions too. They found that the expression of CD81 binding partner CD19 was much reduced in CD81 knockout B-lymphopoietic cells and through transfection of various CD9/CD81 chimeras demonstrated that only the first transmembrane region of CD81 was required to restore expression levels of CD19 (Section 1.1.3.2).

1.1.2.3 EC1 region

The smaller of the extracellular loops, EC1, is composed of under 30 amino acids (Charrin et al., 2009; Seigneuret, 2006). Relatively few functions have been assigned to this region but

Masciopinto *et al.* (2001) found that although the EC1 was not required for CD81-partner interactions, removal of the EC1 led to CD81 retention within the cell, suggesting requirement of this region for efficient translocation. Similarly deletion of the EC1 in CD151 did not affect its association with integrin α3β1 but did prohibit its cell surface expression (Berditchevski et al., 2001). Bioinformatic analysis of CD81 also identified a hydrophobic patch within the EC2 which has been proposed as a "docking site" for the EC1 domain (Seigneuret, 2006); this is thought to aid in EC2 stability and cryo-EM studies of urpolakins have suggested a similar phenomenon (Min et al., 2006). The EC1-EC2 interaction is relatively ambiguous however, because CD81 EC2 crystallised as a homodimer which blocked the proposed EC1 binding site and would therefore prevent this interaction (Kitadokoro et al., 2001; Rajesh et al., 2012).

1.1.2.4 EC2 domain

The EC2 domain makes up a large proportion of the tetraspanin protein accounting for 76-131 amino acids (Boucheix and Rubinstein, 2001; Charrin et al., 2009), and is targeted by many of the available anti-tetraspanin monoclonal antibodies. To date, the only tetraspanin crystal structure available is that of the EC2 domain of human CD81. This particular structure consists of a five helix bundle stabilised by disulphide bonds that the authors describe as having a "mushroom-like" shape comprised of a stalk and head region (Figure 1.1b (Kitadokoro et al., 2001). Kitadokoro *et al.* speculated that this structure is conserved across the tetraspanin family, however later work suggested this is only partly true (Seigneuret et al., 2001). Through sequence alignment, analysis of secondary structures and homology modelling, Seigneuret *et al.* (2006) proposed that the EC2 domain is in fact made of two sub-domains. The more constant of the two subdomains comprises three helices (helices A, B and E) which are thought to be a consistent feature across the family. On the other hand, the hyper-variable subdomain (composed of helices C and D in the CD81 structure) is suggested to have a more varied structure (Seigneuret et al., 2001). Indeed, later NMR analysis by Rajesh *et al* (2012) indicated that the originally dubbed "Helix D" in CD81 may actually have a more dynamic loop structure.

There are four to eight conserved cysteine residues within the EC2 with the majority of members having six, one of which is found within an absolutely conserved CCG motif. These cysteines are thought to take part in di-sulphide bridge formation which is essential for maintaining the structure of the EC2. Interestingly, the specialised tetraspanins perphearin/RDS and ROM-1, located in the photoreceptor outer segment of the eye, have a seventh cysteine involved in intermolecular bonding (Charrin et al., 2009; Loewen and Molday, 2000). Similarly, plant tetraspanins have an uneven number of cysteines (nine), one of which is

located within the EC1 domain and has also been suggested to enable cross-molecule linkage (DeSalle et al., 2010)

The EC2 domain is the most varied region of the tetraspanin proteins and is thought to contribute specificity to different tetraspanin members and as such is primarily considered as the site of partner protein interaction. A number of studies have provided further evidence towards this, for example chimeras of CD151/CD9 showed the EC2 domain was essential for the interaction of CD151 with its binding partner integrin *α3β1.* Moreover Kazarov *et al.* (2002) were able to show that residues 194-196 within the EC2 are required for this association (Berditchevski et al., 2001; Yaucht et al., 2000). Point mutations at two of the conserved cysteines within the EC2 abrogated interaction with partner proteins, therefore also indicating a requirement of disulphide bonds for partner protein associations (Berditchevski et al., 2001). These mutations did not affect interaction with other tetraspanin family members but mutation of the CCG motif did prevent CD151-CD151 interactions, perhaps suggesting different regional requirements for homodimer and heterodimer formation.

The EC2 domain is also responsible for several receptor ligand interactions, for instance the site of CD81 association with the Hepatitis C virus protein E2 has been mapped to the hyper-variable region (Higginbottom et al., 2000b). Binding of the uropathogenic *E. coli* (UPEC) fimbriael protein, FimH, to the uroplakin tetraspanin, UP1a, takes place within the EC2 domain and CD9 interaction with its ligand, PSG17, similarly requires the EC2 domain (Ellerman et al., 2003; Zhou et al., 2001).

Many of the mutations which lead to disease in humans are mutations of residues within the EC2 domains again demonstrating the importance of this particular region. For instance mutation of residue 172 within the hypervariable region of tetraspanin TM4SF2 leads to mental retardation (Zemni et al., 2000). Furthermore, mutations in perpharin/RDS (a tetraspanin found in photoreceptor cells within the eye) leads to severe retinal disease and 70% of mutations that display this phenotype are located within the EC2, many being within the hypervariable region (Stipp et al., 2003).

1.1.2.5 Post translational modification

All tetraspanins undergo post-translational modification with the vast majority of the family being *N*-glycosylated within the EC2 domain at a classical Asn-X-Thr/Ser motif (Martin et al., 2005). The exceptions to this are CD9, which is glycosylated within the EC1 domain, and CD81 and NET-2 which are not glycosylated at all (Boucheix et al., 1991; Maecker et al., 1997). The exact function of glycosylation is unknown however it is required for normal tetraspanin

function in several processes. Glycosylation of CD82 and CD9 is required for their ability to impose a pro-apoptotic anti-metastatic effect in Krieger's ldlD 14 (D14) cells, therefore suggesting a role of tetraspanin glycosylation in cancer suppression (Ono et al., 1999). Point mutation of glycosylation sites in CD82 also resulted in a systematic increase in α5 integrin association and a concurrent decrease in cell motility (Ono et al., 2000). This demonstrates an inhibitory role of tetraspanin glycosylation in partner protein association and a physiological downstream consequence (Ono et al., 2000). Binding and subsequent infection of UPEC is mediated through FimH interaction with the uroplakin UPaI. Interestingly, this binding requires UPaI glycosylation, and the non-mannose residues used in UP1b glycosylation mean that this related tetraspanin is not amenable to FimH binding. This not only demonstrates a role for tetraspanin glycosylation in ligand binding but also shows a level of specificity towards glycosylation patterns (Xie et al., 2006).

Palmitoylation is the covalent attachment of a palmitate group to a cysteine residue (or less commonly a serine/threonine residue) and in contrast to glycosylation, all of the tetraspanins family members without exception undergo this form of modification (Yang et al., 2002). In tetraspanins, palmitoylation takes place on cytoplasmic juxtamembrane cysteines (the number of which vary between members) and several reports have shown the importance of this modification in tetraspanin interactions and trafficking. Although palmitoylation deficient CD9 was still found in the detergent resistant fraction of sucrose gradients (indicating its inclusion within a TEM), its interaction with other tetraspanins was diminished (Charrin et al., 2002). Similarly, abolition of CD151 palmitoylation prohibited its interaction with other tetraspanins (CD63 and CD81) and also reduced its interaction with palmitoylated integrin *α3β1* (Berditchevski et al., 2002). Yang *et al.* (2002) also suggest a contribution of palmitoylation to cellular distribution of CD151, however Berditchevski *et al.* (2002) did not see the same effect and suggest this may be instead due to the C-terminal GFP tag affecting a targeting motif. Interestingly, elimination of palmitoylation in CD81 had no effect on its binding to HCV protein EW2 but did lead to a decrease in HCV susceptibility. Because this mutation led to a decrease in CD81 association with other tetraspanins, the apparent resistance to HCV infection is thought to arise from palmitoylation deficient CD81s inability to exist within TEM (section 1.1.3.1) (Zhu et al., 2012). Additionally, analysis of palmitoylation deficient CD9 indicated that palmitoylation is required for confinement of CD9 into tetraspanin enriched areas (Espenel et al., 2008). Overall, this data would suggest a role for palmitoylation in tetraspanin microdomain formation and interaction with other palmitoylated proteins including other tetraspanin family members. A small number of tetraspanins have also been shown to be ubiquitinated, for example, ubiquitination of CD82 by the ubiquitin ligase gp78 targets it for

degradation (Tsai et al., 2007) and similarly ubiquitination of CD151 promotes its degradation (Lineberry et al., 2008)

1.1.3 Tetraspanin function

1.1.3.1 TEMs

Tetraspanins are primarily thought to function as "molecular facilitators", a role in which they organise proteins within the plasma membrane to form functional clusters which can for example, increase efficiency of signal transduction or increase receptor avidity within a specific area (Kropshofer et al., 2002; Maecker et al., 1997; Yáñez-Mó et al., 2009). Tetraspanins capacity to organise other membrane proteins comes as a result of a number of tetraspanin-partner and tetraspanin-tetraspanin interactions which form a network of proteins at the cell surface often referred to as the tetraspanin web, which includes discreet tetraspanin enriched microdomains (TEM) (Figure 1.2) (Hemler, 2003; Rubinstein et al., 1996). Evidence for the tetraspanin web first came from biochemical studies in which co-immunoprecipitation revealed a plethora of proteins to which tetraspanins associate. Partner proteins include adhesion molecules such as integins, receptor proteins, Ig domain containing proteins and ectro-enzymes, amongst others. Moreover, many of the tetraspanins were found to associate with one another (for an extensive list of binding partners see (Yáñez-Mó et al., 2009)). There is also some evidence for association with intracellular signalling molecules, however it is not clear is this is a direct interaction (Charrin et al., 2014). By varying the strength of detergent used for extraction, it was found that the degree of interaction varied (Rubinstein et al., 1996). Primary interactions refer to those that are retained under the most stringent detergents when tetraspanin-tetraspanin interactions have been abolished; these include specific highly stoichiometric associations between tetraspanins and partner molecules. Weaker detergents maintain secondary interactions (including those between tetraspanins) which are thought to represent association of two proteins through an intermediary tetraspanin-tetraspanin interaction. For example, the metalloproteinase MT1-MMP will co-immunoprecipitate with CD9 but is only in Förster resonance energy transfer (FRET) distance of CD151 (Yanez-Mó et al., 2008). Tertiary interactions include a broad array of proteins and are only found when using the mildest of detergents (such as CHAPS) for lysis. Little is known about the nature of these interactions, although the physical proximity of interacting proteins has been confirmed (Szöllósi et al., 1996; Yáñez-Mó et al., 2009).

Tetraspanin-tetraspanin interactions are thought to initiate in the Golgi resulting in homo and heterodimers which are then transported to the cell surface (perhaps by aid of a transmembrane chaperone) where they act as TEM building blocks

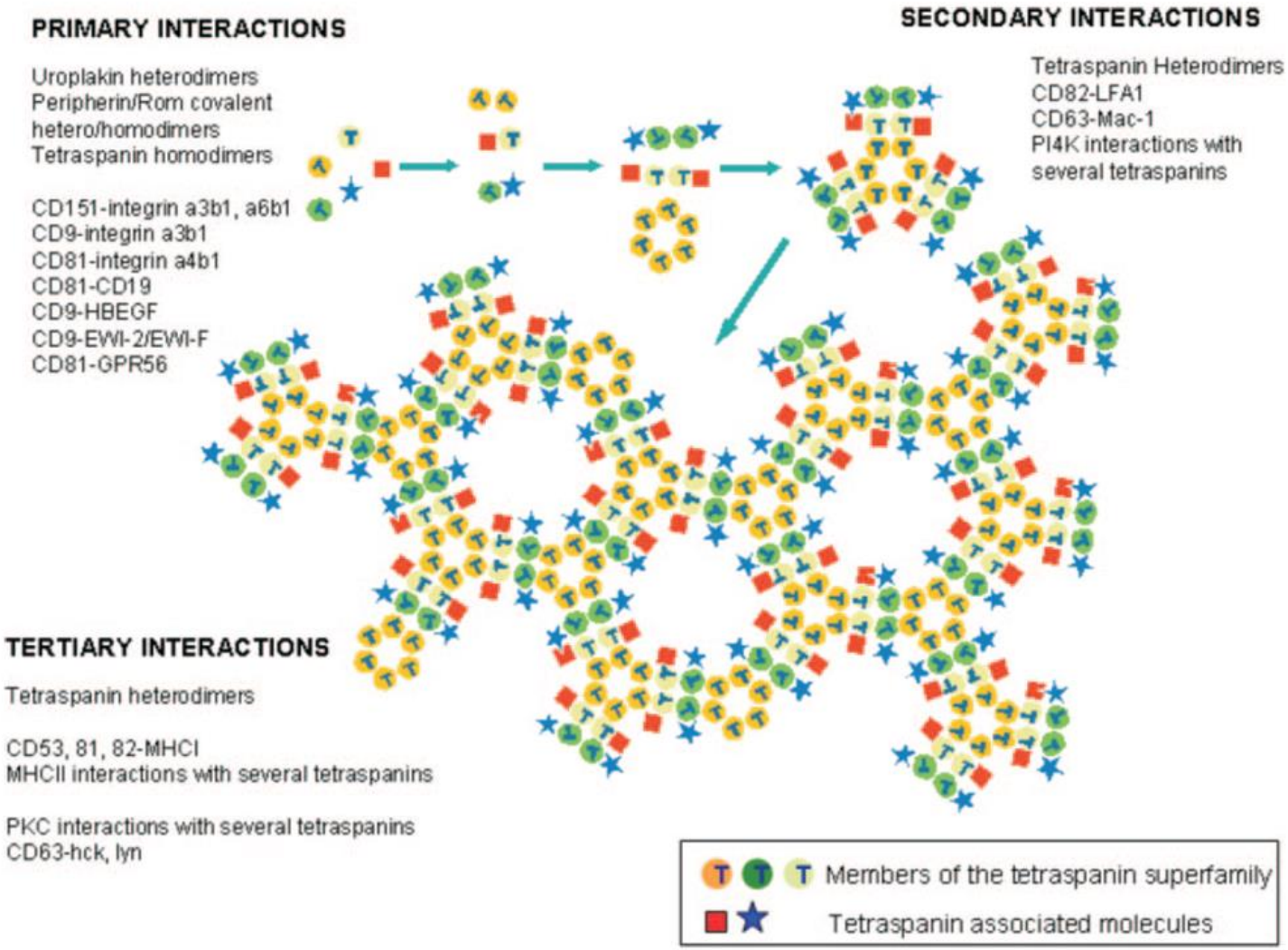

Figure 1.3 Diagrammatic representation of proposed TEM architecture. Robust highly stoichiometric primary interactions are followed by secondary interactions (including those between tetraspanins) which enable the coalescence of tetraspanin-partner complexes and interaction of different primary partners. The coming together of multiple tetraspanin-partner units through tetraspanin-tetraspanin interactions results in the formation of a large multi-molecular complex with tertiary interactions resulting from this higher order structure. The depicted hexagon structure is based on those found in urothelial plaques composed of the specialised uroplakin tetraspanins. Taken from (Martin et al., 2005)

(Berditchevski and Odintsova, 2007; Kovalenko et al., 2004). Several tetraspanin-partner interactions have also been shown to take place in early biosynthesis with tetraspanins proposed to aid in partner protein trafficking (section 1.1.3.2). Partner proteins have been shown to vary depending on the cell type, for example CD81 associates with CD19 in B cells whilst in T cells it associates with CD4 (Charrin et al., 2009). Moreover, partner protein have even been shown to change during tumour progression (Le Naour et al., 2006).

Co-immunoprecipitation after extraction in mild detergents can result in incomplete membrane solubilisation which may give rise to a number of false positives when determining tetraspanin binding partners (Claas et al., 2001). However, more advanced techniques have since corroborated the existence of such associations. For instance, CD9 and CD151 association with the adhesion molecules ICAM-1 and VCAM-1 has been evidenced by FRET (Barreiro et al., 2008) as was the association of CD151 with the metalloproteinase MT1-MMP (Yanez-Mó et al., 2008). A lack of mAbs towards many tetraspanin members made confirming tetraspanin-tetraspanin association difficult also; but these have similarly been proven using various alternative methods. For example, chemical cross linking of CD9 showed homodimers formed in the Golgi (Kovalenko et al., 2004) and FRET analysis demonstrated the existence of CD9-CD151 heterodimers along with CD9-CD9 homodimers at the cell surface (Barreiro et al., 2008). A number of studies have evidenced secondary associations which take place via a tetraspanin intermediary. For instance, the CD9 binding partner, CD9P-1, only interacts with CD81 when CD9 is also expressed (Charrin et al., 2003a) and interaction of the CD151 binding partner, integrin α1β3, with other tetraspanins is abrogated in the absence of CD151 (Takeda et al., 2007) .

The existence of TEMs has also been proven using advanced microscopy techniques. For instance the diffusion patterns of a single CD9 molecule were monitored using total internal reflection fluorescence (TIRF) microscopy (Espenel et al., 2008). In the study, regions of the membrane were identified which were enriched in both CD9 and CD81 and the stability of these tetraspanin enriched areas (TEAs) was unaffected by cholesterol depletion or cytoskeletal elements and was therefore suggested to be dependent on protein-protein interaction. CD9 molecules outside of TEAs displayed Brownian motion and were thought to form transient homodimers due to the propensity of two CD9 molecules to co-diffuse for short intervals. Unusually the increased size of the co-diffusing molecules did not reduce their rate of diffusion (which would normally be expected). This led the authors to suggest their existence within a cluster of other tetraspanins and partner proteins. Inside the TEAs, CD9 showed a more restricted , lower diffusion rate than in the rest of the cell, indicating an area of confinement (Espenel et al., 2008). Fluorescence recovery after photo bleaching (FRAP) by

Barreiro *et al.* (2008) also demonstrated that tetraspanins and other members of TEMs diffused at much slower rates than the lipid raft marker GPI-EGFP.

The web phenomenon is perhaps best exemplified in the bladder urothelium, in which the specialised tetraspanins UPIa and UPIb interact with partner protein UPII and UPIII respectively. Interaction of these proteins leads to the formation of 16nm urothelial plaques which cover the bladder surface and help to maintain a permeability barrier (Wu et al., 2009). Cryo-EM studies and cross linking analysis on these naturally forming 16nm particles demonstrated that tetraspanin partner interaction is facilitated through both transmembrane and extracellular regions and varying levels of protein-protein interactions lead to the formation of a distinct microdomain (Min et al., 2006; Wu et al., 1995)

The discovery of membrane microdomains has seen the original fluid mosaic model of the plasma membrane somewhat disregarded/altered in favour of one in which related proteins are grouped to carry out functions more efficiently. However the idea of membrane protein organisation is not unique to TEMs. In 1997 Simons *et al* (1997) proposed the idea of distinct platforms enriched in sphingolipids and cholesterol which contain mostly saturated phospholipids. These platforms are now known as lipid rafts and are thought to form a liquid ordered phase within a liquid disordered environment, leading to protein segregation and clustering. Other membrane microdomains also exist, such as caveolae which appear as flask shaped invaginations in the cell membrane. These micromdomains are linked to endocytosis, and as well as being enriched in glycosphingolipids and cholesterol, they also contain the membrane proteins caveolin (Thomsen et al., 2002).

There are a number of common features between TEMs and lipid rafts, for instance both contain cholesterol, gangliosides and glycosphingolipids. Lipid rafts partition into the detergent resistant fraction of density gradients and in some circumstances tetraspanins do also. Palmitoylation is required for the partitioning of proteins into lipid rafts and is also required for many tetraspanin-tetraspanin interactions (Charrin et al., 2002, 2003a; Claas et al., 2001; Yang et al., 2004). However, a number of physical and molecular differences reveal TEMs as a distinct type of microdomain. Firstly in their composition; there has been no reported associations of tetraspanins with GPI-linked proteins or caveolin (which are used as markers for lipid rafts and caveoli) and proteomics of lipid raft-resident proteins has not identified any tetraspanin family members (Foster et al., 2003; Le Naour et al., 2006) a number of G-protein subunits have been identified in both lipid rafts and TEMs however (Le Naour et al., 2006). Their physical properties also differ, in contrast to lipid rafts, TEMs are disrupted with Triton X-100 at 4°C but are maintained at 37°C under milder detergents (Le Naour et al., 2006).

Moreover, TEMS are more resistant to cholesterol depletion than lipid rafts (although are still partially disrupted) (Charrin et al., 2003b; Hemler, 2005). Finally, FRAP analysis by Barreiro *et al.* (2008) revealed that TEM associated proteins diffused at much slower rates than a commonly used lipid raft marker.

This organising potential of TEMs along with the multitude of partner proteins has led to their implication in a plethora of different processes both in normal physiology and also in disease, some of which will be discussed here.

1.1.3.2 Protein trafficking

In addition to their organising capacity at the cell surface, tetraspanins have also been shown to aid trafficking of their associated protein partners, with just a few instances being discussed here.

The immunoglobulin family member CD19 is the molecular partner of tetraspanin CD81 in B lymphocytes and its surface expression is significantly reduced in CD81 knockout mice (Tsitsikov et al., 1997). CD19 mRNA levels were unaffected in $CD81^{-/-}$ cells indicating a posttranscriptional involvement of CD81; which was also suggested due to CD19s significantly slower transit from the ER to the Golgi in these cells (Shoham et al., 2003). Gene knockouts of other tetraspanins had no such effect and the use of CD9/CD81 chimeras demonstrated that the CD81 EC2 domain was not required for CD19 expression. Surprisingly the first transmembrane domain (TM1) alone was sufficient to restore CD19 surface expression; this is suggested to be because this region can facilitate the release of CD19 from a transmembrane chaperone (Shoham et al., 2006).

In contrast to CD81, CD151 knockout cells did not show diminished expression of CD151 integrin partners, α3β1 or α6β4, at the cell surface (Winterwood et al., 2006). However, RNAi mediated silencing of CD151 in carcinoma cells led to reduced motility on certain surfaces, due to the loss of CD151 not only preventing integrin association with TEMs, but also significantly reducing their internalisation rate, leading to persistence at the surface and increased adhesive contacts. CD151 trafficking is suggested to involve the C-terminal YXXϕ motif previously mentioned (section 1.1.2.1), thought to enable selection for clathrin dependent endocytosis by interaction with adaptor complexes (Winterwood et al., 2006)

Some of the less well characterised tetraspanins which contain eight cysteine residues (TspanC8) also aid in the trafficking of their partner proteins, specifically a surface metalloproteinase, ADAM10, which cleaves and activates the transcription factor Notch. In this

instance the TspanC8 proteins regulate ADAM10 release from the ER and in doing so are able to regulate its cleavage ability and subsequent notch signalling (Dornier et al., 2012)

1.1.3.3 Migration and adhesion

Integrins are a family of membrane proteins composed of αβ heterodimers, through interaction with other cells and extracellular matrix components, they can alter cellular adhesion and migratory properties (Hemler, 1990). Integrins are prime examples of primary tetraspanin partner proteins which exhibit strong tetraspanin interactions that are stable in a variety of detergents. It is perhaps unsurprising then that tetraspanins have been implicated in a number of adhesion and migratory processes.

Tetraspanin-integrin associations are known to take place early in their biosynthesis and tetraspanins have been shown to regulate integrin trafficking and turnover. CD151 is perhaps most well-known for its interaction with integrins and, as previously mentioned, CD151 mediated endocytosis of α3β1 and α6β4 has pronounced effects on cellular migration (Liu et al., 2007). A role of CD151 in adhesion strengthening has also been shown using fibroblasts expressing mutant CD151 which lacks the C-terminal tail. Although initial adhesion was unaffected in these mutant cells, the strength of adhesion to laminin did not increase over time (in contrast to cells expressing wild-type CD151) (Lammerding et al., 2003). This is thought to result from loss of CD151 C-terminus interaction with unidentified membrane proximal elements following integrin α6β1 attachment which would normally result in adhesion strengthening. CD81 has also been shown to affect adhesion strengthening although in different cell types (monocytes and B cells). Interestingly CD81 also enhanced initial capture events of α4β1 to VCAM-1 (Feigelson et al., 2003).

In addition to integrins, tetraspanins also associate with the integrin receptors ICAM-1 and VCAM-1, which enables another means by which they are able to regulate adhesion and migration. Barreiro *et al.* (2005) showed that treatment of endothelial cells with recombinant CD9 or CD151 EC2 domains, or siRNA knockdown of CD9 and CD151 resulted in reduced lymphocyte transmigration and increased detachment under shear stress. This is thought to happen due to the disruption of TEMs (also called endothelial adhesive platforms (EAPs)) which result from co-recruitment of tetraspanins and adhesion molecules to specific lymphocyte engagement sites. These form a docking structures on endothelial cells, clustering adhesion molecules and in so doing enable more efficient capture and transmigration (Barreiro et al., 2008).

1.1.3.4 Cell fusion

One of the most well documented tetraspanin roles is that of CD9 in sperm-egg fusion. From the first observation in 2000 that $CD9^{-/-}$ oocytes were unable to fuse with sperm cells, it has since been discovered that treatment of oocytes with recombinant CD9-EC2 domains or anti-tetraspanin monoclonal antibodies is also sufficient to inhibit fusion (Miller et al., 2000; Le Naour et al., 2000; Zhu et al., 2002). Interestingly, pre-incubation of sperm with CD9-EC2 domains has no effect on fusion and male CD9 knock-out mice do not exhibit reduced fertility, thus indicating an in-*cis* effect of CD9 at the oocyte surface (Kaji et al., 2000). CD9 has since been suggested to coordinate the formation of adhesion sites at the egg surface, resulting in a tight interface between the gametes, enabling cell fusion (Jegou et al., 2011).

This is not the only instance of tetraspanins being involved in cellar fusion; they have also been implicated in fusion of muscle cells to form myotubes, renewal of photoreceptor outer discs and monocyte fusion (Boesze-Battaglia et al., 2003; Tachibana and Hemler, 1999). Monocytes do not traditionally undergo fusion and instead circulate in the blood before differentiating in the tissues to form mononucleate macrophages. In the rare event of monocyte fusion, the resultant cells are known as osteoclasts when found in the bone and multinucleated giant cells (MNGCs) when found in cases of chronic inflammation (Chen et al., 2007). Monocytes are thought to form these larger entities to enable more efficient resorption of bone, or for the extracellular killing of microbes. Given that this is not the traditional route of monocyte progression it is a tightly regulated process and investigation into tetraspanin involvement has displayed varied effects for different members. Antibodies towards CD9 and CD81 were shown to enhance Con-A induced MNGC formation whereas anti-CD63 antibodies had the inverse affect and CD151 had no significant affect (Parthasarathy et al., 2009; Takeda et al., 2003). The inhibitory role for CD9 and CD81 was also exhibited by $CD9^{-/-}$ and $CD81^{-/-}$ monocytes which showed enhanced fusion individually and spontaneous fusion when knocked-out together (Takeda et al., 2003). Interestingly, the EC2 domain of CD9 and CD63 when added exogenously to the cells as a recombinant GST fusion proteins also inhibited cell fusion whereas CD81 EC2 had no significant effect suggesting a more direct role of CD9 in this type of fusion (Parthasarathy et al., 2009; Takeda et al., 2003)

Tetraspanins have also been linked to viral induced cell fusion that results in multinucleated giant cells known as syncytium, proposed to aid in viral dissemination in an infected host. For instance, overexpression of CD9 or CD63 in HeLa or Jurkat cells results in a significant decrease in HIV induced syncytium formation and the reciprocal effect is seen when expression of these proteins was knocked down (Weng et al., 2009). It is not known exactly how this happens but

the recruitment of viral proteins GAG and ENV into TEMs has been implicated. In contrast to CD9 and CD63, a positive regulatory role has been described for CD81 in HTLV-1 syncytium formation as anti-CD81 antibodies have been shown to reduce syncytium formation and CD81 associates with a number of viral proteins on the plasma membrane and on intracellular vesicles (Fanaei et al., 2011).

1.1.3.5 Immune function

T helper cells (T_h) are activated by interaction with class II major histocompatibility complexes (MHC) on the surface of antigen presenting cells (APCs). A single signal in isolation is not sufficient for T cell activation and instead there is a requirement for T-cell receptors to engage multiple, peptide primed MHC molecules on the opposing cell. Clustering of MHC molecules on APCs at the point of T-cell engagement (also known as the immunological synapse) is crucial for activation and is now known to involve TEMs (Kropshofer et al., 2002). Interestingly, lipid rafts have also been shown to cluster MHC molecules, however far more MHC complexes can be isolated from TEMs and their peptide composition is more restricted than those isolated from rafts, indicated another physiological difference between the two microdomains. (Kropshofer et al., 2002). Disruption of the membrane microdomains using the glycoside, saponin, significantly reduced T cell activation. Similarly Unternaehrer *et al.* (2007) found that knocking out CD9 led to disruption of heterologous MHC molecules dimers, also suggesting a role for tetraspanins in enhancing T cell stimulation. It is therefore surprising that knocking out tetraspanins CD37 and CD151 in dendritic cells led to a hyperstimulatory phenotype (Sheng et al., 2009). Investigation into this response found that these two tetraspanins have differing roles in T-cell activation with CD37 being involved in MHC clustering and CD151 regulating co-stimulation. The authors suggest that the unexpected phenotype is a result of tetraspanin members having differing functions in T-cell activation some stimulatory and some inhibitory.

CD81 was original found as the target of an anti-proliferative antibody towards B cells and has since been linked to a number of immune functions (Oren et al., 1990). Along with its requirement for efficient glycosylation, transport and activation of CD19 in B cells, CD81 is also thought to act as a co-stimulatory molecule in T cells (Witherden et al., 2000). Its activity was akin to that of another co-stimulatory molecule, CD28, although the two pathways are distinct and lead to differing cytokine profiles. Additionally, antibody cross linking of CD81 and CD63 on natural killer (NK) cells leads to increased migration towards various cytokines, an effect thought to be mediated through increase phosphorylation of ERM proteins (a family of proteins which link the membrane to the actin cytoskeleton (Arpin et al., 2011; Krämer et al., 2009).

1.1.3.6 Disease

Tetraspanins are linked to a number of pathologies, perhaps most evidently to those which are a direct result of mutations within the tetraspanin genes. For instance, mutation of tetraspanin Tspan7 results in X-linked mental retardation (Abidi, 2002) and mutation of CD81 EC2 leads to severe immune deficiency from an inability to mount an antibody mediated immune response (Van Zelm et al., 2010). A premature stop codon in CD151 results in renal failure, skin blistering and deafness which reflects this proteins importance in basement membrane formation in the kidney and skin and mirrors the effect seen of various integrin mutants (Crew et al., 2004). Finally mutation in the EC2 domain of Tspan 12 leads to progression vision loss in the form of familial exudative vitreoretinopathy (FEVR)(Yang et al., 2011). This is thought to arise from developmental issues and subsequent deficiencies in signalling through norrin/β-catenin (Junge et al., 2009)

Tetraspanins involvement in cancer was initially as markers for cancer type, progression and prognosis, for instance CD63 (initially known as melanoma associated antigen) is highly expressed in early melanoma stages and is much reduced in later phases (Hotta et al., 1988). Tetraspanins are now known to regulate cell behaviour at multiple cancer stages, for instance, although they are not as strongly linked to initial tumour formation, ablation of CD151 in breast cancer xenograft models reduced tumour initiation through integrin redistribution (Yang et al., 2008). Many reports using anti-CD9 antibodies or genetic knockdown of CD9 have demonstrated its ability to inhibit cancer metastasis (Powner et al., 2011). Similarly CD82 is also able to reduce metastasis and low expression levels of both CD9 and CD82 is linked to a poor prognosis (Boucheix and Rubinstein, 2001). On the other hand introduction of CD151 or Tspan8 results in enhanced metastasis (Zöller, 2009), again exhibiting the contrasting role which tetraspanins can display. The exact mechanism by which tetraspanins modulate cancer activity is in the most part unknown, but is most likely due to their association with integrins and proteinases which can themselves alter cellular migration.

Tetraspanins have been identified as the initial pathogen binding partners (enabling subsequent infection) in several infectious diseases. One of the most prominent is hepatitis C (HCV) infection of hepatocytes mediated through viral protein E2 binding of tetraspanin CD81 (Pileri et al., 1998). CD81 not only enables entry of HCV but is also involved in downstream processes. For example, in CD81 negative cells, the viral protein E1E2 was retained in the ER, whilst in those which were transfected with human CD81, E1E2 was transported through the Golgi and found within exosomes which are suggested to fuse to and infect other cells (Masciopinto et al., 2004). Tetraspanins are also indirectly linked to HIV entry, as recombinant

EC2 domains of several tetraspanins along with an anti-CD63 mAb block macrophage infection by HIV (Ho et al., 2006; von Lindern et al., 2003). CD63 silencing also inhibited HIV reverse transcription and CD63 is suggested to exhibit these pro-infectious properties due to its trafficking of CXCR4 (a GPCR which acts as a HIV co-receptor) (Yoshida et al., 2008). These are just two examples of tetraspanin involvement in viral infection; however there are a number of other instances (Hassuna et al., 2009; Martin et al., 2005; Monk and Partridge, 2012)

Tetraspanins are also linked to bacterial infection with the most well characterised interaction being between the uroplakin UP1a and uropathogenic *E. Coli* (UPEC). Similarly to CD81-HCV interaction, the UP1a-FimH association acts as an initial point of pathogen binding and enables subsequent infection of the bladder epithelium (Wu et al., 1996). Interestingly, it was more recently shown that following initial binding of FimH to a mannose moiety on UP1, a global conformation change takes place across the uroplakin complex both extracellularly and in the transmembrane regions (Wang et al., 2009). Despite this being the only documented direct interaction of tetraspanins with bacteria, they have been linked indirectly to many other bacterial infections also. For instance CD81 knockout HeLa cells exhibited its importance in *listeria* internalisation and work by our group showed several anti-tetraspanin antibodies and recombinant EC2 were able to prohibited meningococcal adhesion to endothelial cells (Green et al., 2011; Tham et al., 2010). Moreover, tetraspanins have also been implicated in a number of fungal and even plasmodium infections (Monk and Partridge, 2012)

1.1.3.7 Trans associations and specialised functions

Although tetraspanins are mainly known for their lateral associations within the membrane there are a number of instances of trans associations, for example with a specific ligand or a surface protein on another cell. The first identified tetraspanin ligand was pregnancy specific glycoproteins 17 (PSG17) and the use of blocking antibodies and knockouts exhibited its specificity for CD9 (Waterhouse et al., 2002). Later results showed that PSG17 binding requires SFQ residues within the CD9 EC2 domain which are also those required to enable sperm-egg fusion (Ellerman et al., 2003). Yeast-two-hybrid screening identified CD63 as the binding partner of the matrix metalloproteinase inhibitor TIMP-1, (which was later confirmed using shRNA knockdown of CD63) (Jung et al., 2006). TIMP-1 binding of CD63 is required for its cell surface association and intergrin co-localisation. The same study also showed that CD63 is required for several TIMP-1 functions for instance promoting cell survival through inhibition of the caspase pathway. Finally two instances of tetraspanin ligand interaction were discussed In the previous section (1.1.3.5) with CD81 binding HCV protein E2 and UPIa binding UPEC adhesin Fim-H.

Although the tetraspanins UP1a and UP1b in the bladder and ROM-1 and peripherin/RDS in the eye act in the more convention manner of forming lateral interactions, their specialised functions are distinct from traditional tetraspanins. As previously mentioned (section 1.1.3.1) the two uroplakins UPIa and UPIb form heterodimers with their respective partner protein UPII and UPIII and a network of these hetrodimers results in a plaque which help form a permeability barrier (Min et al., 2006). Peripherin/RDS and Rom-1 are located in the rim membrane of the disc structures found in the outer segment of photoreceptor cells. Peripherin/RDS is required for morphogenesis and stabilisation of the rim, evidenced by the lack of outer segment in homozygous negative mice and disordered structure found in heterozygous mutants (Sanyal and Hawkins, 1981). On the other hand knock-outs of Rom-1 led to larger more disordered discs and mutants have a far less serious phenotype than that of Peripherin/RDS mutants indicating a more supportive role for this protein(Boon et al., 2008; Clarke et al., 2000). As may be expected from tetraspanin family members, these proteins are thought to form multi protein complexes (tetramers) which in turn form larger oligomer structures which are required for disc formation (although in contrast to traditional tetraspanins heterodimers are thought to be stabilised by intermolecular disulphide bonds) (Boon et al., 2008; Loewen and Molday, 2000)

1.1.3.8 Studying tetraspanin

Despite tetraspanins being involved in a multitude of processes, relatively little is known about the effects of individual members. Many different methods have been used to assay their function with varying levels of success. For example, knockout mice frequently display mild phenotypes probably because of a level of redundancy within the tetraspanin web (Charrin et al., 2009; Hemler, 2005; Weng et al., 2009). The occasional phenotypes which are displayed have shed some light on the activities of certain tetraspanins. For instance, the previously mentioned CD9 knock-out mice displayed CD9s importance in fertility, and CD9, CD81 double knockout monocytes exhibited spontaneous fusion (Section 1.1.3.3) (Miller et al., 2000; Takeda et al., 2003). Additionally, further cellular examination of knock-out mice previously considered “normal”, has identified subtle defects such as $CD37^{-/-}$ dendritic cells which have impaired *in vivo* migration, adhesion and spreading and altered T-cell stimulation (Gartlan et al., 2013; Sheng et al., 2009). Anti-tetraspanin monoclonal antibodies have also been shown to modulate tetraspanin function and are often used in collaboration with other techniques to corroborate results. For instance studies have shown that anti-CD151 antibodies inhibit CD151 association with α3β1 and in doing so, greatly reduced the integrins ligand binding capability thus suggesting CD151 stabilises α3β1 in an active conformation (Nishiuchi et al., 2005). Monoclonal antibodies do however have drawbacks: they are difficult to raise against some

tetraspanins due to poor immunogenicity, they may cause remote unrelated results because of their inherent ability to interact with fragment crystallisable (Fc) receptors and they may cross-link both tetraspanins and partner molecules within TEMs due to their divalent nature (Hassuna et al., 2009; Wright et al., 2004)

As mentioned previously (section 1.1.2.4), the high level of variability between EC2 domains of different family members has led to the suggestion that they are responsible for some specific functions of individual tetraspanins. Furthermore, the CD81 crystal structure, NMR and conformationally sensitive antibodies have shown that EC2s domain can be correctly folded when expressed alone (Higginbottom et al., 2003; Kitadokoro et al., 2001; Rajesh et al., 2012). These factors, along with recombinant EC2 domains ability to bind to other tetraspanins and partner proteins has led to the use of these proteins in a number of functional studies (Parthasarathy et al., 2009, Ho et al., 2006, Barreiro et al., 2005), some of which will be discussed here, along with their proposed mechanism of action.

To examine the involvement of TEMs in the adhesion of leukocytes to endothelial cells, Barreiro *et al.* (2005) treated endothelial cells with recombinant CD9-EC2-GST fusion proteins. Electron microscopy revealed that when endothelial cells were treated CD9-EC2-GST the spacing of the reported TEM associated receptors ICAM-1 and VCAM-1 was increased over the untreated counterparts. Furthermore, the pattern of distribution of these two receptors was also altered and this trend was not seen in cells treated with heat inactivated CD9-EC2-GST. Moreover, treatment of the endothelial cells with CD9 EC2 not only decreased CD9 diffusion but also decreased diffusion of CD151, therefore indicating that modulation of one tetraspanin may affect the TEM as a whole. The authors suggest that this occurs due to exogenous CD9-EC2-GST competing with endogenous CD9 for both homotypic interactions with other native CD9 molecules and heterotypic interaction with partner proteins, which in turn disrupts the TEM (Barreiro et al., 2008). In an earlier study by Zhu *et al.* (2002), recombinant CD9 EC2 domains were also used, in this case to study their effects on sperm-egg fusion. When eggs were pre-incubated with CD9-EC2 their rate of fusion was lowered, however, a similar affect was not seen when sperm were pre-incubated. This showed that the EC2 domains were acting in *cis,* leading the authors to again speculate that exogenous CD9 competes with endogenous CD9; however, they did add that the inability of recombinant CD9 EC2 to display the complete function of CD9 is most likely due to the lack of transmembrane regions. Higginbottom *et al.* (2003) similarly used recombinant EC2 domains to study sperm-egg fusion and demonstrated an inhibitory effect with CD81 EC2 (albeit a less dramatic inhibition than CD9 EC2). In this study mutation of specific residues displayed the functional importance of several conserved cysteines within the EC2.

As previously discussed, the use anti-CD9 and anti-CD81 mAbs along with and CD9/CD81 knockout mice led Takeda *et al.* (Takeda et al., 2003) to reported a negative regulatory role for these tetraspanins in monocyte fusion. In addition to these methods, the authors also used recombinant EC2 domains corresponding to CD9. Interestingly anti-CD9 mAbs and GST-CD9 showed opposing effects on cell fusion, with EC2 domains inhibiting monocyte fusion in a dose dependent manner and anti-CD9 mAbs enhancing fusion. This emphasised the different modes of action between mAbs and EC2 domains. In a similar experiment, Parthasarathy *et al.* (2009) showed recombinant EC2 domains of tetraspanin CD63 were also able to inhibit fusion whereas CD81-EC2 and mouse CD9-EC2 had no effect. Not only does this show EC2 domains from different family members have specific interactions (and therefore different outcomes) but also exhibits the variation between EC2 domains originating from different species.

Kelić *et al.* (2001) were able to show specific binding of CD81-EC2-GST to neurones and not astrocytes, despite endogenous expression of CD81 on both cell types. This suggested the existence of a CD81 ligand on neurons, additionally, recombinant CD81 was thought to compete with native CD81 for receptors on the neurone and in doing so block neuron-induced astrocyte proliferative arrest.

1.2 Mast cells

1.2.1 History

Multiple studies have linked tetraspanins to mast cells, with a specific focus on tetraspanins role in the activation of mast cells in response to specific stimuli (Fleming et al., 1997; Köberle et al., 2012; Kraft et al., 2005; Peng et al., 2011). Despite these investigations being able to show tetraspanins involvement in activation there is still no definitive answer as to their specific role, the aim herein was to develop our understanding or tetraspanin involvment in mast cell activation by IgE.

Granulated cells within tissue were first described in 1863 by Friedrich von Recklinghausen, however it was not until 1879 when these cells were first called “Maztzellen” or “Mast cells” (meaning well-fed cells) by Paul Ehrlich (Blank et al., 2013; Ehrlich, 1879). Mast cells have since become known as key players in both immunity and disease and it has been established that they are of the myeloid lineage, originating in the bone marrow and circulating in the blood, before migrating to the tissues where they undergo maturation (Gurish and Boyce, 2006). They have a common morphology with distinct electron dense granules within the cytoplasm. These granules contain cytokines, proteases, histamine and serotonin and in response to certain stimuli these components can be rapidly released to the surroundings. In addition, mast cells are able to release *de novo* synthesised cytokines along with several lipid based signalling molecules (Plaut et al., 1989).

Despite a common morphology, mast cells are a heterogeneous population, which have been divided into a number of groups. The first groups to be established were based on staining differences in mast cells isolated from the rat gastrointestinal mucosa and were entitled mucosal mast cells (MMCs) and connective tissue mast cells (CTMC). Human mast cells were later divided based on their protease content with one group containing only tryptase (MC_T) and the other group containing both tryptase and chymase (MC_{TC}) (Irani et al., 1986). A third group also exists which express chymase and capthesin G (MC_c), although these are much less prevalent (Metcalfe, 2008). Further subdivisions have since been made based on differences in granular content, response to stimuli, drug inhibition, histamine content and proteoglycan composition amongst other factors (Metcalfe et al., 1997). Differences in mast cell properties are suggested to stem from requirements for residing in various tissues or for responding to different pathogens (Abraham and St John, 2010).

The primary function of mast cells was initially unknown, however, the finding that their granules contain histamine along with the prior knowledge that this substance could cause

smooth muscle contraction led to the suggestion of mast cells involvement in anaphylaxis (Riley and West, 1953). Later work recognised the association of mast cells with IgE, a subtype of antibodies initially known as the serum factor, able to transfer hypersensitivity from one animal to another (Ishizaka et al., 1967; Kulczycki et al., 1974). It was not until years later that the beneficial effects of mast cells were hinted upon when it was discovered that they are able to synthesise cytokines, specifically IL-4, opening the possibility for a role beyond allergic effectors (Brown et al., 1987). This possibility was solidified when mast cell activity was exhibited in parasitic (specifically nematode) expulsion and In the following years various studies have shown their ability to phagocytose microbes, process and present antigen and produce vasoactive substances and cytokines (Metcalfe et al., 1997; Woodbury et al., 1984). Mast cells are now seen as an important player in the host immune response, acting as sentries to announce the presence of pathogens, effector cells able to themselves destroy invading microorganisms and signalling cells modulating both innate and adaptive immune responses (Galli et al., 2005).

1.2.3 Mast cells in immunity

1.2.2.1 Pathogen detection

As mast cells are predominantly found in the mucosal tissues at the boundary with the outside environment, they are often one of the first immune cells to encounter infection and so it may not be surprising that mast cells are well equipped for pathogen detection. Similarly to dendritic cells, neutrophils, epithelial and endothelial cells, mast cells are also able to detect pathogens through Toll-like receptors (TLRs) which recognise pathogen associated molecular patterns (PAMPs)(Trinchieri and Sher, 2007). In addition, mast cells contain a number of other non-toll like receptors which are able to recognise features specific to certain pathogens, for example CD48 is able to recognise fimbriated *E. coli* (Malaviya et al., 1999). Furthermore, mast cells also express a number of Fc receptors which enable them to bind to antibodies directed against pathogens. This allows mast cell activation with exquisite specificity against a limitless amount of pathogens to which the host has previously been exposed (Kawakami and Galli, 2002). Moreover, Fc receptors have the added effect of enabling activation towards bacterial “super antigens” which are able to bind to various antibody subclasses indiscriminately thus causing Fc receptor crosslinking and degranulation (Genovese et al., 2000). Interestingly, mast cells can also be activated by substances such as snake and bee venom (Metz et al., 2006). Mast cells are not only activated by external pathogen related sources but can also be activated by endogenous signalling molecules. These include complement components signalling through the C5a receptor, Endothelin-I, substance P, neurotensin, SCF and of course

cytokines (Kulka et al., 2008; Nilsson et al., 1996) (for a comprehensive list of receptors and the signalling molecules by which and receptors see table 2 in (Galli et al., 2005))

1.2.2.2 Signalling

Like other immune cells, mast cells are able to produce a multitude of cytokines, chemokines and growth factors which affect cells in the surrounding area (Table 1.2). Unlike many immune cells, mast cells contain these mediators within granules in their cytoplasm. The ability to immediately release these preformed mediators instead of synthesising molecules upon stimulation, allows a more rapid response to stimulus. The granules are predominantly insoluble structures within the cytoplasm, a proportion of which, once released, will become soluble allowing for signalling within the immediate area. However, thanks to interaction of positively charged proteins with negatively charged carbohydrate molecules, the majority of the granular content will remain in an insoluble form (Metcalfe et al., 1997; Schwartz et al., 1981). Kunder *et al.* (2009) have demonstrated that when TNFα is parcelled in these insoluble heparin containing particles, it is protected from degradation and dilution and is therefore able to signal over long distances to draining lymph nodes (resulting in hypertrophy). This demonstrates the ability of mast cells to signal over large distances using the circulatory system, analogous to the endocrine system but using a smaller amount of signalling molecule.

As previously mentioned, in addition to the release of preformed mediators upon stimulation, mast cells also synthesise molecules *de novo*. These come in the form of lipid based mediators which can be produced rapidly and cytokines and chemokines which have a more delayed production. The lipid mediators are collectively known as eicosanoids and the two subfamilies produced in mast cells are called prostaglandins and leukotrienes (Beaven, 2009). The speed by which they are produced is a result of them being synthesised from arachidonic acid which can be cleaved from the phospholipid bilayer by phospholipase A_2. Arachidonic acid then follows two pathways initiated by the either cyclooxygenase in the case of the prostaglandins or lipoxygenase for leukotrienes. These mediators cause increased vascular permeability and lead to bronchoconstriction in the lungs and “wheal and flare” reactions in the skin (Beaven, 2009)

MHC class I is expressed on the surface of all mast cell subclasses and It has been shown that following enterobacteria phagocytosis, mast cells are able to present processed antigen to T cells (Malaviya et al., 1996). Interaction in this manner was more recently shown to activate and induce proliferation of CD8+ cytotoxic T cells (Stelekati et al., 2009). The case for mast cell involvement in MHC class II signalling is less clear because resting mast cells often show low or no expression of MHC class II; however in several groups its expression is drastically increased

following LPS of IFN-γ exposure (Henz et al., 2001). On the other hand, mast cells isolated from sites of inflammation caused by various diseases were shown not to express MHC class II suggesting a requirement for specific activation and/or maturation (Henz et al., 2001; Lipski et al., 1996). Mast cells are able to attract T cells, for example through secretion of lymphotactin a chemokine with restricted CD8+ specificity and they have also been shown to migrate to the lymph nodes after induced hypersensitivity, demonstrating that they can influence T-cell distally as well as locally (Henz et al., 2001; Wang et al., 1998).

Class	Mediators	Physiological effect
Cytokines	TNF-α, TGF-β, IFN-α, IFN-β, IFN-γ, IL-1α, IL-1β, IL-2, IL-4, IL-5, IL-10, IL-12, IL-6, IL-13, IL-16, IL-17, IL-18	Inflammation, leukocyte migration/proliferation
Chemokines	IL-8 (CXCL8), I-309 (CCL1), MCP-1 (CCL2), MIP-1αS (CCL3), MIP1β (CCL4), MCP-3 (CCL7), RANTES (CCL5), eotaxin (CCL11), MCAF (MCP-1)	Chemoattraction and tissue infiltration of leukocytes
Growth factors	SCF, M-CSF, GM-CSF, bFGF, VEGF, NGF, PDGF	Growth of various cell types, vasodilation, neovascularization, angiogenesis

Table 1.2 Cytokines, chemokines and growth factors produced by mast cells, list is not exhaustive and some produced in vitro may not be found in vivo. Adapted from "Mast cells and mastocytosis" (Metcalfe, 2008) with additions from "Targetting mast cells in inflamtory disease" (Reber and Frossard, 2014).

Mast cells are adaptive and able to alter their mediator production based on the pathogens that they encounter and signals they receive; furthermore, they are also able to alter the extent of their response. For instance when encountering LPS through TLR-4 they produce IL-4 but will not degranulate, but when stimulated by peptidoglycan through TLR-2 they will both produce IL-4 and degranulate (Supajatura et al., 2002). They not only alter their mediator synthesis but can also change the components they store within granules and because they are able to replenish these granules following infection, this has been considered as a type of immunological memory which allows a more specific response in subsequent infection (Abraham and St John, 2010; Toru et al., 1998). Even the protease content of granules is not a predetermined factor and can be altered based on their surrounding environment for instance IL-10 is able to stimulate the production of the mouse mast cell serine protease MMCP-2 (Ghildyal et al., 1992).

1.2.2.3 Mast cell as effectors

One of the most prominent effects of mast cell activation is inflammation. Oftentimes this is viewed in the unfavourable context of allergy, for instance during anaphylaxis or asthma; however this process is also crucial to the recruitment of immune cells to sites of infection. The first inflammatory mediator to be identified was histamine, a small amine which is produced from decarboxylation of the amino acid L-histidine. It acts through G protein-coupled receptors H1R-H4R on target cells resulting in increased vascular permeability and smooth muscle contraction (O'Mahony et al., 2011). Although histamine is perhaps the most studied contributor to mast cell induced inflammation, it is just one of a number of inflammatory mediators including several cytokines and leukotrienes.

Several proteases have also been shown to modulate inflammation, for instance through degradation of extracellular matrix components (Caughey, 2007). The proteases are stored within the acidic granules in an inactive form complexed with proteoglycans, and once released can act on a variety of substrates. They not only contribute to inflammation but can also degrade potentially harmful endogenous signalling molecules attributing them a protective role in certain instances. For example, in mouse sepsis models, expression of the peptidase neurolysin leads to decrease mortality though reduction of neurotensin levels (which is known to promote hypertension during sepsis) (Piliponsky et al., 2008). Endothelein-1 (ET-1) is similarly harmful during sepsis and mast cells have been show to produce, detect and, following activation, reduce ET-1 levels and associated pathology suggesting a homeostatic role for mast cells. Protease activity is not limited to endogenous products as in contrast to the commonly held misbelieve that mast cells contribute to snake and bee venom

mortality, it has now been shown that they actually reduce pathology though production of proteases which breakdown these harmful toxins (Metz et al., 2006)

In addition to microbial killing via phagocytosis, mast cells also constitutively express antimicrobial peptides (AMPs) called cathelicidins (Abraham and Malaviya, 1997; Di Nardo et al., 2003). These small amphipathic α-helical molecules induce microbial killing through intercalation into the membrane. AMPs effect many pathogens including bacteria, fungi enveloped viruses and protozoa and AMP deficient mast cells demonstrated significantly reduced ability to kill streptococci (Di Nardo et al., 2008)

1.2.4 Mast cells in disease

The term anaphylaxis was first coined in 1901 by Paul Portier and Charles Richet when they observed that injecting dogs with *Physalia* tentacle extract for a second time killed them, despite the same dose not doing so in an initial injection. This was counter to the idea at the time that exposure led to protection, and although the mechanism of how it happened was unknown it was deemed anaphylaxis (ana= against, phylaxis = protection) (Blank et al., 2013). Subsequent studies showed that repeat injection of serum led to serum sickness and transferring the serum of someone who suffered from allergy also led to sensitivity in the recipient (Blank et al., 2013). We now know that the transferred serum factor which was responsible for sensitisation is IgE; moreover, this class of allergy is now called type I hypersensitivity and is one of four different classes of allergy proposed by Robin Coombs and Philip Gell in 1963 (Rajan, 2003). Type II hypersensitivity is a result of complement activation initiated through IgG or IgM binding to the cell surface. Type III hypersensitivity occurs when antibodies bind to soluble target antigens in the blood and are deposited on the basement membrane leading to tissue damage. Finally type IV (also known as delayed type) hypersensitivity is not mediated by antibodies but instead by T cells, both through recruitment of macrophages by CD4+ T cells and cell killing by CD8+ T cells (Rajan, 2003).

In 1911 it was observed that histamine was able to cause smooth muscle contraction analogous to anaphylaxis, and years later it was shown that mast cells contained histamine, thus an initial link between mast cells and hypersensitivity was established (Riley and West, 1953). Later work (following the identification of IgE) by Ishizaka *et al.,* identified IgE binding sites on mast cells and showed that IgE could cause histamine release, therefore linking both mast cells and IgE to Type I hypersensitivity (Ishizaka et al., 1967, 1970)

1.2.4.1 IgE receptor signalling

Despite current knowledge of mast cells beneficial roles, much of the work on them still focuses on their involvement in allergy specifically as the main effector cells in Type-1 hypersensitivity. Also known as immediate type hypersensitivity (due to the quick appearance of symptoms), this form of allergy is now known to be instigated by IgE antibodies produced towards an otherwise innocuous multivalent antigen. These antibodies bind to the high affinity IgE receptor (FcεRI) on mast cells and upon subsequent antigen exposure they are cross linked and a signalling pathway is initiated which leads to degranulation and synthesis and release of various mediators (Roberts et al., 1979). Although the focus of this section will be IgE mediated degranulation, there are a number of other pathways by which degranulation can take place. For example, in response to pathogen associated molecular pattern (PAMP) activation of toll like receptors (TLRs), Complement components binding to their respective receptors, stem cell factor binding to c-KIT, and even specific venoms have been shown to stimulate degranulation (Reber and Frossard, 2014)

The high affinity IgE receptor (FcεRI) is a member of the multichain immune recognition receptor (MIRR) protein family. The receptor is made up of four subunits, one IgE binding α domain, a single β domain involved in signal amplification and two di-sulphide linked γ domains where the signalling initiates (Garman et al., 1998; Lin et al., 1996). High-affinity binding of IgE takes place through two Ig-like domains in the extracellular region of the α subunit, which was shown to be essential in mast cell activation in mice (Dombrowicz et al., 1993). Interestingly, binding of IgE to FcεRI is no longer solely thought as a sensitisation step before degranulation, since monomeric binding of IgE has been shown in itself to promote mast cell survival (Asai et al., 2001; Kalesnikoff et al., 2001). β and γ subunits both contain immunoreceptor tyrosine-based activating motifs (ITAMs) within the cytoplasmic tails; however FcεRI lacks intrinsic kinase activity so initial activation require phosphorylation by one of a number kinases belonging to the Src tyrosine kinase family. Downstream signalling is complex, involving multiple pathways which are usually defined by the separate Src proteins which are used to initiate them (Figure 1.3). Although each pathway is distinct in terms of its signal transduction, each of the Src proteins are simultaneously activated by the receptor leading to large protein complexes called signalosomes which are primarily made up of adaptor proteins and kinases (Draber et al., 2012). In the primary pathway (Figure1.3a), upon activation of the receptor, the constitutively associated protein Lyn (a member of the SRC family) phosphorylates intracellular ITAM motifs on γ and β subunits (Pribluda et al., 1994). Signalling molecules which contain SH_2 domains are then recruited, including the kinase Syk (another member of the Src family). The adaptor proteins LAT is one of several Syk targets and

once phosphorylated it recruits a number of cytosolic adapter proteins, GTP exchangers and signalling enzymes which results in the formation of the aforementioned signalasome. One such signalling enzyme PLCγ, cleaves PIP_2, yielding inositol trisphosphate (IP3) and diacylglycerol (DAG). These lead to activation of protein kinase C (PKC) and an increase in intracellular calcium levels which are both required for mast cell degranulation and eicosanoid formation (reviewed in (Metcalfe et al., 2009)). The discovery that Lyn deficient mast cells were able to degranulate to a normal extent (Nishizumi and Yamamoto, 1997) led to the identification of a second pathway (Figure 1.3b) which functions though an alternate Src Kinase Fyn and the adaptor protein GAB-2 (Parravicini et al., 2002). These activate PI3K which in turn activates Akt leading to the phosphorylation of PIP_2. This enabling recruitment of Btk and PLCγ which can function as previously mentioned (Sibilano et al., 2014). More recently a third pathway has also been identified (Figure 1.3c) which utilises the Src proteins Fgr and Hck. Although this is less well characterised, it is known that Fgr and Hck are positive regulators of degranulation and cytokine production (Hong et al., 2007; Lee et al., 2011). Down regulation of degranulation signals is important for fine tuning and prevention aberrant activation and as such there are a number of negative regulators include SHIP1 and SHIP 2 (Src homologue containing inositol phosphatase), PKCδ, allergin-1 and RabGEF-1 (Reber and Frossard, 2014).

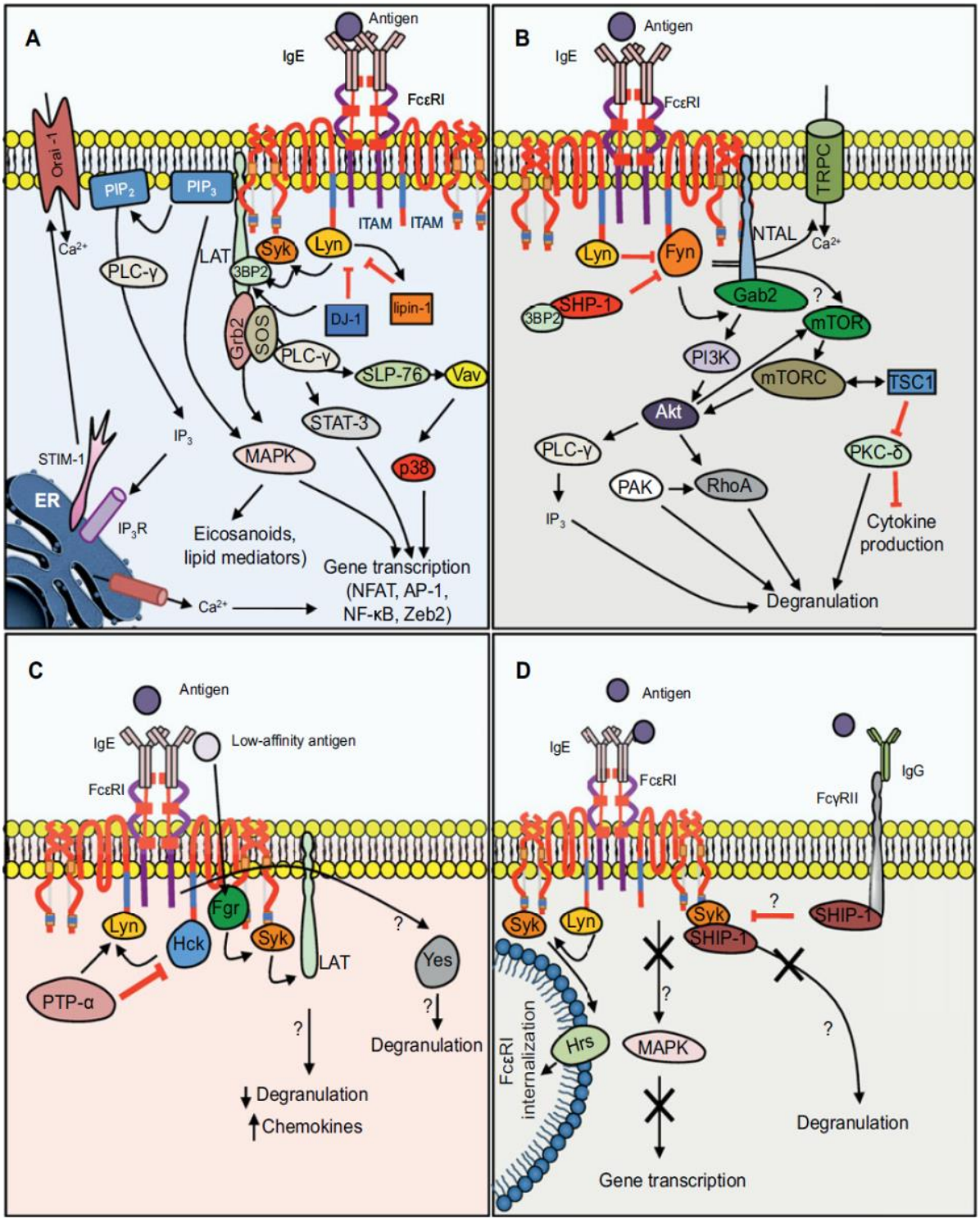

Figure 1.4 Pathways involved in IgE mediated degranulation. (A, B, C) show early steps in mast cell activation pathway following FcεRI crosslinking by antigen. Each panel represents initiration by a differing Src Kinase family member **(D)** molecular pathway of mast cell desensitisation arrows indicate positive signals and red bars show inhibitory signals. Activation pathways are split based on the Src kinase which initiates signalling (either Lyn in (A) Fyn in (B) or Fgr in (C)) taken from from (Sibilano et al., 2014).

1.2.5 Tetraspanins and mast cells

Tetraspanin expression on mast cells and basophils and their involvement in said cells activation is as yet not fully understood. However, a number of studies have shown an association of various tetraspanin family members with Fc receptors (including FcεRI) or have described a functional involvement of tetraspanins in degranulation. CD9, CD63 and CD81 have all been functionally associated with degranulation, CD151 on the other hand has been shown to be expressed on a number of mast cell subtypes but to date its only functional effect has been on cytokine production (Table 1.2.). Here, some of the previous studies of tetraspanins in mast cells will be discussed along with the proposed means in which they are involved.

Tspan	Splice variants	Binding partners	Link to mast cell function
CD9	13	CD9P-1/EWI-F/FPRP EWI-2/PGRL EpCAM Pro-HB-EGF ICAM-1 Claudin-1	Interacts with FcγRII in plate lets (Huang et al., 1992) Antibodies towards human CD9 were able to inhibit degranulation in (Higginbottom et al., 2000a) Co-localises with FcγRI in dendritic cells (Peng et al., 2011) Cross-linking of CD9 during activation increases degranulation (Peng et al., 2011) Possible alternative IL-16 receptor (Yadav et al., 2010)
CD63	16	H+/K+-ATPase	Anti-CD63 antibodies inhibited mast cell degranulation (Kitani et al., 1991) CD63 knockout BMCCs display inhibited degranulation (Kraft et al., 2005) Anti-CD63 antibody inhibited degranulation in rats Antibodies towards a CD63 granular variant inhibit degranulation after a first activation (Schäfer et al., 2010)
CD81	18	CD19 Integrin α4β1 CD9P-1/EWI-F/FPRP EWI-2/PGRL Claudin-1	Anti-CD81 antibodies inhibited RBL cell degranulation Anti-CD81 antibodies reduced passive cutaneous anaphylaxis in rats (Fleming et al., 1997)
CD151	21	Integrin α3β1 Integrin α6β1 Integrin α6β4 Integrin αIIbβ3 VCAM-1 MT1-MMP	CD151 deficient mast cells give a different cytokine profile after activation (Abdala-Valencia et al., 2015)

Table 1.3 Tetraspanin involvement in degranulation and mast cell function. Binding partners taken from (Charrin et al., 2009), number of splice variants from www.ensembl.org.

1.2.5.1 CD9

CD9 is expressed on a number of mast cell subtypes and basophils and was shown to interact with FcγRII in platelets and FcεRI in monocytes (Peng et al., 2011; Qi et al., 1996). RBL-2H3 cells transfected with human CD9 were used to investigate its involvement in IgE mediated degranulation. In said study, three out of four mAbs towards human CD9 were able to stimulate degranulation (Higginbottom et al., 2000a). Upon further investigation it was found that $F(ab')_2$ fragments alone could not induce this effect and required the addition of an anti-F(ab') antibody to restored this function. This led the authors to suggest CD9 cross linking was not sufficient to stimulate degranulation and required Fc receptor interaction. Indeed, this degranulation was later inhibited via co-incubation with monomeric IgE (and not IgG_1) which indicated an involvement of the high-affinity IgE receptor; this was also corroborated via co-immunoprecipitation. Subsequently two models were suggested for CD9 involvement; in the first, CD9 monomers are brought together in complex with FcεRI resulting in its activation. In the second, dimers or multimers of CD9 are connected by antibody binding and FcεRI receptors are "enmeshed" by involvement through their Fc receptor domains with degranulation resulting from FcεRI immobilisation. More recently Peng *et al.* (2011) observed a relationship between expression patterns of CD9, CD81 and FcεRI on monocytes, which prompted them to evaluate a possible molecular association. Using both immunoprecipitation and fluorescence microscopy they were able to show an association of both tetraspanins and FcεRI. Further experiments by the same group also showed that CD9 antibodies were able to unregulated IL-10 production following FcεRI crosslinking.

CD9 has also been implicated in other forms of mast cell signalling, specifically as an alternate IL-16 receptor. Mast cells respond to IL-16; however some subtypes do not express the primary IL-16 receptor CD4. The suggestion of CD9 as an alternate receptor arose from observations that anti-CD9 antibodies were able to inhibit the chemotactic response to, and BMMC activation by, IL-16 (Qi et al., 2006). More recently, however, this observation has been questioned due to the inability of anti-CD9 antibodies to alter the cytotoxic effects of IL-16 on $CD4^-$ A549 cells and the suggestion that its capacity to modulate the chemotactic effect is in fact an artefact (Yadav et al., 2010)

1.2.5.2 CD63

One of the first studies to associate tetraspanins with FcεRI showed that high concentration of a mAb towards (the then unidentified) CD63 was able to inhibit degranulation in RBL-2H3 cells (Kitani et al., 1991). It was shown that the inhibition was not due to impeding IgE binding to its receptor; however antibodies directed towards FcεRI could stop anti-CD63 binding, indicating

a close proximity to FcεRI. Later work has shown CD63 also localised to a number of secretory granules in a range of different cells and has subsequently been used as an activation marker for basophils and mast cells (Knol et al., 1991; Nishikata et al., 1992). Work by Smith *et al.* (1995) used human CD63 transfected RBL-2H3 cells to investigated human CD63 (hCD63) involvement in degranulation. In these experiments a number of antibodies directed towards hCD63 were able to induce degranulation without further stimulus. Furthermore, one antibody was able to partially inhibit degranulation caused by IgE crosslinking. The differing responses to various anti-CD63 mAbs indicated that crosslinking is not sufficient to induce activation and the authors suggest mAbs are acting in place of a natural hCD63 ligand. However, later work by the same group suggests that the results may be at least partly explained by interaction of the anti-CD63 antibodies with FcεRI as described above (Higginbottom et al., 2000a).

More recent work by Kraft *et al.* (2005) also used an anti-CD63 monoclonal antibody to further examine the role of CD63 in degranulation. In this study the mAb was again able to inhibit IgE mediated RBL-2H3 degranulation, however it was shown to only affect adherent cells. Tyrosine phosphorylation and calcium mobilisation (early stages in the IgE primary activation pathway) were not affected by the mAb however it did exhibit a capacity to reduce adhesion to fibronectin and vitronectin. These results led to the suggestion that CD63 was acting through a common pathway which is able to modulate both adhesion and degranulation. CD63's known interaction with α chain of β1 integrins (which bind to the aforementioned ECM components) revealed a possible mechanism, and further analysis led to the identification of changes within the PI3K, GAB-2 degranulation pathway. The authors concluded with three possible mechanisms. Firstly, anti-CD63 could sterically hinder integrin binding to ECM thus stopping positive degranulation signals. Secondly, a similar reduction in positive degranulation signals could result from general disruption of CD63 containing complexes which uncouple integrins and signalling partners. Finally, anti-CD63 could be sequestering CD63 along with associated signalling molecules. More recently work by Kraft *et al.* (2013) favoured the latter hypothesis and suggested that the treatment may have been affecting endocytosis (being as CD63 is predominantly found on intracellular membranes). They also showed that mast cells from CD63 knockout mice exhibited significantly reduced degranulation, and indicated a possible link between CD63 and t-SNARE activity (a protein required for membrane fusion)(Südhof and Rothman, 2009). Interestingly, being as BMMC grow in suspension, in this instance the reduction in degranulation was not reliant on the cells being adhered to a surface which was suggested to be a "particularity" of the RBL-2H3 cells originally used.

Schafer *et al.* (Schäfer et al., 2010) demonstrated the existence a distinct variant of CD63 expressed on intracellular granules of cord blood human mast cells (CBHMCs). This variant is distinct from the surface expressed CD63, it is thought to be a different glycoform resulting from an alternative synthesis pathway or due to a different environment. Single amino acid mutation identified specific variation at residues C170 and N172. A mAb which bound only to the so called "granular variant" of CD63 was not only shown to be a useful as a marker of degranulation, but was also able to inhibit subsequent rounds of degranulation. The authors indicate a potential therapeutic application in which primary mast cell degranulation can function as normal but repeat degranulation is impeded.

1.2.5.3 CD81

Similarly to CD63, a mAb towards CD81 has also been shown to inhibit IgE mediated degranulation in RBL cells (Fleming et al., 1997). This antibody did not affect calcium mobilization or tyrosine phosphorylation either and was shown to affect degranulation *in vivo* also. The authors did not speculate as to a possible mode of action, however a similar modulation of mast cell signalling was shown in $CD81^{-/-}$ mice which exhibited reduced allergen induced airway hyperactivity (Deng et al., 2000). Köberle *et al.* (2012) suggest that these phenotypes may result from disruption of CD81-FcεRI interactions which regulates signaling.

1.2.5.4 CD151

Although evidence for CD151 involvement in degranulation is limited, in a recent study BMMCs from CD151 knockout mice displayed increased expression of pro-inflammatory cytokines following FcεRI stimulation. Although no affect was seen on FcεRI mediated degranulation in these cells, the authors suggest a negative regulatory role for CD151 in FcεRI mediated cytokine production (Abdala-Valencia et al., 2015)

1.3 Hosts for recombinant protein expression

Recombinant proteins are those which are produced from recombinant DNA technology, for instance molecular cloning, which brings together DNA which would not conventionally be found (in most instances a coding gene and a vector). Since its discovery in the 1970s the field of recombinant protein production has developed vastly both in terms of large scale production of therapeutics and industrial enzymes and in small scale protein production which is common practice in many research laboratories (Demain and Vaishnav, 2009). Recombinant protein production still follows the common pathway of generation of an expression construct, introduction into the desired host, expression and downstream processing, but improved understanding of genetics and protein production has seen refinement and variation in each area to suit the needs of the user. Variables are primarily altered based on the desired properties of the final protein product, but one must also consider the ease of use, cost and time associated with the different systems. One of the primary considerations which must be made is the choice of host for expression, as each one has its own benefits and downsides (Wurm, 2004)

1.3.1 Bacteria

The Gram-negative bacteria *Escherichia coli* was the one of the first, and is still one of the most used, host for recombinant protein expression; this stems from its ease of use, quick growth and high yields (Terpe, 2006). Furthermore, its long standing use in research has led to excellent genetic characterisation thus enabling easy manipulation (Baneyx, 1999). Many strains of *E. coli* are available commercially, which are tailored for different requirements through the inclusion or deletion of different genetic elements. To name just a few; the frequently used stain BL21 is deficient in certain cellular proteases thus reducing breakdown of the desired product, Rosetta contain tRNA for codons which are rarely seen in *E. coli* facilitating the expression of proteins from other organisms and Origami cells have mutated reductases, resulting in an oxidising environment in the cytoplasm which is beneficial for disulphide bond formation (Demain and Vaishnav, 2009).

Although *E. coli* is a common first choice for protein expression, other bacterial species have proven useful for different applications. Perhaps the most used (after *E. coli*) are the Gram-positive class of bacterial *Bacillus.* These do not contain LPS within the cell wall therefore resultant product will not contain endotoxin contamination and *Bacillus* are thus favoured for the production of food stuffs (Westers et al., 2004). Moreover, they naturally have high efficiency of secretion and transport many enzymes to the growth media which enables easier downstream purification (Westers et al., 2004). Traditionally, high levels of protease secretion

into surrounding growth media meant certain *Bacilli* species were not amenable to recombinant protein expression but mutant stains are now available which show drastically reduced protease activity (Wu et al., 1991).

Recombinant proteins are frequently expressed into *E. coli* cytoplasm due to the potentially higher yields (Terpe, 2006); however it is also possible for expressed proteins to be transported to the periplasmic space or secreted into the growth media. Expression into the periplasm is often favoured for proteins which contain disulphide bonds because it (a) removes them from the reducing environment of the cytoplasm which is detrimental to disulphide bond formation and (b) contains disulphide bond isomerase chaperones such as DsbA which aid in disulphide formation (Joly and Swartz, 1994). Expression into the periplasm or growth media also offers the advantage of simplified downstream purification due to there being fewer unwanted proteins here than the cytoplasm (the expressed protein can be released from the periplasm by osmotic shock or permiabilisation of the cell wall). Additionally, fewer proteases in the periplasm or growth media means there is less chance of unwanted proteolysis of the protein product (Shokri et al., 2003). Transport to the periplasm or indeed secretion from the cell is achieved through inclusion of a leader sequence at the proteins N-terminus. There are multiple secretions sequences to select from, with the choice often determined on a trial and error basis (Choi and Lee, 2004). Once synthesised in the cytoplasm, proteins commonly enter the periplasm in an unfolded state through the Sec pathway before being exported through a type II secretion system (if applicable) with the leader sequence being cleaved by membrane bound proteases once the protein has been successfully translocated (Choi and Lee, 2004). Consideration must be given to the ability of the cells to translocate the protein as this must be equal to, or greater than, their capacity to produce said proteins or it may retained within the cytoplasm where they will likely form inclusion bodies (Choi and Lee, 2004).

Inclusion bodies are intracellular insoluble protein aggregates formed from unfolded or partially folded proteins. These are often viewed as an unwanted consequence of heterologous protein overexpression, arising due to insufficient amounts of chaperones, thus allowing hydrophobic surfaces of proteins to form intermolecular associations before the proteins can fold correctly (Carrió and Villaverde, 2002; Terpe, 2003). Co-expression of chaperones has been shown to help in the folding of over- expressed protein (Levy et al., 2001), However, inclusion bodies are not always undesirable because it is possible to recover soluble, functional protein from these insoluble aggregates (Buchner and Rudolph, 1991). The aggregates must first be solubilised (usually using a strong denaturing agents) and reduced

before the proteins are refolded (Demain and Vaishnav, 2009); however this is a timely process and on average refolding is only 10%-50% efficient (Carrió and Villaverde, 2002)

Despite the advantages discussed, there are a number of drawbacks to the use of a bacteria host for expression. Firstly, most bacterial species are unable to glycosylate their proteins and although this is not always required, it can mean that the resultant proteins behave differently than their glycosylated counterparts (Demain and Vaishnav, 2009). For instance, they may exhibit reduced half-life or solubility and may not display full biological activity. Furthermore, antibodies raised against a non-glycosylated recombinant protein may not recognise the native mammalian protein (Jenkins and Curling, 1994). Proteins produced In Gram-negative bacteria also contain endotoxin contamination meaning they cannot be used for therapeutic application and are unsuitable for many research-based applications where LPS may elicit a response (unless the LPS is removed during downstream purification) (Terpe, 2006). Finally bacteria are not equipped to cope with the folding of larger proteins >100 kDa with more complex folding patterns often resulting in their aggregation (Demain and Vaishnav, 2009)

1.3.2 Mammalian cell lines

The first protein to be produced from recombinant mammalian cells was human tissue plasminogen activator in 1986, an enzymes which breaks down blood clots and is thus used to treat stroke patients (Kim et al., 2012). Since then, mammalian cells have become the principle host for production of therapeutic agents. Although there are many different cell types available for the production of recombinant proteins, as of 2007, 70% of therapeutics produced in mammalian cells were produced in Chinese hamster ovary (CHO) cells (Jayapal et al., 2007). This is in part because past products have shown that CHO cells are safe for therapeutic production, making approval from regulatory agencies easier to attain. Additionally, they produce proteins with glycosylation patterns which make them active in humans, and systems have been developed which enable high specific productivity from these cells (Kim et al., 2012). HEK-293 cells are often used in research laboratories because they are readily transfected by a number of means and can be easily adapted to serum-free suspension growth. COS-1 cells are also frequently utilised, however this cell line is predominantly used for transient expression because they express the SV40 large T-antigen which enables vector replication through the SV40 origin of replication leading to increase in gene copy number and higher expression (Dalton and Barton, 2014).

DNA is usually introduced into mammalian cells by non-viral means, for instance using lipofectamine, electroporation, calcium phosphate or a polymer based method, and the DNA is normally integrated into the host genome through non-homologous recombination (Finn et

al., 1989). The site of integration is often random and can impact on protein expression levels (position effect variegation), for instance if the gene integrates in euchromatin then it should be expressed, whilst integration into heterochromatin can result in little to no expression (Wurm, 2004). Several methods have been developed to stop these effects such as blocking histone deacetylation (which promotes euchromatin formation) (Gorman et al., 1983) and including flanking regions in the DNA which stop the effects of the chromatin structure (Zahn-Zabal et al., 2001). A more recent development is the use of a specific recombinase enzyme such as the phage protein Cre or yeast derived Flp recombinase. These enzymes catalyse recombination at pre-defined sites leading to integration at a transcriptionally active location (Wurm, 2004). Transient gene expression can also be utilised, in which the gene is expressed from an extrachromosomal plasmid; this offers the advantages of quicker time from transfections to purified protein but it requires a far greater amount of both transfection reagent and recombinant DNA which may be prohibitively expensive (Dalton and Barton, 2014)

Proteins which are produced in mammalian cells are usually correctly folded with glycosylation patterns which are most like those found *in vivo*. Additionally, proteins produced in mammalian cells have relatively homogenous glycosylation patterns and once a stable cell lines has been established it can be stored indefinitely in liquid nitrogen (Dalton and Barton, 2014). However, cell culture is expensive due to the high price of media and disposable plastic ware and specialist facilities are required for mammalian cell culture. Moreover the time commitment for mammalian expression is far greater than for prokaryotic expression (weeks to months to establish a stable cell line).

1.3.3 Other hosts

Insect cells can carry out post-translational modification and are well equipped for producing proteins with complex folding patterns (Britain et al., 1991). The most commonly used insect cells are Sf9 cells, originating from the fall army worm *Spodoptera frugiperda.* These cells grow in suspension culture which enables high cell densities to be achieved along with easy scale-up of production. Insect cells are commonly transfected using baculovirus DNA vectors with the gene of interest under the control of the polyhedron promoter. This strong promoter enables high expression of the desired protein during the very late phase of the viral lifecycle (Altmann et al., 1999). The main advantage of insect cells is their ability to cope with proteins containing complex folding patterns and di-sulphide bonds, and their capacity to post translationally modify their expressed proteins. However, as with each expression system, insect cells also have a number of shortcomings. For instance, the lytic lifestyle of the baculovirus means that

cellular contents are released during expression, this can comprise protease enzymes resulting in degradation of the desired proteins. Furthermore, baculovirus infection leads to the inevitable death of the host cells meaning cells must be re-infected for subsequent round of expression (and viral stocks cannot be stored indefinitely) (Dalton and Barton, 2014). One of the foremost problems with insect cells is the manner in which they glycosylate their proteins. They often utilise N-glycans which are less complex than those found in mammalian cells and proteins can be underglycosylated also (Altmann et al., 1999; Demain and Vaishnav, 2009). Due to the high culture cost of insect cells they frequently overlooked in favour of mammalian expression which can produce higher protein yields at a similar cost with the added benefit of being able to produce more complex glycosylation patterns (Dalton and Barton, 2014).

The single celled eukaryotes yeast (usually in the form of *S. cerevisiae* or *P. pastoris*) offer similar advantages to *E. coli*, they too give high protein yields, grow rapidly and are cost effective due to inexpensive media and reusable glass culture vessels (Dalton and Barton, 2014). However, in contrast to *E. coli*, yeast are able to cope with proteins containing disulphide bonds and more complex folding patterns and are also able to glycosylate the proteins they produce (Demain and Vaishnav, 2009). However, glycosylation patterns produced by yeast vary significantly to those found in mammalian host. For instance, through inclusion of high-mannose sugar moieties and over glycosylation of N-glycosylation sites the produced protein can exhibit reduced activity and half-life (Wildt and Gerngross, 2005). Furthermore, yeast express a number of extracellular and cell bound proteases which can degrade or truncate the produced proteins (Macauley-Patrick et al., 2005).

Although not readily applicable for production of recombinant protein for many research groups, transgenic animals have been used to produce large amounts of recombinant proteins for industrial and therapeutic applications. Proteins are normally expressed into the milk of the transgenic animal because of the large volumes produced and easy collection methods. “Biofarming” has the potential to produce large amounts of proteins (100s of Kgs) at low production costs; however, it does come with a number of issues. The length of time required in order to assess protein production in transgenic animals can be extremely long, ranging from 3.5 months to 32 months depending on the organism used (Demain and Vaishnav, 2009), with high prices of keeping animals this can represent a large financial investment. Moreover, the likelihood of successful protein production following this lengthy initial phase is low and there is a possibility of animal viruses and prions contaminating the final protein products (Larrick and Thomas, 2001). Transgenic plants have similarly been used and have some distinct benefits over the other hosts. For instance, they are able to produce oligomeric proteins such as antibodies whilst microbes cannot, and large scale production of proteins in plants is

suggested to be far more cost effective than when using large microbial or mammalian bioreactors. Unlike transgenic animals, plant products do not contain human pathogens such as viruses and prions. Plants are able to carry out post translational modifications, however inclusion of noval glycan structure and production of many different protein glycoforms means the resultant protein may not have use therapeutically (Larrick and Thomas, 2001).

Expression System	Advantages	Disadvantages
Bacterial	• Rapid expression • High yields • Inexpensive • Cost effective	• Proteins containing disulphide bonds are difficult to express • Proteins are not glycosylated • Protein preparations contain endotoxins • Proteins can be expressed in inactive inclusion bodies
Yeast	• High yield • Cost effective • Can produce isotope labelled proteins • Fast growth • Can produce disulphide containing proteins • Can express glycosylated proteins	• Proteases may break down expressed proteins • Glycosylate proteins with high mannose sugars
Insect cells	• Post translationally modify their proteins • Easy scale up of production • Safe to work with	• Unusual glycosylation patterns with many protein being over glycosylated • Unable keep cryogenic stocks
Mammalian cells	• Post translationally modify proteins • Most like in vivo protein when expression mammalian targets	• Expensive • Specialist facilities required •
Plants	• Cost effective • Can accumulate protein in plant tissue • Wont contain animal pathogens • Post translationally modify their proteins	• Unusual glycosylation patterns • Can express complex oligomeric proteins
Transgenic animals	• Cost effective for large scale protein production	• May contain pathogens • Low chance of selecting stable cell lines • Large time and money investment

Table 1.4 Summary of advantages and disadvantages of expression systems. (Demain and Vaishnav, 2009)

1.4 Project aims

As discussed throughout section 1.1.3, tetraspanin EC2 domains have proven useful in dissecting the roles of various tetraspanins in a range of different processes. Our group has traditionally used these recombinant domains in the form of GST fusion proteins produced in *E. coli.* Unfortunately, proteins made in such a manner inherently contain bacterial contaminants which render them unusable in certain circumstances. Moreover, antibodies raised against these recombinant proteins were unable to recognise their native counterpart, which is suggested to arise because the recombinant preparations contain both folded and unfolded proteins. To address some of the issues found in recombinant protein expressed in bacteria, the initial aim of this project was to clone and express the EC2 domains using mammalian or insect cells as a host for expression. The next aim was to use the purified recombinant proteins for functional studies or for raising monoclonal antibodies that were specific to the native protein(s). As discussed in section 1.3 mammalian and insect cells are better equipped for the complex folding patterns resulting from multiple disulphide bonds and would produce products free from endotoxin contamination therefore suitable for a wider range of applications (Wakelin et al., 2006). Additionally, both mammalian and insect cells are able to glycosylate their expressed proteins, therefore the produced EC2 domains may be able to shed more light on the involvement of glycosylation in tetraspanin function. Initial efforts aimed to express three tetraspanin EC2 domains (CD9, CD151 and Tspan5) so that the increasing complexcity of the EC2 domains could provide some indication as to how well mammalian systems could cope with the folding patterns.

After efforts to produce recombinant EC2 domains in eukaryotic systems were unsuccessful, it was decided to instead focus on expression in *E. coli* which was already an established means of producing recombinant EC2 proteins. Although these bacterially expressed proteins are in limited by possible contamination and incorrect folding, they can be produced in relatively high amounts, are suitable for a number of applications, and have proven useful in a number of functional assays by our group and others (Barreiro et al., 2008; Green et al., 2011; Parthasarathy et al., 2009; Zhu et al., 2002). Four tetraspanins have been linked to mast cell degranulation (Table 1.2) however it is not clear exactly what their involvement in this process is, so in an effort to shed more light on their function the EC2 domains of CD9, CD63 CD81 and CD151 were expressed as recombinant GST fusion proteins in *E. coli*. Following initial purification and characterisation via Western blot, the expression and purification procedures for these proteins were optimised. It was hypothesised that the IgE receptor responsible for initial steps in mast cell activation may be organised by tetraspanins so the recombinant

proteins were used in conjunction with RBL-2H3 cells to determine if they were able to modulate IgE-mediated degranulation.

In initial attempts to dissect their mode of action, the binding of the recombinant tetraspanin EC2 binding to the surface of different mammalian cell types was investigated. Work was also undertaken to assess the possible effects of LPS contamination of the EC2 proteins in a cell:cell fusion assay. Finally cleavage of the GST tag from the recombinant EC2 domains was optimised prior to CD spectroscopy analysis, which was carried out to further characterise the EC2 domains in terms of their secondary structure.

Chapter 2: Materials and Methods

2.1 Materials

2.1.1 Prepared Reagents and Buffers

Reagent	Preparation
Acid ethanol (1%)	1ml HCl, 99ml ethanol
Agar plates	10g tryptone, 5g yeast extract, 10g NaCL, 15g agar made up to 1L with dH_2O
Agarose gel (1%)	1g of MetaPhor agarose (Lonza) in 100ml 1x TAE buffer, heat until dissolved
BBN	1g BSA, 0.5g sodium azide add to 500ml HBSS (with divalents)
Blocking buffer	5g milk powder, 10ml 10x TBS, 90ml dH_2O, 150µl tween 20
Blotting buffer 10x	20.23g Tris, 144g glycine made up to 1L with dH_2O
Blotting buffer 1x	100ml 10x blotting buffer, 200ml methanol, 700ml dH_20
Carbonate-bicarbonate buffer (100mM)	3.03g Na_2CO_3, 6g $NaHCO_3$ made up to 1L with dH_2O, pH adjusted to 9.6 with HCl
Citrate buffer (200mM)	5.85 citric acid, 6.47g sodium citrate
Coomassie blue stain	500ml methanol, 2.5g Coomassie Brilliant Blue R-250 (BioRad), 100ml acetic acid made up to 1L with dH_2O
Coomassie de-stain	400ml methanol, 100ml acetic acid, 500ml dH_2O
EDTA 500mM	18.6g EDTA, 90ml dH_2O, adjust pH to 7.0 with HCl, make up to 1L with dH_2O
Freezing solution	9ml FCS, 1ml DMSO
Glutathione elution buffer (25mM)	30.8mg reduced glutathione, 60.6mg Tris, made to 10ml with dH_2O pH 8.0
Glycerol 60%	12ml 100% glycerol, 6ml dH20. Sterile filtered through a 0.22µm filter
Imidazole binding buffer (10mM)	6.9g NaH_2PO_4, 17.54 g NaCl, 0.68g imidazole

	make up to 1L with dH_2O adjusted pH to 8.0 with HCl
Imidazole Elution buffer (500mM)	6.9g NaH_2PO_4, 17.54 g NaCl, 34g imidazole make up to 1L with dH_2O adjusted pH to 8.0 with HCl
LB (Lysogeny broth)	10g tryptone, 5g, yeast extract, 10g NaCl made up to 1L with dH_2O
Nitrocellulose membrane stripping buffer	15g glycine, 1g SDS, 10ml tween20, pH to 2.2 with HCl made up to 1L with dH_2O
PBST 1x	100ml 10x PBS, 900ml dH_20, 250µl tween20
Phosphate buffered saline (PBS) 10x	80g NaCL, 2g KCL, 14.4g Na_2HPO_4, 2.4g KH_2PO_4 Made up to 1L with dH_2O
Release buffer	500ml HBSS (with divalents) with 0.1%BSA (0.5g)
SDS-PAGE loading buffer (non-reducing) 4x	5ml 0.5M Tris adjust pH to 6.8 with HCl, 2ml 20%SDS, 4ml glycerol, 1ml 2mg/ml bromophenol blue
SDS-PAGE Loading buffer (reducing) 2x	5ml 0.5M Tris adjust pH to 6.8, 2ml 10% SDS, 2ml 60% Glycerol, 1ml β-mercaptoethanol, 0.5ml 2mg/ml bromophenol blue
SDS-PAGE Running buffer 10x	30g Tris, 144g glycine, 10g SDS made up to 1L with dH_2O
Separating gel (12.5%)	2.5ml H_2O, 3ml 30% acrylamide, 1.9ml 4x separating buffer, 112µl 10% APS, 5µl TEMED
Separating gel buffer (4x)	18.7g Tris base, 4ml 10% SDS, pH adjusted to 8.8 with HCl, made up to 100ml with dH_2O
Sodium bicarbonate (1M)	840mg $NaHCO_3$ dissolved in 10ml dH_2O, pH adjusted to pH 8.3 with NaOH
Sodium phosphate buffer 100mM (pH7.4)	77.4ml 1M sodium phosphate dibasic, 22.6ml sodium phosphate monobasic, made up to 1L with dH_2O
Sodium phosphate dibasic (1M)	142g Na_2HPO4 made up to 1L with dH_2O
Sodium phosphate monobasic (1M)	138g $NaH_2PO_4.H_2O$ made to 1L with dH_2O
Stacking gel (5%)	1ml H_2O, 300µl 30% acrylamide, 444µl 4x stacking buffer, 25µl 10% APS, 5µl TEMED

Stacking gel buffer (4x)	6.06g Tris, 4ml 10%SDS, pH to 6.8 with HCl, made up to 100ml with dH_2O
Sulforhodamine B 0.4%	400mg sulforhodamine B sodium salt (Sigma) dissolved in 100ml 1% acetic acid
TAE buffer 50x	242g Tris, 700ml dH_2O, 57.1ml acetic acid, 100ml 500mM EDTA (pH8) made up to 1L with dH_2O
TBST 1x	100ml 10x TBS, 900ml dH_2O, 250µl tween20
Tris 1M (pH9.0)	121.14g of Tris dissolved in 800ml dH20, adjust to 9.0 with HCl and make up to 1Litre
Tris buffered saline (TBS) 10x	24.2g Tris, 87.66g NaCl pH to 7.6 with HCl made up to 1L with dH_2O
Tris HCl	18.171g Tris dissolved in 100ml dH_2O, pH adjusted to 8.8 with NaOH
Tris unbuffered (50mM)	6.06g Tris in 1L dH_2O
B-Hexosaminidase substrate solution	Naphthol AS-BI N-acetyl-β-D-glucosaminide diluted to 50mM stock in DMSO

Table 2.1: Recipes for prepared buffers and reagents.

2.1.2 Antibodies

Antigen	Target Species	Clone	Isotype	Label	Source
GST	-	Polyclonal	IgG	HRP	Sigma
GST	-	Polyclonal	IgG	FITC	Abcam
CD9	Human	602.29	IgG1	-	Prepared in house from hyridoma (Andrews et al., 1981)
CD9	Rat	RPM7	IgG3, κ	-	BD biosciences
CD81	Mouse	EAT2	IgG1	-	AbD serotec
CD81	Human	1.3.3.22	IgG1, κ	-	Thermo fisher
CD151	Human	14A2	IgG1	-	L. Ashman, Aus
CD151	Human	11G5a	IgG1	-	Thermofisher
CD63	Human	H5C6	IgG1	-	Prepared in house from hyridoma (Azorsa et al., 1991)
CD63	Rat	AD1	IgG1	-	AbD serotec
Rat IgE	Rat	LO-ME-3	IgG1	FITC	AbD serotec
DNP	-	Polyclonal	IgE	-	Prepared in house from hyridoma (Eshhar et al., 1980)
Mouse IgG	Mouse	Polyclonal	IgG	HRP	Sigma
Mouse IgG	Mouse	Polyclonal	-	FITC	Sigma
Mouse IgE	Mouse	23G3	IgG1	-	Southern biotech
Hamster IgG	Hamster	Polyclonal	-	FITC	Abcam
Isotype IgG3	Mouse	J606	IgG3, κ	-	BD biosciences
Isotype IgG1	Mouse	JC1	IgG1	-	Prepared in house from hyridoma (Muranova et al., 2003)
Isotype Hamster	Hamster	eBio299Arm	IgG	-	Affymetrix

Table 2.2 Concentration, specificities, isotype and suppliers of various antibodies.

2.1.3 Restriction enzymes

Name	Used for
HindIII	Mammalian EC2 cloning, Flp-in/ Rat CD63 expression
AgeI	Mammalian EC2 cloning, Flp-in
NheI	Mammalian EC2 cloning, Flp-in
XbaI	Mammalian EC2 cloning, pCINEO
EcoRV	Mammalian EC2 cloning, pCINEO
BamHI	Cloning for insect cells
NotI	Cloning for insect cells
EcoRI	Rat-CD63 cloning

Table 2.3 Endonuclease restriction enzymes and their application. All restriction enzymes were purchased from Promega and used with Multi-core™ buffer where applicable.

2.1.4 Bacterial strains

E. coli Strain	Characteristics	Souce
Rosetta-gami	F– *ompT* hsdS_B(r_B–m_B–) *gal dcm lacY1 aphC* (DE3) *gor522*::Tn*10 trxB* pRARE^2 (Cam^R , Kan^R , Tet^R)	Novagen
DH5α	F^- Φ80*lac*ZΔM15 Δ(*lac*ZYA-*arg*F) U169 *rec*A1 *end*A1 *hsd*R17(r_k^-, m_k^+) *pho*A*sup* E44 *thi*-1 *gyr*A96 *rel*A1 λ^-	Life technologies

Table 2.4 Bacterial strains and their characteristics

2.1.5 Antibiotics

Carbenicillin	Stock preparation (mg/ml)	Diluted in	Working concentration (ug/ml)
Chloramphenicol	34	100% ethanol	34
Tetracycline	12.5	70% ethanol	12.5
Kanamycin	15	water	15
Carbenicillin	50	water	50
Hygromycin	50	-	1000
Zeocin	100	-	300
Geneticin (G418)	250	DMEM	300/1000
Penicillin/Streptomycin	10000 units/ 10mg/ml	Growth media	10 units/ml / 100
Amikacin	50	water	500

Table 2.5 Antibiotic stock and working concentrations.

2.1.6 Cell lines

Name	Source	Culture medium	Used for
CHO	Chinese hamster ovary (ECACC)	DMEM + 10%FCS	Expression of EC2 domains
HEK-293	Human embryonic kidney (ECACC)	DMEM + 10%FCS	Expression of EC2 domains
HEC-1B	Human endothelial carcinoma (ECACC)	EMEM + 10%FCS	Binding of EC2 domains, bacterial adhesion studies
KM3	Rat (kind gift from Peter Hersey, Newcastle Hospital, Newcastle, Australia (Moseley et al., 2003))	DMEM + 10%FCS	Positive control for tetraspanin CD9 expression
RBL-2H3	Rat basophil leukaemia (kind gift from Dr Birgit Helm, MBB, University of Sheffield)	DMEM + 10%FCS +P/S	Binding of EC2 domains, degranulation assays
SF9	*Spodoptera frugiperda* (insect cells) (ECACC)	SF900, Insect Xpress	Expression of EC2 domains
J774	Mouse macrophage (ECACC)	EMEM + 10%FCS	Giant cell formation assay

Table 2.6 Cell lines, growth media used and their application.

2.1.7 Plasmids

Plasmid name	Application	Origin
pGEX-KG	Expression of GST tag for use as negative control, cloned tetraspanin EC2 domains into	(Guan and Dixon, 1991)
pGEX-CD9	Expression of tetraspanin CD9 EC2 domain in Rosetta-gami B(DE3) cells	Previously produced by our group
pGEX-CD63	Expression of tetraspanin CD63 EC2 domain in Rosetta-gami B(DE3) cells	Previously produced by our group
pGEX-CD81	Expression of tetraspanin CD81 EC2 domain in Rosetta-gami B(DE3) cells	Previously produced by our group
pGEX-CD151	Expression of tetraspanin CD81 EC2 domain in Rosetta-gami B(DE3 cells	Previously produced by our group
pGEX-RCD63	Expression of rat tetraspanin CD63 EC2 domain in Rosetta-gami B(DE3) cells	This work
pCI-neo	Genes encoding EC2 domains of tetraspanins CD9 and CD151 cloned into this vector for expression in CHO and HEK-293 cells	Promega
pCI-neo-CD63	Used in a previous study for expression of human CD63 in HEK-293 cells	Previously produced by our group
pSecTag-link	Modified vector of the Flp-in system, use to express EC2 domains in CHO and HEK cells	Modification of pSecTag/FRT/V5-His by I. Wilkinson University of Sheffield, Medical School
pSecTag-GHstop	Template for expression of IgGκ leader sequence	I. Wilkinson, University of Sheffield, Medical School
pOG44	Expresses Flp-recombinanse, co-transfected in pSecTag to insert EC2 encoding genes into the genome	Life Technologies
pVL1393	Expression of full length tspans in insect cells	Life Technologies
pAcSec1	Expression of EC2 domains in insect cells	Allele Biotechnology
pEGFP-N2	Reporter of transfection efficiency	Clonetech

Table 2.7 Plasmids used in this work and their origin. For vector maps see appendix

2.2 Methods

2.2.1 Cell culture methods

2.2.1.1 Passage of adherent mammalian cells

Cells were routinely cultured in a humid atmosphere at 37^{o}C and 8% CO_2. Once cells became confluent they were sub-cultured for later use. To split cells in a T75 flask (Nunc), media was removed from the flask and cells were washed with 10ml HBSS without divalents (Lonza). Cells were dissociated from the flask by adding 4ml of Trypsin/EDTA (Sigma) or cell dissociation solution (Millipore) and incubating for 10 minutes. Following incubation, 6ml of DMEM containing 10%FCS (Lonza) was added and cells were removed by repeatedly pipetting up and down. Cells were transferred into a sterile falcon tube and the flask was washed again with 10ml of HBSS to remove any remaining cells which were then also added to the falcon. Cells were centrifuged at 200*g* for 5 minutes before being resuspended in the required volume of DMEM and transferred to another plate. (Penicillin/streptomycin (Sigma) was routinely added to growth media for culture of RBL cells)

2.2.1.2 Counting mammalian cells

Cell numbers for experiments were determined using an Improved Neubauer haemocytometer with a counting chamber of 0.1mm depth. If viability of the cells was required the cell suspension was mixed 1:1 with trypan blue before counting, dead cells took up the dye whilst viable cells did not.

2.2.1.3 Freezing mammalian cells

Cells were passaged at least once before being frozen. Once cells reached 90% confluence they were dissociated using trypsin, centrifuged at 400*g* for 5 minutes and resuspended in freezing solution (Table 2.1) at a cell density of $1x10^6$ per ml. 1ml of cell suspension was transferred to each cryovial, vials were transferred to a feezing plug (Jencons) and suspended in the vapour phase of a liquid nitrogen dewar to cool slowly for 90 minutes before transfer into the liquid nitrogen.

2.2.1.4 Thawing mammalian cells

Cryovials were removed from nitrogen and transferred to a water bath at 37°C until most of the frozen pellet had thawed. The 1ml of cell suspension was then transferred to 9ml of growth media and centrifuged for 5 minutes at 200*g*. After centrifugation, growth media containing freezing solution was discarded and the cell pellet was resuspended in 10ml of fresh growth media and transferred to a 10cm dish or T75 flask.

2.2.1.5 RBL cell degranulation/release assay

The amount of degranulation taking place in treated RBL cells was monitored using an enzymatic assay which produces a quantifiable colour changed based on the amount of β-hexosaminidase released by the cells (Ortega et al., 1991). RBL cells were dissociated using cell dissociation solution (CDS, Sigma) and plated at a density of $5x10^4$ per 100µl per well in a flat bottomed 96-well plate (Corning). After incubating at 37°C for one hour, 100µl of DNP-specific IgE (diluted 1 in 500 with growth media) was added to each well and cells were cultured overnight.

The following day, cells were inspected to ensure confluence, then the growth media was removed by flicking into Virkon and cells were washed twice with 50µl of HBSS with divalents (Lonza). Cells were incubated for 10 minutes in 30µl HBSS at 37°C, 8% CO_2. After incubation, 10µl antibody or recombinant protein (at 4x final concentration) or HBSS was added to the cells and they were incubated for a further hour. Cells were then stimulated to degranulate by incubating with 10µl of DNP-BSA at varying concentrations for 15 minutes. After 15 minutes, 40µl of cell supernatant was transferred to another flat-bottom 96-well plate containing 40µl of β-hexosaminidase substrate (Sigma) (diluted 1/25 in 0.2M citrate buffer) which was then incubated for 2 hours. The reaction was stopped by addition of 120µl 1M Tris (pH9.0) and the absorbance was measured using a LabTech-LT4000 plate reader at 405nm. Background absorbance values (from cells to which no DNP was added) were subtracted from test values and these were normalised to the maximum value attained from cells incubated with antigen and HBSS alone. Data points are shown mean ± standard error of the mean (SEM) unless otherwise stated.

2.2.1.6 Indirect flow cytometry binding assay

Cells were harvested by incubating for 15 minutes with cell dissociation solution, during which time recombinant proteins were diluted with BBN (Table 2.1) in a U bottom 96-well plate and stored on ice. Harvested cells were centrifuged for 5 minutes at 400*g* then resuspended in growth medium and transferred to a U bottomed 96-well plate (100µl per well, $1x10^5$ cells per well). The cells were washed twice by centrifuging the plate at 400*g* for 2 minutes and resuspending the cells in 100µl of BBN. The cell pellets were then resuspended in 50µl of BBN only or the appropriate concentration of recombinant protein and incubated for 45 minutes on ice. Cells were washed twice (as above) and fixed by resuspending in 100µl of 2% PFA and incubating for 15 minutes. After fixation, cells were washed twice and resuspended in 25µl of FITC conjugated anti-GST antibody (Table 2.2) and incubated in the dark on ice for 45 minutes. Cells were again washed twice (as above) and resuspended in 150µl of BBN and analysed using an Attune Autosampler flow cytometer (LifeTechnologies).

2.2.1.7 Direct flow cytometry binding assay

Cells were harvested, plated in U bottom 96-well plates and washed as described previously whilst dilutions of labelled recombinant proteins were prepared in BBN and stored on ice. Cell pellets were resuspended in the 50µl of the appropriate concentrations of labelled protein and incubated for 45 minutes in the dark on ice. The cells were washed twice more, resuspended in 150µl of BBN and analysed on an Attune Autosampler.

2.2.1.8 Immunofluorescent protein labelling

22mm diameter cover slips (SLS) were carefully added to the bottom of a sterile 24-well plate (Corning) using sterile forceps. Cells were harvested and seeded atop the coverslips at a density of $5x10^4$ per 500µl per well, cells were then incubated overnight. The following day cells were inspected to check even distribution, growth media was removed and cells were washed by addition and removal of 500µl PBS. Labelled proteins were added at varying concentrations and incubated for 45 minutes. Following incubation the proteins were aspirated from the wells and cells washed twice with PBS before being fixed by addition of 500µl 2% PFA for 10 minutes. Once fixed the cells were again washed twice with PBS before the coverslips were carefully removed from the 24 well plate with a needle. Cover slips were affixed to microscope slides using Vectashield mountant (VectorLabs) and sealed with nail varnish to prevent slides drying out.

2.2.1.9 Immunological staining of mammalian cells

Cells were harvested and seeded in each chamber of an 8-chamber Lab-Tek™ slide (Nunc) at a density of $5x10^4$ per chamber in 500µl then incubated overnight. The following day, cells were inspected to ensure an even distribution, growth media was removed and cells were washed by addition of 500µl PBS. PBS was removed and cells were fixed by incubating with 500µl of acetone. Acetone was removed and each well washed twice with PBS before submerging in PBS for 5 minutes. After incubation, PBS was removed and 150µl of primary antibody (10µg/ml), isotype control (10µg/ml) or PBS only was added to each well at an appropriate dilution, plates were then incubated for 1 hour on ice. After incubation, cells were washed twice with PBS and submerged in PBS for 5 minutes. Once washed, cells were incubated with 150µl of FITC labelled secondary antibody (5µg/ml) for one hour in the dark, on ice. Secondary antibody was removed and the cells were washed twice with PBS and submerged in PBS for 5 minutes. To stain the cell nuclei 150µl of propidium idodide was added to each well for 3 minutes and the cells were again washed. The Lab-Tek chambers were removed from the slide with the provided tool and cells were carefully aspirated to remove and residual PBS. 5µl of Vectorshield mountant was added to each chamber and a cover slip was carefully lowered

over the slide. Sides of the chamber were sealed with nail varnish, which was allowed to set for one hour. Slides were stored at 4^{o}C in the dark until needed.

2.2.1.10 Fluorescent imaging of mammalian cells

Slides were imaged using a Nikon A1 confocal microscope, random fields from each sample were selected and images were taken in both the FITC and DAPI channel for expression studies and FITC and brightfield channel for binding assays. Images were processed using the Fiji software (http://fiji.sc/Fiji).

2.2.1.11 Antibiotic sensitivity testing

The cells under investigation were harvested, counted and plated in each well of a 6-well plate (Corning) at a cell density of 1x10^{5} per 3ml per well and grown overnight. The following day the cells were inspected to ensure they were healthy and around 50% confluent, the growth media was removed and replaced with growth media supplemented with a range of concentrations of antibiotic. In each experiment one well was replaced with growth media containing no antibiotics (as a negative control) and one with growth media containing an excess of antibiotic (positive control). Media was changed every two days and growth of cells monitored visually over the course of two weeks. A concentration of antibiotic for transfection was selected that successfully killed all cells after two weeks.

2.2.1.12 Mammalian cell transfection via electroporation

A 90% confluent T175 flask of cells was harvested using trypsin, counted, centrifuged (500*g*, 5 minutes) and resuspended in serum free growth media at a density of 1x10^{7}ml^{-1}. 0.8ml of the cell suspension was transferred to a pre-chilled electroporation cuvette (Biorad, 0.2cm gap width) on ice. 10µg of plasmid DNA was added to the cuvette (for the Flp-in system both pOG-44 and the expression vector were mixed in an eppendorf in a 1:9 ratio before being transferred to the cuvette). The cuvettes were gently tapped to distribute the cells they were then incubated on ice for 10minutes. Following incubation, cuvettes were transferred to the electroporator (BioRad Gene Pulser II with capacitance extender) and pulsed at 250V (CHO) 350V (HEK-293) and 975µF. After electroporation, cells were incubated on ice for a further 30 minutes before being plated on 4 10cm dishes in growth media supplemented with FCS. The following day, growth media was replaced with one containing selective antibiotics. Cells were grown for two weeks with media being replaced every 2 days; after two weeks resistant cells were transferred to a fresh growth vessel.

2.2.1.13 Mammalian cell transfection via Turbofect™

Cells were plated in a 6-well plate at a density of $1x10^5$ per well in 3ml of growth media and cultured overnight. The following day the cells were checked to ensure they were healthy and at a sufficient confluencey (40-60%). 3µg of DNA was mixed with 6µl of Turbofect transfection reagent (Life Technologies) in 400µl of serum free DMEM per well and left to incubate for 20 minutes at room temperature (with intermittent mixing). 400µl of the DNA-Turbofect dilution was added in a drop-wise fashion to the top of each well, the plate was gently rocked before returning to the incubator overnight. Controls were included in each transfection, one without DNA and one without DNA and Turbofect. The following day the growth media was aspirated from the cells and replaced with growth media containing selective agent, media was replaced every other day for 2 weeks before assessing expression.

2.2.1.14 Insect cell transfection

Insect cells were routinely cultured in a shaking incubator at 27°C in SF-900 media (LifeTechnologies). $3.5x10^5$ SF9 cells were plated in each well of a 6-well plate and grown overnight. The following day 1µg of baculovirus DNA (Saphire, Allelebiotech) was mixed 1:1 with DNA expression plasmid and in a separate tube 10µl Cellfectin (Life Technologies) reagent was added to 100µl serum free SF-900 media. The diluted Cellfectin was added to the DNA mixture and incubated at room temperature for 20 minutes. During incubation the cells were gently washed with 2ml of serum free media three times. After washing the cells the DNA Cellfectin mixture was added in a drop wise fashion to the top of each well. Each plate was carefully wrapped in clingfilm and incubated at 27°C for 6 hours with gentle shaking every 30 minutes for the first 2 hours. After 6 hours, media was replaced with serum supplemented media and cells were left to grow for 5 days. After 5 days the cell media (containing primary viral isolate) was removed and centrifuged 500*g* for 5 minutes. Fresh SF9 cells were seeded at a density of $1x10^6$ per ml in a 5ml volume and the primary viral isolate added atop the cells at a 1:1000 dilution. After five days of growth the secondary viral isolate was harvested in the same fashion as the first. Fresh SF9 cells were seeded in a new flask in Insect-Xpress™ media (Lonza); once the cells had reached a density of $2.5x10^6 ml^{-1}$ the secondary viral isolate was added at a 1:200 dilution. Cells were grown for 2 weeks after which time protein expression was analysed.

2.2.1.15 Detergent based mammalian cell lysis

CHO and HEK-293 cells were lysed using CellLytic M Cell Lysis Reagent (Sigma) according to manufacturer's instructions. Briefly; cells were grown and harvested from a T175 flask, counted and centrifuged at 200*g* for 5 minutes. Cells were washed with HBSS and then

resuspended in CelLytic M Cell Lysis Reagent (125µl per 1x10^6 cells) and protease inhibitor cocktail (Sigma)(1µl per 1x10^6 cells). Cells were incubated for 30 minutes on ice with vortexing every 5 minutes. Finally, lysates were centrifuged at 12000g for 15 minutes after which the protein containing supernatant was transferred to a chilled Eppendorf and stored at -80^{o}C for later use.

2.2.1.16 *Burkholderia thailandensis* – induced mammalian cell fusion assay

J774.2 cells were harvested using a cell scraper and seeded in a 96-well plate at a density of 2x10^4. The following day cells where washed twice with sterile PBS then incubated for one hour with PBS only, 500 nM of tetraspanin EC2-GST or GST alone as a control. After one hour cells were again washed twice with PBS and infected with *Burkholderia thailandensis* at an MOI of 3:1 for 2 hours. After infection, cells were washed as previously then incubated in growth medium supplemented with 500 µg/ml kanamycin and amikacin for 14 hours. The following day, cells were fixed with acid ethanol (Table 2.1) at room temperature for 10 minutes after which time they were washed as previous and stained by incubation with of 0.1% Giemsa solution for 10 minutes at room temperature. Finally cells were washed with dH_2O and allowed to air dry before being visualised. 10 random fields were taken for each well and results are displayed as: $Fusion\ index = \frac{number\ of\ nuclei\ in\ an\ MNGC}{(total\ number\ of\ nuclei)}$

Or $MNGC\ size = \frac{number\ of\ nuclei\ in\ MNGC}{Number\ of\ MNGC's}$

2.2.1.17 Sulforhodamine B (SRB) assay

A colorimetric assay was employed to determine the amount of cellular protein remaining in wells following treatment with EC2 domains and thorough washing (Vichai and Kirtikara, 2006). RBL-2H3 cells were plated in a 96-well plate at 2x10^5 per 50 µl per well. EC2 proteins or GST were diluted to 2x concentration in 50µl of growth media and added atop the cells and incubated overnight. If necessary, the cells were washed by removing growth media and adding 100µl of pre-warmed media then rocking for 5 minutes before the growth media was replaced. Cells were then fixed by adding 50µl TCA to each well and incubating for one hour at 4^{o}C. TCA was removed and wells were washed five times by adding dH_2O to each well and flicking the plate into Virkon. The plate was left inverted on a paper towel at room temperature until dry and cellular protein was then stained by adding 100 µl of 0.4% (Table 2.1). The plate was incubated for 30 minutes and excess stain was then removed by flicking into Virkon, wells were then washed four times with 1% acetic acid. The plate was again dried on a paper towel at room temperature and then dye was solubilised by adding 50 µl of 10mM

unbuffered tris (Table 2.1) to each well. The plate was incubated for 5 minutes with gentle agitation before its absorbance was read at 570nm.

2.2.1.18 Flow cytometry

Cells were harvested and seeded in a 96-well plate at a density of $1x10^5$ per well in 100µl volume. After centrifugation at 200 *g,* growth media was removed and cells were washed twice with 100µl HBSS. HBSS was removed and 100µl of primary antibody (10µg/ml) , isotype control (10µg/ml) or PBS only was added to each well at an appropriate dilution, plates were then incubated for one hour on ice. After incubation, cells were washed twice with HBSS and were incubated with 100µl of FITC labelled secondary antibody (5µg/ml) for one hour in the dark, on ice. Secondary antibody was removed and the cells were washed twice with HBSS before being resuspended in 150µl BBN and analysed using an Attune Autosampler flow cytometer.

2.2.2 Molecular biology methods

2.2.2.1 Primer design

The boundaries of the EC2 domain encoding genes where initially defined according to previous work from our group based on hydrophobicity analysis to determine the position of the TM domains (Higginbottom et al., 2000b) along with a number of publications which aligned various EC2 domains. EC2 encoding sequences were analysed using the NEB cutter software to identify any potential restriction sites and appropriate restriction enzymes for cloning were determined. Restriction sites were added to the sequence along with several GC base pairs to accommodate the restriction enzymes themselves, keep coding sequences in frame and add a GC clamp to the primer ends. For overlap extension PCR, Primers were designed corresponding to the 5' and 3' end of the tetraspanin EC2 domains and contained a leader sequence overlap and a restriction site respectively. Primers were also designed to anneal to the 5' and 3' end of the leader sequence and contained a restriction site and EC2 overlap respectively. Leader sequence forward primers also contained a start codon and a Kozak sequence. Once potential primer pairs were designed the Tm values were checked and primers were adjusted accordingly, cloning was then simulated using Clone manager suite 7. The EC2 domains amplified along with their amino acid position can be seen in Table 2.8

TSpan	**EC2 domain boundaries**	**Amino acid sequence**
CD9	113-192	HKDEVIKEVQEFYKDTYNKLKTKDEPQRETLKAIHYALNCCGLAGGVEQFISD ICPKKDVLETFTVKSCPDAIKEVFDNK
CD63	107-202	FRDKVMSEFNNNFRQQMENYPKNNHTASILDRMQADFKCCGAANYTDW EKIPSMSKNRVPDSCCINVTVGCGINFNEKAIHKEGCVEKIGGWLRKN
CD81	115-199	NKDQIAKDVKQFYDQALQQAVVDDDANNAKAVVKTFHETLDCCGSSTLTA LTTSVLKNNLCPSGSNIISNLFKEDCHQKIDDLFSGKLY
CD151	114-219	YYQQLNTELKENLKDTMTKRYHQPGHEAVTSAVDQLQQEFHCCGSNNSQ DWRDSEWIRSQEAGGRVVPDSCCKTVVALCGQRDHASNIYKVEGGCITKLE TFIQEH
Tspan5	115-232	FKDWIKDQLYFFINNNIRAYRDDIDLQNLIDFTQEYWQCCGAFGADDWNL NIYFNCTDSNASRERCGVPFSCCTKDPAEDVINTQCGYDARQKPEVDQQIVI YTKGCVPQFEKWLQDN

Table 2.8 EC2 domain boundaries and amino acid sequence.

2.2.2.2 Touchdown PCR

Touchdown PCRs were utilised which start with a high initial annealing temperature which is thought to reduce the amount of nonspecific priming. Annealing temperature is gradually decreased in subsequent rounds of amplification when the specific target has been amplified (Don et al., 1991). Reactions were carried out in a 20µl reaction volume which consisted of

Component	Volume/ Final concentration
Water	10µl
10x HF Buffer	2µl
dNTPS	200µM
Forward primer	200nM
Reverse primer	200nM
Template	500ng
Phusion DNA pol	1.25units/50µl

Table 2.9 PCR components Phusion DNA polymerase and buffer HF were purchased from NEB, 10mM dNTPS from Sigma. Primers were used from a 1:10 dilution of the initial 100pmol stock supplied by eurofins. Template DNA was initially diluted to 100ng/ml before inclusion.

For amplification the thermocycler (Techne Genius) was programmed for an initial denaturation step of 95^{o}C for 5 minutes followed by 35 rounds of:

- 95^{0}C for 30 seconds
- X^{0}C for 30 seconds
- 72^{0}C for 45 seconds

After this, a final extension took place at 72^{o}C for 10 minutes before the reaction was held at 4^{o}C. The annealing temperature (X) was determined based on the Tm values of primer pairs

2.2.2.3 Overlap extension PCR

Overlap extension PCRs were utilised to combine two pieces of DNA (the EC2 encoding gene and leader sequence) (Ho et al., 1989). Primers used in this PCR included an overhang which corresponded to the gene to be added (for example a forward primer for an EC2 domain included a leader sequence overhang see Figure 2.1). For this kind of amplification "Touchdown PCR" was used (Don et al., 1991) in which a high initial annealing temperature reduces nonspecific primer binding and is reduced in subsequent rounds which reduces the stringency of the reaction. The Themocycler program was as in the previous section (2.2.2.2). However the annealing temperature (X) started at the primer Tm value + 2^{o}C and after every 5 round of amplification was dropped by 2^{o}C for a total of 35 rounds.

2.2.2.4 Small scale plasmid purification

Small scale plasmid purifications were carried out using a Qiagen Plasmid Mini Kit according to manufacturer's instructions. Briefly, single colonies were picked using a sterile cocktail stick and inoculated into 5ml of LB containing selective antibiotics. Cultures were grown overnight (37^{o}C, 225 rpm) after which time they were centrifuged at 5500*g* for 10 minutes. Pellets were

resuspended in 250µl of buffer P1, vortexed and transferred to Eppendorf tubes, 250µl of buffer P2 was added and the solutions mixed by inversion. 350µl of buffer P3 was added and the tubes were again mixed thoroughly by inversion after which they were centrifuged at 13k *rpm* for 10 minutes to pellet the cell debris. Supernatant was decanted into to a Qiagen spin column which was then centrifuged again at 13k rpm in a microfuge for 1 minute; columns were then washed with 750µl of buffer PE and centrifuged again as above. After washing, the DNA was eluted in 50µl of RNase free water or elution buffer.

2.2.2.5 Large scale plasmid purification

Larger plasmid purifications were carried out using a Qiagen HiSpeed Plasmid Midi kit according to manufacturer's instructions. In short, single bacterial colonies were picked from an agar plate using a sterile cocktail stick/pipette tip and inoculated into 5ml of LB containing selective antibiotics and cultured overnight (37^{o}C, 225 rpm). The following day 1ml of bacterial culture was added to 50ml of LB containing selective antibiotics, which was again cultured overnight. 50ml cultures were centrifuged at 5500*g* for 30 minutes and supernatant discarded. Bacterial pellets were resuspended in 4ml of buffer P1, 4ml of buffer P2 was added and samples mixed by inversion then incubated on ice for 15 minutes. 4ml of buffer P3 was added and the samples were again mixed thoroughly by inversion then centrifuged for 30 minutes at 5500*g*. Supernatant was then passed through a previously equilibrated QIAGEN-tip then the tip was washed with 10ml of buffer QC twice. DNA was eluted from the tip into a sterile falcon tube using 5ml of buffer QF and then precipitated with 3.5ml of isopropanol. Precipitated DNA was added to a QIA precipitator module and washed with 2ml of 70% ethanol. DNA was eluted from the precipitator module using 1ml of buffer TE or RNAse free DNase free water.

2.2.2.6 Transformation of competent cells

20µl of Rosetta-gami or DH5α competent cells were thawed on ice for 10 minutes. 1ul of expression plasmid at 100ng/µl or ligation mixture was added and cells were incubated for a further 20 minutes. Following incubation cells were heat shocked at 42°C for 45 seconds and then incubated on ice for a further 2 minutes. 250 µl of SOC buffer was added to the bacteria and they were then transferred to 37°C to recover for 45 minutes. Cells were then plated on agar plates containing selective agent and grown overnight.

2.2.2.7 DNA sequencing

DNA sequencing was carried out at The University of Sheffield Core Genomic Facility. Results were read using the software FinchTV and aligned using EMBOSS NEEDLE Pairwise Sequence

Alignment (http://www.ebi.ac.uk/Tools/psa/emboss_needle/). For primer sequences see Appendix.

2.2.2.8 Preparation of glycerol stocks

A single colony of transformed bacteria was transferred into 5ml of LB containing appropriate antibiotics, which was then grown overnight (37^{o}C, 250 rpm). The following day 750 ml of the bacterial culture was transferred to a cryovial (Nunc) along with 250µl of 60% glycerol (Table 2.1), vials were immediately transferred to a -80^{o}C freezer until further use. To thaw cells from glycerol stocks some of the frozen pellet was scraped from the vial using a pipette tip and transferred to LB containing antibiotics.

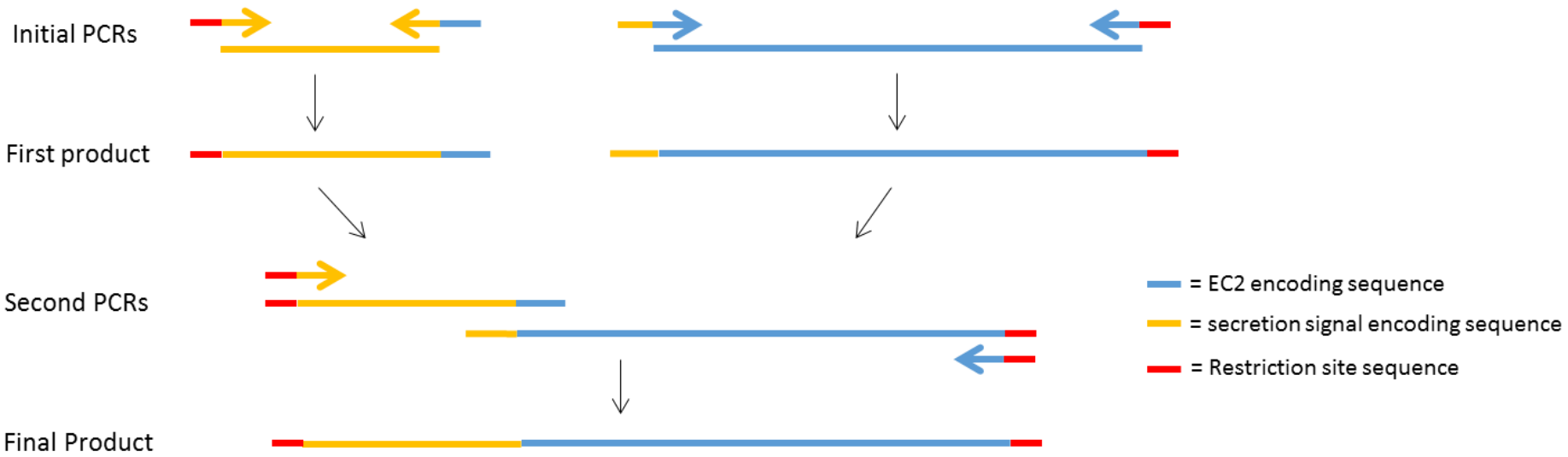

Figure 2.1: Schematic diagram depicting the different steps in overlap extension PCR. Short arrows represent primers and long lines either products or templates. Initial PCRs incorporate restriction sites and overlaps onto either the leader sequence or EC2 encoding sequence. Products from the first PCRs are able to anneal and are used as a template in a second PCR which combines both leader sequence and EC2 encoding gene.

2.2.2.9 Agarose gel electrophoresis

1g of agarose was heated with 100ml of TAE buffer (Table 2.1) and once cooled sufficiently, 3µl of 10mg/ml ethidium bromide was added and the gel was poured into a DNA gel tank with comb. DNA samples were diluted with 6x DNA loading dye (Bioline). Once the gel had set, the comb was removed and 15µl of each diluted DNA sample was loaded into each well, 5µl of the DNA ladder Hyperladder I (Bioline) was included with each gel. Gels were run at 100 volts for 50 minutes and then imaged using a gel imaging system (UVP gel doc).

2.2.2.10 Gel extraction

Gel extraction was carried out using QIAquick Gel Extraction Kit according to manufacturer's instructions. In short, after conducting DNA electrophoresis (Section 2.2.2.9) samples were briefly illuminated using a UV block. Gel bands corresponding to the required DNA fragment were removed from the gel with a sterile scalpel and transferred to an Eppendorf tube. After weighing each gel slice, 3 volumes of buffer QG was added to 1 volume of gel, samples were then dissolved in a 60^{o}C heat block with intermittent vortexing. After the gel slice had completely dissolved the solution was added to a spin column and centrifuged at 13k rpm in a benchtop centrifuge (Eppendorf minispin) for 1 minute. The column was washed with 750µl of buffer PE and after washing the column was again centrifuged at max speed for 1 minute to remove and residual wash buffer. DNA was eluted using 40µl of RNase free water into a clean Eppendorf tube.

2.2.2.11 PCR purification

PCR purifications were carried out using a QIAquick PCR Purification Kit according to manufacturer's instructions. In brief, PCR samples were diluted with 5 volumes of buffer PB and added to a QIAquick spin column then centrifuged at 13k rpm for 1 minute in a microfuge. 750µl of buffer PE was added and the columns were again centrifuged for 1 minute. After an additional centrifuge step to remove any residual wash buffer DNA was eluted from the column using 50µl of RNAse free DNAse free water.

2.2.2.12 Restriction digest

Digestion of inserts was carried out using ~ 400ng of PCR product (Section 2.2.2.2), 4µl of multicore buffer (Promega), 4µl of BSA (1ng/ml) and 1.5µl of each enzyme, made up to 40µl with RNase incubated at 37^{o}C for 3 hours. Digestion of vector was achieved through two individual single digests, which were then combined into one double digest. Single digests comprised 400ng of vector DNA, 2µl multicore-buffer, 2µl BSA and 1µl of the required enzyme

made up to 20µL using RNase free water. Single enzyme digests of the vector were incubated at 37°C for 1.5 hours after which time they were pooled and incubated for another 1.5hours.

2.2.2.13 Ligation

Ligations were set up using a 3:1molar ratio of insert to vector according to the equation:

$$\frac{Vector\ amount\ (ng) x\ Insert\ size\ (bp)}{Size\ of\ vector\ (bp)}\ x\ molar\ ratio\ insert{:}\ vector = Amount\ of\ insert\ (ng)$$

Ligations were carried out in a 20µl reaction volume which consisted of:

Component	Volume
Water	Made up to 20µl
Buffer	2µl
Insert	Xµl (See equation)
Digested vector	Xµl (50ng)
T4 DNA Ligase	1unit/50µl

Table 2.10 Ligation reaction components: buffer and ligase were both part of the T4 DNA ligase kit (NEB) vector and insert volume was determined based on DNA concentration volume using the equation above

The ligation mix was incubated for 3 hours at 37°C after which 1µl of the ligation mix was used for transformation of DH5α competent cells (Section 2.2.2.6).

2.2.2.14 Genomic DNA extraction from mammalian cells

Genomic DNA was extracted using the PureLink genomic DNA extraction kit (Invitrogen) as per the manufacturer's instructions. Briefly, cells were harvested and $3x10^6$ cells were resuspended in 200µl of HBSS. The cell suspension was added to 20µl of proteinase K to which 20µl of RNase A was added, the sample was then vortexed and incubated for 2 minutes at room temperature. 200µl of PureLink Lysis/binding buffer was added and the mixture was again vortexed and incubated for 10 minutes at 55°C. 200µl of absolute ethanol was then added and the solution was vortexed. This sample was added to a spin column which was centrifuged at 13k rpm in a micofuge for 1 minute, then the column was washed with 500µl Wash buffer 1 and 2 and finally the DNA was eluted in 100µl elution buffer.

2.2.2.15 Preparation of cDNA from mammalian cells

To assess the presence of specific RNA within mammalian cells cDNA was first prepared from whole cell extracts. Total nucleic acid was isolated using a Qiagen RNeasy Mini Kit according to

manufacturer's instructions. Briefly, cells were harvested and $3x10^6$ cells were resuspended in 350µl buffer RLT, 350µl of 70% ethanol was added and the sample was mixed thoroughly by pipetting. The lysate was transferred to an RNeasy mini column and centrifuged for 15 seconds at 13k rpm, then the column was washed with 700µl RW1 and 500µl RPE. After washing, the nucleic acid was eluted in 30µl of elution buffer.

An Ambion DNA-free kit was used to remove DNA from the sample. A mixture consisting of 2µl 10x buffer, 2µg of nucleic acid and 1µl of DNase was made up to 10µl with RNase-free water. Samples were incubated for 20 minutes at room temperature before 2µl of inactivation reagent was added and the sample vortexed. After a further 2 minute incubation (with intermittent mixing) the samples were centrifuged for 10 minutes at 13k rpm in a microfuge and the RNA containing supernatant removed.

RT-PCR was carried out using a High-Capacity RNA-to-cDNA kit (Applied Biosystems). A 2x master mix was made for each reaction consisting of:

Component	**Volume**
Water	3.2µl
10x RT Buffer	2µl
25x dNTP mix (100mM)	0.8µl
10x RT Random primers	2µl
MultiScribe Reverse transcriptase	1µl
RNase inhibitor	1µl

Table 2.11 Components of the reverse transcription master mix. Random primers, reverse transcriptase, dNTPs and RNase inhibitor were all from the High Capacity RNA-to-cDNA kit (Life technologies).

10µl of this master mix along with 10µl of the previously produced RNA were added to a PCR tube and run in a thermocycler for: 10 minutes at 25^{o}C, 120minutes at 73^{o}C and 5 minutes at 85^{o}C. Once produced the cDNA was stored at 4^{o}C for later use or -20^{o}C for long term storage.

2.2.3 Protein biochemistry methods

2.2.3.1 SDS-PAGE

Protein gels consisting of a 12% separating gel and 8% stacking gel were prepared according to Table 2.1. Once gels were set they were removed from the casting apparatus and transferred to a Biorad mini-protean tetra cell. Protein samples were diluted with either non-reducing protein loading dye (Table 2.1), for Western blots using conformationally sensitive antibodies, or reducing protein loading dye (Table 2.1). The gel tank was filled with SDS running buffer (Table 2.1) and gels were run at constant voltage of 160v for around 2 hours before being removed from the tank

2.2.3.2 Coomassie staining and de-staining

Gels were carefully removed from the glass plates, transferred to a container and then incubated with Coomassie brilliant blue stain (Table 2.1) for one hour with gentle rocking. Once stained, the gel was briefly washed with dH_2O and transferred to de-stain (Table 2.1) for 4 hours or until sufficiently de-stained. Gels were then imaged using a UVP gel doc.

2.2.3.3 Western blot

Once gels had finished running (Section 2.2.3.1) they were carefully removed from glass plates and transferred to a Western blot "sandwich" consisting of cassette, sponge, blotting paper, PAGE gel, high bond ECL nitrocellulose membrane (Amersham), blotting paper and finally sponge. This sandwich was assembled under blotting buffer (Table 2.1) and any air bubbles were removed with a roller. Once assembled, the sandwich was loaded into the blotting apparatus along with 1L of blotting buffer (Table 2.1). Blotting was carried out for 1 hour at 100 volts or overnight at 10 volts then the membranes were transferred to blocking buffer (Table 2.1) for one hour. Membranes were then washed by incubating twice in TBST (Table 2.1) for 10 minutes then transferred to a universal tube containing 5ml of primary antibody diluted in blocking buffer to 1µg/ml. Membranes were incubated for one hour on a rotary mixer, washed twice as before then transferred to a second universal tube containing HRP-linked secondary antibody, also diluted in blocking buffer. Membranes were incubated in secondary for one hour then washed before being incubated with SuperSignal West Pico Chemiluminescent Substrate (Life Technologies) for 5 minutes with gentle rocking. Membranes were transferred to a Western blot cassette and incubated with X-ray film (Pierce) for varying lengths of time. Finally the films were removed from the cassette and immersed in developing solution, washed with tap water then immersed in fixing solution.

2.2.3.4 Expression of tetraspanin EC2 domains in *E. coil*

After Rosetta-gami cells had been transformed with pGEX-KG plasmids (Section 2.1.7) a single colony was picked from an agar plate using a sterile pipette tip and transferred to 5ml of LB containing the appropriate antibiotics (Table 2.1.5). Starter cultures were grown for 8 hours at 37^{o}C 250rpm, then the 5ml culture was added to a larger 200ml flask of LB (also containing antibiotics) which was grown overnight (37^{o}C 250rpm). The overnight culture was then added to 500ml flasks of LB containing antibiotics at a 1/25 dilution. The cultures were grown at 37^{o}C 250rpm until an OD_{600} of 0.6 was achieved at which point expression was induced using 0.1mM IPTG and cultures were incubated for 4 hours. Bacteria were harvested by centrifuging at 4500*g* for 20 minutes, supernatant was decanted into Virkon and bacterial pellets were weighed and frozen until lysis and purification

2.2.3.5 Cell lysis by sonication

Bacterial cell pellets collected previously (Section 2.2.3.4) were thawed on ice and resuspended in lysis buffer consisting of 1x PBS (Table 2.1) and Halt protease inhibitor cocktail (Lifetechnologies) diluted 1/100 (5ml lysis buffer per 1g of bacterial pellet). Resuspended cultures were lysed by sonicating at 15 microns for two 15 second rounds, at which point there were mixed and sonicated again for a further 3 rounds (5 round in total). Tubes were then balanced using PBS and centrifuged at 24000*g* for 20 minutes to pellet unwanted cell debris. Cell lysates were transferred to fresh universal tubes for downstream purification and cell pellets containing the insoluble protein fraction were frozen for later analysis.

2.2.3.6 Affinity purification of GST tagged proteins –Batch method

An appropriate volume of GST Sepharose beads (GE Healthcare) (100µl of beads for every gram of bacterial pellet) were transferred to a 1.5ml Eppendorf tube, centrifuged (500g, 5 minutes) and the head volume (containing ethanol) discarded. The beads were resuspended in 5 bed volumes of PBS centrifuged again and the head volume discarded, this wash process was repeated twice more for a total of 3 washes. Washed beads were incubated at room temperature with cell lysates for 2 hours on a rotary mixer. Beads were then centrifuged and the head volume containing unbound protein was removed, (the final 100-200µl of supernatant was removed using a gel loading tip to prevent unwanted transfer of beads). The beads were washed with 5 bed volumes of PBS, centrifuged and the head volume was once again removed (wash 1). This process was repeated twice more yielding the Wash 2 and Wash 3 fractions, after which the beads were incubated for 15 minutes with 25mM reduced glutathione (Table 2.1) (0.5ml of elution buffer for each gram of bacterial pellet). After incubation the beads were pelleted and the head volume (eluate 1) was transferred to a pre-

chilled Eppendorf for later dialysis. The elution process was carried out once more using half the initial volume to remove any protein which may have remained on the beads (eluate 2).

2.2.3.7 Affinity purification of GST tagged proteins – Column method

An appropriate volume of GST Sepharose beads) (100µl of beads for every gram of bacterial pellet) were added to a Poly-Prep chromatography column (BioRad) and left to settle. To remove the 70% ethanol the beads are supplied in, 2 bed volumes of PBS were added to the top of the column and allowed to pass though – this was repeated until 5 bed volumes had passed through the column. The column was then capped, cell lysates were added and the lid was securely fitted. Lysates were incubated with the beads for 2 hours with end-over-end rotation at room temperature. After incubation the column was allowed to settle for 5 minutes before both caps were removed and the lysate was allowed to flow through and collected (unbound fraction). The beads were washed three times by adding 5 bed volumes of PBS to the top of the column and allowing it to empty under gravity then the beads were incubated with 25mM reduced glutathione for 20 minutes with end over end rotation (0.5ml per gram of bacterial pellet). After incubation, the eluate was passed through the column and collected; any residual liquid was forced through the column using a syringe (eluate 1). To remove any remaining protein the column was again incubated with 25mM reduced glutathione (0.25ml per gram of bacterial pellet) for 20 minutes and the eluate collected (eluate 2)

2.2.3.8 Nickel affinity chromatography

Cell supernatant or lysate samples containing His tagged proteins were concentrated to a volume less than 10ml and simultaneously buffer exchanged into 10mM Imidazole binding buffer (Table 2.1) using centristrat columns (section 2.2.3.8). Once samples had buffer exchanged, samples were added to a Ni-NTA agarose column (approximately 20mg of protein per 1ml of resin) and incubated for 2 hours at room temperature with on a rotary mixer. Following incubation the column was uncapped and unbound protein was eluted and collected. The column was washed with 5 bed volumes of 10mM imidazole before the bound proteins were eluted. Initial elution was carried out with 500µl of 500mM imidazole elution buffer (Table 2.1) and subsequent elutions with a two-fold lower concentration for a total of 3 elutes. Eluted proteins were stored at 4^{o}C for immediate use or -80^{o}C for later analysis

2.2.3.9 Dialysis

16mm snakeskin dialysis tubing with 3.5kDa molecular weight cut-off (Life Technologies) was soaked in 1x PBS and one end of the tubing was tied and clipped. Proteins eluates were

pipetted into the tubing, the tubing was gently pressed to remove any air and the open end was tied and clipped. Proteins were incubated in 5 litres of PBS overnight at 4^{o}C with gentle agitation. The PBS was then replaced and proteins were incubated for a further 6 hours before they were transferred to an Eppendorf on Ice. Protein was then quantified and aliquots were stored at -80^{o}C

2.2.3.10 Bradford assay protein quantification

A Bradford assay was used to quantify proteins in a sample by comparing aborbance to samples of known protein concentration (Bradford, 1976) 12 BSA standards spanning a range of concentrations were generated by serially diluting a stock of BSA in PBS. 10µl of these standards along with 10µl of test proteins were added in triplicate to a 96-well plate. Protein Assay Dye Reagent Concentrate (BioRad) was diluted 1:5 with dH_2O and 200µl of this diluted dye was added to each sample. The plate was gently rocked to distribute the dye and then incubated for 5 minutes to ensure a complete colour change. The absorbance was read on a plate reader at a wavelength of 595nm. A standard curve was generated using the absorbance values of the proteins standards from which the unknown protein concentrations could be determined.

2.2.3.11 Protein concentration using molecular weight cut-off columns

EC2-GST fusion proteins were concentrated using Centrisart I Concentrator columns with 5kDa molecular weight cut off (Sigma). Protein was added to the column to the 2.5ml mark and then the inner tube was inserted and left to stand for 5 minutes. Columns were then centrifuged at 2500g for 30-45 minutes. After centrifugation the filtrate was removed and the outer tube was again filled to the 2.5ml mark. This process was repeated until samples were sufficiently concentrated.

2.2.3.12 LPS quantification

LPS levels were quantified using a LAL Chromogenic Endotoxin Quantitation Kit (Pierce) according to manufacturer's instructions. Briefly, standards were prepared using provided LPS and endotoxin free water and protein samples were diluted with endotoxin free water to fit within range of LPS standards. 50µl of recombinant protein or LPS standards were added in duplicate to a 96-well plate and incubated for 5 minutes at 37^{o}C. After incubation 50µl of LAL (Limulus amebocyte lysate) was added to each well, the plate was gently shaken and then incubated for a further 10 minutes at 37^{o}C. Exactly 10 minutes following incubation 100µl of substrate solution was added to each well, again the plate was gently shaken and incubated for an additional 6 minutes. Finally 50µl of 25% acetic acid was added to stop the reaction and

absorbance was read at 410nm on LT-4000 Labtech plate reader. Background values were subtracted before a standard curve was established to determine LPS levels in test proteins.

2.2.3.13 GST cleavage –batch method

Recombinant GST tagged proteins were incubated with prewashed glutathione Sepharose beads with end-over-end rotation for 2 hours in a protein LoBind tube (Eppendorf) (10mg of protein per 1ml of glutathione Sepharose). Beads were then centrifuged for 5 minutes at 500g and the head volume (containing any non-bound protein) was removed. Beads were then washed 3 times with 5 bed-volumes of PBS to ensure any residual unbound protein was removed. An appropriate amount of Thrombin (GE healthcare) was diluted in PBS/phosphate buffer (1.5 units per 100µg of protein) and was then used to re-suspend the GST-Sepharose beads, which were then incubated for 16 hours with end-over-end rotation at room temperature. Samples were then centrifuged at 500g for 5 minutes and the head volume containing cleaved protein was removed using a gel loading tip to avoid transfer of any GST-beads. Cleaved protein was incubated with washed p-aminobenzimade agarose (Sigma)(2µl per unit of thrombin) for 30 minutes after which samples were centrifuged at 13k rpm 5 minutes. The head volume containing cleaved protein was then transferred to another LoBind tube using a gel loading tip and cleaved protein was then stored at 4^{o}C for immediate use or -80^{o}C for later use.

2.2.3.14 GST cleavage – column method

Recombinant GST tagged proteins were incubated with washed glutathione sepharose beads with end-over-end rotation for 2 hours in a BioRad Polyprep chromatography column (10mg of protein per 1ml of glutathione Sepharose). The beads were then allowed to settle for 5 minutes before the column was uncapped and unbound proteins allowed to flow through and collected. The beads were washed 3 times with 5 bed volumes of PBS before thrombin diluted in PBS was added to the column. The column was sealed and incubated overnight with end-over-end rotation at room temperature. The column was then uncapped and cleaved protein was collected in a LoBind tube. To remove any residual protein from the column, additional PBS was added and pushed through the column with a syringe. Cleaved protein was incubated with washed p-aminobenzimade-agarose (Sigma) (2µl per unit of thrombin) for 30 minutes after which, samples were centrifuged at 13k rpm on a microfuge for 5 minutes. The head volume containing cleaved protein was then transferred to another LoBind tube using a gel loading tip and the cleaved protein was then stored at 4^{o}C for immediate use or -80^{o}C for later use.

2.2.3.15 CD spectroscopy

CD spectroscopy was utilised to estimate the secondary structures of proteins. All circular dichroism experiments were carried out using a Jasco J-810 spectrophotometer with a cell of pathlength of 0.02cm. Data were obtained at 15^{o}C with start and end points of 350 and 190nm respectively. A data pitch of 1nm, response time of 8 seconds and scan speed of 20nm/min were used and readings were averaged over 5 accumulations. To allow for more direct comparison results are displayed as mean residue elipticity [Θ]MRW (deg·cm2 dmol-1) which was calculated using the following equation.

$$[\theta]mrw = \frac{MRW\ x\ \theta obs}{10\ x\ P\ x\ C}$$

where MRW is mean residue weight, P is the path length in cm and C is the concentration in mg/ml. Absorbance values were read in an environment of nitrogen gas and if required, recombinant proteins were buffer exchanged into 20mM sodium phosphate buffer before being analysed. 115µl of protein sample was added to the recess on one glass slide then the second slide was placed on top and excess protein removed with a lens wipe. The filled slides were placed in the spectrophotometer and the program parameters used were as previously described. If assessing effects of temperature on circular dichroism the spectra was measured at a constant 222nm and a temperature gradient from 10^{o}C-90^{o}C was used with responses every 2^{o}C. Spectra were deconvoluted using the online software Dichroweb (Whitmore and Wallace, 2004)

2.2.3.16 Alexa488 Protein labelling

Alexa488 dye (Life Technologies) was dissolved in 100µl of DMSO to generate a 10mg/ml stock which was stored in aliquots at -20^{o}C. The quantity of Alexa488, $NaHCO_3$ and Tris-HCL to use were determined based on the number of moles of protein to be labelled, using a molar excess of 20 (as suggested by the manufacturer). A minimum of 200µg of recombinant protein was added to a 0.5ml Eppendorf wrapped in foil and appropriate volumes of Alexa488 and $NaHCO_3$ were added then incubated for 2 hours with end over end rotation at room temperature. During incubation PD-SpinTrap G-25 columns (GE healthcare) were prepared by removing storage buffer and washing the column 5 times with 300µl of PBS. After the 2 hours incubation free succinyl groups were quenched with Tris-HCL and the samples were added to the previously prepared columns (one column could accommodate 130µl sample). Columns were centrifuged at 13k rpm on a microfuge for 3 minutes and flow through containing labelled protein was collected. The OD_{280} and OD_{494} of the resulting samples were read on a Nanodrop

(Nanodrop 1000 Thermo) and used to determine the degree of labelling using the following equation.

$$DOL = \frac{OD494\ x\ dilution\ factor}{71000\ x\ protein\ concentration\ (M)}$$

2.2.3.17 Enzyme linked immuno assay (ELISA)

100µl of cell supernatant or recombinant protein at appropriate initial concentrations were serially diluted in carbonate-bicarbonate buffer (Table 2.1) across a 96-well ELISA plate (Nunc). Plates were wrapped in cling-film and incubated overnight at 4^{o}C. Excess protein samples were discarded from the wells and the plate was washed twice with PBST and patted dry on paper towels. 150µl of blocking buffer (Table 2.1) was added to the wells and the plate was incubated again for 2 hours at 37^{o}C. The blocking buffer was then discarded and the plate was again washed twice with PBST and patted dry. 50µl of primary antibody diluted in blocking buffer to 10 µg/ml was added to each well and the plate was incubated at 37^{o}C for 1 hour. The primary antibody was then discarded and the plate was washed and dried as previously, 50µl of secondary HRP-linked antibody was added to each well and the plate was again incubated for 1 hour at 37^{o}C. The plate was washed twice with PBST and twice with dH_2O after which 50µl of TMB substrate (Sigma) was added to each well. The colour was allowed to develop for 15 minutes before the reaction was stopped by addition of 50µl of 2M H_2SO_4, The absorbance was read on a plate reader a 450nm.

2.2.3.17 Statistical analysis

Data was analysed using tools within the GraphPad Prism 6 software. To reduce variation between experiments, degranulation values are normalised to those seen when no treatment were used in conjunctions with the highest concentration of DNP-HSA (this value was fixed to 100%). Unless otherwise stated, data are presented as mean +/- SEM. Significance was determined by one way ANOVA using Bonferroni post hoc multiple comparison.

Chapter 3: Production and analysis of tetraspanin EC2 domains

3.1 Introduction

Despite tetraspanin proteins being almost ubiquitous in the human body, and involved in a multitude of important cellular and pathological processes (see section 1.1.3), relatively little is known about the functions of individual members. This is in part due to the limited availability of monoclonal antibodies and the mild phenotypes observed in a number of tetraspanin knock-out mutants (probably due to a level of redundancy) (Hemler, 2005). Our group and others have previously had success in dissecting individual tetraspanin functions using recombinant tetraspanin EC2 domains (Section 1.1.4); however, these bacterially expressed recombinant proteins lack post-translational modifications, specifically glycosylation, so may not exhibit a tetraspanins full function. Furthermore, due to the complex folding patterns of tetraspanin EC2 domains and a lack of specific chaperones in *E. coli,* which help with this folding, it has been suggested that a heterogeneous group of both folded and unfolded proteins may be expressed. Additionally, previous work by our group (Fanaei, 2013) has also considered the effects of contaminating LPS resulting from the use of bacteria as a host for recombinant protein expression.

The initial aim of this chapter was to express the EC2 domains of the human tetraspanins: CD9, CD151 and Tspan5, in a mammalian or insect host. These specific tetraspanins were selected as candidates for mammalian expression as they contain a varied number of theoretical di-sulphide bonds (2, 3 and 4 respectively). This is thought to contribute to a more complex protein structure and could give an indication as to how well these systems can express more “difficult” proteins. As both mammalian and insect cells are able to carry out post translational modifications (albeit with different patterns of glycosylation) it was hypothesised that the resultant proteins could shed light on the contribution of glycosylation in the function of tetraspanin EC2 domains. Additionally, due to the more sophisticated cellular machinery present in both cell types, it was thought that these systems may be better equipped to handle the complex folding of the EC2 domains, resulting in a more homologous, higher quality end product (Section 1.3.1). Moreover, using a non-bacterial host for protein expression eliminates the possibility of LPS contamination in the proteins produced, which would enable the use of these proteins in LPS sensitive assays.

Later aims were to express recombinant EC2 domains of the human versions of tetraspanins CD9, CD63 and CD151 in bacteria. These specific family members were selected based on their association with mast cell degranulation, with the later view to using them in furthering our understanding of tetraspanin involvement in this area. The EC2 domain on Rat CD63 was also expressed to enable a comparison between the effects of EC2 domains originating from different species. Following this, work was carried out to optimise the expression of said proteins to enable studies that require higher protein concentrations.

3.2 Results

3.2.1 Cloning of tetraspanin EC2 domains for mammalian expression

Boundaries for the tetraspanin EC2 domains had previously been defined by our group based on hydrophobicity analysis and alignment of the primary amino acid sequence of multiple human tetraspanin EC2 domains, in addition to work carried out by Todd *et al.* (1998) and Rob *et al.* (2001). To allow for easier downstream purifications it is desirable to have the products secreted into the surrounding growth media; this was achieved through the inclusion of a leader (or secretion) sequence at the 5' end of the gene sequence (here the leader sequence of the IgGκ light chain was used (Young et al., 1995)) . DNA sequences for the tetraspanin EC2 domains, each containing an IgGκ leader sequence, were generated by overlap extension PCR (Section 2.2.2.3) using the gene specific primers displayed in the Appendix (Table 7.1). PCR reactions were carried out using Phusion high fidelity polymerase (NEB) with initial rounds of PCR resulting in products ranging from ~260-380bp for the EC2 domains and ~90bp for the leader sequences (Figure 3.1a). Subsequent rounds of amplification (overlap extension) combined the leader sequences with the EC2 genes, resulting in products ranging from 330bp-450bp (Figure 3.1b). PCR products prior to and following overlap extension were run adjacent to one another and the increased size after the second round of amplification also indicated successful combination of leader sequence and EC2 encoding gene.

The resultant fragments were cloned into the plasmid pSec-Tag-link, a modified version of the pSecTag/FRT/V5-His plasmid from the Flp-in system (Life Technologies). In this particular vector the multiple cloning site was altered to remove the V5 epitope to make the resulting recombinant protein more representative of its native counterpart. The Flp-in system was selected as it had been used for transfections of other (non-tetraspanin) genes by our group and offers a number of advantages over traditional transfection systems. It involves the insertion of a coding gene from one plasmid (pSecTag/FRT/V5-His) into a Flp recombinase

target (FRT) site in the host genome using a Flp-recombinase encoded on a second plasmid (pOG44) (O'Gorman et al., 1991). Integration at a predefined site ensures that the gene will not be inserted at an inactive region of the chromosome, therefore overcoming position effect variegation (Barnes et al., 2003). Furthermore, this method results in a clonal population following transfection, eliminating the need for downstream cloning. In this instance AgeI or HindIII were used as a 3' restriction site allowing for the inclusion or omission of a C-terminal His-tag on the recombinant protein produced.

PCR fragments were purified and digested with the relevant restriction enzymes (as was the vector pSecTag-link). The digested EC2-encoding inserts and vector were ligated according to section 2.2.2.13 and transformed into chemically competent *E. coli* DH5α cells. Overnight cultures were created from the resulting transformants and the plasmid DNA was then isolated via a plasmid miniprep. Plasmid DNA was quantified and an analytical restriction digest was carried out using the restriction sites either side of the multiple cloning site. Digestion products were run on a 1% agarose gel and the presence of an excised fragment indicated a successful ligation (Figure 3.2). Bands in the 350 to 400 bp region of Figure 3.2 are visible in lanes 1, 3, 5 and 8, and indicate successful ligations (their faint appearance is due to the small size in relation to the larger plasmid, 450 bp vs 5000 bp). Successful ligations were then sequenced to confirm the presence of the correct EC2 domain. DNA sequencing was carried out using CMV forward primers and BHG reverse primers (Appendix Table 7.1) to show that the vectors aligned with desired sequence, were in frame and contained no mutations. Once the sequences had been confirmed, fresh transformations were made, scaled up and midi-preps carried out to generate more DNA for subsequent transfections.

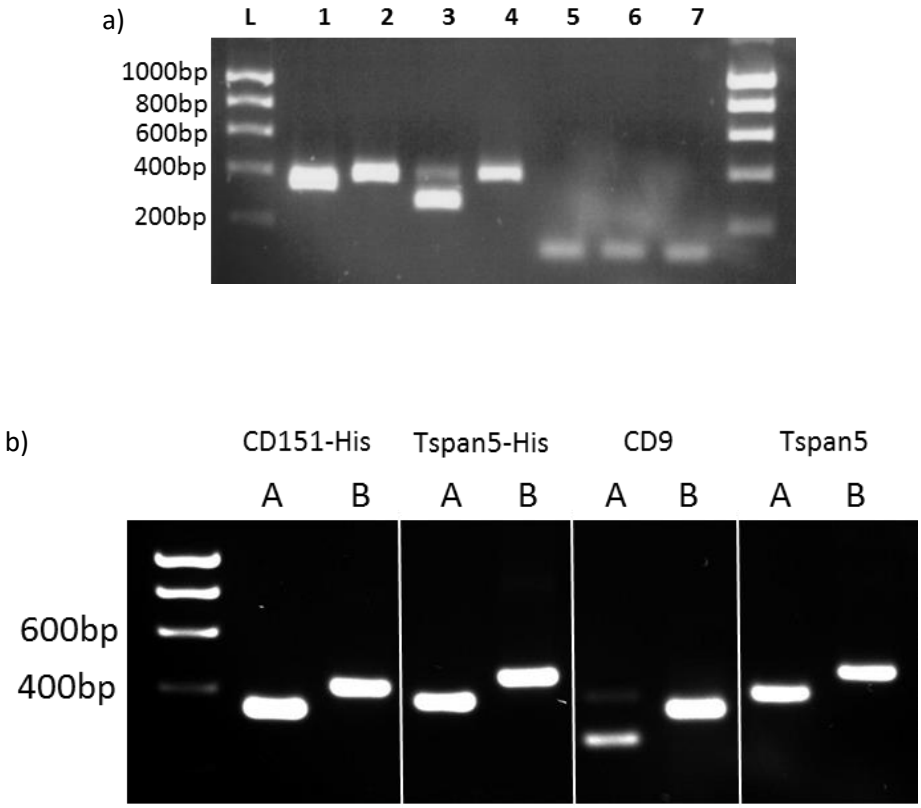

Figure 3.1: PCR amplification of human CD9 and CD151 EC2 genes to generate EC2-leader sequence constructs for cloning into mammalian expression vector. (a) EC2 encoding genes from pGEX bacterial expression vectors and leader sequences from pSec-GHstop plasmid were amplified by PCR. Samples were run on a 1% agarose gel. L: Hyperladder 1kb (Bioline), 1: 151 AgeI, 2: Tspan5 Age1, 3: CD9 HindIII, 4: Tspan5 HindIII, 5: Leader CD9, 6: Leader CD151, 7: Leader Tspan5. (**b**) Following overlap extension PCR products were run on a 1% agarose gel alongside the fragments without addition of a leader sequence. **A** shows the original PCR and **B** shows the fragment with addition of a leader sequence. Both gels show 4 of the 6 inserts that were eventually cloned.

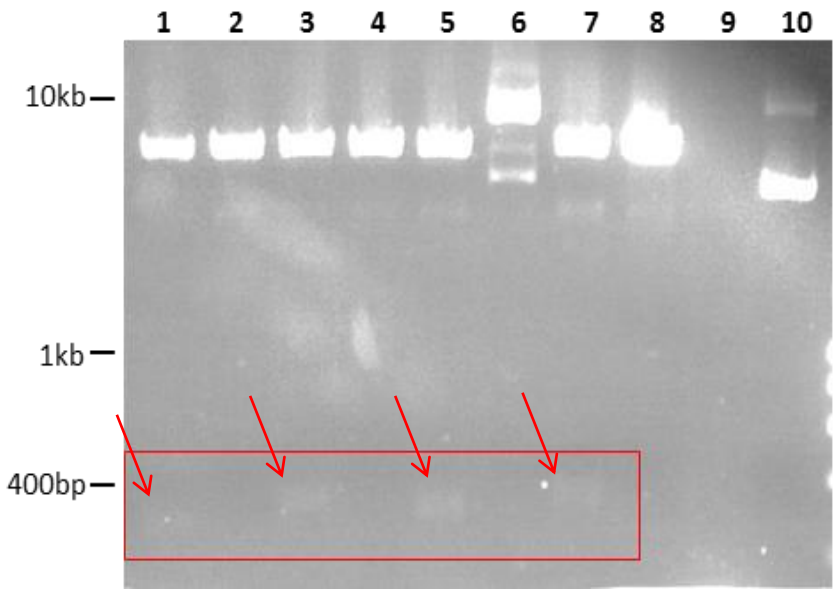

Figure 3.2: Restriction digest analysis of EC2- encoding constructs to confirm ligation. Analytical restriction digests were carried out on potential pSecTAG constructs to check for the presence of the desired tetraspanin EC2 domains inserts Products of digestion were run on a 1% agarose gel and arrows denote insert fragments in lanes 1, 3, 5 and 7. 1-2: CD9-his, 3-6: CD151-his, 7: Tspan5-his, 8: Digested vector 10: Uncut plasmid DNA.

3.2.2 Expression of recombinant EC2 domains in mammalian cells.

CHO and HEK-293 mammalian cell lines were used as hosts for mammalian expression, both of which have been used extensively in industry for recombinant protein expression (Jayapal et al., 2007). CHO cells are very amenable to genetic manipulation and can reach high cell densities in suspension culture allowing for greater protein yields per litre (Jayapal et al., 2007); whilst HEK293 cells, being of human origin, are able produce human patterns of glycosylation so proteins produced may better reflect native tetraspanins in terms of function. Both HEK-293 and CHO cells already containing FRT (Flp recombinanse target) sites were available to us (a kind gift from I. Wilkinson, University of Sheffield, Medical School). These cells were co-transfected via electroporation (Section 2.2.1.12) with an EC2-encoding pSecTag plasmid and the recombinase-encoding plasmid pOG44; some samples were also mock transfected with the pOG44 plasmid alone as a negative control. After selection in hygromycin, supernatant from confluent resistant cells was analysed for tetraspanin protein content.

Supernatants from transfected and non-transfected cells were analysed by Western blot and ELIS using relevant antibodies (as no anti-Tspan5 antibodies are available an anti-his antibody was used instead, figure not shown). Recombinant EC2 proteins previously produced from bacteria were included as a positive control (Figure 3.3). Although positive controls were clear in all blots and ELISA experiments (data not shown), no tetraspanin proteins could be detected in the cell supernatant samples from either transfected CHO or HEK-293 cells when probing with anti-CD9, anti-CD151 or anti-his antibodies. In Figure 3.3(a) and 3.3(b) bands representing CD9 and CD151 respectively are clear in the 27-35kDa region of the positive control lanes along with higher molecular weight bands which are perhaps due to higher order oligomers. However, bands which would be expected at 10 kDa and 13 kDa are absent from lanes containing supernatant from CD9 or CD151 transfected cells respectively.

It was considered that low protein expression levels may have resulted in tetraspanin concentrations in the supernatant being insufficient for detection; therefore efforts were made to increase the amount of protein in each sample. Cells were allowed to grow until 100% confluent before supernatant was again collected and concentrated tenfold as described in 2.2.3.11. Samples were again analysed by Western blot and ELISA. In Figure 3.3(C) and 3.3(d) intense bands are clear in the 37-25 kDa region for positive controls; however there was still no detectable protein in the supernatant of transfected cells and ELISA absorbance values were

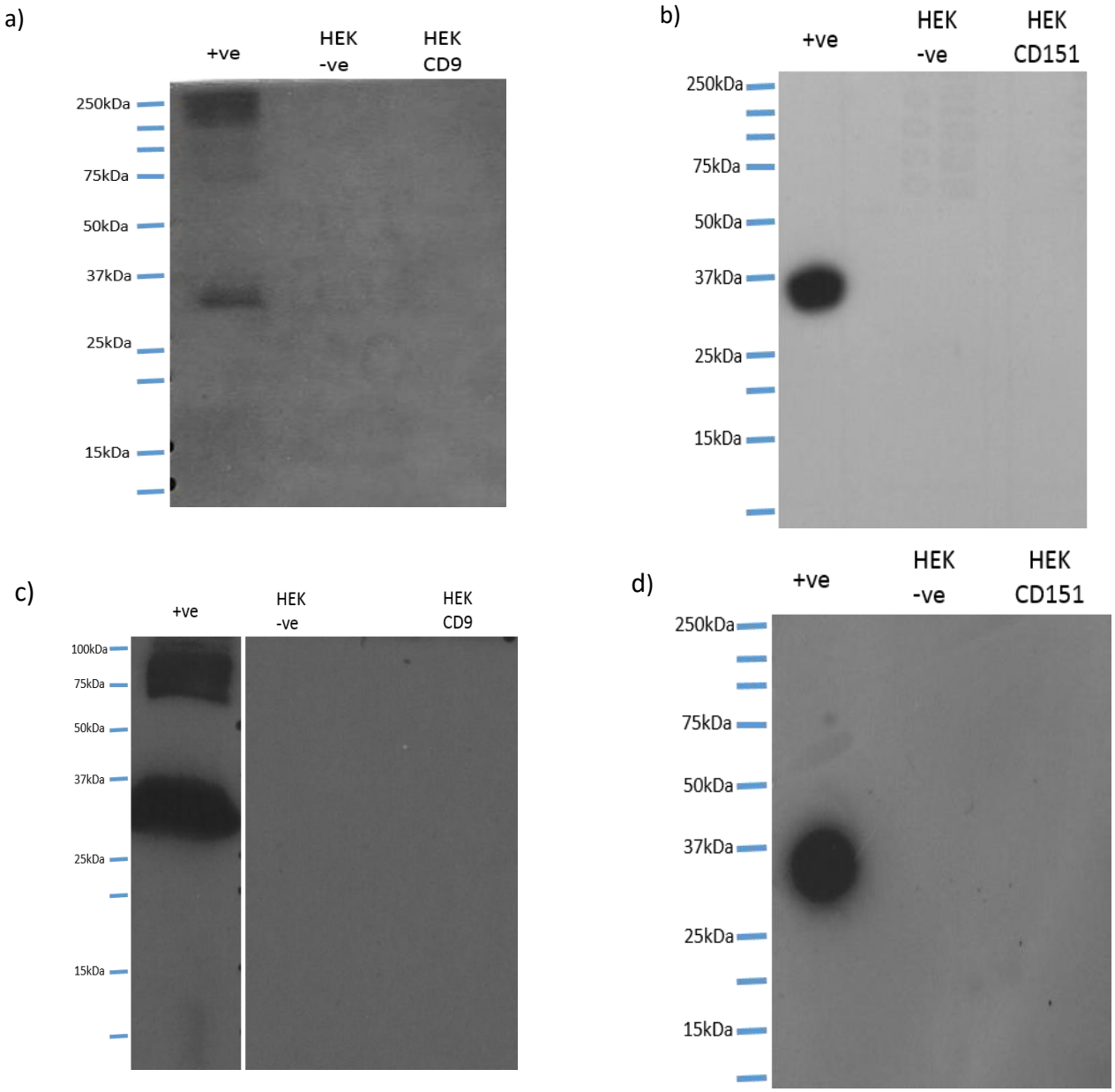

Figure 3.3: Attempts to detect soluble tetraspanin EC2 production in transfected cell supernatants. (a +b) Supernatants from CD9 and CD151 transfected and non-transfected HEK-293 (-ve) cells were analysed via Western blot using relevant specific monoclonal antibodies. Recombinant CD9 EC2 or CD151 EC2 produced in bacteria (~25ug/ml) was included as a positive control (+ve). **(c + d)** as in a+b but supernatant samples were concentrated 10x using Centrisart columns (5kDa cut off) and X-ray films were incubated with membrane overnight rather than the traditional five minutes.

zero (data not shown). A similar result was also seen for CHO transfections and anti-His Western blots used to detect Tspan5 were also negative (data not shown).

The anti-CD9 antibody 602.29 appeared to be the more sensitive of the two anti-tetraspanin antibodies, giving more intense bands with equal amounts of recombinant protein. To determine the limits of detection, bacterially expressed recombinant CD9 was serially diluted and probed with 602.29 in Western blotting. Bands were visible across the membrane down to a minimum of 6µg/ml (Figure 3.4 (a)). A similar approach was taken to determine the sensitivity of an anti-CD9 ELISA with figure 3.4(b) showing an absorbance reading in wells with protein quantities as low as ~80ng/ml.

It was next considered that the protein may be being retained within the cells, if for example the leader sequence was not functioning as intended. To check this, lysates were prepared from, both transfected and non-transfected cells (Section 2.2.1.15) and were then analysed by Western blot and ELISA. An anti-actin Western blot was included to ensure lysis had been successful. Lanes 2 and 3 of figure 3.5(a) show no CD9 protein could be detected in the lysate samples from either transfected or non-transfected CHO cells while bands just below 50 kDa in figure 3.5(b) represent actin, indicating successful lysis. Western blots of HEK-293 cell lysates (data not shown) also displayed endogenous full-length CD9 which further suggests successful lysis and also acts as an additional positive control. As no protein could be detected in intra or extracellular samples, it was speculated that the protein was not being expressed at all (i.e. as a result of problems in translation or transcription). It was considered that the transfection efficiency may be low resulting in very few cells containing the required DNA, but which are able to give passive resistance to the rest of the population.

a)

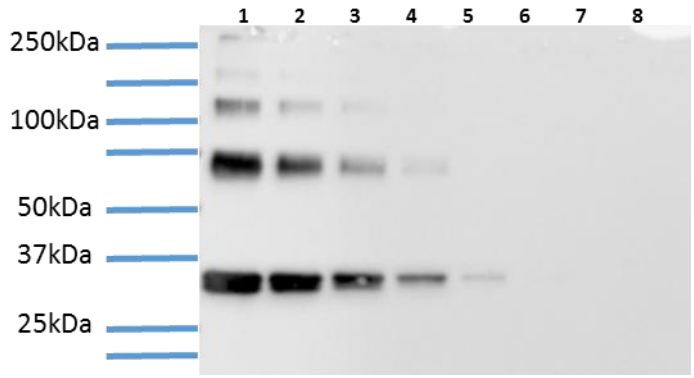

CD9 content (µg/ml)	Detected	Lane
100	Y	1
50	Y	2
25	Y	3
12.5	Y	4
6.25	Y	5
3.13	N	6
1.56	N	7
0.78	N	8

b)

CD9 content µg/ml	10	5	2.5	1.25	.625	.313	.156	.078	.039	.019	.01
10	1.08372	1.31415	1.00313	1.22589	1.35864	1.43232	1.84499	0.954617	0.379711	0.185646	0.10455
5	1.22975	1.47258	1.00903	1.4829	1.67728	1.93713	0.932066	0.381302	0.165939	0.101186	0.070723
2.5	1.28478	1.18935	1.4573	1.78516	1.88349	0.996142	0.393621	0.161146	0.119078	0.091814	0.068388
1.25	1.34881	1.25319	1.74527	1.95137	1.02218	0.336101	0.157859	0.09192	0.072215	0.056764	0.05588
0.625	1.17631	1.48617	1.95641	0.956406	0.393058	0.150348	0.091322	0.091069	0.078013	0.09845	0.05389
0.313	1.14711	1.99898	0.98072	0.431666	0.242423	0.110908	0.104091	0.101925	0.086634	0.145242	0.071004
0.156	1.64498	1.03002	0.485916	0.168586	0.160255	0.083604	0.075776	0.080915	0.07269	0.126425	0.092449

Figure 3.4: Determination of the sensitivity of CD9 EC2 detection in Western blots and ELISA. **(a)** Recombinant CD9 EC2 protein produced in bacteria was diluted with non-reducing loading dye (concentration indicated in the table), run on an SDS-PAGE gel and blotted. Membranes were probed with anti-CD9 antibody, 602.29 (the blot was developed for 5 minutes). **(b)** From a starting concentration of 20 µg/ml recombinant CD9 EC2 was serially double-diluted down and across the wells of a 96-well ELISA plate. Antigen was detected using 602.29 antibody as described in 2.2.3.18. Absorbance readings at 410nm are shown

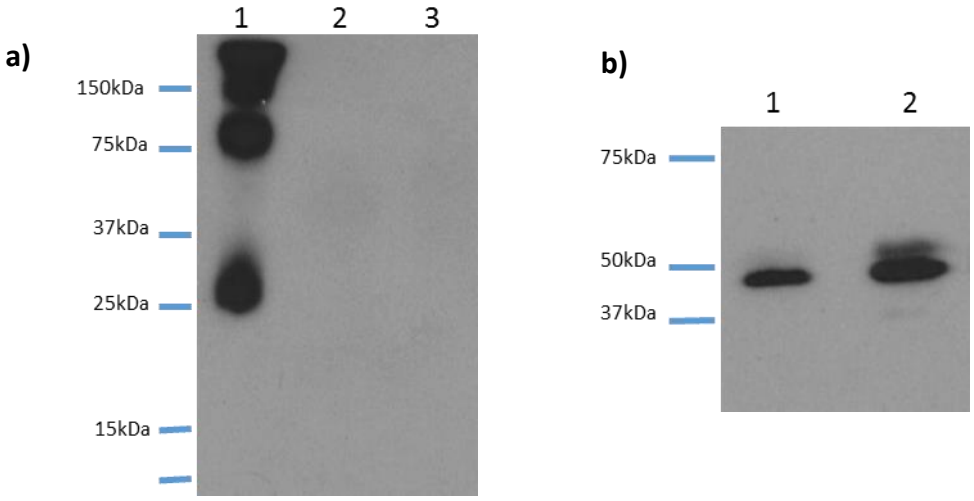

Figure 3.5 Analysis of Lysates of transfected CHO cells by Western blotting. (a) Transfected and non-transfected CHO cells ($5x10^6$) were lysed as in section 2.2.1.15. Lysates (lanes 2 and 3) were run on an SDS PAGE gel under reducing conditions along with Recombinant CD9 EC2 from bacteria (25 µg/ml) which was included as a positive control. Following transfer, membranes were probed with anti-CD9 antibody. 1: bacterially expressed positive control, 2: transfected cell lysate, 3: non-transfected cell lysate **(b)** Cell lysates were also probed with an anti-actin antibody. 1: transfected cell lysate, 2: non-transfected cell lysate

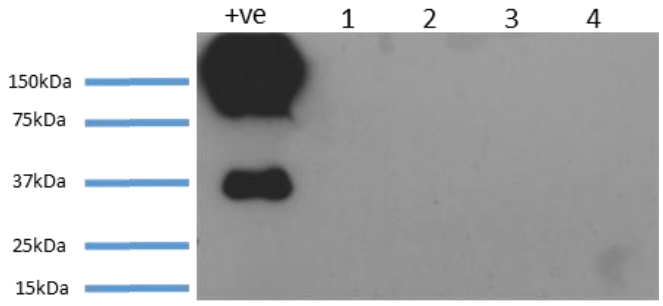

Figure 3.6 Analysis of supernatant and lysates from CHO cells transfected with CD9 encoding plasmid via Turbofect. Supernatant from transfected and non-transfected CHO cells were concentrated tenfold as described in Figure 3.3 and lysates were collected according to section 2.2.1.15. Samples (along with bacterially expressed CD9 as a positive control) were probed by Western blot using an anti-CD9 antibody as described previously. 1: non-transfected cell supernatant, 2: CD9 transfected cell supernatant, 3: non-transfected cell lysate, 4: CD9 transfected cell lysate.

Turbofect™ transfection reagent (Life Technologies) reportedly results in a greater efficiently of transfection than electroporation (I. Yaseen, unpublished data). The reagent consists of a cationic polymer which forms a positively charged complex with DNA in order to deliver DNA to the cell (Oba and Tanaka, 2012). To compare the transfection efficiencies of both methods and to ensure that the methods of transfection were working, CHO cells were initially transfected with a GFP expression vector (pEGFP-N1). Three days following transfection there was a marked difference in the appearance of cells transfected by different the methods, with electroporation initially giving fewer viable cells which were able to adhere. Once cells transfected by both methods had become confluent they were viewed using a Nikon A1 fluorescent microscope. Both methods did yield transfected, fluorescent cells, indicating that the experimental procedures used were sufficient to successfully deliver DNA. However, Turbofect ™ transfection gave a greater proportion of fluorescent cells (approximately 90% vs 60% (Data not shown)). With this apparent increase in transfection efficiency, CHO and HEK cells were once again transfected with the EC2 expression vectors using Turbofect™. However, despite improved initial viability compared to electroporation, still no protein could be detected in concentrated supernatant or lysate samples by Western blot (Figure 3.6) or ELISA (data not shown)

After a number of unsuccessful attempts to detect EC2 protein following transfections with two different cell lines, five expression constructs (CD9, CD151 with and without His and Tspan5) and two transfection methods it was decided to try a different system for expression which forgoes the need for co-transfection. This system uses the expression vector pCI-neo and has previously been used successfully by our group for expression of human CD63 in HEK-293 cells (Jirvairiyakul, 2010). Being as the CD63 pCI-neo construct was already available, cloning into the vector did not require overlap extension PCR and instead the CD9 and CD151 encoding inserts were cloned down-stream of the existing leader sequence. Tspan5 was not cloned into this particular vector because no anti-Tspan5 mAbs are available, making its detection more difficult. Concentrations of G418 to use for selection were established prior to transfection and Turbofect™ was again used for these transfections. Two weeks following transfection, resistant colonies were clear (Figure 3.7). However, upon testing lysate and concentrated supernatant samples of CD9 transfected cells, these proteins still could not be detected by Western blot (Figure 3.8) or ELISA analysis (data not shown) (the same results were seen for CD151 transfection and when using HEK-293 cells, data not shown).

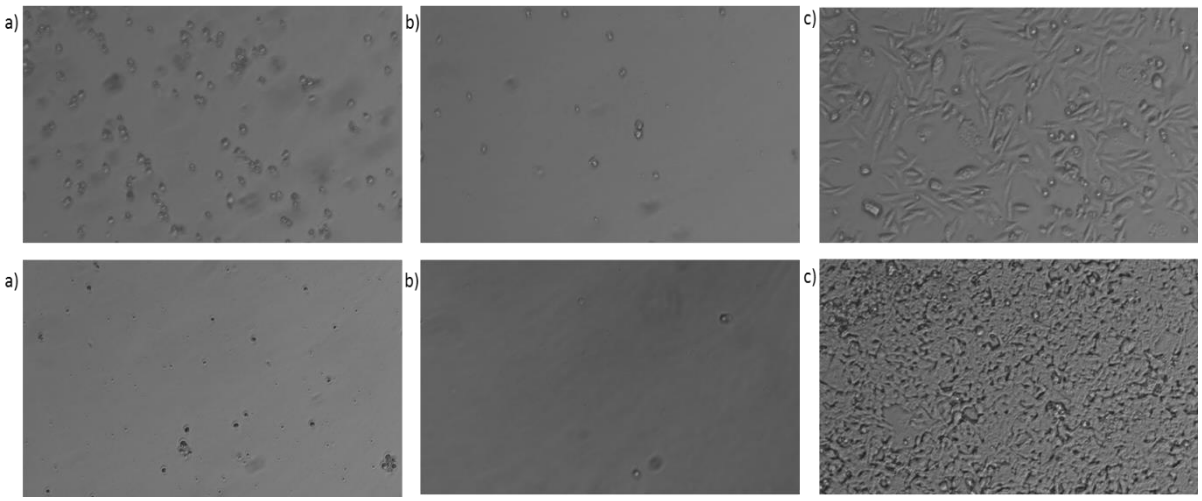

Figure 3.7 Images of CD9 pCI-neo transfected CHO and HEK-293 cells following selection using G418. Following transfection, cells were grown in DMEM containing G418 (1mg/ml CHO, 500µg/ml HEK-293) for two weeks **(a)** non transfected **(b)** mock transfected **(c)** CD9 pCI-neo transfected. Random fields were captured using a Nikon Diaphot brightfield microscope using a 10x objective.

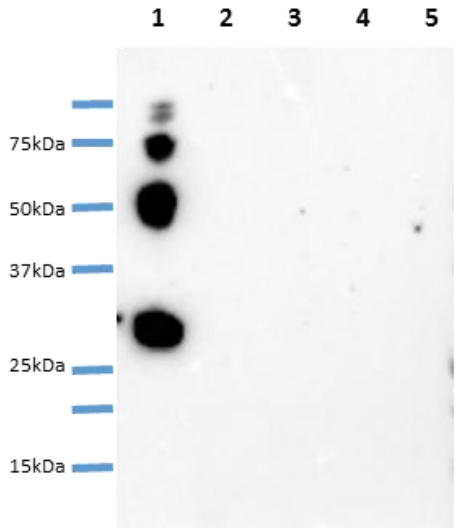

Figure 3.8: Analysis of Supernatant and Lysates from CD9 pCI-neo transfected CHO cells. Supernatant and lysates from CHO cells transfected with CD9 pCI-neo and non-transfected CHO cells were collected. After SDS-PAGE and blotting, membranes were probed using an anti-cd9 antibody as described previously, using bacterially expressed CD9 as a positive control. 1: Bacterially expressed positive control, 2: non-transfected cell supernatant, 3: CD9 transfected cell supernatant, 4: non-transfected cell lysate, 5: CD9 transfected cell lysate.

3.2.2.1 Analysis of mammalian transfection

To determine if the initial stages of transfection had been successful, attempts were made to check if the CD9 EC2 encoding DNA has been stably introduced into the cells. Genomic DNA was isolated from CD9 transfected HEK-293 FLP-in cells from pCI-neo transfected CHO cells, along with their non-transfected counterparts. The isolated nucleic acid was used as a PCR template to detect if the encoding DNA for CD9 EC2 was present (Figure 3.9). In both instances positive controls bands are clear, as are bands in the transfected cell samples, with no amplification product in non-transfected negative controls. This demonstrates that the coding DNA is present in the cells; however, it is possible that the DNA is not being transcribed.

To address the possibility that the gene encoding CD9 EC2 was not being transcribed, levels of cellular RNA were investigated. Total cellular nucleic acid was firstly isolated from the CD9 EC2 transfected HEK-293 and CHO cells as described in section 2.2.2.14. DNA in the samples was digested to leave only the RNA fraction and reverse transcription was carried out on each sample to produce cDNA (Section 2.2.2.15), in some cases the reverse transcriptase was omitted to give negative control samples for contaminating cellular DNA. The cDNA samples were used as PCR templates to amplify either the β-actin RNA as a positive control or CD9 EC2 encoding RNA (Figure 3.10). Actin control bands can be seen in each sample with the reverse transcriptase and are not present in those without it, thus indicating that the only DNA present in the samples results from reverse transcription of RNA. CD9 EC2 bands can be seen in transfected cells but not in the non-transfected negative control lanes (Figure 3.10b), indicating that the CD9 encoding DNA being transcribed.

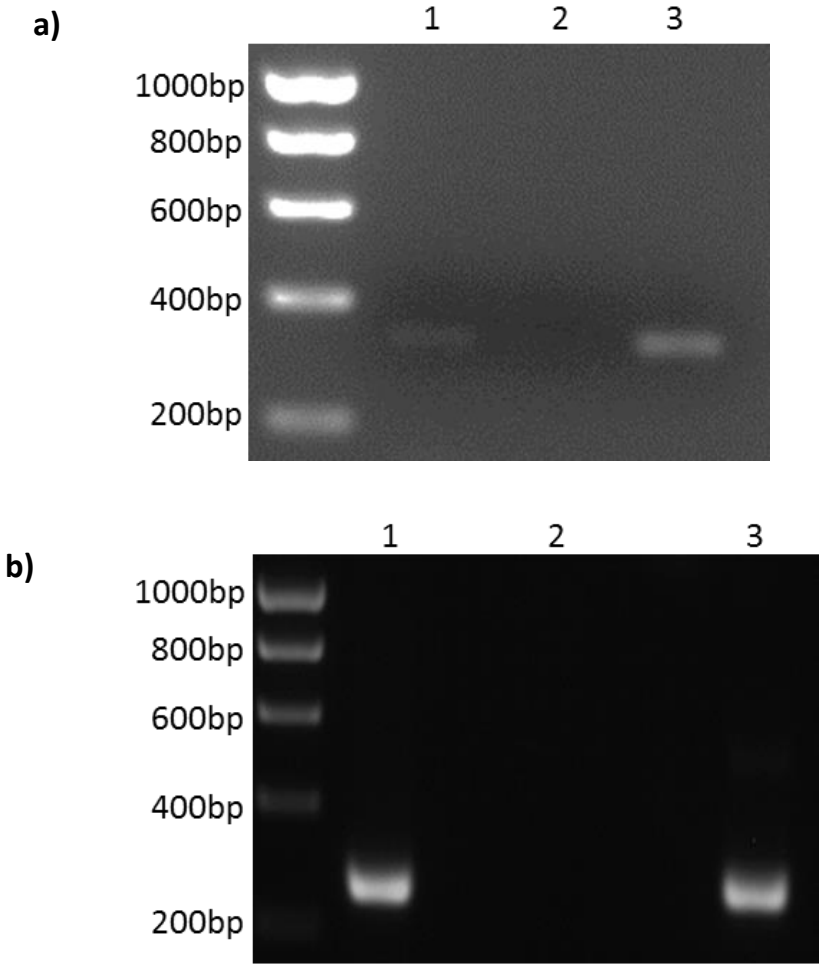

Figure 3.9: PCR analysis of Flp-in and pCI-neo transfected cells to check for incorporation of expression gene. (a) Genomic DNA was isolated from pSecTag-CD9 transfected HEK-293 cells and non-transfected HEK-293 cells according to section 2.2.2.14. Purified expression vector DNA from bacteria or genomic DNA from non-transfected or transfected cells was used as a template for PCR using leader sequence forward and CD9 reverse primers for amplification (Appendix Table 7.1) 1: Positive control (expression vector DNA purified from bacteria), 2: Genomic DNA from non-transfected cells, 3: Genomic DNA from transfected cells. **(b)** Genomic DNA was isolated from CD9-pCI-neo transfected CHO cells and non-transfected CHO cells. Purified expression vector from bacteria or genomic DNA from non-transfected or transfected cells was used as a template for PCR using CD9F and CD9R primers (Appendix table7.1) 1: Positive control (expression vector DNA purified from bacteria), 2: Genomic DNA from non-transfected cells, 3: Genomic DNA from transfected cells.

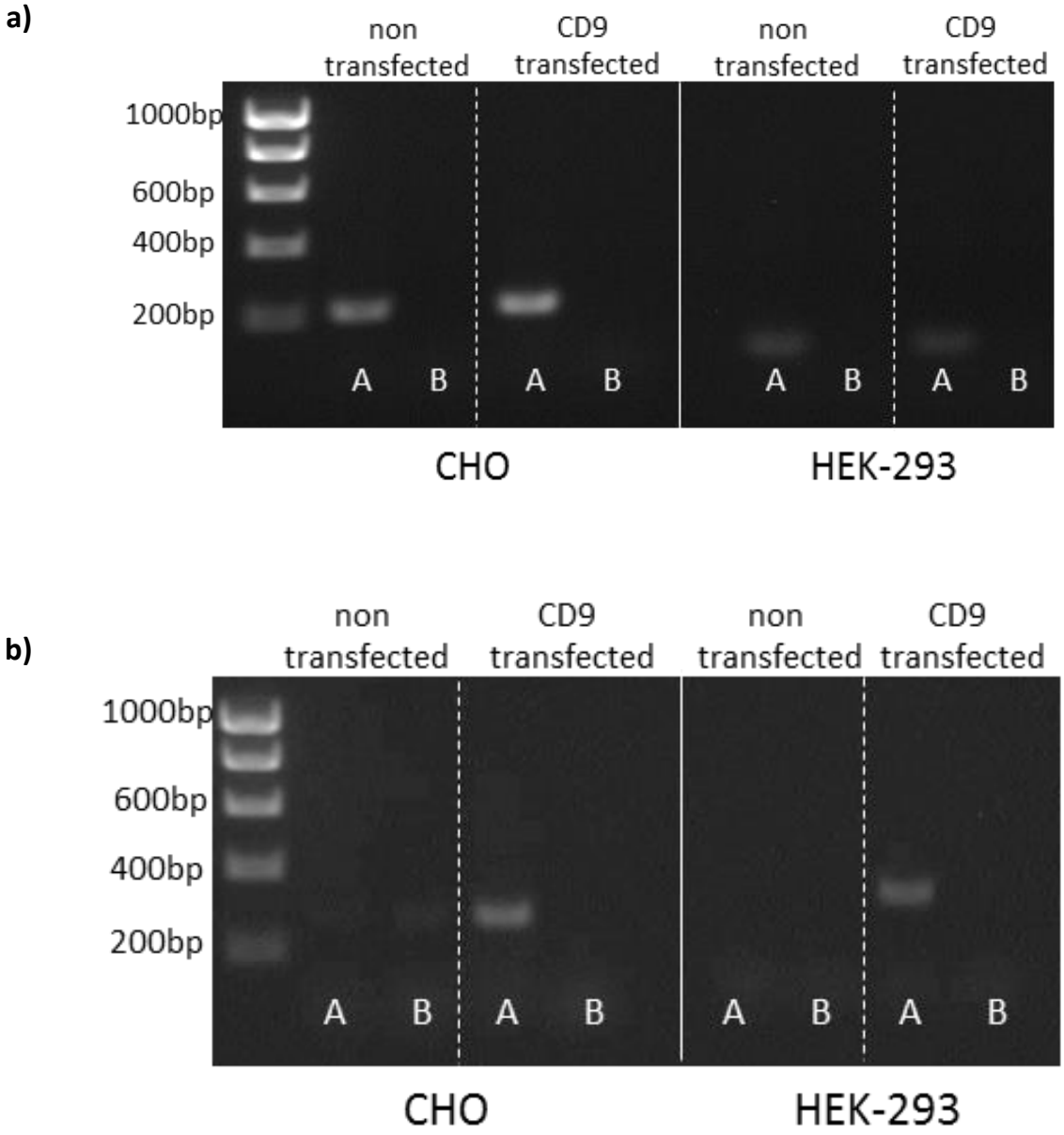

Figure 3.10: PCR analysis to check for CD9 EC2 encoding mRNA in transfected CHO and HEK-293 cells. Total nucleic acid was isolated from transfected and non-transfected CHO and HEK cells and DNA was digested using DNase. In A samples reverse transciptase was added to make cDNA, in B samples reverse transcriptase was omitted. cDNA was used as a template for PCR using **(a)** actin primers (Appendix table 7.1) **(b)** CD9 EC2 primers described in Figure 3.9. amplification is specific for recombinant DNA and not for endogenous CD9 encoding DNA.

3.2.3 Expression of recombinant EC2 domains in insect cells

Since numerous attempts to produce recombinant EC2 domains from mammalian cells using different approaches were unsuccessful, it was proposed that insect cells, specifically Sf9 cells, might be a suitable alternative for protein expression. Insect cells are able to perform post-translational modifications so would produce glycosylated EC2 domains, and their ability to produce correctly folded proteins is second only to mammalian cells (Altmann et al., 1999). Furthermore, as they grow in suspension, high cell densities are more easily attained, which could lead to higher protein yields.

CD9 and Tspan5 were selected as initial candidates for insect expression as the different numbers of theoretical disulphide bonds (2 and 4 respectively) should give an indication as to how well this system can cope with the tetraspanin EC2 domain folding patterns. Genes for both the EC2 domains and full-length versions of CD9 and Tspan5 were amplified with the view to later structural studies. Primers were designed to introduce his-tags at either the N- or C- terminal ends of the tetraspanin proteins. The tetraspanin genes were amplified from constructs corresponding to the EC2 regions in the p-GEX vectors (Higginbottom et al., 2003) or full length tetraspanins in pEE6 vectors (Higginbottom et al., 2000a) that had previously been generated in the laboratory, and amplification products were run on a 1% agarose gel (Figure 3.11). Bands at ~250 bp in lanes 1, 2, 5 and 6 are the correct size for the EC2 domain encoding regions, whilst products at 650 bp in lanes 3, 4, 7 and 8 are the correct size for full length tetraspanin genes. PCR products were digested and ligated into either pACSEC1 (which contains a gp64 leader sequence) for EC2 expression or pVL1393 for the full length protein. The ligation products were used to transform *E. coli* DH5α competent cells as described in 2.2.2.6.

Once the tetraspanin-encoding sequences had been confirmed as correct, the plasmids were mixed with baculovirus DNA as described in section 2.2.1.14. During incubation, homologous recombination takes place which incorporates the gene of interest into the viral genome. The gene of interest is under the control of the polyhedron promotor, a strong very late stage promotor at its maximum during the lytic phase of the virus cycle. The baculovirus expression/DNA mixture was combined with the cationic lipid, Cellfectin (Life Technologies), which results in the formation of a cationic lipid-DNA complex. This complex was incubated with the cells where it fuses with the cell membrane and enters via subsequent endocytosis. After culturing the cells for five days, primary viral isolates were harvested and used to infect a larger volume of cells; secondary viral isolates were subsequently used to infect further cells.

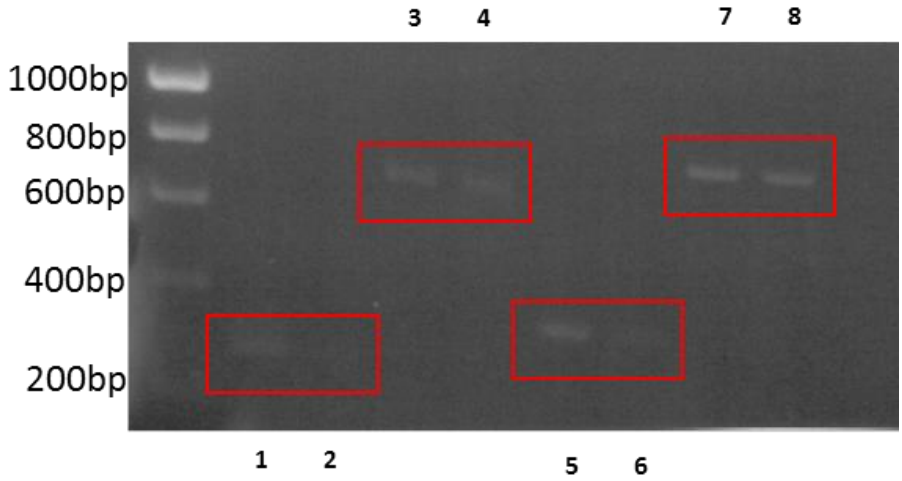

Figure 3.11 PCR amplification of full length CD9 and Tspan5 and EC2 domains CD9 and Tspan5 for cloning into insect expression vectors. DNA encoding CD9 and Tspan5 EC2 domains and full length protein were PCR amplified from pGEX and pEE6 expression vectors respectively. PCR products were run on a 1% agarose gel. 1 = CD9 EC2 5'His, 2= CD9 EC2 3' His, 3= CD9 full length 5' His, 4 = CD9 full length 3'His, 5 = Tspan5 EC2 5' His, 6 =Tspan5 EC2 3' His, 7 = Tspan5 full length 5' His, 8 = Tspan5 full length 3'His.

Once these insect cell cultures had reached the desired density, cells were harvested and frozen at -80ºC whilst supernatants were subjected to nickel affinity chromatography (Section 2.2.3.8) in an attempt to isolate his tagged protein. Samples were taken at each step of the purification and run on a polyacrylamide gel along with the eluted protein. Recombinant CD9 EC2 protein produced in bacteria was used as a positive control for the anti-CD9 Western blots as described in previous sections.

An absence of bands in lanes 1-4 and lanes 6-9 of Figure 3.12a show that no CD9 EC2 protein could be detected in the column flow through, wash or fractions eluted with imidazole from the attempted purification of CD9 EC2 His-tagged at the N- or C- terminal ends. Again it was considered that protein could be being retained within the cells, so cell pellets were thawed and lysed by sonication as described in 2.2.3.5. Cell lysates also underwent nickel affinity chromatography; flow-through, wash and eluted samples were again subjected to Western blot analysis. Lanes 2-9 of Figure3.12 (b) again show that no CD9 protein could be detected in any fractions of the purification. Further attempts were made using different titres of secondary viral isolates for the infection of more cultures; however similar results were observed with no tetraspanin EC2 proteins being detected (data not shown).

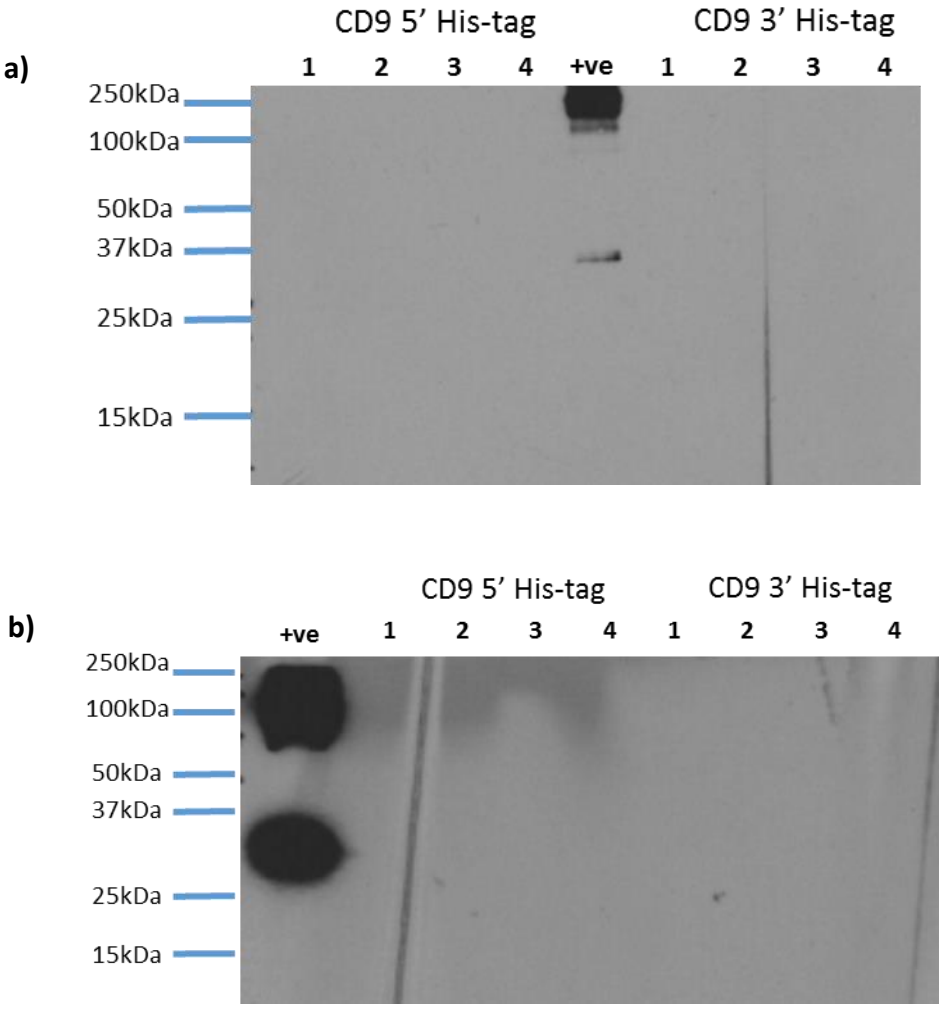

Figure 3.12 Attempted purification of His-tagged CD9 EC2 protein from insect cell supernatants using nickel affinity chromatography. (a) Supernatants collected from transfected insect cells (2.2.1.14) were subjected to nickel affinity chromatography (2.2.3.8). Samples from each step of purification were run on a SDS-PAGE polyacrylamide gel, blotted and the membranes probed with anti-CD9 antibody. 1= Initial flow through, 2= Wash, 3= 500mM imidazole elutate 1, 4= 250mM imidazole eluate, +ve: CD9 EC2 control. **(b)** Cell lysates from transfected cells were also subjected to nickel affinity chromatography and were analysed as described in (a) 1= Flow through, 2= Wash, 3= 500mM imidazole eluate, 4= 250mM imidazole eluate, +ve= Positive control.

3.2.4 Expression of recombinant EC2 domains in bacteria

3.2.4.1 Rationale for bacterial expression

Although the recombinant EC2-GST fusion protein expressed in *E. coli* have some limitations (e.g. lack of glycosylation and possible contamination with LPS) they have shown biological activity in a number of functional studies and have proven useful in finding out more about tetraspanins as a whole (Green et al., 2011; Ho et al., 2006; Parthasarathy et al., 2009; Takeda et al., 2003; Zhu et al., 2002). Because of the problems encountered in trying to express soluble EC2 proteins in the eukaryotic systems described above, the EC2 domains of CD9, CD63, CD81 and CD151 were subsequently expressed in *E. coli* to provide protein for use in later functional studies (Chapters 4 and 5).

Expression of disulphide containing proteins in bacteria is challenging due to the reducing environment of the cytoplasm. This issue can be circumvented in a number of ways, for example by expressing the proteins into the periplasmic space where Dsb enzymes facilitate the formation of disulphide bonds (Baneyx and Mujacic, 2004; Qiu et al., 1998). Here, however, a strain of *E. coli* called Rosetta-gamiB(DE3) (Novagen) were used, which have mutations making them amenable to the expression of di-sulphide containing protein in the cytoplasm. For di-sulphide bonds to form, enzymes must be present to oxidise amino acid thiol groups. In the *E. coli* cytoplasm thioredoxins TrxA and TrxC along with the three glutaradoxins, are capable of doing this, but are kept in a reduced state by a thioredoxin reductase (TrxB) and Glutathione (Gor) respectively. In Rosetta-gami cells *trxB* and *gor* mutations result in the oxidised form of the thioredoxins and glutaradoxins, thus enabling disulphide bond formation (Bessette et al., 1999). Rosetta-gami also contain a pRARE plasmid which encodes the tRNA for codons rarely seen in *E. coli,* enabling the expression of human proteins more efficiently (Brinkmann et al., 1989)

The proteins were expressed as GST-fusion proteins via the use of the vector, pGEX-KG. This enables simple one-step purification through glutathione chromatography, and in some cases the GST tag has been suggested to aid in the solubility of the tagged protein (Shih et al., 2002). This particular vector includes a thrombin cleavage site for downstream removal of the GST tag along with a flexible glycine rich linker region to improve cleavage efficiency (Guan and Dixon, 1991).

3.2.4.2 Bacterial expression of EC2 domains and subsequent purification

Previously generated pGEX-KG expression vectors encoding N-terminal GST tagged EC2 domains were used to transform Rosetta-gami competent cells (Section 2.2.2.6). After induction with IPTG, cultures were harvested and bacteria lysed as described in 2.2.3.5 and GST tagged proteins were then purified by affinity chromatography as described in 2.2.3.6. Samples from each step of the purification were run on a SDS PAGE gel and subsequently stained with Coomassie blue (Figure 3.13).

The eluted protein from each purification (shown in lanes 6 and 7) was largely composed of the full length tetraspanin EC2-GST fusion protein (indicated by a red arrow); however there are a number of contaminating bands also. Lower MW bands are most likely products of truncation or proteolytic cleavage of the GST tag, indeed a band indicative of free GST can be seen at ~25 kDa. An anti-GST Western blot of the eluted proteins (Figure 3.14a) shows GST containing products at intervals below the expected full length fusion protein; this further indicates that bands of lower molecular weights are indeed a result of degraded full length protein or truncated expression.

The insoluble protein fraction was resuspended in loading dye and run alongside the samples from affinity purification (Figure 3.13 lane 1) and in each case a band can be seen at positions corresponding to the respective tetraspanin EC2 fusion proteins. Interestingly the size of the band seems to inversely correlate with the final protein yield (shown in table 3.2); this suggests that lower yields of soluble protein (e.g. for CD63 and CD151 purifications) are a result of the protein forming insoluble protein aggregates. Additionally, small amounts of tetraspanin protein can be seen in the wash steps (lanes 3, 4 and 5) of CD9 and CD81 purifications; this is probably due to oversaturation of beads as these bands cannot be seen in CD63 and CD151 purification. Eluate protein concentration was quantified using absorption at 280 nm and the proportion of correctly folded material (indicated by a red arrow) determined by densitometry using the software ImageJ.

The EC2-GST fusion proteins were recognised via Western blotting using anti-tetraspanin antibodies, with bands being detected at the expected molecular weights in the non-reduced lanes of Figure3.14 (b). Higher molecular weight bands can also be at ~75 kDa and are thought to represent oligomers or protein aggregates. As these larger bands are not observed in Coomassie stained polyacrylamide gels of proteins under reducing conditions, it may be that these higher order structures are reliant on the correct folding of the proteins or that they are a result of some aberrant disulphide bond formation. Additionally, GST contains four solvent

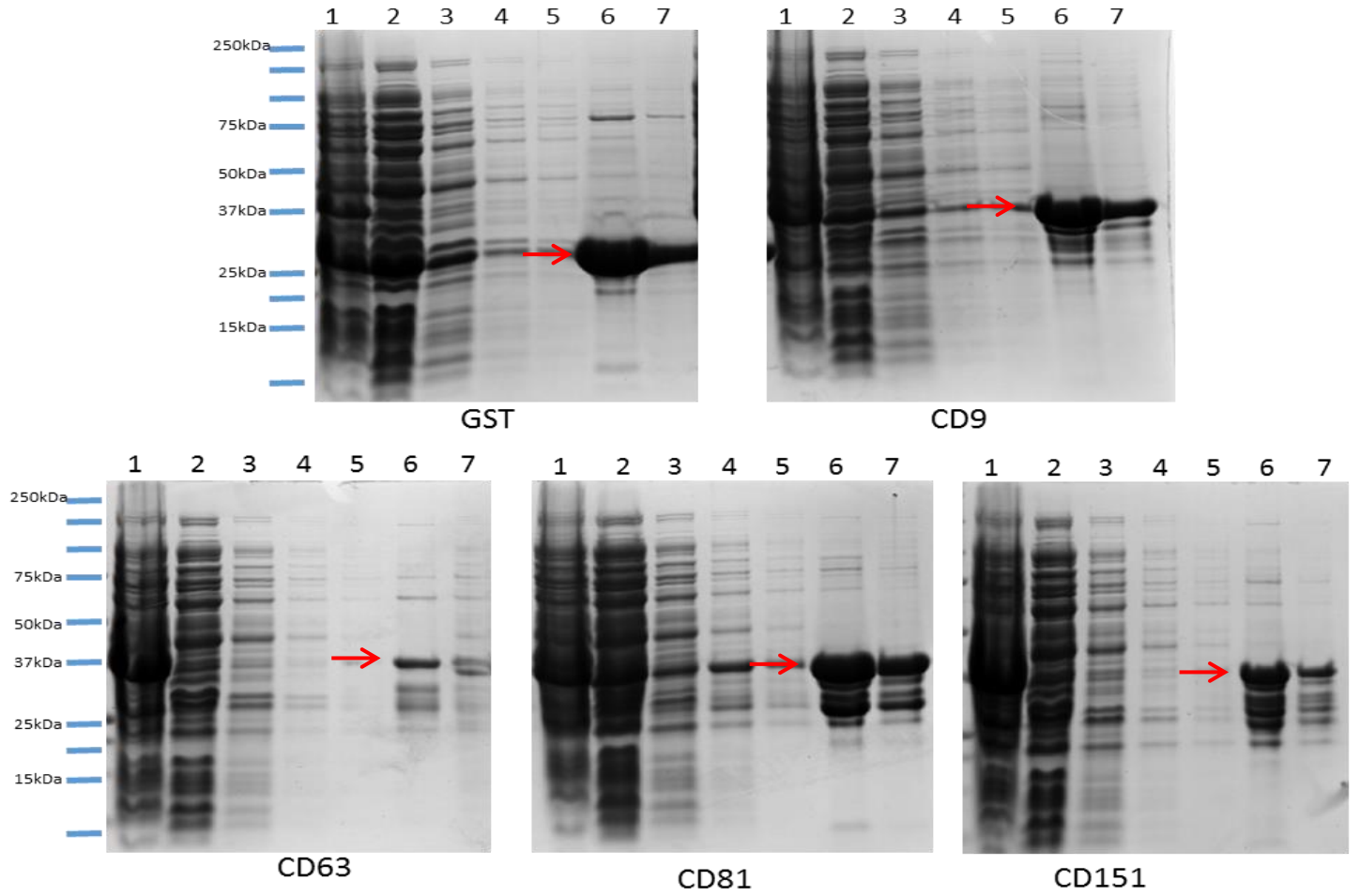

Figure 3.13: Glutathione affinity purification of GST and four tetraspanin EC2 domains from Rosetta-gami cells. Rosetta-gami B(DE3) *E. coli* cells transformed with tetraspanin EC2 encoding pGEX vectors were used to express GST-tagged proteins as described in 2.2.3.4.. Lysates underwent glutathione affinity chromatography (Section 2.2.3.6) and samples taken at each stage of the purification, (and the insoluble fraction which was retained after lysis and resuspended in 1x reducing loading buffer) were run on a polyacrylamide gel and stained with Coomassie blue. 1 = insoluble fraction, 2 = Not bound to beads, 3 = 1st wash, 4 = 2nd wash, 5 = 3rd wash, 6 = Eluate 1, 7 = Eluate 2.

Protein	Yield per gram of bacteria (mg)
GST	3.529
CD9	1.979
CD63	0.255
CD81	2.532
CD151	0.964

Table 3.1: Tetraspanin EC2 protein produced per gram of bacterial pellet as determined by absorbance at 280 nm. Purified proteins were quantified using a nanodrop.

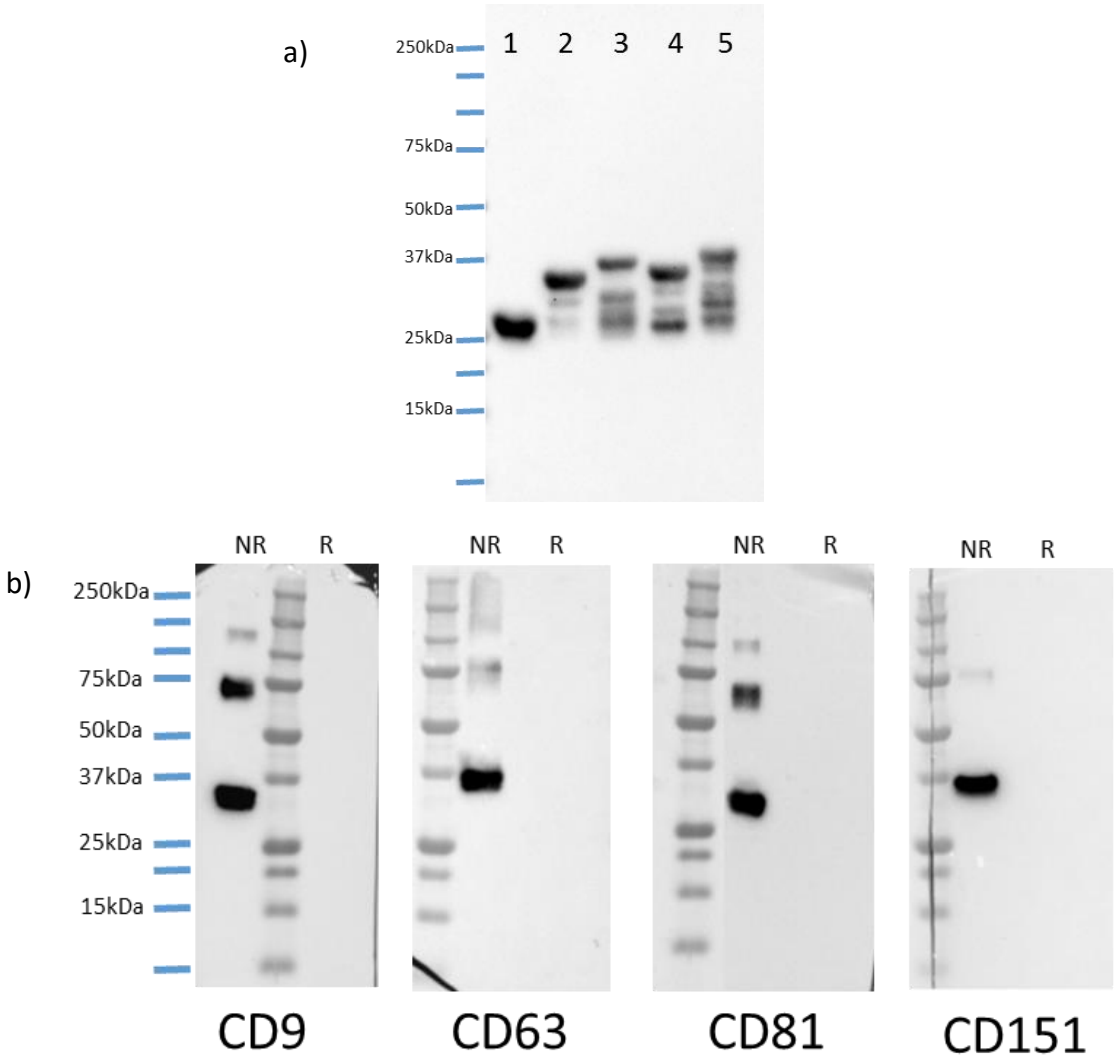

Figure 3.14 Western blot analyses of purified tetraspanin EC2 domains. (a) Purified Proteins (50 µg/ml) were run under reducing conditions on a polyacrylamide gel, blotted and probed with an anti-GST antibody. 1 = GST, 2 = CD9 EC2, 3 = CD63 EC2, 4 = CD81 EC2, 5 = CD151 EC2 **(b)** Purified tetraspanin proteins (50 µg/ml) were run under reducing (R) or non- reducing (NR) conditions on a polyacrylamide, blotted and probed with the relevant anti-tetraspanin antibodies.

exposed cysteine residues which can contribute to the formation of protein aggregates upon oxidation (Kaplan et al., 1997). Western blotting (Figure 3.14 (b)) also demonstrates that recognition of the tetraspanin EC2 proteins by their respective antibodies is abolished under reducing conditions. This indicates that the monoclonal antibodies used are conformationally sensitive and exhibits a requirement of di-sulphide bonds for the correct folding of the EC2 domains.

3.2.4.3 Optimisation of bacterial EC2 domain expression

Visual inspection of Coomassie-stained polyacrylamide gels (Figure 3.13), along with the data presented in Table 3.2, indicates the relative protein yield from the expression and purification of each EC2 domain. Although only small amounts of EC2-GST fusion proteins are generally required for functional assays, it is desirable to optimise protein yields to reduce additionally rounds of expression and facilitate experiments which require higher quantities of protein (e.g. structural studies). Furthermore, alternative methods of purification might reduce contaminants in the final product. In an attempt to increase the amount of soluble protein from the purification a number of parameters were altered.

IPTG is used as an inducer of the Lac promoter (or derivatives thereof) but at high concentrations can inhibit cell growth (Marbach and Bettenbrock, 2012). The effect of varied IPTG levels on CD63 expression by pGEX-CD63 transformed Rosetta-gami cells was investigated. Western blot analysis (Figure 3.15) showed a decrease in the band intensity with increasing levels of IPTG indicating that lower concentrations of IPTG favour higher amounts of correctly folded CD63 EC2-GST but that this effect plateaus at a concentration of 0.1 mM (indicated by the small difference between 0.1 and 0.25mM IPTG). As the entire cellular contents were loaded here, these results reflect total protein production and not levels of soluble protein.

Rajesh and co-workers (2012) also expressed EC2 domains in *E. coli* and favour longer incubation (12hours) at lower temperatures (18^{o}C) post induction. To determine the effects of prolonged incubation on EC2 expression, cells transformed with pGEX-CD81 were incubated for varying lengths of time after IPTG induction. GST tagged proteins were purified from the soluble fraction as described previously (Section 2.2.3.6) and samples were analysed on polyacrylamide gels. As shown in Figure 3.16, there is a decrease in full length protein (indicated by a red arrow) as soon as six hours after induction and a simultaneous increase in a band at 25 kDa indicative of free GST. These results suggest that prolonged incubation leads to far greater occurrence of aberrant proteolytic cleavage of the GST tag.

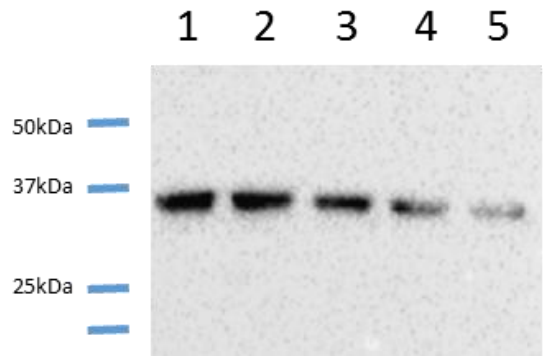

IPTG used (mM)	Density, relative to 0.1mM	Lane
0.1	1.00	1
0.25	0.98	2
0.5	0.73	3
0.75	0.44	4
1	0.21	5

Figure 3.15: Effect of increasing concentration of IPTG on CD63 expression. *E. coli* transformed with p-GEX encoding CD63 EC2 were grown to an OD_{600} of 0.6 before being induced with varying concentrations of IPTG. After four hours, bacteria were harvested by centrifugation and resuspended in 1x non-reducing SDS loading buffer, boiled and run on an polyacrylamide gel. After blotting membranes were probed with an anti-CD63 antibody.

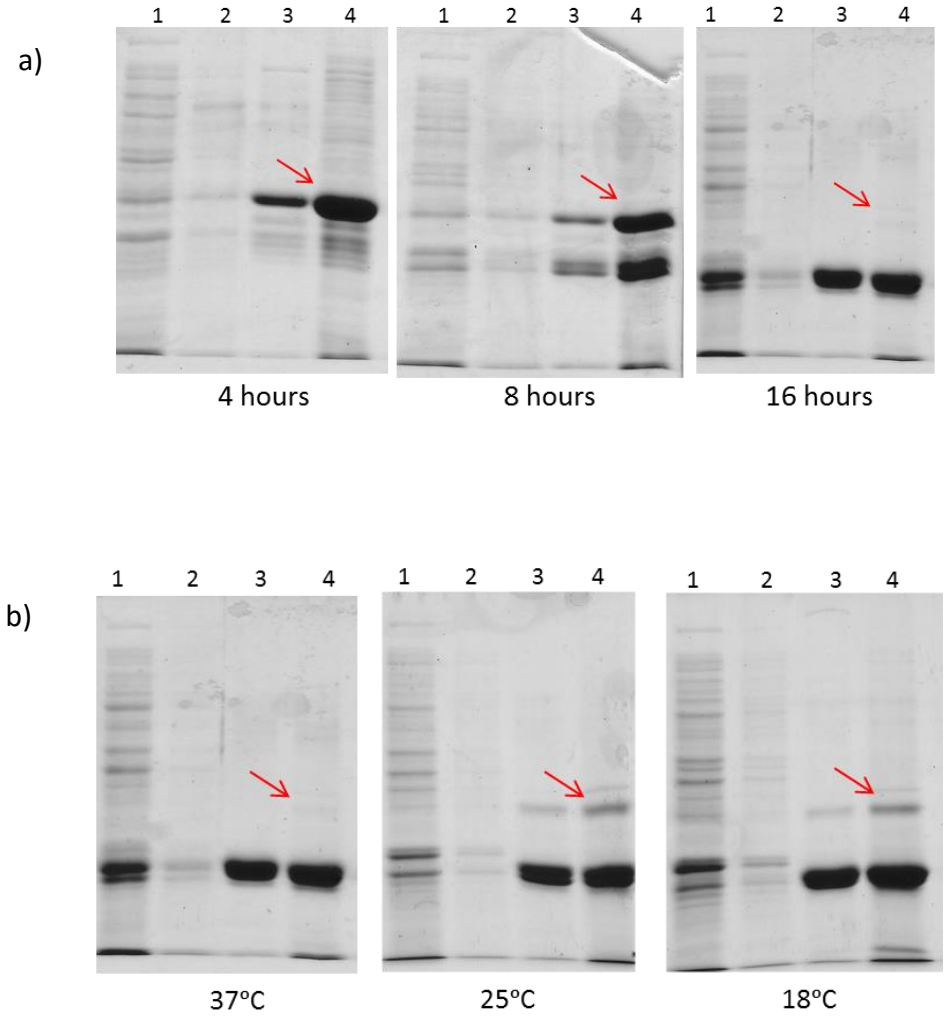

Figure 3.16: Effect of prolonged incubation (post IPTG induction) and temperature on CD81-EC2 expression. (a) *E. coli* transformed with pGEX-CD81 were grown to an OD_{600} of 0.6, induced with 0.1mM IPTG, incubated for varying lengths of time then harvested by centrifugation and frozen. Cell pellets were subsequently resuspended lysed and lysates were used for glutathione affinity purification (2.2.3.6). Samples from each stage of the purification were run on a polyacrylamide gel and stained with coomassie blue. 1= 1st wash , 2= 2nd wash 2, 3= eluate 1, 4= Protein remaining on GST beads **(b)** As in (a) but cells were incubated at the temperatures shown for 16 hours post induction.

Decreasing the temperature used for prolonged incubation after induction (Figure 3.16) reduces the amount of cleavage taking place but yields are still lower than those attained from the four hour expression period. Column and batch methods of affinity purification of GST-tagged tetraspanin EC2s were also compared. Our group has recently favoured the use of a batch method of glutathione affinity purification over the previously used column method (sections 2.2.3.6 and 2.2.3.7 respectively). This is mostly due to the increased control over elution volumes in the batch method; if for example a higher concentration of protein is required, a lower elution volume can be used. However, it is conceivable that different methods of purification may result in slightly different end products, with one concern being that EC2 proteins purified by the batch method might contain higher levels of contaminants, such as LPS. Both methods were compared using Rosetta-gami cells transformed pGEX-CD9. Following expression and lysis, half of the lysate was used in a batch method of purification and half in the column method (Figure 3.17a and 3.17b). Similar yields of protein were recovered from each purification method, eluted proteins (lanes 5 and 6) have a similar appearance in terms of lower molecular weight bands and the amount of full length protein (determined by densitometry) was almost identical (~48% for the batch method and ~47% for column). The second and third wash steps (lanes 3 and 4) of the column method contain more protein, however the weight of the proteins suggest that it is CD9 EC2 eluting from the column rather than contaminating protein so may not be indicative of more thorough washing. LPS levels in recombinant CD9 EC2 proteins resulting from both methods of purification were also similar (displayed figure 3.16c) and would indicate that, with respect to endotoxin contamination, neither method is favourable.

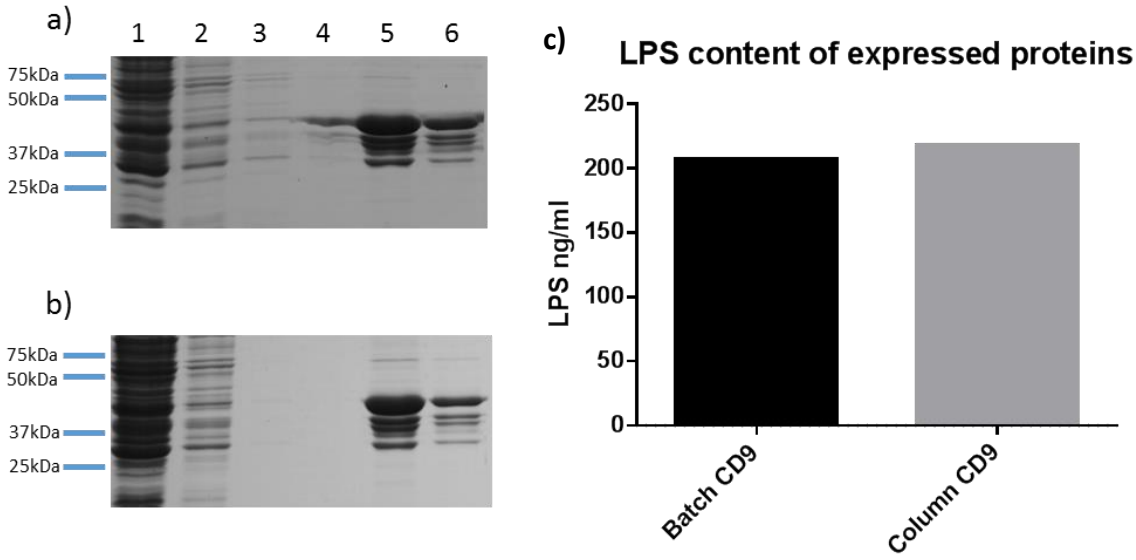

Figure 3.17: Comparison of batch and column purification methods. *E. coli* transformed with pGEX-CD9 were grown, harvested and lysed as described in 2.2.3.4 and 2.2.3.5. GST-tagged proteins purified by glutathione affinity purification according to **(a)** batch method (2.2.3.6) or **(b)** column method (2.2.3.7). Samples from each step of the purifications were run on a polyacrylamide gel which was stained with Coomassie blue. 1= Non-bound protein, 2= 1st wash, 3= 2nd wash, 4 = 3rd wash, 5= eluate 1, 6 = eluate 2 **(c)** LPS levels in a 500nM solution of CD9 EC2 (eluted 1, lane 5) from each method of purification were quantified using a Pierce LAL endotoxin quantitation kit (2.2.3.13) data is representative of two repeats.

3.2.5 Cloning and expression of rat CD63 EC2 domain

The majority of recombinant EC2 domains used by our group are those corresponding to human tetraspanins, however, previous reports have suggested that EC2 domains originating from different species can have significantly different effects in functional assays (Ho et al., 2006; Parthasarathy et al., 2009). For use in functional assays involving rat cells (described in Chapter 4), rat CD63 was chosen to be expressed (becuase of the tetraspanins investigated here, this member shows the most variation between rat and human orthologues (see Appendix).

A plasmid containing the full-length rat CD63 cDNA was purchased from OriGene. Primers were designed to amplify the EC2 domain (Appendix Table 7.1) and included restrictions sites to allow incorporation in the pEX-KG plasmid. Once amplified (Figure 3.18a), the PCR product corresponding to the EC2 domain and the pGEX-KG vector were digested and ligated (2.2.2.12 and 2.2.2.13). *E coli* DH5α cells were transformed with the ligation product used to isolate and amplify vector DNA. An analytical digest was carried out to check for the presence of an insert (Figure 3.18b) (shown by fragments within the red box) and the construct was sequenced.

Once the correct rat-CD63 EC2 sequence was confirmed, rat CD63 p-GEX plasmid was used to transform Rosetta-gami cells and GST-tagged protein was express and purified as described previously (Sections 2.2.3.4 and 2.2.3.6). As shown in Figure 13.19a the eluate (lane 5) contains a predominant band at the correct molecular weight for rat CD63. Samples of the eluate and previously generated human CD63 EC2 were compared Western blots probed with antibodies towards either rat CD63 (AD1) or human CD63 (H5C6) and the results are shown in Figure 3.19b. The rat and human CD63 EC2 proteins only show reactivity with their respective antibodies (which are species specific) indicating that expression of rat CD63 had been successful (although yields were relatively low).

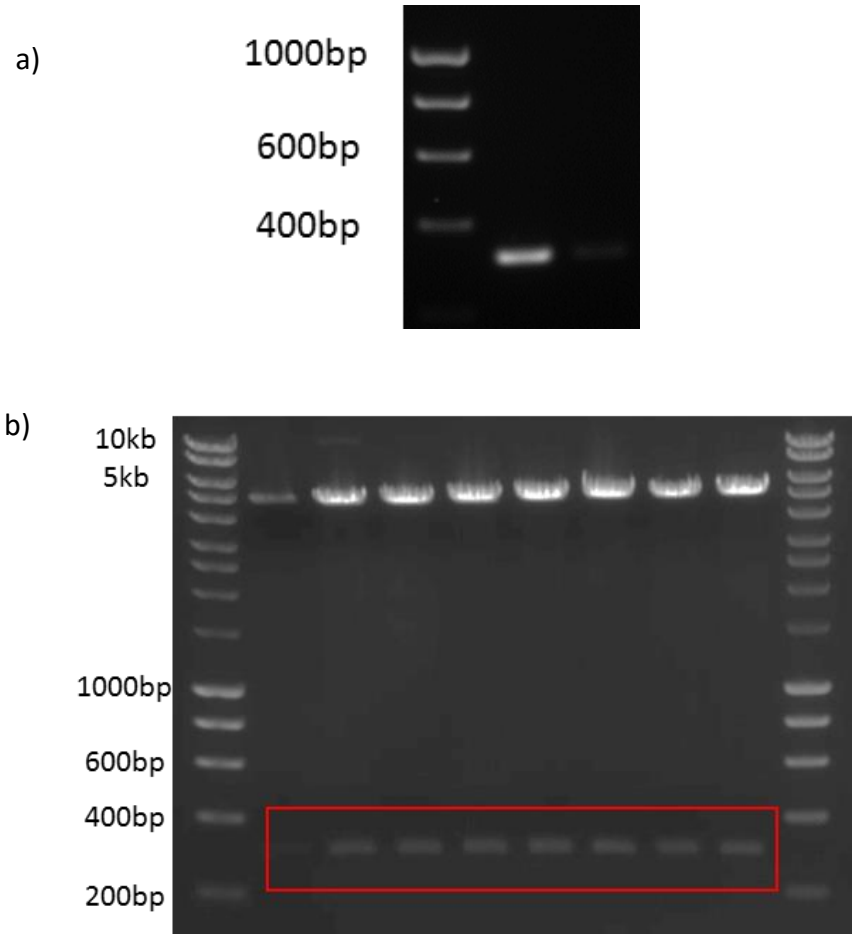

Figure 3.18: PCR of rat CD63 EC2 and analytical digest of rat CD63 EC2 expression vector to check for EC2 encoding insert. (a) PCR amplification products of rat CD63 EC2 from full length rat CD63 in the pCMV6-Entry vector were run on a 1% agarose gel **(b)** Restriction digest of pGEX-ratCD63 (using EcoRI and HindIII) DNA from transformed DH5α *E. Coli* cells. Digestion products were run on a 1% agarose gels, each lane represents different tranformants insert fragments can be seen at 290 bp.

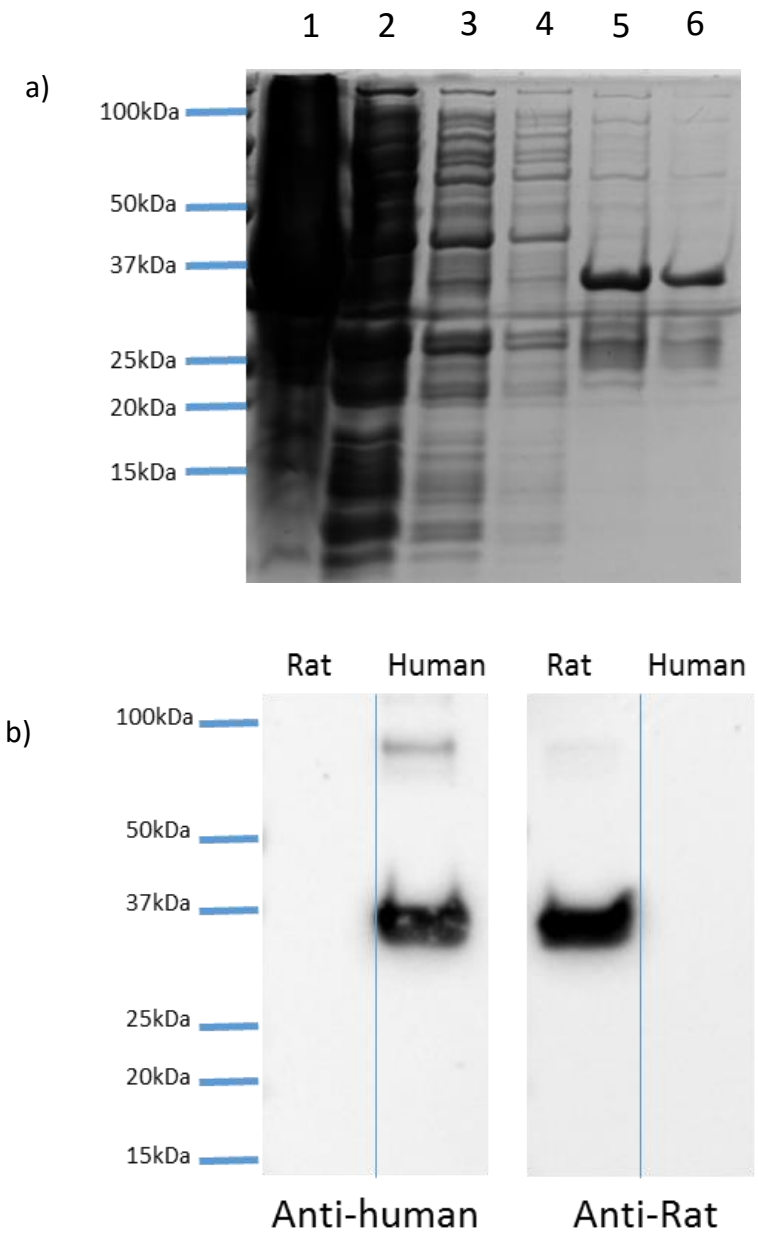

Figure 3.19: Steps in the glutathione purification of rat CD63-EC2 from bacterial lysates. (a) Transformed *E. coli* were cultured and lysed as described previously and GST-tagged proteins purified by affinity purification. Samples were run on a polyacrylamide gel under reducing conditions and stained with Coomassie blue 1= insoluble fraction, 2= Non-bound protein, 3= 1st wash, 4 = 2nd wash, 5 = eluate 1, 6 = eluate 2. **(b)** Samples of purified rat and human CD63 EC2 were run on a polyacrylamide gel and blotted; each membrane was probed with either anti-rat CD63 (AD1) or anti-human CD63 (H5C6) monoclonal antibodies.

3.3 Discussion

Mammalian and insect cells are more able to cope with complex folding patterns than bacteria and produce proteins which are glycosylated and free of endotoxin contamination (Section 1.3), therefore many attempts were made at producing recombinant EC2 domains in both systems. For mammalian expression, two cell lines were transfected by two separate methods using seven different vectors (Five for the Flp-in system and two for pCI-neo). Resistant cells were clear, yet no protein could be detected in supernatant samples or cell lysates by Western blot or ELISA. Similarly for insect cells, multiple vectors yielded no protein. This was surprising because the pCI-neo expression vector has been used by our group previously for CD63 EC2 expression in HEK-293 and the Flp-in systems offers a number of benefits over this vector (Jiraviryakul, 2010). One of the most apparent advantages of the Flp-in system is the use of site specific recombination which stops the possibility of gene incorporation into a transcriptionally inactive site (Barnes et al., 2003). Although this improvement has not led to production of the desired protein in this instance, it has at least enabled this issue to be ruled out as the reason for the absence of protein. There are a number of other possible explanations for the lack of detectable protein, some of which will be discussed here.

Firstly, DNA constructs were all sequenced and found to be in frame with no mutations indicating that the coding DNA was not at fault. With both HEK-293 and CHO transfections resistant colonies were apparent when comparing transfected cells with mock transfected cells. The presence of the CD9 coding DNA in genomic extractions from both FLP-in or pCI-neo transfected cells (Figure 3.9) indicates that there was no issue with introducing the DNA to the cells. Reverse transcription PCR (Figure 3.10) demonstrated that the CD9 transfected CHO and HEK-293 cells were producing CD9 encoding mRNA also. In both instances it is unlikely that the PCR products are a result of amplification of endogenous CD9 DNA/RNA, in CHO cells (which are hamster in origin) a forward primer corresponding to human CD9 was used and in the human HEK-293 cells an IgGκ forward primer (corresponding to the secretion tag) was used. These results show that the DNA is being transcribed and has therefore been introduced into the desired site. This therefore suggests an issue with translation of the mRNA into the desired protein product, or a problem with the produced protein, which renders it undetectable.

Expression of CD9 encoding mRNA had been confirmed through RT-PCR on cellular RNA, however random primers were used for amplification leading to the amplification of all the cellular RNA, including that which is not processed (where as poly dT primers would amplify only polyadenylated RNA). It is possible that the small size of the RNA means it is poorly

processed (for example not polyadenylated), which could result in it not being translated (Ntini et al., 2013). In future, poly dT primers could be used for RT-PCR to assess whether the CD9 encoding RNA is polyadenylated, it may also be beneficial to use longer DNA constructs for expression; for instance by including a streptavidin tag or V5 epitope which were omitted in this work with the hopes of expressing products closer to the native proteins.

Mammalian cells traditionally produce less protein than *E. coli* expression systems, therefore initial thoughts were that the proteins were expressed but were at concentrations too low to be detected. However, analysis of Western blot and ELISA detection limits indicated that the methods used here should be sufficiently sensitive to detect proteins even with modest estimates of protein expression. For example, Western blots to determine the detection limits of the anti-CD9 antibody (Figure3.4a) were able to detect a protein concentration as low as 6 µg/ml. In a supernatant sample concentrated 10x, as little as 0.6 µg/ml or 600µg/litre in the original sample would be detected via Western blot analysis, and ELISA experiments have proven even more sensitive, with absorbance readings being detected in wells with CD9 quantities as low as 80 ng/ml, therefore theoretically requiring transfected cells to produce as little as 80 µg/litre. It is still possible that the recombinant proteins were being produced at lower than detectable quantities, however if this was the case, then these yields would be too low to make these hosts feasible for expression.

An alternative explanation for lack of detectable EC2 protein is once the proteins are expressed they are rapidly degraded prior to detection. This could happen non-specifically by cellular proteases or via the unfolded protein response, in which proteins are broken-down in response to accumulation of unfolded protein within the ER (Cao and Kaufman, 2012). If the EC2 domains are not broken down there is also the possibility that they are forming insoluble protein aggregates as a result of non-native interactions between protein folding intermediates (Kopito, 2000). This may have led to the loss of conformational epitopes required for the anti-tetraspanin antibody to bind, however it is likely that His-tagged variants would still be detected with anti-His antibodies. Finally there is the potential that the expressed tetraspanin EC2 domains are toxic for the host cells and therefore production of the EC2 domains is lost over time.

Expression of EC2 domains by other groups is predominantly undertaken using *E. coli* as a host for expression (Barreiro et al., 2005; Kitadokoro et al., 2001; Petracca et al., 2000; Takeda et al., 2003; Zhu et al., 2002) with one instance of a yeast (*Pichia pink)* expression system being utilised (Curti et al., 2013), and another where mammalian cells (HEK-293) are used (Rajesh et

al., 2012). The group which used a cell line for EC2 expression favoured transient transfection (Rajesh et al., 2012), in which a large volume of cells are transfected and express protein for a short amount of time before the protein is harvested. It is possible that the expression from a high copy number plasmid could lead to more protein (Balbás, 2001). Additionally, with regards toxic proteins, transient transfection or inducible expression may be favourable because the cells are not subjected to the negative selection for a long period of time and cell viability is less of an issue over the short expression period.

One instance where stable cell lines have been successfully used for expression of tetraspanin EC2 domains was by our group for the expression of CD63 in HEK-293 cells (Jiraviryakul, 2010). However, there are a number of properties of the CD63 construct that may make it more amenable to this method of expression. Firstly, the construct used contained a streptavidin tag, glycine linker and thrombin cleavage site and is therefore larger than the ones produced here. This will result in longer RNA which could be more readily processed. Furthermore, of the proteins which we have attempted to express in mammalian cells (CD9, CD63, CD151 and Tspan5) CD63 has a much lower theoretical stability index (Table 3.3). This value is based on the presence of specific dipeptides within the protein which have been correlated to its half-life, proteins with values below 40 are considered stable, so CD63 with a stability index of 28.83 may remain in solution for longer periods of time (Guruprasad et al., 1990). Furthermore, CD63 is unusual within the tetraspanin family as it is often found in intracellular vesicles and in some cases, lysosomes. With this localisation it is possible that CD63 has adaptations to prevent proteolytic degradation, for example, being heavily glycosylated as evidenced by the smear it shows as on Western blots (Jiraviryakul, 2010(Russell et al., 2009). Finally, CD63 has a much higher PI than the other members discussed here (Table 3.3). The mammalian cell lines used for expression are cultured in DMEM medium (pH of 7.4); however once cells reach a high density the pH does drop (indicated by changes phenol red indicator). This could favour the solubility of CD63 with a high pI and but negatively impact the solubility of the other tetraspanin protein with lower pI values.

The EC2 domains of the four tetraspanins under investigation (CD9 CD63, CD81, CD151) and a GST control were successfully produced and purified from Rosetta-gami *E. coli* cells (Figure 3.13) and the final purified products were effectively recognised by their respective antibodies (Figure 3.14b). Since these antibodies are conformationally sensitive and reliant upon the presence of disulphide bonds, this indicates that the resultant proteins are (at least in part) correctly folded. For the majority of the EC2 domains produced, over 50% of the final product was composed of the full length protein with much of the remainder being lower molecular

weight products. An anti-GST Western blot (Figure 3.14a) shows that the lower molecular weight bands are GST containing proteins; it is therefore likely that they are a result of premature termination of protein translation or degradation of the full length product (perhaps from aberrant proteolysis following cell lysis). The lowest band appears at ~ 26kDa and represents free GST from cleavage of the tag from the EC2 domain, however high bands also suggest that proteolysis is not just taking place at the GST cleavage site. This phenomenon has been observed by other groups expressing GST tagged EC2 domains (Azorsa et al., 1999; Barreiro et al., 2005; Petracca et al., 2000), with some opting for the inclusion of a second affinity tag (usually a His-tag) at the opposing end of the protein (Petracca et al., 2000). This secondary tag enables an additional round of purification, which can purify the full length His containing products from the truncated proteins that do not include the 3' His-tag. Not only would this method result in an end product with fewer unwanted protein contaminants but could also be beneficial when cleaving the bulky GST tag from the proteins (Section 5.3.3). Some groups have also utilised more rigorous methods of protein purification to remove the unwanted contaminating protein, such as reverse phase HPLC (Parthasarathy et al., 2009; Zhu et al., 2002)

Coomassie staining of the insoluble protein fraction indicates that a relatively large amount of the desired protein is ending up in an insoluble form. This is more apparent in the low yielding purifications of CD63 and CD151, both of which contain six disulphide bonds. The relatively low yields of these EC2 domains, along with the increased proportion of insoluble protein is thought to result from an inability of the host *E. coli* cells to cope with the increased complexity of folding caused by a greater number of putative di-sulphide bonds. Reducing the level of recombinant protein expression (i.e. by using a lower concentration of IPTG) results in decreased a metabolic load on the cells which can lead to a lower incidence of protein aggregation and degradation (Baneyx and Mujacic, 2004). The results here would suggest that decreasing the concentration of IPTG does favour a higher incidence of soluble protein.

When expressing CD81 EC2, Rajesh *et al.* (2012) utilised longer (12 hour) periods of expression at a lower temperature of 18^{o}C. These same conditions were mimicked for expression of our pGEX-CD81 vector. However, Figure 3.16 indicates that incubations longer than 4 hours result in a decrease in the 35 kDa full length protein, and a simultaneous increase of 27 kDa free GST. Cleavage of the tag from the EC2 protein does not seem to be entirely responsible for the reduction in full length protein as there is no substantial increase in the 10 kDa band indicative of untagged EC2 protein. This suggests that there is a greater incidence of degradation when using longer incubations post induction. It is possible that the slight difference in the defined

EC2 boundaries (residues 112-202 for Rajesh *et al.* vs residues 114-203 for our construct) could impact on the expression and folding of the resultant protein. Alternately, the flexible glycine linker within the pGEX-KG vector used by our group may have the unintended effect of increasing the likelihood of unwanted proteolytic degradation of the EC2 domains. Using lower temperatures for expression increased the proportion of full length EC2 protein, with ~9% of the final protein being full length at 18^{o}C incubation, whereas less than 1% was full length at 37^{o}C. However, the proportion of full length protein was still lower than traditional expression for four hours, where ~70% of the protein was the desired full length CD81-GST. Experiments were attempted using lower temperatures for shorter periods of expression however extremely low amounts of bacteria were harvested after 4 hours. Simultaneous expression of chaperones from psychrophilic bacteria has been reported to enable high *E. coli* growth rates when using temperatures as low as 4^{o}C for recombinant protein expression (Ferrer et al., 2004). What's more these low temperatures facilitated a higher degree of protein folding and would presumably limit the activity of cellular proteases. Although principally for the expression of heat liable proteins this "pCold" system may be beneficial for the expression of protein with complex folding patterns such as the tetraspanin EC2 domains.

Changing the purification method seemed to have little effect on the final protein product with coomassie profiles and LPS content appearing very similar (Figure 3.17). This enables more direct comparison between results gained from EC2 domains produced by either method and enables a choice of methods based on application. Column purification was the quicker of the two as there was no need for multiple centrifugation steps and was more suited to larger purification. However considerably more elution buffer had to be used to pass through the column which when producing low yield proteins may be an issue.

EC2 domains from different species sometime exhibit differing functional effects, for example the EC2 domain of human CD9 but not mouse CD9 was able to inhibit multinucleated giant cell formation (Parthasarathy et al., 2009). In other instances they function similarly, for example injecting either mouse or human CD9 mRNA into CD9 -/- ooyctes restored their fusogenic ability to equal extents (Zhu et al., 2002). In terms of the EC2 domains under investigation here, Rat and Human CD63 show the most variation in amino acid sequence (Appendix Figure 7.2). It was therefore decided to express rat CD63, for later studies on the effects of EC2 domains from different species on degranulation. Figure 3.19 shows that this recombinant protein was successfully expressed and shows good reactivity with its respective antibody.

CD Name	Tspan name	Amino acid size (kDa)	Amino acid size of EC2 (kDa)	Number of cysteine	Amount of glycosylation (within EC2)	Theoretical pI	Hydrophobicity	Stability index
CD9	Tspan29	228aa (25.4)	80 (9.195)	4	2/1 (0)	5.65	-0.64	46.18
CD63	Tspan30	238aa (25.6)	96 (11.037)	6	3 (3)	8.59	-0.745	28.84
CD81	Tspan28	236aa (25.8)	89 (9.797)	4	0 (0)	5.09	-0.371	37.31
CD151	Tspan 24	253aa (28.3)	106 (12.12)	6	1 (1)	5.67	-0.837	47.22
-	Tspan5	268aa (30.3)	118 (13.9)	8	4 (3)	4.31	-0.631	39.64

Table 3.2: Physical properties of the tetraspanins under investigations. EC2 sizes were determined by multiple sequence alignment. Theoretical pI, hydrophobicity and stability index were all resourced from http://web.expasy.org/protparam/ and are for the EC2 domain alone. Stability index is based on the presence of specific dipeptides within the protein which have been correlated to its half-life, proteins with values below 40 are considered stable

Chapter 4: Effects of tetraspanin EC2 domains on RBL-2H3 cell degranulation

4.1 Introduction

4.1.1 Degranulation and allergy

The beneficial role of Mast cells in immunity is becoming more appreciated, such as their numerous methods of pathogen detection, ability to phagocytose microorganisms and signal locally as well as over long distances (Section 1.3). However, chronic or systemic activation of mast cells along with aberrant activation, towards an otherwise innocuous antigen for example, can result in a number of diseases such as arthritis and allergy (Brandt et al., 2003; Reber and Frossard, 2014). For this reason it is becoming increasingly important to understand the molecular mechanisms involved in mast cell activation which may enable the development of more treatments for mast cell associated diseases.

Mast cell prevalence in allergy and autoimmunity has led to a number of therapeutic agents which stop or down regulate their activation. Some such agents prevent activation by stabilising the mast cell membrane, for example, cromolyn sodium and nedocromil sodium which are used to treat asthma amongst other diseases (Reber and Frossard, 2014). Other treatments stop specific means of activation, for instance, tyrosine kinase inhibitors prevent mast cell stimulation by inhibiting the tyrosine kinase growth factor receptor c-Kit, which is essential for mast cell activation (El-Agamy, 2012). One of the first tyrosine kinase inhibitors to be used medically, Imatanib, acts by blocking an ATP binding site on the c-Kit receptor, maintaining it in an inhibited state (Mol et al., 2004). Some therapeutics seek to minimise the effects of mast cell derived products, such as anti-histamines which function as reverse agonists of G protein coupled receptors (GPCR) targeted by histamine. However, reverse agonists for therapeutic use are currently only available towards two of the four histamine targeted GPCRs (H1-4R) (Simons and Simons, 2011). One of the main goals of allergy treatment is to prevent mast cell activation through the high affinity IgE receptor; one such method uses an anti-IgE antibody known as Omalizumab. This binds to IgE at the same site where interaction with the high affinity IgE receptor would take place, thereby stopping this association thus preventing activation (Chang, 2000). Although other strategies are currently in development (Borriello et al., 2014), Omalizumab is currently the only means to prevent IgE activation directly and its high price limits its use (Harvima et al., 2014).

A number of tetraspanins have been linked with mast cells and the process of degranulation, either through association with the FcεRI receptor or through the modulating effects exhibited by various anti-tetraspanin monoclonal antibodies and tetraspanin gene knockouts (Section 1.2.5). For instance, It was previously shown that incubating RBL-2H3 cells with antibodies towards either CD63 or CD81 prior to degranulation was able down-regulate the degranulation response (Fleming et al., 1997; Kitani et al., 1991; Kraft et al., 2005). Some of the authors propose mechanisms by which these mAbs may affect degranulation but the specifics of tetraspanin involvement in IgE signalling are currently unknown, however the association of FcεRI with several tetraspanins could indicate its inclusion in TEMs. Recombinant forms of tetraspanin EC2 domains have previously shown biologically activity in a number of functional studies (Section 1.1.4), and what is more they do not inherently interact with the Fc receptors or cross link target proteins so their alternate mode of action to mAbs may shed more light on tetraspanins function. In this chapter, EC2-GST fusion proteins corresponding to four tetraspanins which have been implicated in IgE signalling (CD9, CD63, CD81 and CD151) are used in conjunction with RBL-2H3 cells in an attempt to further our understanding of tetraspanins involvement in degranulation and act as a preliminary investigation into any potential therapeutic application. RBL-2H3 cells do not express endogenous CD9, however it is unclear if homotypic interactions are required in order for EC2 domains to impart an effect so this EC2 domain was still used on in conjunction with non-transfected RBL cells. Furthermore, RBL cells transfected with human CD9 were also used because previous studies have shown that treatment of RBL cell transfected with human CD9 with anti-human CD9 antibodies was enough to stimulate degranulation and it was hypothesised that EC2 domains might display a similar outcome (Higginbottom et al., 2000a).

Despite RBL-2H3 cells originating from basophils, they are frequently used as a model for mast cells and degranulation. This is because they share a number of mast cell properties, for example they express the mast cell proteins rat mast cell protease II and c-Kit (albeit a constitutively active variant) (Mol et al., 2004; Passante and Frankish, 2009; Seldin et al., 1985). Furthermore, they are straightforward to culture and forgo timely isolation methods used for primary mast cells (which usually result in low cell numbers) (Siebenhaar et al., 2014). As mentioned previously (Section 1.2.1), mast cells display heterogeneity and their properties can differ significantly according to the stimuli they receive from their surrounding environment. For this reason it is difficult to take a property displayed by one subset of mast cells investigated in vitro and ascribe that to other mast cell populations (Galli et al., 2005). However, when considering IgE mediated release, RBL-2H3 cells display a characteristic bell-shaped dose-response curve and are considered a reliable model for early screens of this

particular process (Passante et al., 2009).Being of Rat origin these cells endogenously express rat tetraspanin family members, this may preclude interaction with the recombinant human EC2 domains being used here, however, previous studies have shown that tetraspanins from one species can interact with cells from another (Zhu et al., 2002)(Our group, unpublished data). Furthermore, rat and human EC2 domains have fairly similar homology (64.6-86.8% identity) and the EC2 domains of rat CD63 EC2 (which shows the most variation) is also being used to see if rat EC2 domains show greater effects on degranulation. Here, the degree of degranulation has been tracked through the release of β-hexosaminidase. The function of this enzyme in the degranulation response is unknown; however it is released in parallel to histamine and can be easily quantified by monitoring the breakdown of its substrate (Passante et al., 2009).

4.2 Results

4.2.1 Expression of tetraspanins on RBL-2H3 cells

Before investigating the effects of recombinant EC2 domains on RBL-2H3 cells, the level of tetraspanin expression on the cell surface was established by flow cytometry using tetraspanin-specific monoclonal antibodies according to section 2.2.1.9. In Figure 4.1a the median fluorescence intensity (MFI) of the resultant populations are shown relative to their respective isotype control antibodies (RFI), giving an indication of the level of surface expression, whilst in Figure 4.1b the "percentage positive of parent" is displayed and indicates how many cells in the overall population are expressing a specific tetraspanin. Figure 4.1c shows how gates are generating following an expression assay, with isotype control cells being used as negative populations to establish a positive gate to the right hand side, therefore any cells which have a higher fluorescence than the negative control cells and are farther to the right will be included in the positive gate. CD9 shows no expression on either plot which corroborates previously reported results (Higginbottom et al., 2000a). CD151 shows relatively low expression levels on a small population of cells (18%). However, whilst the other antibodies used were specific for rat tetraspanins, the only mAb available for CD151 was raised against human CD151. Although it is reported cross-react with the rat tetraspanin by the suppliers, this may be partial and so not reflect the true levels of expression. CD81 has the highest level of surface expression and is expressed on nearly all RBL-2H3 cells (96%). Finally, CD63 was found to be expressed on the majority of cells (82%) however it has relatively low intensity, which is most likely due to its predominantly intracellular expression (Boucheix and Rubinstein, 2001).

Overall expression levels were also analysed qualitatively via fluorescent microscopy in which cells were fixed and permeabilized before being stained with primary anti-tetraspanin antibodies or isotype controls (Section 2.2.1.9). (Figure 4.2). In each instance random fields depict expression of each tetraspanin on RBL-2H3 cells along with their respective isotype controls. Because the cells have been permeabilized, images represent the entire cellular content, as such CD63 shows up with more vivid staining than would be expected from flow cytometry. CD9 again shows no expression whilst CD151 and CD81 have moderate staining. Human CD9 transfected RBL-2H3 cells were also included which stained vividly indicating high transfection efficiency, which again would corroborate previous reports (Higginbottom et al., 2000a)

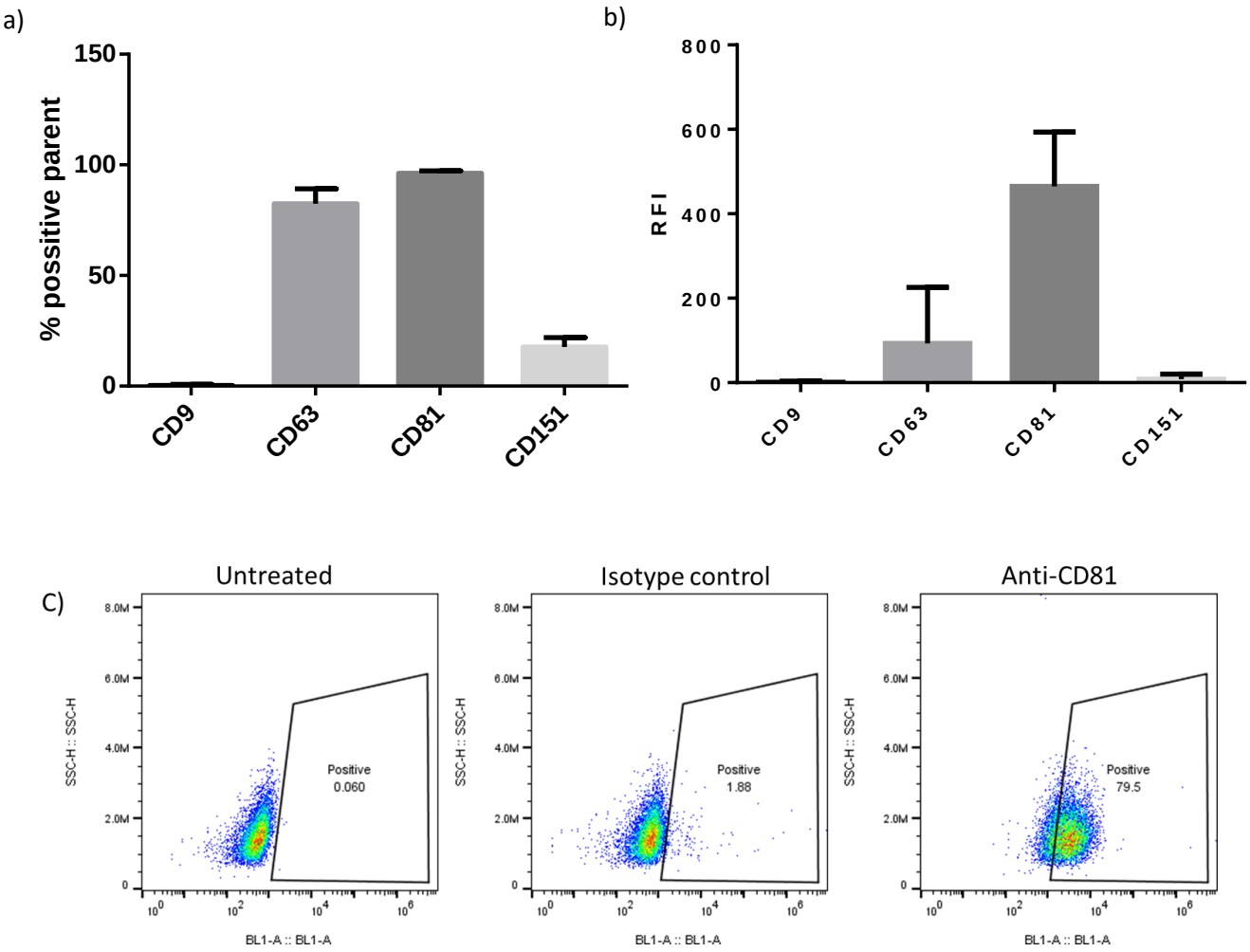

Figure 4.1: Flow cytometry of RBL-2H3 surface expression of four tetraspanin members. Expression of tetraspanin on the RBL-2H3 cell surface was analysed by flow cytometry according to section 2.2.1.18. Briefly, RBL-2H3 cells were incubated with primary anti-tetraspanin antibodies (Table 2.2), appropriate isotype control antibodies or BBN alone for one hour. Cells were washed and stained with secondary FITC conjugated antibodies before cells were analysed on an Attune Autosampler. (**a**) Background values (buffer alone) were removed from isotype control and anti-tetraspanin values. MFIs of anti-tetraspanin values are shown relative to isotype control values as relative fluorescence intensitry (RFI) (**b**) Control gates were set based on isotype control populations and used to define positive cells in samples where anti-tetraspanin antibodies were used. (**c**) 10000 events are collected per treatment and displayed as cell side scatter vs fluorescence. Positive gates were made which exclude cells from the untreated control. For gating of each antibody please see appendix Figure 7.5. Data points are mean ± standard error of the mean (SEM) from a minimum of three repeats carried out in duplicate.

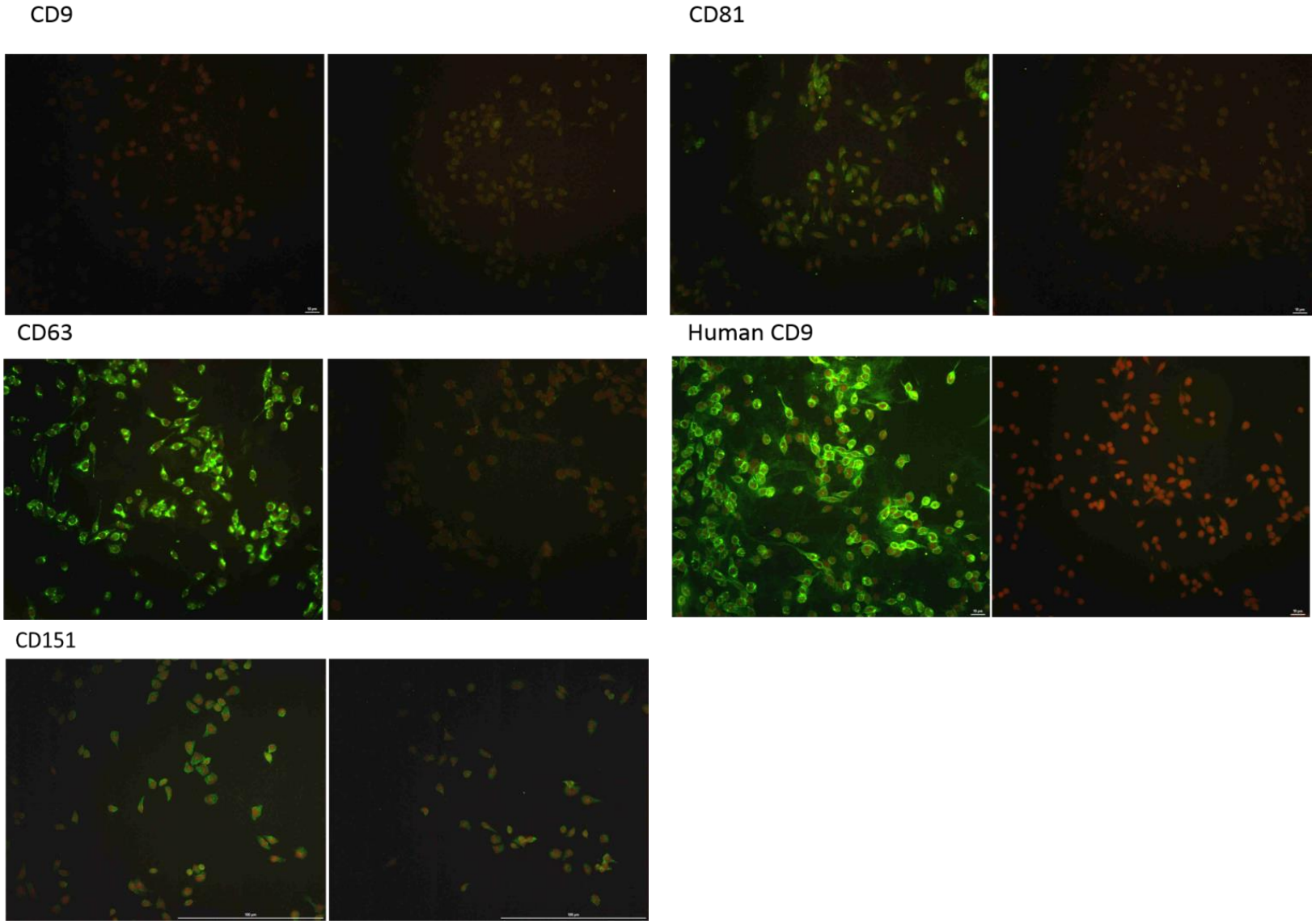

Figure 4.2: Immunofluorescence microscopy on permeabilized RBL-2H3 cells to check for tetraspanin expression. RBL-2H3 expression of tetraspanins (both on the cell surface and intracelluarly) was visualised according to section 2.2.1.9, Briefly, RBL-2H3 cells were stained with the relevant anti-tetraspanin monoclonal antibodies (or isotype control antibodies) followed by secondary FITC-conjugated antibodies. Random fields were photographed for each population using a Nikon A1 confocal fluorescence microscope at 10x objective. Images are representative of two experiments carried out in duplicate

4.2.2 Effects of pre-incubation with EC2-GST fusion proteins on degranulation

In initial experiments examining the effect of recombinant tetraspanin EC2-GST fusion proteins on degranulation, RBL-2H3 cells that had been pre-sensitised with mouse anti-DNP IgE overnight as described in 2.2.1.5, were pre-incubated with various recombinant tetraspanin EC2 domains for one hour prior to stimulating degranulation. A concentration of 500 nM of recombinant protein was used because this concentration shows clear activity in a number of other functional assays (Green et al., 2011; Parthasarathy et al., 2009). Despite CD9 not being expressed on these cells, recombinant CD9 EC2 was also used to see if homotypic interactions are required for an effect to be displayed. Because the EC2 domains are tagged with GST, and contain LPS (as a result of the *E. coli* used to express them) RBL-2H3 cells were also pre-incubated with recombinant GST (produced in the same manner as the EC2 domains) and LPS as negative controls. Dinitrophenol conjugated to Human Serum Albumin (DNP-HSA) was used as a multivalent cross-linking reagent and in each case, conditions were run in triplicate and a minimum of three biological repeats were carried out. The resultant graphs have a bell shaped profile because at higher antigen concentrations, the IgE receptors are not as frequently cross-linked by one antigen molecule and are instead bound by separate molecules. To account for differences in degranulation efficiency between cells, comparisons were only made between conditions on the same 96-well plate (shown on the same graphs). The raw data was normalised to the maximum release given when the cells were not pre-treated with recombinant protein or LPS, allowing for more direct comparisons by accounting for differences in plating density and changes in degranulation efficiency over time. In each experiment the amount of release induced by cross-linking was also related to the total cellular β-hexosaminidase which was determined by lysis with Triton X-100 (Figure 4.3d and 4.3e) and if maximum DNP concentrations with no pre-treatment did not induce at minimum of 20% release, the cells were deemed inefficient and results were excluded. The amplitude and mean DNP of each condition was compared within each experiment using a one-way ANOVA. This represents the maximum amount of β-hexosaminidase released upon degranulation and amount of DNP required to cause maximal release respectively.

Interestingly, one hour pre-treatment of the RBL-2H3 cells with any of the EC2-GST fusion proteins, GST alone or LPS had no effect on the maximal β-hexosaminidase release or DNP required to cause maximal release (Figure 4.3). The way in which EC2 domains are able to impart their effects is still unknown and it was considered that whilst the antibody treatment previously described (section 1.3) shows an effect after just one hour of treatment, this length

of time may not be sufficient for recombinant EC2 domains to modulate RBL-2H3 activity. Furthermore, tetraspanins have been associated with the high affinity IgE receptor and although anti-CD63 mAbs did not interfere with IgE binding (Kitani et al., 1991) it is possible that EC2 domains may affect initial stages of IgE priming. It was therefore decided to apply IgE and EC2 domains to the RBL-2H3 cells simultaneously, 16 hours before degranulation

Similarly to one hour pre-incubation, overnight treatment with the EC2 domains also showed no activity on maximal degranulation or the concentration of DNP required for maximal release (Figure 4.4). This indicates that the EC2 domains do not interfere with IgE binding to the high affinity IgE receptor and that sustained exposure to the recombinant EC2 domains is also unable to modulate degranulation.

4.2.3 Effect of anti-CD63 antibody AD1 and higher EC2 concentrations on degranulation

In prior studies which monitor the effect of monoclonal antibody treatment on degranulation, serotonin and histamine have been used as a marker for degranulation. Although β-hexosaminidase is released in parallel with histamine it was considered that changes in the experimental method may affect the ability of such a screen to effectively display inhibition or enhancement of degranulation. In an attempt to reproduce the results previously documented by Kitani *et al.* (1991) RBL-2H3 cells were pre-incubated with the same anti-CD63 antibody used by Kitani and co-workers, AD1. The effects of anti-CD63 were quite apparent (Figure 4.5) and when results were compared by a one way ANOVA a significant (P<0.005) decrease in the amount of β-hexosaminidase released by the cells was observed. This indicated that the method being used should be sufficient to display any modulating effects that the recombinant EC2 domains may be having. Kitani *et al.* (1991) also reported that a high concentration (100μg/ml) of antibody was required to see this significant decrease in degranulation and when used at a lower concentration (10 μg/ml) (Figure 4.6) only a slight and non-significant decrease was exhibited. It was therefore considered that a higher concentration of EC2 domains may be required in order to affect a response. Consequently, RBL-2H3 cells were incubated with a threefold higher concentration (1.5μM as opposed to 500nM) of recombinant EC2 protein, GST and LPS, for one hour. However, again there was no significant change in degranulation under any of these experimental conditions (Figure 4.7).

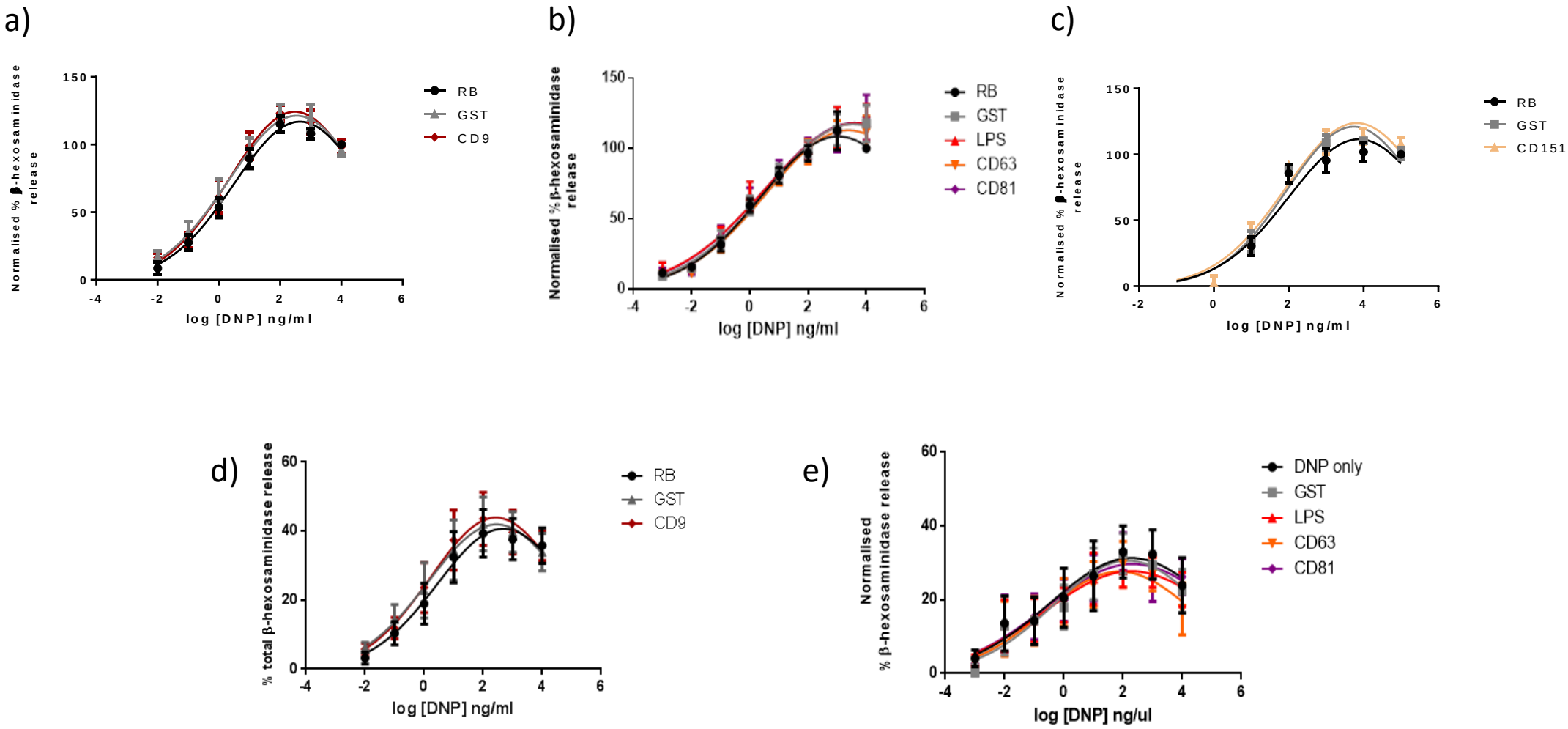

Figure 4.3: DNP stimulated degranulation following one hour pre-incubation with recombinant tetraspanin EC2 domains. RBL-2H3 cells that had been pre-sensitised with mouse anti-DNP IgE overnight as described in 2.2.1.5 were treated with 500nM GST-EC2 fusion proteins, GST alone, LPS or release buffer only (RB) for one hour prior to stimulating degranulation with a range of concentrations of DNP-HSA. β-hexosaminidase release was determined as described in 2.2.1.5 by measuring absorbance at 405 nm. Background absorbance values were removed from test values which in **(a, b and c)** were then normalised to the highest amount of degranulation seen when stimulating degranulation with antigen alone. **(d+e)** Values are shown in relation to the total cellular β-hexosaminidase determined by lysis with 1% TritonX-100. Data points are mean ± standard error of the mean (SEM) from three repeats carried out in duplicate. Amplitude and mean values were compared by one way ANOVA.

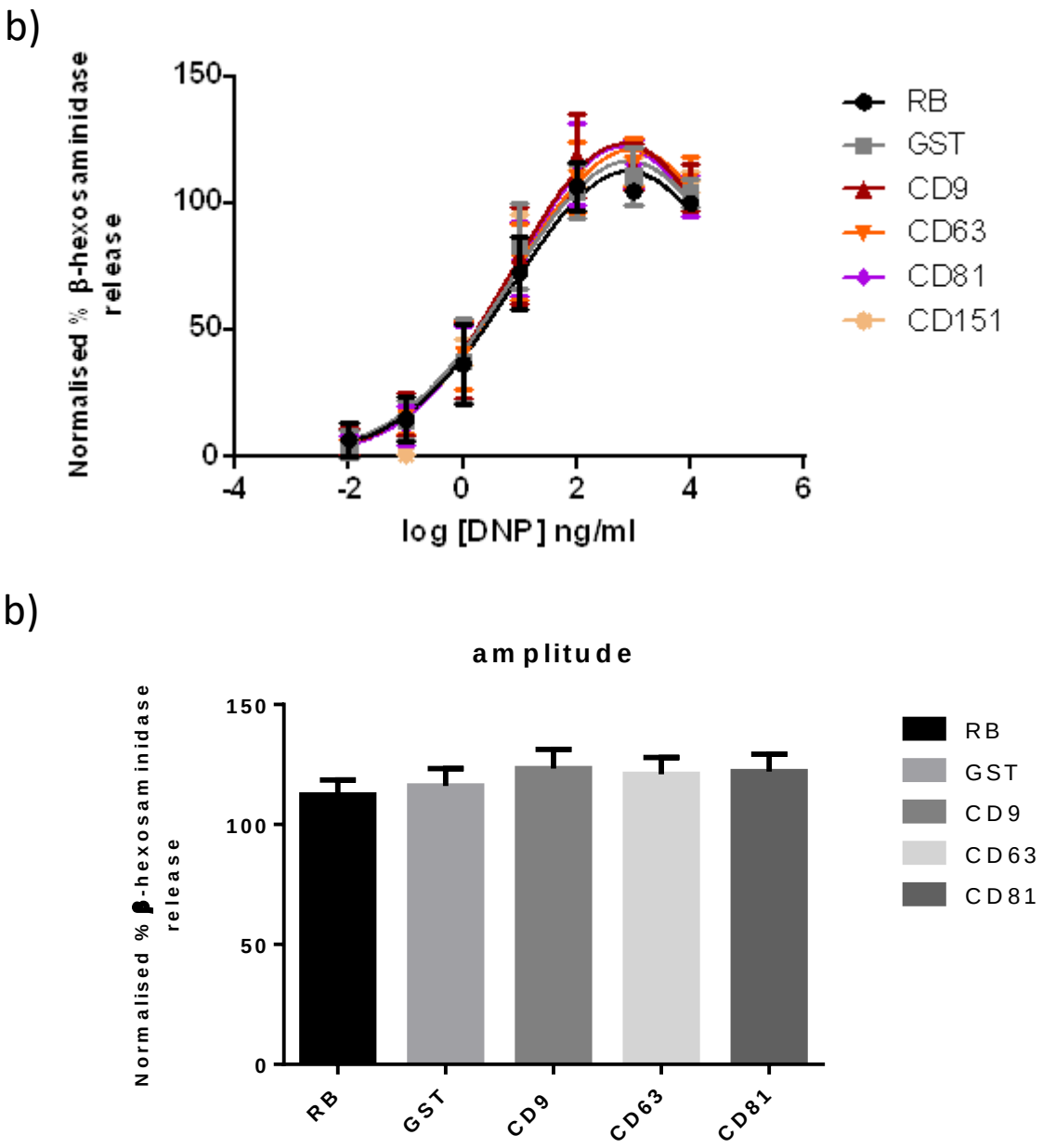

Figure 4.4: DNP stimulated degranulation following 16 hour pre-incubation with recombinant tetraspanin EC2 domains. (**a**) RBL-2H3 cells were treated with 500 nM of the GST-EC2 fusion proteins, GST alone, or release buffer only for 16 hours along with anti-DNP IgE prior to stimulating degranulation with a range of concentrations of DNP-HSA. Background absorbance values were subtracted from test values which were then normalised to the highest amount of degranulation seen when stimulating degranulation with antigen alone. (b) The highest amount of degranulation seen with each treatment (amplitude values) were compared by one way ANOVA. Data points are mean ± standard error of the mean (SEM) from four repeats carried out in duplicate.

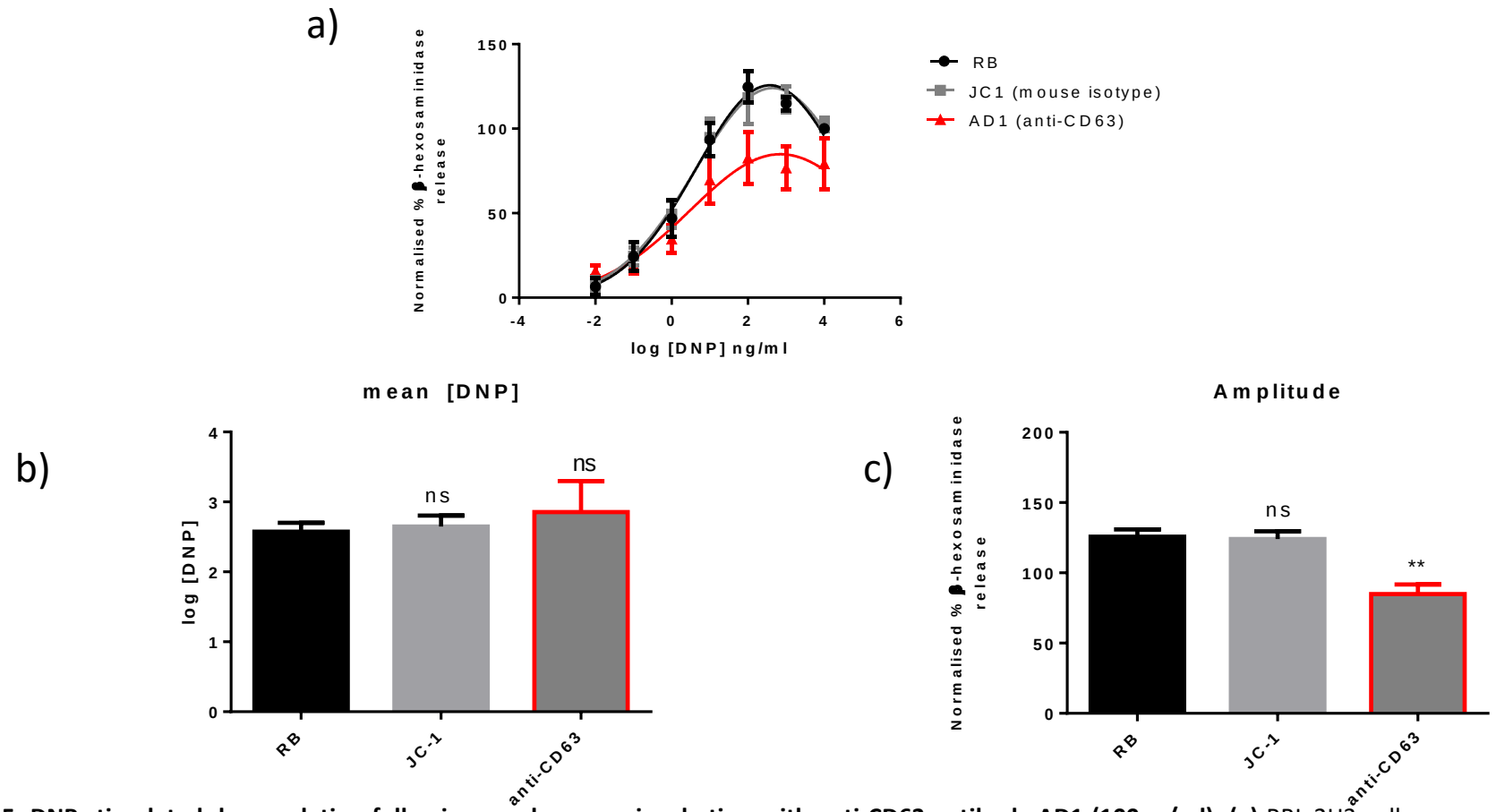

Figure 4.5: DNP stimulated degranulation following one hour pre-incubation with anti-CD63 antibody AD1 (100µg/ml). (a) RBL-2H3 cells pre-sensitised with mouse IgE anti-DNP were treated with monoclonal anti-rat CD63 antibody (AD1) at 100 µg/ml, isotype control antibody (100 µg/ml) (JC-1) or release buffer for one hour prior to stimulating degranulation with a range of concentrations of DNP-HSA. Background absorbance values were subtracted from test values which were then normalised to the highest level of degranulation seen when stimulating degranulation with antigen alone. **(b)** For each condition the mean DNP concentrations (which shows how much DNP was required for maximum release) were compared by one way ANOVA **(c)** The amplitudes (representing the maximum degranulation) were also compared by one way ANOVA. Data points are mean ± standard error of the mean (SEM) from three repeats carried out in duplicate.

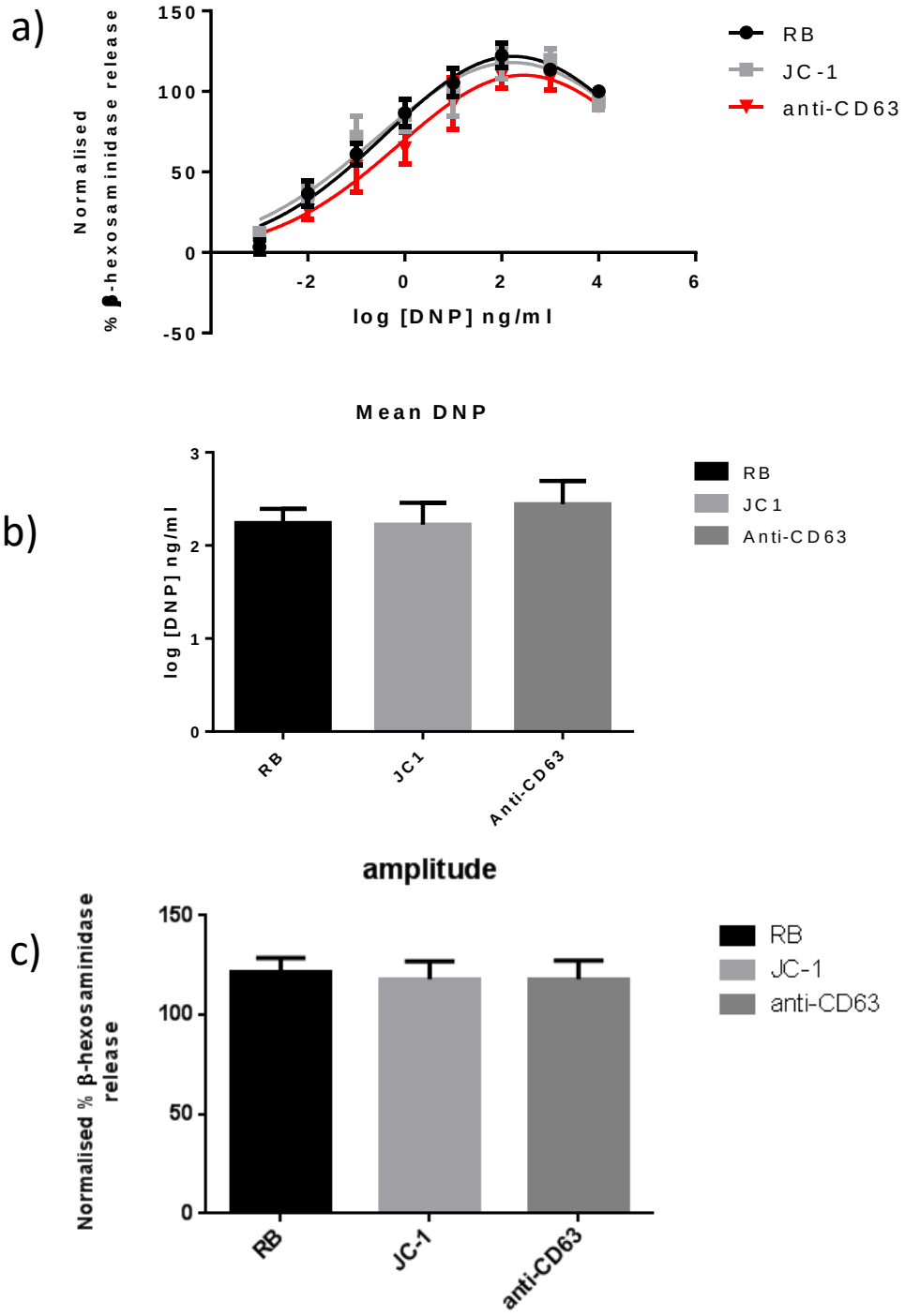

Figure 4.6 DNP Stimulated degranulation following one hour pre-incubation with anti-CD63 antibody AD1 (10µg/ml). (a) RBL-2H3 cells pre-sensitised with mouse IgE anti-DNP were treated with anti-CD63 antibody (AD1) (10 µg/ml) , isotype control antibody (10 µg/ml) or release buffer for 1 hour prior to stimulating degranulation with a range of concentrations of DNP-HSA. Background absorbance values were subtracted from test values which were then normalised to the highest level of degranulation seen when stimulating degranulation with antigen alone. **(b)** For each condition the mean DNP concentrations (which shows how much DNP was required for maximum release) were compared by one way ANOVA **(c)** The amplitudes (representing the maximum degranulation) were also compared by one way ANOVA. Data points are mean ± standard error of the mean (SEM) from three repeats carried out in duplicate.

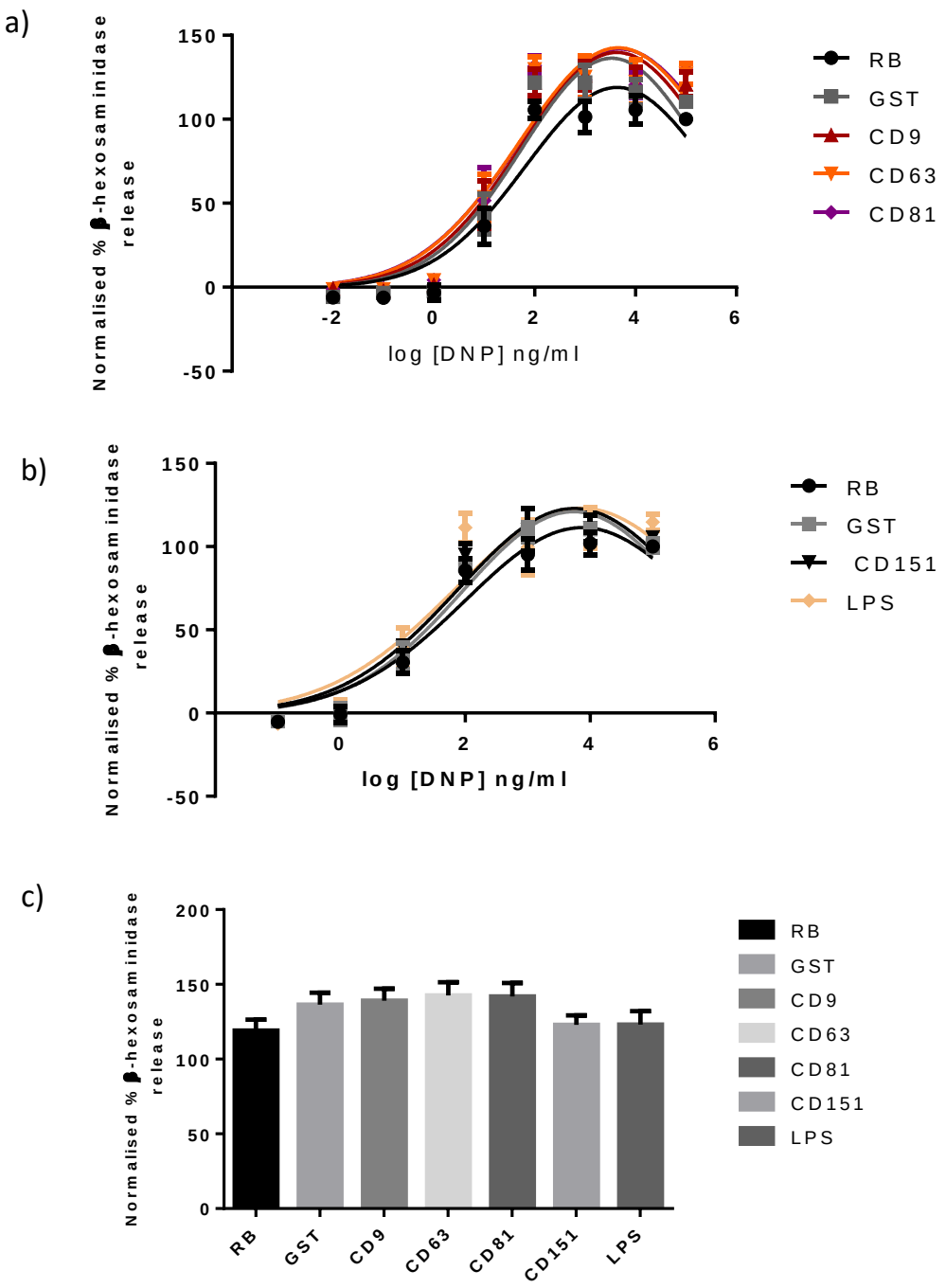

Figure 4.7: DNP stimulated degranulation following one hour pre-incubation with 1.5µM recombinant tetraspanin EC2 domains. (a+b) RBL-2H3 cells pre-sensitised with mouse IgE anti-DNP were treated with 1.5 µM GST-EC2 fusion proteins, GST alone, LPS or release buffer for 16 hours prior to stimulating degranulation with a range of concentrations of DNP-HSA. Background absorbance values were subtracted from test values which were then normalised to the highest amount of degranulation seen when stimulating degranulation with antigen alone (**c**) maximum degranulation values were compared via one way ANOVA. Data points are mean ± standard error of the mean (SEM) from three repeats carried out in duplicate.

4.2.4 Effects of tetraspanin EC2 domains on anti-IgE induced degranulation

DNP-HSA Is commonly used to stimulate degranulation as it is a multivalent antigen, easily able to cross-link FcεRI bound anti-DNP IgE. However, this may not be ideal when looking at subtle effects involving less extensive cross-linking of the FcεRI. It was considered that the potential effects of the tetraspanins EC2 domains might be being masked by the extensive cross-linking induced by DNP-HSA.

To investigate the effects of the tetraspanin EC2s on degranulation triggered by a lower valency molecule, an IgE specific monoclonal antibody was selected as this bivalent antibody would still be able to cross-link IgE bound to FcεRI, but each antibody molecule should only cross-link two receptors on the cell surface. To determine the suitability of this approach, preliminary FACS analysis was undertaken to ensure that the IgE specific IgG antibody was able to bind to the IgE when it was bound to the high affinity IgE receptor. Figure 4.8a shows low levels of non-specific binding of both the isotype control and the anti-IgE antibody (probably through Fcγ receptor binding); however the majority of anti-IgE binding takes place when cells are primed with IgE, indicating that this antibody is suitable for cross-linking. RBL-2H3 cells pre-sensitised with IgE were treated (as previously) with EC2 proteins for one hour. A range of concentrations of anti-IgE mAb were used to stimulate degranulation and the results are shown in Figure 4.8a. The anti-IgE antibody was able to trigger degranulation to a similar extent as DNP-HSA, with ~40% maximal degranulation being exhibited relative to the total cellular β-hexosaminidase (Data not shown), but again no significant effect was seen with the tetrasapnin EC2 proteins on maximal degranulation or the amount of IgG required causing maximal degranulation.

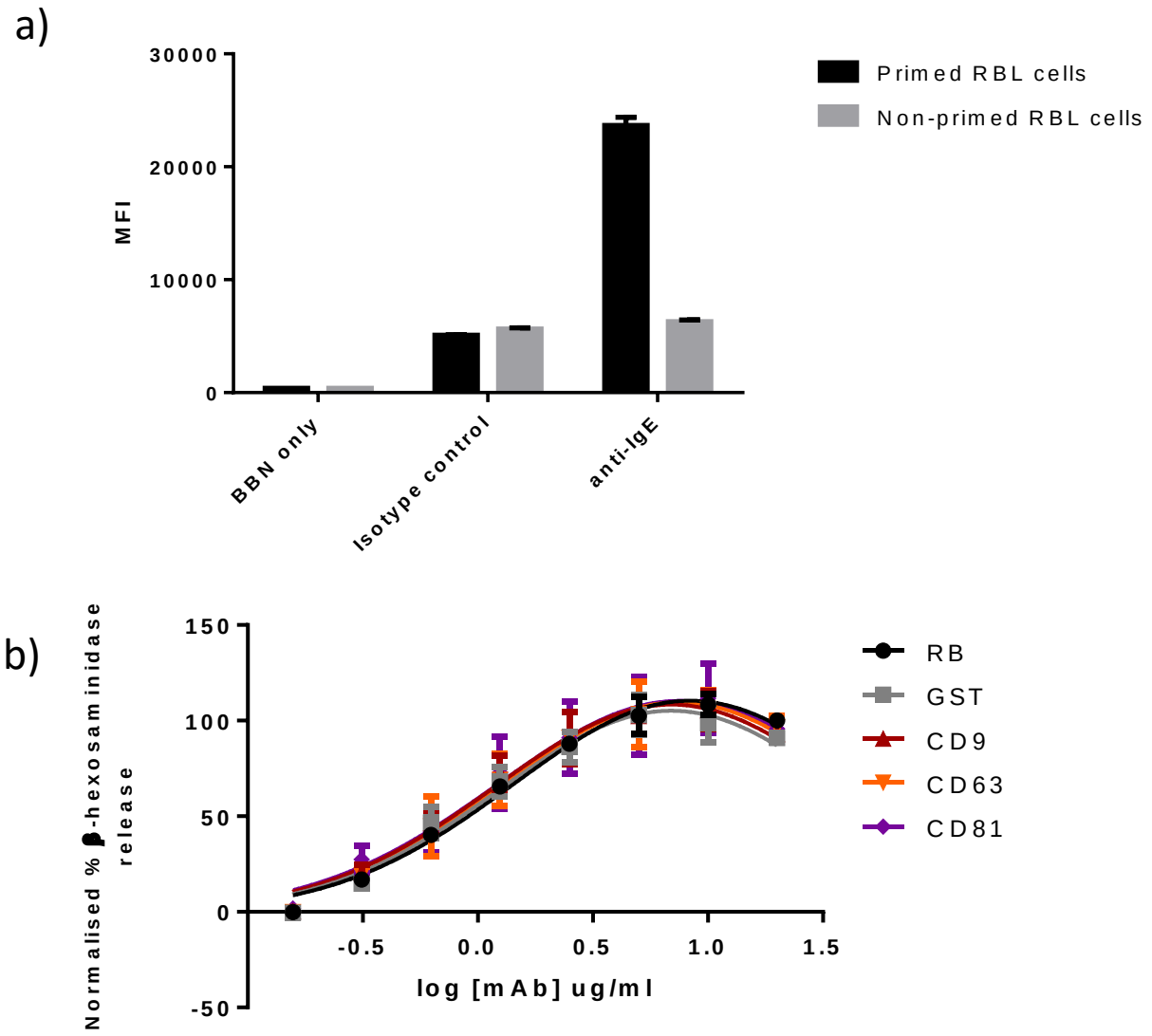

Figure 4.8: Anti-IgE stimulated degranulation following one hour pre-incubation with recombinant tetraspanin EC2 domains (**a**) RBL-2H3 cells were plated overnight with or without the addition of anti-DNP IgE. The following day cells were washed and probed with an anti-IgE monoclonal antibody or isotype control antibody. After incubating for one hour, cells were washed and incubated with a secondary FITC labelled anti-IgG antibody, cells were then washed and analysed via flow cytometry. For percentage positive values see appendix Figure 7.6 (**b**) RBL-2H3 cells pre-sensitised with mouse IgE anti-DNP were treated with 500 nm GST-EC2 fusion proteins, GST alone, LPS or release buffer for one hour prior to stimulating degranulation with a range of concentrations of anti-IgE mAb. Background absorbance values were subtracted from test values which were then normalised to the highest amount of degranulation. Data points are mean ± standard error of the mean (SEM) from three repeats carried out in duplicate.

4.2.5 Effect of rat CD63 EC2 domain on degranulation

Previous studies using EC2 domains have reported differences when using the EC2 domains from one species or another. For example Takeda *et al.* (2003) saw an inhibitory effect of human CD9 EC2 on monocyte fusion however mouse CD9 EC2 had no effect. Similarly Higginbottom *et al.* (2003) demonstrated that in contrast to human CD9 EC2, mouse CD9 EC2 is unable to inhibit sperm oocyte binding. Being as RBL-2H3 cells are of rat origin, it was considered that the human tetraspanin EC2 domains used thus far may not be able to compete with endogenous tetraspanins. It was therefore decided to use a rat homologue for comparison. As time and expense constraints made it difficult to produce rat variants of each of the tetraspanins, it was instead decided to produce one rat EC2 domain for preliminary investigations. The EC2 domain of CD63 was selected as a candidate for expression because of the tetraspanins under investigation, this member shows the most variation between species (65% identity vs 84-87%, see Appendix Figure 7.2) so is perhaps more likely to exhibit a difference between orthologues. Moreover, there is more evidence for CD63 involvement in degranulation than the other three members. Once the recombinant EC2 was produced (Section 3.2.5) it was used to pre-treat RBL-2H3 cells for one hour prior to stimulating degranulation as previously described. Although there is a slight increase in the maximal degranulation (Figure 4.9) this is not significant which suggests that the use of human tetraspanin EC2 domains is not the reason for a lack of apparent effect of EC2 domains.

a)

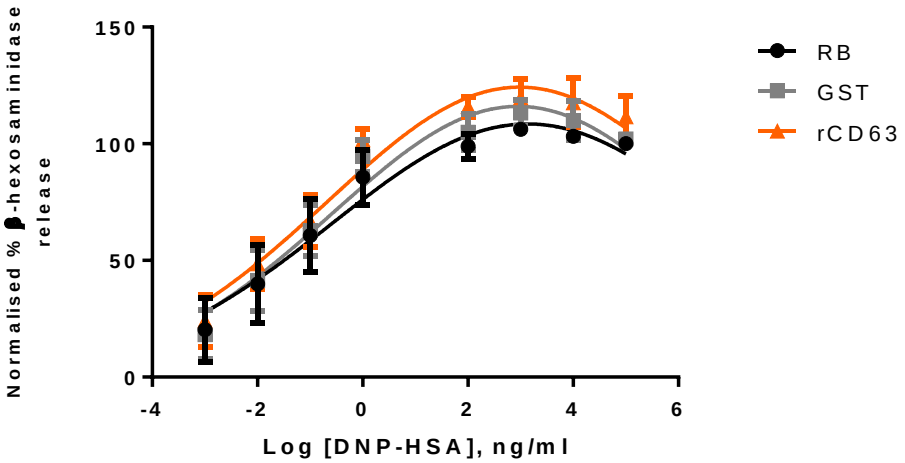

b)

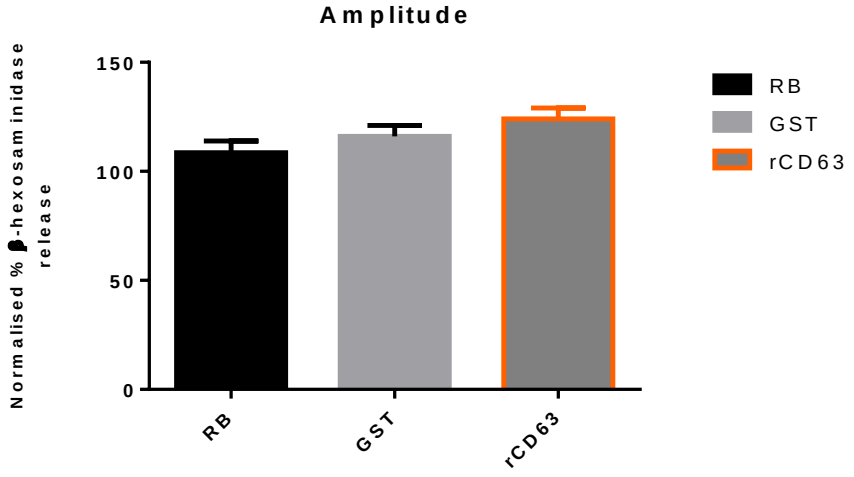

Figure 4.9: DNP stimulated degranulation following one hour pre-incubation with recombinant rat CD63 EC2 (a) RBL-2H3 cells pre-sensitised with mouse IgE anti-DNP were pre-incubated with rat-CD63 EC2 (rCD63), GST or release buffer alone for one hour before stimulating degranulation with a range of concentrations of DNP-HSA. Background absorbance values were subtracted from test values which were then normalised to the highest level of degranulation seen when stimulating degranulation with antigen alone. **(b)** Amplitude values were plotting on a column graph and compared via one way ANOVA. Data points are mean ± standard error of the mean (SEM) from three repeats carried out in duplicate.

4.2.6 Effects of CD9 EC2 on degranulation of human CD9 transfected RBL-2H3 cells

Although CD9 it not expressed in RBL-2H3 (Figure 4.1), it has previously been implicated in activation of both eosinophils and platelets (Kim et al., 1997; Qi et al., 1996). Moreover, a panel of antibodies directed towards human CD9 were shown to induce degranulation in human CD9 transfected RBL cells. In said studies the Fc region was shown to be critical for mAbs to impose their effects (Higginbottom et al., 2000a). Here it was hypothesised that the alternate mode of action of recombinant EC2 domains might enable further dissection of CD9s interaction with the high affinity IgE receptor. Human CD9 transfected RBL cells were incubated with CD9 EC2 for one hour prior to stimulating degranulation. Although there is a slight increase in degranulation this was not significant when compared to the GST control (Figure 4.10a). Furthermore, when using an anti IgE antibody to stimulate degranulation there was no change in the degranulation profile (Figure 4.10c).

Peptides corresponding to different regions of the CD9 EC2 domain (Appendix Figure 7.4) have previously been shown to be functionally active and in some circumstances show activity at lower concentrations than the entire EC2 domains (D. Cozens, unpublished data). Two such peptides which are active in preventing bacterial adhesion (D. Cozens, unpublished data) were used to examine effects on degranulation. Scrambled versions of the peptides were also used as a negative control. RBL cells were pre-treated with 500 nM of each peptide and scrambled control for one hour before stimulating degranulation with either DNP or anti-IgE mAb. Again no significant effect was seen with any treatment (Figure 4.11).

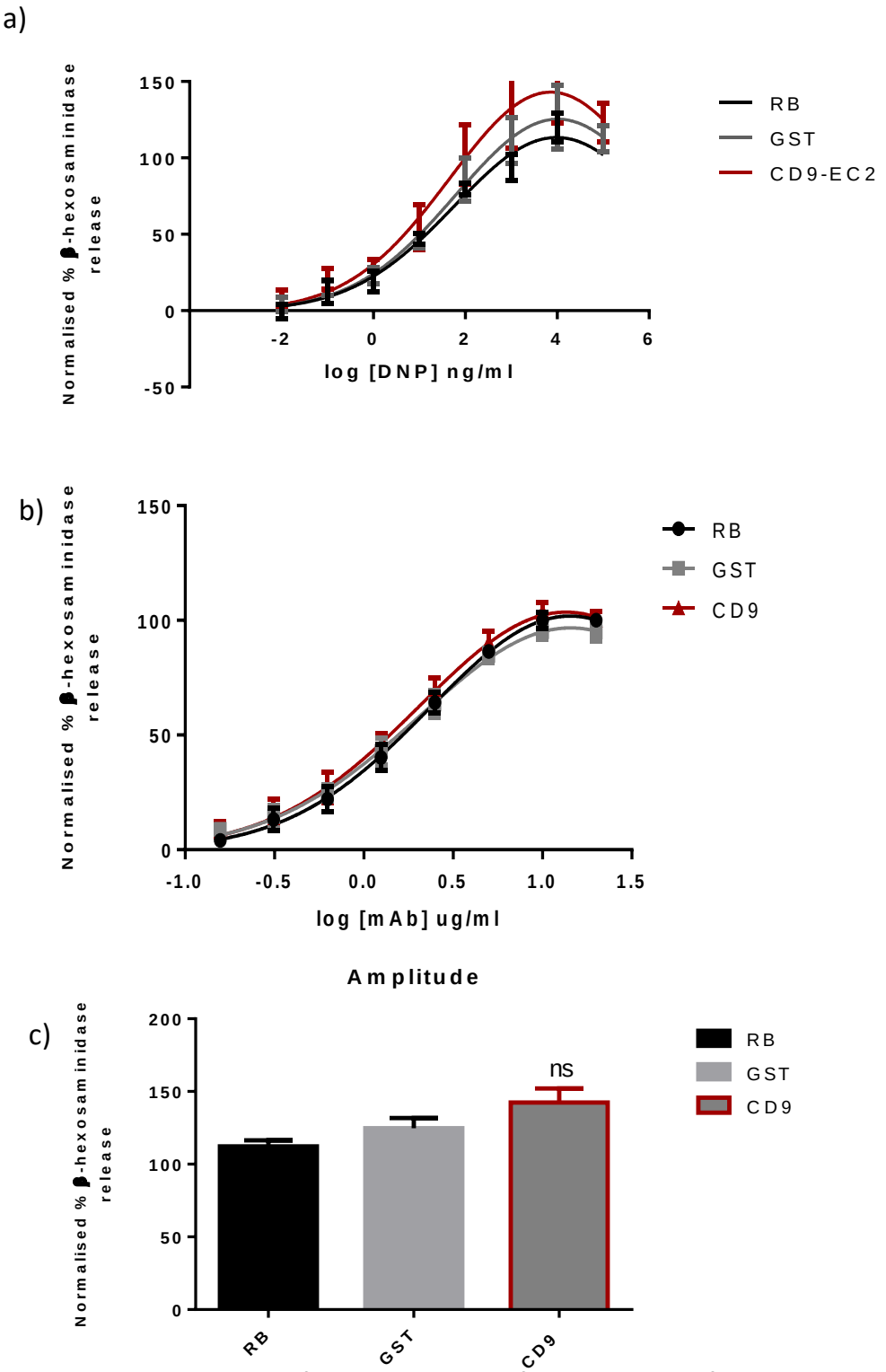

Figure 4.10: Degranulation of human CD9 transfected RBL cells following pre-incubation with recombinant CD9 EC2. Human CD9 transfected RBL cells sensitised with IgE were pre-treated for one hour with CD9-EC2, GST or release buffer alone before being stimulated to degranulate with **(a)** DNP or **(b)** an anti-IgE mAb. **(c)** Amplitude values collected when using DNP to stimulate degranulation were compared via one way ANOVA. Data points are mean ± standard error of the mean (SEM) from a four repeats carried out in duplicate

a)

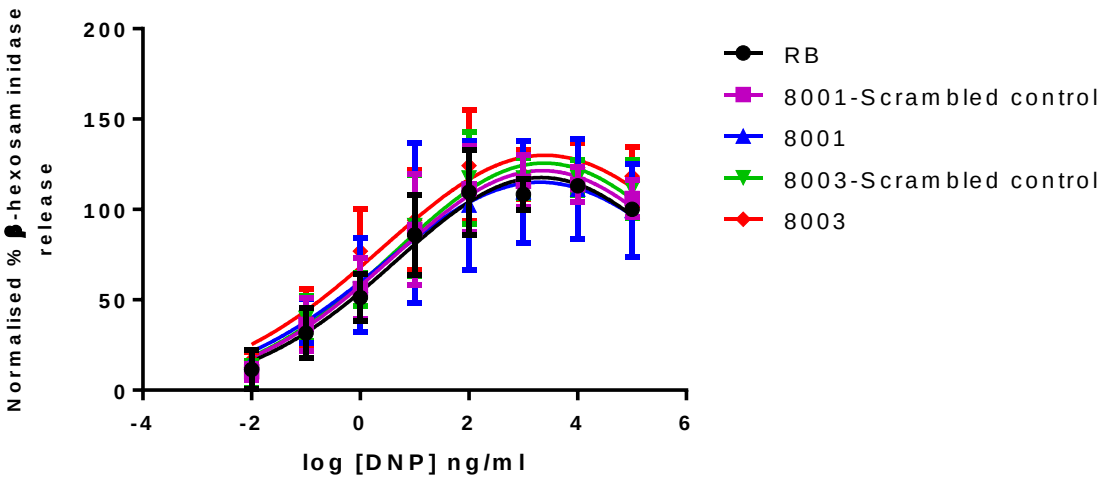

b)

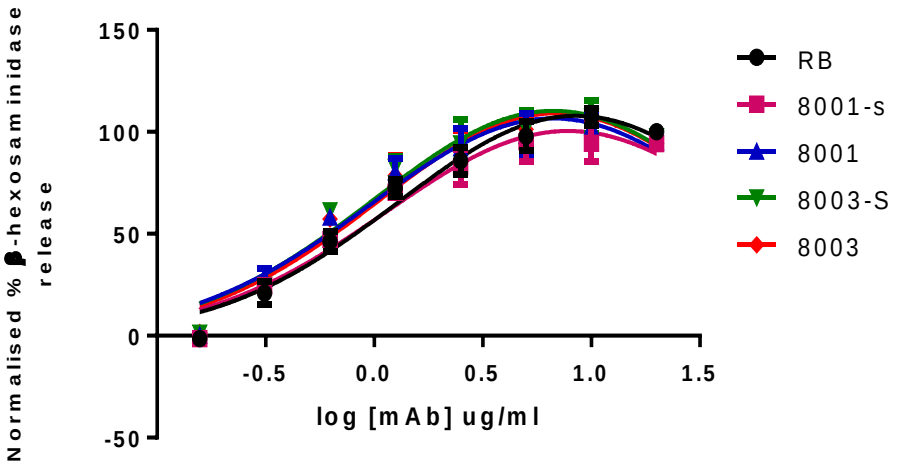

Figure 4.11: DNP and anti-IgE stimulated degranulation following one hour pre-incubation with CD9 EC2 peptides. Human CD9-transfected RBL-2H3 cells sensitised with IgE were pre-incubated with 500 nm of CD9 EC2 peptide, scrambled control peptide or release buffer only for one hour prior to stimulating degranulation with either various concentrations of **(a)** DNP-HSA or **(b)** anti-IgE mAb. Work carried out in part by W. Hazelton and E. McKeefry, data analysed by the author. Data points are mean ± standard error of the mean (SEM) from three repeats carried out in duplicate.

4.2.7 Effects of EC2 domains on cell adhesion

Previous reports have shown that RBL-2H3 cells which are adhered to different substrates are able to degranulate to a greater extent than non-adhered RBL-2H3 cells (Apgar, 1997; Hamawy et al., 1992). The exact mechanism linking degranulation and adhesion is currently unknown however the "augmented degranulation" was shown to result from cell spreading rather than adhesion alone. Integrin binding of ECM components is primarily responsible for cellular adhesion and spreading (Hynes, 1992) and is therefore thought to contribute to increased degranulation. Several tetraspanins are known to have primary associations with various integrins, for instance one of the most studied primary interactions is between CD151 and integrin α3β1 (Yauch et al., 1998), CD81 regulates VLA-4 and VLA-5 adhesion strengthening (Feigelson et al., 2003) and CD63 binds to integrin VLA-3 and VLA-6 (Berditchevski et al., 1995). Antibodies towards CD63 are able to inhibit both adhesion and degranulation, supposedly by down-regulation of the GAB-2, PI3K signalling pathway common to both processes. Initial suggestions were that this occurs through antibody blocking of integrin-ECM interaction, disruption of membrane complexes or antibody sequestering of CD63 and its associated signalling molecules (Kraft et al., 2005). Later studies exhibited reduced degranulation in CD63 knock out bone marrow derived mast cells (BMMC); being suspension cells this favoured the later hypothesis. CD9 EC2 domains have similarly been able to reduce adhesion (although in endothelial cells), however from this work it is evident that they are unable to alter degranulation. Due to the relatively undefined relationship between degranulation and adhesion it was also decided to carry out an initial screen to see if the EC2 domains are able to alter RBL-2H3 adhesion properties.

An sulforhodamine B (SRB) colorometic assay (Skehan et al., 1990) was carried out as in section 2.2.1.17 to determine levels of cellular adhesion following EC2 treatment. Briefly, RBL cells were treated overnight with 500 nm or 1.5 µm of each recombinant EC2 domain, with GST and PBS being used as negative controls. Non-adherent cells were removed by washing and cells were then fixed and cellular protein remaining in the wells was stained with sulforhodamine B. The absorbance at 570nm thus relates to the number of remaining adherent cells. A one-way ANOVA was used to compare readings from each condition and none of the recombinant EC2 treatments (or controls) resulted in a significant reduction in cellular protein within the wells when used at either concentration. This initial screen indicates that EC2 domains are not significantly affecting adhesion or viability of the cells, however, more rigorous methods with differentiate between adhesion and viability may be desirable in future.

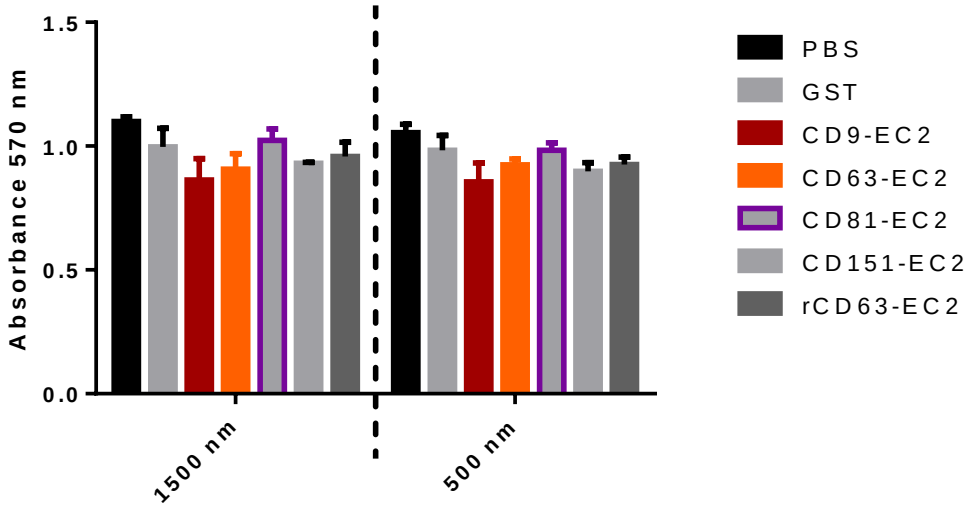

Figure 4.12: RBL-2H3 adhesion following overnight treatment with recombinant EC2 domains. RBL-2H3 cells were pre-incubated with 500 nm or 1500nm EC2 protein, GST or PBS only for 16 hours. After washing an SRB colorometric assay was carried out as in section 2.2.1.17, where absorbance at 570nm relates to the number of remaining adherent cells. Data points are mean ± standard error of the mean (SEM) from three repeats performed in triplicate. Values were compared by one-way ANOVA.

4.3 Discussion

There have been many reports of tetraspanins association with FcεRI or involvement in degranulation, for instance CD9 and CD81 both co-localize and co-immunoprecipitate with FcεRI (Higginbottom et al., 2000a; Peng et al., 2011). In addition, CD151 knockout mice show increased pro-inflammatory cytokine production upon mast cell activation and CD63 knock out BMMC have significantly reduce degranulation in response to IgE cross-linking (Abdala-Valencia et al., 2015; Kraft et al., 2013). On a number of occasions anti-tetraspanin monoclonal antibodies have been shown to affect the IgE-mediated degranulation response in RBL-2H3 cells. Kitani *et al.* (1991) used an anti-CD63 antibody (AD1) which significantly reduced degranulation when used at a high concentration (a result which has been reproduced here). Fleming *et al.* (1997) later showed a similar effect when pre-incubating with an anti-CD81 antibody, and also observed effects with the antibody on mast cells *in vivo*. More recently Kraft *et al.* (2005) also showed that an anti-CD63 mAb inhibited degranulation and linked this to its capacity to reduce cellular adhesion to various extracellular matrix components. RBL cells transfected with human CD63 were stimulated to degranulate in response to certain anti human-CD63 mAbs (Smith et al., 1995). Likewise, Higginbottom *et al.* (2000a) showed that human CD9 transfected RBL cells could be stimulated to degranulate in response to certain (mouse IgG1) anti-human CD9 antibodies; this response required CD9 cross linking along with the antibody Fc domain, which appeared to interact with the FcεRI receptor. With these observations in mind it has been speculated that FcεRI may be within a TEM where separate FcεRI molecules are clustered to enable more efficient cross linking upon antigen encounter.

Several studies have been complicated by intrinsic antibody properties, such as Fc receptor interaction, target protein cross-linking, along with their propensity to cross-link tetraspanin partner proteins also (Wright et al., 2004). Recombinant EC2 domains may therefore be useful alternative tools to discover more about tetraspanins functions in degranulation. In some cases, treatment with these recombinant proteins can result in a similar outcome to their respective monoclonal antibodies, whilst in other instances different effects are observed. Thus Takeda *et al.* (2003) found that anti-CD9 antibodies promoted monocyte fusion whilst recombinant CD9 EC2 inhibited fusion, a finding which was corroborated by our group (Parthasarathy et al., 2009). On the other hand CD81 mAbs and recombinant CD81 EC2 both inhibited sperm egg fusion (Higginbottom et al., 2003; Takahashi et al., 2001). The manner in which EC2 domains function is not fully understood, although several groups suggest that the they are able to compete with endogenous EC2 domains for binding of various receptors and in doing so disrupt signalling pathways (Barreiro et al., 2008; Zhu et al., 2002). Their disruptive effect could be in the context of TEMs where multiple interactions with both tetraspanins and

partner proteins lead to an ordered structure within the membrane. If FcεRI is located within a TEM then EC2 domains may lead to decreased clustering of the receptors and therefore reduce cross-linking and degranulation. Alternatively recombinant EC2 domains could reduce associations with other downstream signalling molecules which might be present in TEMs such as several membrane bound adaptor proteins. Moreover, previous studies have linked levels of degranulation to cellular adhesion (Kraft et al., 2005) and because recombinant EC2 domains have previously been shown to alter endothelial adhesion properties (Barreiro et al., 2005, 2008) it is also conceivable that they could affect degranulation by altering RBL-2H3 adhesion.

Expression assays using EC2-specific monoclonal antibodies confirmed the presence of the relevant tetraspanins on RBL-2H3 cells (including CD9 on human CD9 transfected cells) (Figure 4.2). However, initial degranulation assays indicated that recombinant EC2-GST fusion proteins were unable to affect IgE-mediated degranulation (Figure 4.3). Interestingly, LPS was also shown not to alter degranulation despite expression of TLR-4 on RBL-2H3 cells, however RBL-2H3 insensitivity towards LPS has previously been reported and suggested to be due to absence of CD14 which is required for downstream signalling (Bieneman et al., 2005; Passante and Frankish, 2009). To make any potential effects of EC2 pre-incubation more pronounced, higher concentrations of recombinant EC2 domains and longer periods of incubation were used, however no effect on degranulation was observed (Figure 4.4, 4.7). It was speculated that perhaps the high valency of the DNP-HSA antigen (30-40 DNP moieties per HSA) used to trigger degranulation might mask any potential disruption of FcεRI within TEM caused by recombinant EC2 domains. For this reason it was decided to use a monoclonal anti-IgE as a cross-linking reagent, with lower valency. However, despite this hypothetically more sensitive approach the recombinant EC2 domains again had no significant effect on RBL-2H3 degranulation (Figure 4.8).

The tetraspanins are generally well conserved across species, with these particular members being 65-85% conserved between rat and human (Appendix Figure 7.2). Additionally, previous work have shown that recombinant human EC2 domains have been able to affect cells from other species, for instances reducing fusion of mouse macrophages (Figure 5.6) and in some instances tetraspanin knockout phenotypes can be restored using mRNA of tetraspanins from a different species (Zhu et al., 2002). However, some reports have suggested a level of species specificity, for example, human CD81 EC2 could inhibit HCV infection of human liver cells whereas rat and mouse could not (Flint et al., 2006). This is presumably due to either tetraspanin-tetraspanin or tetraspanin-partner interactions requiring regions of the EC2 domain which vary between species. It is therefore possible that the use of human

recombinant EC2 domains here limited the amount of interaction with the endogenous rat proteins, thereby precluding any effect on degranulation. To address this, recombinant rat CD63 EC2 was generated as described in 3.2.5 , this particular member was chosen as it is the most divergent of the tetraspanins under investigation and has the largest body of evidence for involvement in degranulation. It was hoped that the use of recombinant rat CD63 may overcome this, however no modulation of degranulation was exhibited by the rat variant of CD63 EC2 (Figure 4.9).

Due to the lack of CD9 in RBL-2H3 cells, human CD9 transfected cells were used to investigate the role of this particular tetraspanin. This cell line was previously shown to degranulate in response to anti-CD9 mAbs with no other stimulus (Higginbottom et al., 2000a) and an association between the human CD9 and FcεRI was suggested. However, when pre-incubating with CD9-EC2 then stimulating degranulation with DNP or anti-IgE there was no significant effect on degranulation (Figure 4.10). CD9/CD81 chimeras have shown that certain areas of the recombinant EC2 domains are more important than other for their functional effects in other assays (Hulme et al., 2014) and the use of short synthetic peptides corresponding to different regions of the CD9 EC2 domain have in some cases shown greater efficacy than the full recombinant EC2 domain (D. Cozens unpublished observations). This is purportedly because their small size enables easier intercalation where the larger EC2-GST fusion proteins may be sterically hindered. Furthermore, these short synthetic peptides have the advantage of not being synthesised in *E. coli*, therefore should not contain any LPS contamination making them amenable to use in LPS sensitive assays. However, in this assay the selected peptides also have no significant effect on degranulation (Figure 4.11). It is interesting that the recombinant EC2 treatments did not affect degranulation, as they have displayed an effect in an number of other functional assays in our group (Figures 5.1, 5.6), yet there are a number of possible reasons as to why this is this case, some of which will be discussed here.

Firstly, It is possible that in previous reports of EC2-GST activity, the recombinant protein are not intercalating within the TEM giving a general disrupting effect as hypothesised (Barreiro et al., 2008; Parthasarathy et al., 2009; Zhu et al., 2002), but are operating by a different mechanism. For example, they could be disrupt specific interactions between tetraspanins and partner proteins, leading to a change in cell behaviour. This mechanism may not be applicable to FcεRI signalling if tetraspanins and FcεRI do not directly interact. Although co-immunoprecipitation and antibody studies suggest interaction between a number of tetraspanins and FcεRI (Kraft et al., 2005; Peng et al., 2011) it is possible that these are secondary or even tertiary interactions rather than FcεRI being primary tetraspanin partner.

Secondly, although the IgE receptor appears to interact with a number of tetraspanins, there is the potential that it is not within a TEM. Tetraspanins are dynamic within the membrane and their inclusion within a TEM is transient, it is therefore possible that the interaction with FcεRI is not in the context of a TEM (Espenel et al., 2008). This would mean that the proposed general disruption of a TEM caused by EC2 treatment would not affect FcεRI distribution and therefore degranulation. EC2 domains might still be expected to disrupt FcεRI interactions with their respective tetraspanins, but due to limited understanding of tetraspanin involvement in this signalling pathway it is not clear what effect this would have. It is plausible that the anti-tetraspanin monoclonal antibodies are able to modulate activity due to their high affinity binding to their target protein, whilst EC2 domains are likely to bind with much lower affinity and may therefore require TEM involvement for effects to be displayed.

A number of previous reports have provided evidence for lipid raft involvement in IgE mediated signalling, for instance, FcεRI has been isolated from low density Triton X-100 resistant microdmains which are characteristic of lipid rafts (Field et al., 1995). Moreover, cholesterol depletion, which is known to disrupt lipid rafts and to a lesser extent TEMs, stops FcεRI partitioning into the detergent resistant fraction, reduces its tyrosine phosphorylation (the first step in its activation) and its association with the tyroskine kinase Lyn (which is responsible for initial signal transduction)(Kato et al., 2003; Sheets et al., 1999). Additionally, Lyn isolated from the detergent soluble fraction was shown to have a fourfold lower activity than “raft-associated” Lyn, which is suggested to be because of exclusion of specific phosphatase enzymes from lipid rafts (Young et al., 2003). TEMs and lipid rafts are often viewed as distinct microdomains so the involvement of FcεRI with lipid rafts may limit the possibility its presence within a TEM. On the other hand, it is not clear if these microdomains are mutually exclusive, indeed there has been certain examples of coalescence between the two (Hogue et al., 2011) so this might not definitively exclude FcεRI from TEMs.

Finally, these results could indicate that intercalation of recombinant EC2 domains into the TEM is insufficient to disrupt IgE receptor signalling. In studies where EC2 domains do exhibit an effect, for example in membrane fusion and bacterial adhesion (Green et al., 2011; Parthasarathy et al., 2009), TEMs may play a more sophisticated role, perhaps coordinating a complex interplay between separate signalling molecules rather than the proposed function here of holding equivalent receptors within a defined area. This more elaborate role could be more easily disturbed by the EC2 treatment.

The results here suggest that the EC2 domains do not have any therapeutic application with regards to mast cell activation. However, these negative data have enabled speculation into

tetraspanin association with FcεRI and possible mechanisms of recombinant EC2 domain activity. It is important to note that the suggested reasons for lack of activity are speculative and further work would be required to confirm any of the proposed explanations. For instance using a defined ECM component to which the cells could adhere during degranulation may give more information about potential reduction in adhesion caused by the EC2 domains. Nearest neighbour analysis was previously used to see if the spacing of two adhesion receptors was altered following CD9 EC2 treatment of endothelial cells (Barreiro et al., 2008). This involves immune-gold labelling and scanning electron microscopy to identify the receptors under investigation followed by statistical analysis of their location in respect to one another. A similar method could be undertaken following treatment of RBL cells with recombinant EC2 domains to show more definitively if they are able to alter the spacing of the IgE receptor.

Chapter 5: Physical studies of tetraspanin EC2 domains

5.1 Introduction

Recombinant tetraspanin EC2 domains exhibit activity in a number of functional assays, such as inhibiting cell:cell fusion, viral infection and bacterial adhesion to cells (Barreiro et al., 2008; Green et al., 2011; Ho et al., 2006; Parthasarathy et al., 2009; Rajesh et al., 2012; Takeda et al., 2003; Zhu et al., 2002). It is still not completely clear how the EC2 domains impart their effects, although it has been commonly suggested that they intercalate into and disrupt existing TEMs (Barreiro et al., 2008; Green et al., 2011; Ho et al., 2006). Since they show activity in so many processes associated with tetraspanins, it was somewhat surprising that several recombinant EC2 domains were unable to modulate degranulation in RBL-2H3 cells, as described in the previous chapter. Some studies have shown that recombinant EC2 domains only bind to specific cells (regardless of whether the respective tetraspanin is expressed) (Kelić et al., 2001), or to cells under specific conditions (Parthasarathy et al., 2009), suggesting interactions with surface molecules present only on specific cell types or that are upregulated during certain processes. The first aim of this chapter was to investigate the binding of EC2 domains to RBL-2H3 cells and to the human epithelial cell line, HEC-1B this experiment was carried out due to the hypothesis that the EC2 domains may have to bind the cells in order to impart an effect. The latter was chosen as EC2 domains have been shown to significantly reduce bacterial adhesion to these cells by a mechanism proposed to involve disruption of “adhesion platforms” on the epithelial surface (Green et al., 2011).

As mentioned previously (Chapter 3), a potential problem of using recombinant proteins produced in bacteria is that they may be contaminated with endotoxin (LPS), a component of the bacterial cell wall which can affect mammalian cell behaviour by inducing signalling through the TLR4 receptor (Bausinger et al., 2002; Wakelin et al., 2006). An interest of our group has been the role of tetraspanins in the fusion of monocytes/macrophages to form multinucleated giant cells (Hulme et al., 2014; Parthasarathy et al., 2009). Recombinant EC2 proteins representing CD9 and CD63 inhibited Concanavalin A (ConA)-induced giant cell formation from monocytes *in vitro*, whereas CD81 EC2 and mutated versions of CD9 EC2 were inactive (Hulme et al., 2014; Parthasarathy et al., 2009; Takeda et al., 2003). Some workers have indicated that monocyte/macrophage fusion is inhibited by LPS, which is present in the EC2 preparations (Takashima et al., 1993) (Fanaei, 2013), whereas others have shown no effect of LPS (Parthasarathy et al., 2009). Our group has recently started to investigate the role

of tetraspanin proteins in fusion induced by the bacterium *Burkholderia thaillandensis.* This non-pathogenic, gram-negative bacterium is used as a model of the pathogen *Burkholderia pseudomallei* which is the causative agent of mellioidosis, a potentially fatal disease comprising a broad array of clinical manifestations affecting animals and humans predominantly in Australia and South-East Asia (Boddey et al., 2007; Kespichayawattana et al., 2000). *B. pseudomallei* is thought to induce cell fusion as a means of spreading within an infected host and in doing so forms large multinucleate giant cells containing many intracellular bacteria. Interestingly the bacteria is resistant to killing by phagocytes due to its ability to escape the phagosome into the cytoplasm, and has been shown to induce giant cell formation in both phagocytic and non-phagocytic cells both *in vivo* and *in vitro* (Kespichayawattana et al., 2000). Recombinant EC2 proteins generated as part of this project were found to inhibit *B thaillandensis* fusion by co-worker Atiga Elgawidi. The second aim of this chapter was therefore to determine LPS contamination levels in the EC2 proteins to see if there was any correlation with inhibitory activity. The levels of LPS present might also be relevant to other cell functional studies and would inform the inclusion of appropriate controls or the need to reduce endotoxin contamination.

Rajesh *et al.* (2012) have used CD spectroscopy to show that their bacterially expressed CD81 EC2 has a characteristic α-helical content consistent with that found in the CD81 crystal structure (Kitadokoro et al., 2001). However, differences in expression methodology (for instance different vectors, EC2 boundaries and expression conditions) mean these findings may not be readily applicable to the EC2 domains produced by our group. Moreover, some of the EC2 domains produced by our group contain a greater number of putative disulphide bonds than CD81 which attribute them with a more complex folding structure making them more liable to misfold (Qiu et al., 1998). The principle of circular dichroism is based on chiral molecules (including 19 out of 20 amino acids) capacity to absorb left-handed and right-handed circularly polarised light to different extents. This difference in absorbance measured over a range of wavelengths is known as circular dichroism spectroscopy and in proteins is mainly influenced by the macromolecules overarching structure rather than the absorbance of its constituent residues. A protein secondary structure (i.e. its α-helical and β-sheet content) can be calculated based on its absorbance in the far UV region (190-260nm) as these particular structural features have a characteristic absorbance profile at these wavelengths (Greenfield, 2007). Online software, such as Dichroweb, use algorithms to give an estimation of the overall secondary structure by comparing its absorbance profile to those gained when using reference proteins that contain alpha helix and beta sheet character. CD spectroscopy is often utilised to learn more about a proteins secondary structure but can also be used to track a protein

denaturation over time. In contrast to NMR and X-ray crystallography, CD spectroscopy is a low resolution method but has fewer requirements in terms of protein sample and time investment (Kelly et al., 2005) . The final aim of this chapter was to use CD spectroscopy to determine more definitively if the EC2 domains produced by our group are correctly folded; however the GST tag within the recombinant fusion proteins makes up a large proportion of the overall recombinant EC2 domains (around 26kDa of the 36kDa proteins) and it too has a secondary structure. This could lead to difficulties when attempting to discern between readings contributed by the tag and by the protein under investigation. It was therefore necessary to first remove the GST prior to analysis (Kelly et al., 2005). Removal of the tag may also be desirable for later structural or functional studies in which effects of the GST tag must be negated.

5.2 Results

5.2.1 Binding of recombinant EC2 domains

To examine their cellular specificity, binding of the EC2 domains to two cell lines, HEC-1B cells, and RBL-2H3 cells, was investigated. As described in Chapter 4, the EC2 domains have yet to show any activity on RBL-2H3 cells, however, CD9, CD63 and CD151 EC2 domains have been demonstrated to reduce bacterial adhesion to HEC-1B cells (Green et al., 2011) and using the EC2 proteins generated during this project we were able to reproduce this effect (CD151 was also shown to have an inhibitory role, however this affect was not tested here) (Figure 5.1). Thus in the presence of CD9, CD63 and CD151 EC2 there is a significant reduction in both number of number of bacteria per 100 cells and the number of infected cells, whilst CD81 EC2 had no such effect. Importantly, both cell lines express some of the tetraspanins under investigation, with the notable exception of CD9 in RBL-2H3 cells (Figure 4.1) and the relatively low expression of CD151 in Hec-1B cells (Figure 5.1b).

Initial attempts to dissect EC2 binding were indirect, using an anti-GST antibody as a means of quantifying the amount of bound EC2 protein (2.2.1.6). In brief, RBL cells were incubated with EC2-GST fusion proteins, then the cells were washed, fixed and then incubated with a FITC conjugated anti-GST antibody before being washed again and analysed by flow cytometry. Cells which were not incubated with an initial GST containing protein (no treatment, Figure5.2a) still exhibited high MFI readings (around 56% of the overall MFI) which are most likely due to non-specific or Fc receptor binding by the fluorescent anti-GST antibody. A clearer picture could be seen when this background was removed from the original values (Figure 5.2b) and showed each concentration of the tetraspanin proteins had slightly more binding over the equivalent GST only control. However, GST binding was unexpectedly high and when

the MFI values of the cells which were incubated with the highest protein concentrations were compared by one-way ANOVA, only the CD81 treatment showed a significant ($P < 0.05$) increase over GST (Figure 5.2c).

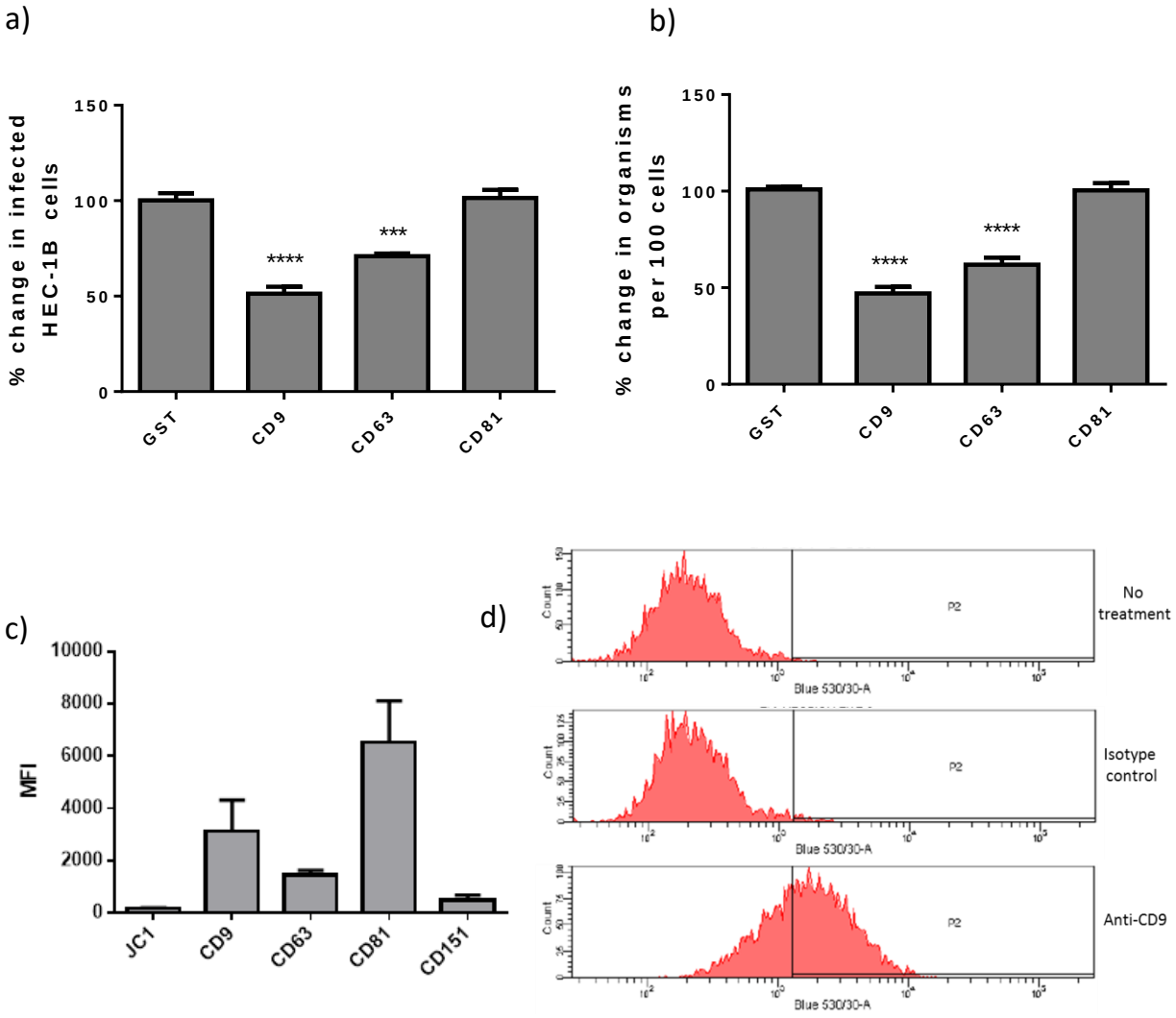

Figure 5.1: Effect of recombinant tetraspanin EC2 domains on *N. meningitidis* adhesion to HEC-1B cells and expression of several tetraspanins on the HEC-1B cell surface. (a+b) Bacterial adhesion assay carried out by D. Cozens. Briefly, Hec-1b cells were seeded on coverslips and blocked using bovine serum abumin (BSA). The cells were then washed and treated with recombinant GST fusion proteins for 30 minutes. Excess protein was removed by washing and the cells were then incubated with bacteria (MOI 300) for 60 minutes. Cells were washed and fixed then treated with anti-miningococci antibodies followed by FITC-labelled secondary antibodies in order to visualize external bacteria. Nuclear DNA was stained with DAPI and coverslips were then mounted, slides were visualised and 100 cells were counted along with the number of associated bacteria. Results are from four biological repeats displayed as means ± standard error values. Significance is shown relative to the GST control *** = P<0.001, **** = P<0.0001 **(c)** Tetraspanin expression on HEC-1B cells was analysed according to section 2.2.1.9 carried out by F. Ali. MFI readings of cells probed with anti-tetraspanin antibodies or an isotype control antibody (JC-1) are displayed. (**d**) Example of gating used in Flow cytometry to determine expression of tetraspanins on HEC-1B cells. Data points are mean ± standard error of the mean (SEM) from three repeats carried out in duplicate.

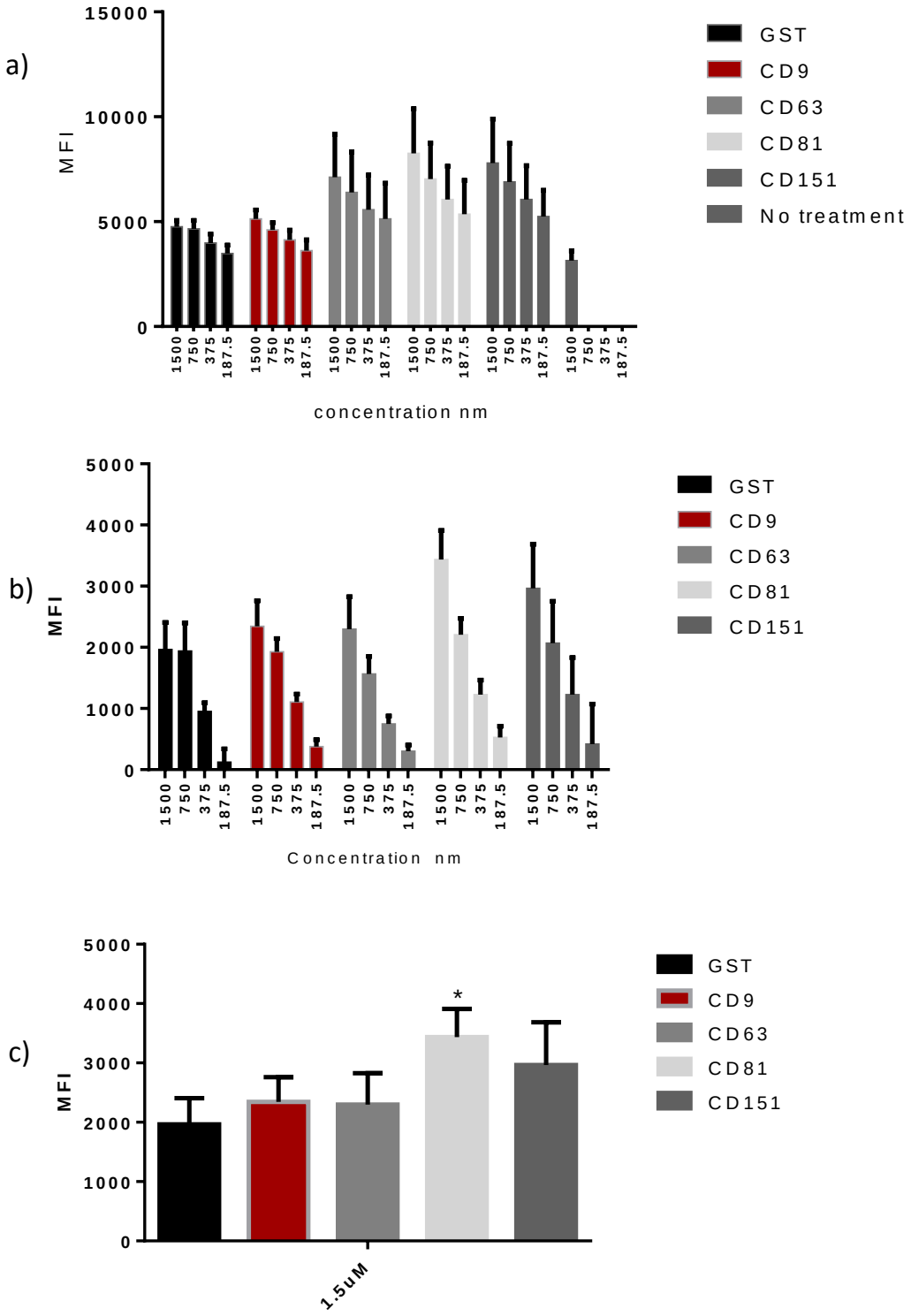

Figure 5.2: Indirect analysis of EC2 binding to RBL-2H3 cells via flow cytometry. EC2 domains were incubated with RBL-2H3 cells for one hour, after which time they were fixed and incubated with a FITC labelled anti-GST antibody. Binding was analysed by flow cytometry (**a**) Original MFI values (**b**) MFI with background reading subtracted (**c**) one way ANOVA used to compare readings when using the highest concentration of recombinant EC2 domains. Results are means ± standard error from four experiment performed in triplicate * = P <0.05.

It was considered that the high level of non-specific/Fc receptor antibody binding might be masking much of the EC2 interaction, therefore a more direct method for assessing binding was used next (Section 2.2.1.7). Firstly recombinant EC2 domains and GST were fluorescently labelled with Alexa488 (Section 2.2.3.16) and the efficiency of labelling (representing the number of molecules of fluorescent dye per protein) was calculated to allow corrections to be made based on differences in labelling (Table 5.1). These proteins were incubated with the RBL-2H3 or HEC-1B cells, and after thoroughly washing, the cells were analysed by flow cytometry (Figure 5.3). Curves were generated to examine the binding profile of each protein (Figure 5.4) and the amount of binding exhibited by the EC2 domains at each concentration was analysed relative to the equivalent concentration GST control (Figure 5.4).

In RBL-2H3 cells, at higher recombinant protein concentrations (above 300 mM) each EC2 domain exhibited significantly higher binding than the equivalent GST control and CD81 EC2 showed significance at even lower concentrations (Figure 5.4), suggesting that the indirect analysis identified this EC2 domains due to its higher degree of binding. The binding of EC2 domains to HEC-1B cells, although higher than RBL-2H3 cells in terms of total MFI, does not show as clear significance in relation to the GST control due to the higher amount of GST interaction (Figure 5.4). Furthermore, CD151 binding is not significantly higher than GST at any of the concentrations tested. Interestingly, the MFI values do not correlate with the expression of the respective tetraspanins, for instance the highest MFI readings with HEC-1B cells were given for incubation with CD9, despite CD81 being the most highly expressed, and CD9 gave similarly high readings when incubated with RBL-2H3 cells despite CD9 not being expressed on these cells (Figure 4.1). Furthermore, the binding pattern does not relate to the degree of protein labelling, and the very similar DOL values would also suggest that this is not responsible the different MFI values seen. Unfortunately it was not possible to attain high enough concentrations of labelled proteins to determine if binding could be saturated so these results do not show the complete binding profile of each recombinant EC2 domain and EC50s could not be calculated which made comparisons between cell types difficult. The MFI values of EC2 treated HEC-1b cells were greater than those of the RBL-2H3 cells suggesting a higher amount of overall EC2 binding to this cell type; however GST binding was also higher so there could be a non-specific contribution to the EC2 binding to these cells.

Protein name	DOL
GST	3.295
CD9 EC2	3.629
CD63 EC2	4.327
CD81 EC2	4.628
CD151 EC2	3.827

Table 5.1: Degree of labelling of recombinant proteins. Recombinant proteins were labelled with Alexa488 and the degree of labelling calculated according to section 2.2.3.16.

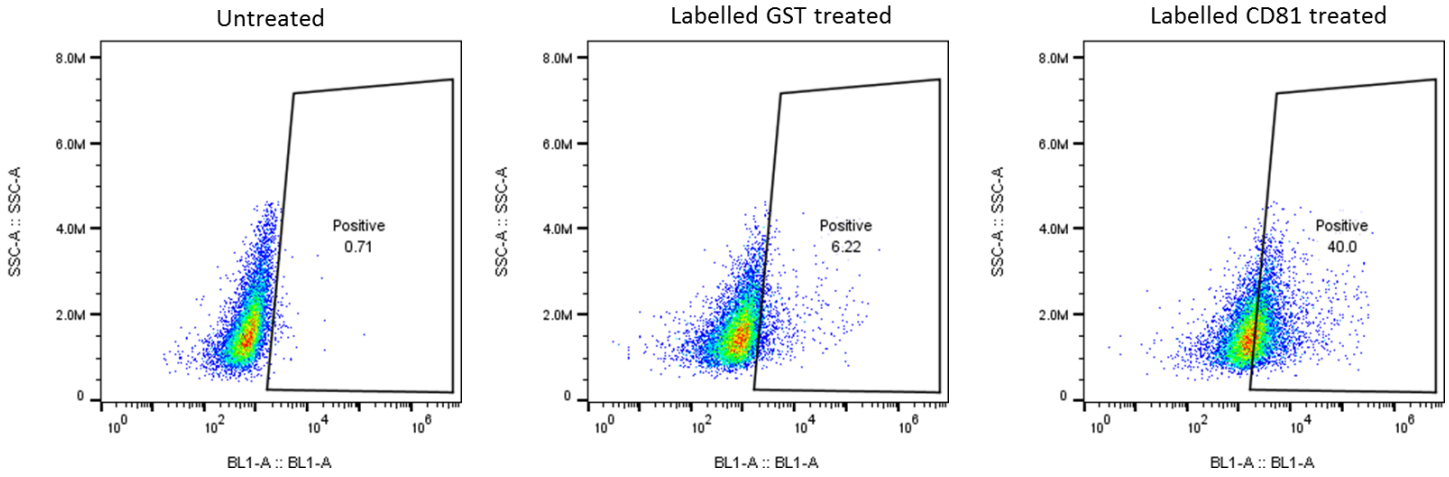

Figure 5.3: Scatter plots representative of untreated and labelled GST and CD81 EC2 treated RBL-2H3 cells. Following 40 minute incubation with labelled proteins, RBL cells were washed and then analysed by flow cytometry. To calculate % positive, negative control gates were established using non-treated cells and applied to cells which had been treated with the various EC2 domains. Scatter plots are one method of depicting the data with the percentage values being transferred to a line graph for easier comparison at multiple protein concentrations (Figure 5.4)

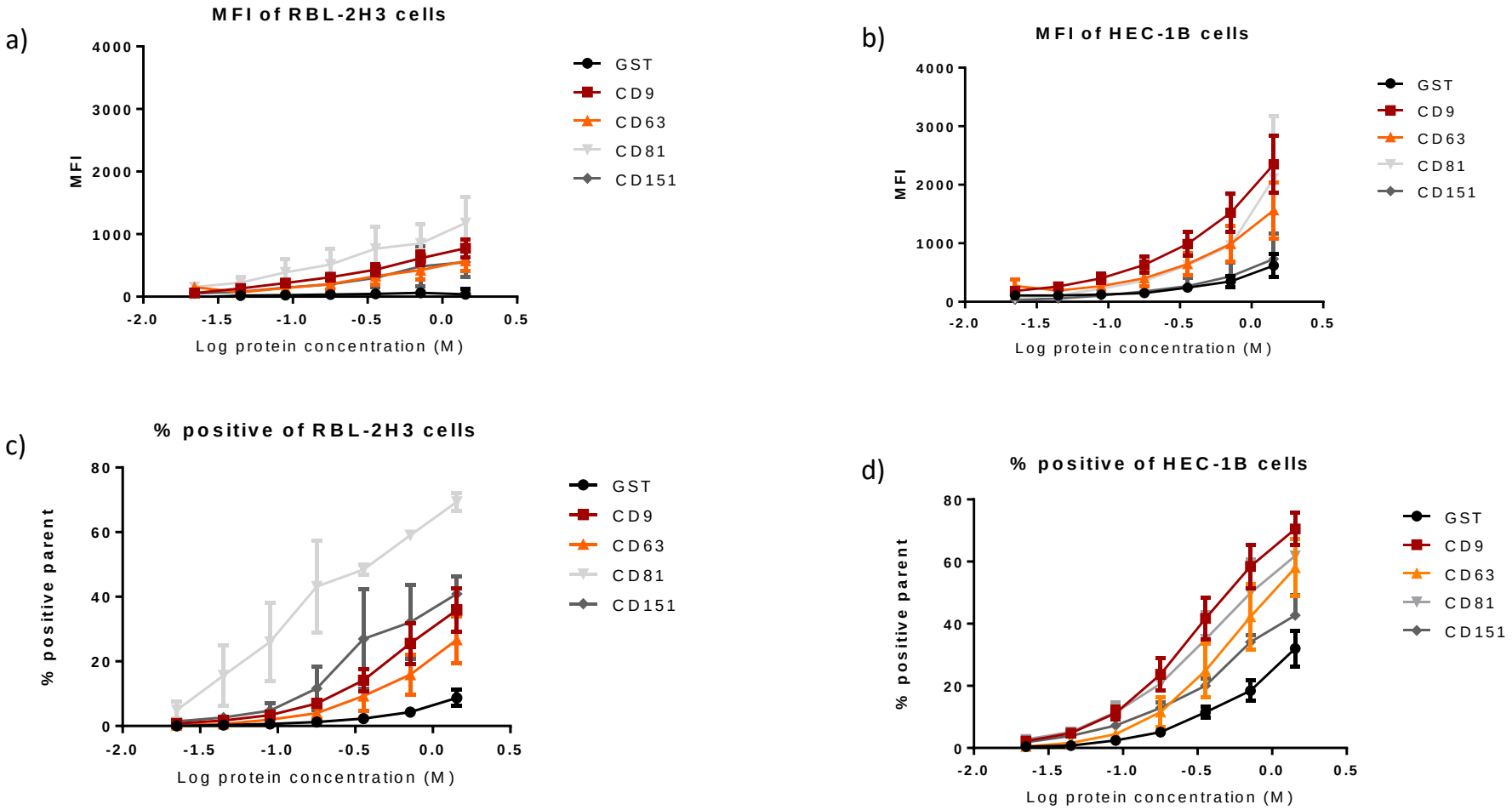

Figure 5.4: Direct analysis of EC2 binding to HEC-1B cells and RBL-2H3 cells via flow cytometry. Fluorescently labelled EC2 domains were incubated with RBL-2H3 cells or HEC-1B cells for 40minutes before cells were washed and analysed by flow cytometry. Results for both cell types are displayed as **(a+b)** MFI which was determined by removing background MFI values from those attained from treated cells and **(c+d)** % positive cells when compared to control cells (determined according to Figure 5.3). Data points are mean ± standard error of the mean (SEM) representative of a minimum of two repeats performed in triplicate.

Although there is a dose dependent increase in binding of the recombinant proteins and a clear distinction between levels of GST and EC2 binding, it is not clear if the binding is specific (i.e. if they are binding to specific surface proteins). To determine if this was the case, competitions assays were performed where the cells were first incubated with a range of concentrations of unlabelled EC2 protein, before a binding assay was carried out using a fixed concentration of labelled protein. Labelled proteins were used at concentrations that gave half maximal binding in the previous binding assays, whilst unlabelled proteins were used at an initial ten-fold higher concentration in an effort to maximise any inhibitory effects. There was a notable decrease in MFI values of RBL-2H3 cells when treated with increasing concentrations of both CD9 and CD63 proteins (Figure 5.5a) suggesting some specific nature to the binding. However, readings for HEC-1B cells showed a greater amount of variation but, due to time constraints the binding of CD9 and CD151 could not be examined further.

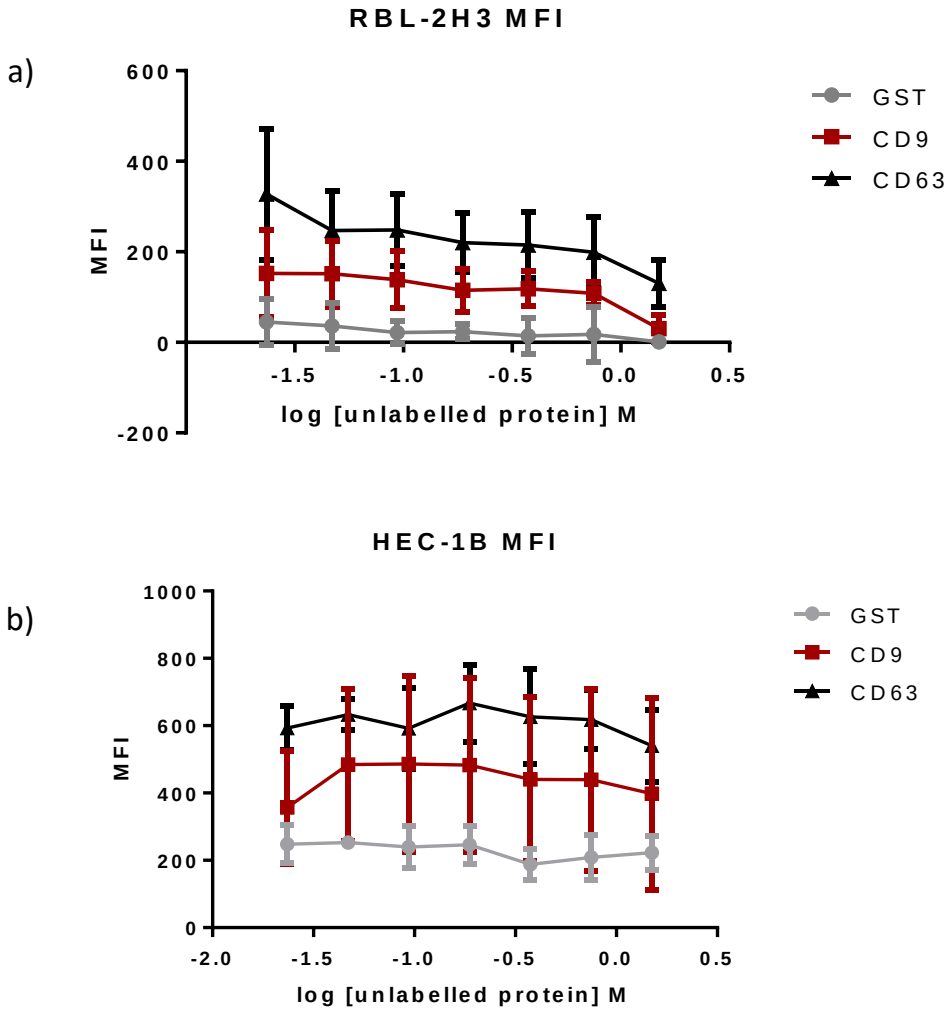

Figure 5.5: Competitive binding of labelled and unlabelled EC2 domains to RBL-2H3 cells and HEC-1B cells. Cells were incubated with an excess of unlabelled recombinant EC2 domains for 15minutes to saturate any specific binding sites which may be present. Cells were then treated with labelled EC2 domains at a concentration which gave half maximal signal in binding experiments (Figure 5.4) for 40 minutes. Cells were then washed and analysed by flow cytometry **(a)** MFI of RBL-2H3 cells incubated with CD63 and CD9 EC2 **(b)** MFI of HEC-1B cells treated with CD9 and CD63. Data points are mean ± standard error of the mean (SEM) and representative of a minimum of three repeats performed in triplicate.

5.2.2 Effect of recombinant EC2 domains on *B. thaillandensis* induced cell fusion and correlation with LPS levels

B. thaillandensis induced fusion of the mouse macrophage cell line J774.2 was studied by A. Elgawidi as described in section 2.2.1.16 (data analysed by the author). Although J774.2 cells are a murine macrophage cell line, the human EC2 domains display high identity to the mouse orthologues (Appendix Figure 7.3) and human CD9 has previously been shown to compensate for the loss of its mouse counterpart (Zhu et al., 2002). Cells were treated with various recombinant EC2 domains prior to infection with *B. thaillandensis* and after allowing fusion to take place, the number of giant cells and the number of nuclei within giant cells were determined. The average size of the resultant giant cells is displayed as the typical number of nuclei within a giant cell and the fusion index represents the number of nuclei within giant cells in relation to the total number of nuclei. To account for variation between experiments (for instance slightly different plating densities), both results are normalised to the values seen in cells with no pre-treatment but non-normal values ranging from 6-20 nuclei per cell with 10-60% of cells taking part in fusion. Giant cell size is significantly decreased when pre-treating the cells with CD9-EC2 and CD63-EC2, with no decrease being exhibited after CD151-EC2 or Tspan 2-EC2 treatment (Figure 5.6a). Similarly CD9 and CD63 are also able to significantly reduce fusion index, whilst CD151 and Tspan2 showed no affect (Figure 5.6b). Moreover, as only two of the four tetraspanins studied were able to reduce fusion, it suggests a specific involvement of these tetraspanin members in the process. To confirm that LPS was not the active constituent, the amount of LPS within the proteins was determined (2.2.3.12) and correlated to the inhibitory effect that each protein has on fusion.

Figure 5.7a shows that amounts of LPS varies between different EC2 domains, and it is also interesting to note that different preparations of the same EC2 domain, made under the same conditions, can exhibit varied LPS levels (as can be seen when comparing CD9(1) with CD9(2) and CD63(1) with CD63(2)). The amount of LPS within a sample does not correlated with its effect on either fusion index or average MNGC size, and it is clear that in each instance there is no relationship between the amount of LPS within a sample and its effect on either parameter. This result indicates that, in this instance, the inhibitory effect of the recombinant proteins on MNGC formation relates to the specific EC2 protein rather than any activity of LPS.

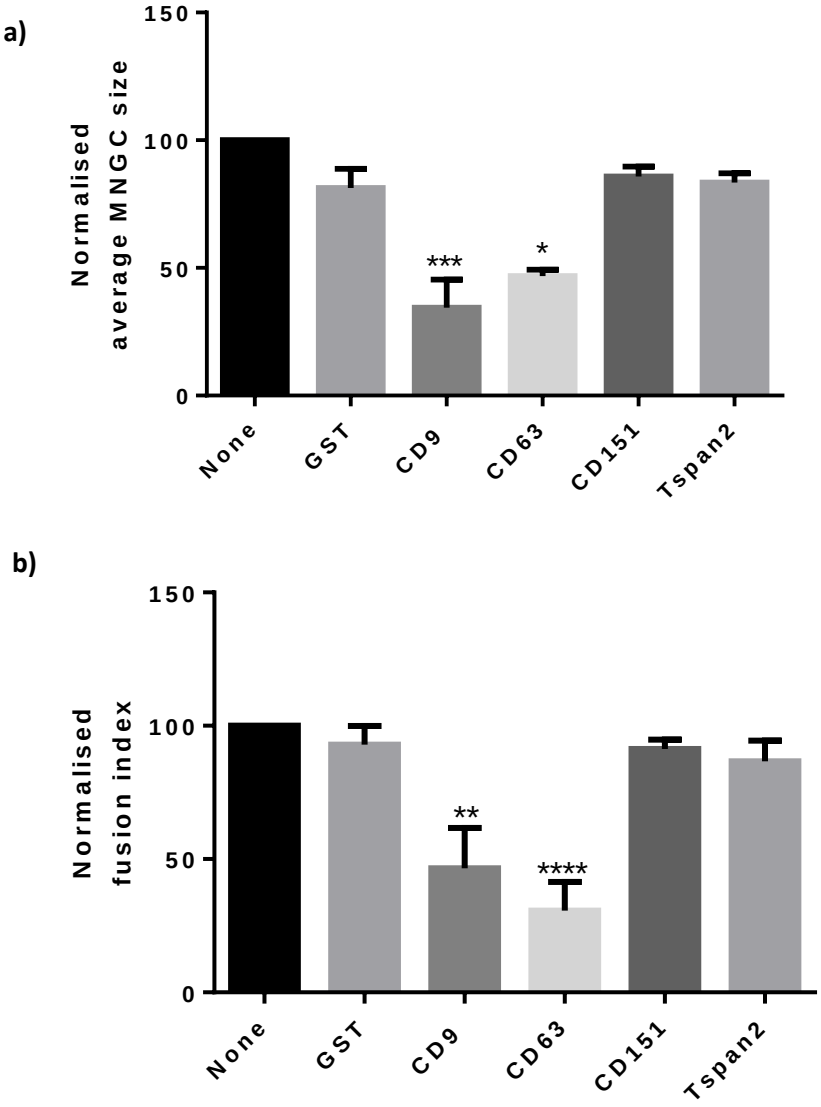

Figure 5.6: Recombinant tetraspanin EC2 domains effect on *B. thailandensis* induced fusion of J774.2 cells. J774.2 cells were treated with 500nM of various EC2 or GST alone for one hour prior to infection with *B. thailandensis.* After infection, external bacteria were killed and cells were allowed to fuse overnight after which they were fixed and stained with Giemsa solution. 10 random fields were taken from each condition and nuclei were counted. Results were normalised and are displayed as **(a)** MNGC size which indicates the average number of nuclei within a giant cell and **(b)** Fusion index which represents the proportion of nuclei found within giant cells. Results are means ± standard error from three experiment performed in triplicate, values were compared to the GST control by one way ANOVA with Holm-Sidak's multiple comparison correction * = P<0.05, ** = P<0.001, **** = P<0.0001.

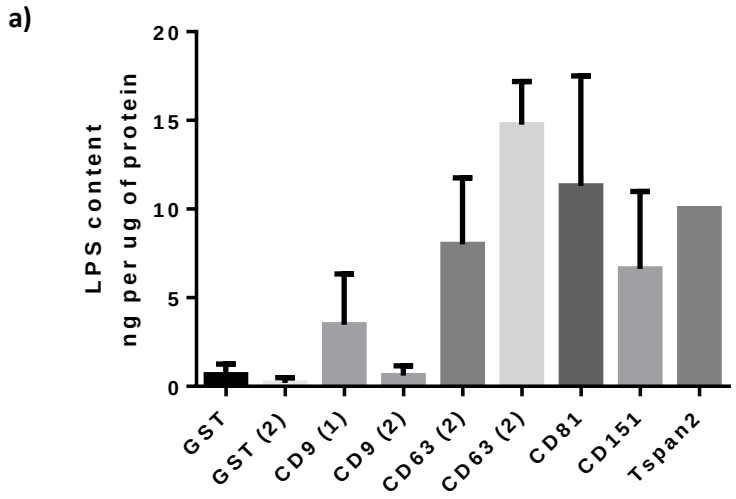

Figure 5.7: LPS content of recombinant EC2 domains and correlation to effect on giant cell formation. (a) LPS content of recombinant proteins was determined using a Pierce LAL endotoxin quantification kit. CD9 (2) and GST (2) were produced by a previous lab member and CD63 (2) indicates CD63 produced from a separate round of purification than that which made CD63 (1). (**b**) The amount of LPS within a recombinant protein preparation plotted against the amount which it reduced MNGC size **(c)** As in (b) but plotted against EC2 ability to reduce cell fusion. Data points are mean ± standard error of the mean (SEM) from a minimum of two repeats carried out in duplicate.

5.2.3 Recombinant EC2 cleavage and CD spectra

5.2.3.1 Optimisation of EC2-GST cleavage

To enable CD spectra to be attained from the EC2 proteins without interference of the large GST tag, the tag first had to be removed. The inclusion of a cleavage site in the vector enables removal through incubation with thrombin, and the flexible glycine linker within the pGEX-KG vector is thought to enable cleavage to take place more efficiently (Guan and Dixon, 1991). Previous students utilised a batch method of cleavage described in section 2.2.3.13, where proteins are incubated with glutathione Sepharose beads cleaved and separated from the beads by centrifugation. Recovery from this method of cleavage was reported to be only 5% however (Hulme, 2010), so efforts were undertaken to improve the experimental design.

According to manufacturer's guidelines (GE healthcare), one unit of thrombin, cleaves 100 µg of protein when incubated for 16 hours at 22^{o}C, however this is subject to change based on the target protein. Here, CD9 EC2-GST was cleaved using 0.5, 1 and 1.5 units of thrombin; additionally, a range of incubation times were used to determine which was most favourable. The protein attained from each cleavage condition was analysed by SDS PAGE followed by Coomassie staining (Figure5.8a) or Western blotting (Figure5.8b). Densitometry analysis of the anti-CD9 Western blot indicated that overnight incubation using one unit of thrombin resulted in the highest yield of cleaved protein. However, Coomassie staining of the cleaved protein (Figure 5.8a) shows bands at both 37 kDa and 26 kDa indicating both uncleaved protein and cleaved, free GST in the final sample. A proteins purity of 95% (as determined by Coomassie staining) is recommended for CD spectroscopy (Kelly et al., 2005), so it was therefore important to try to remove these unwanted proteins from the final samples. Repeat incubation with glutathione Sepharose beads followed by centrifugation reduced the amount of contaminating protein (data not shown); however contaminants still represented over 5% of the final sample. It is likely that these bands are a result of some of the glutathione Sepharose beads transferring into the final solution (despite using gel loading tips). It was not possible to quantify how much of the bead fraction had transferred into the final sample so comparison of cleavage efficiency between test conditions was not reliable. During later attempts at batch cleavage, these contaminating bands were still visible, so a column method of purification was subsequently employed, which should eliminate the transfer of Sepharose beads. The column cleavage method was carried out as in section 2.2.3.14, and the length of incubation with the thrombin was again adjusted. Western blot analysis (Figure 5.9c) followed by densitometry showed that overnight incubation resulted in the highest amount of cleaved CD9 protein.

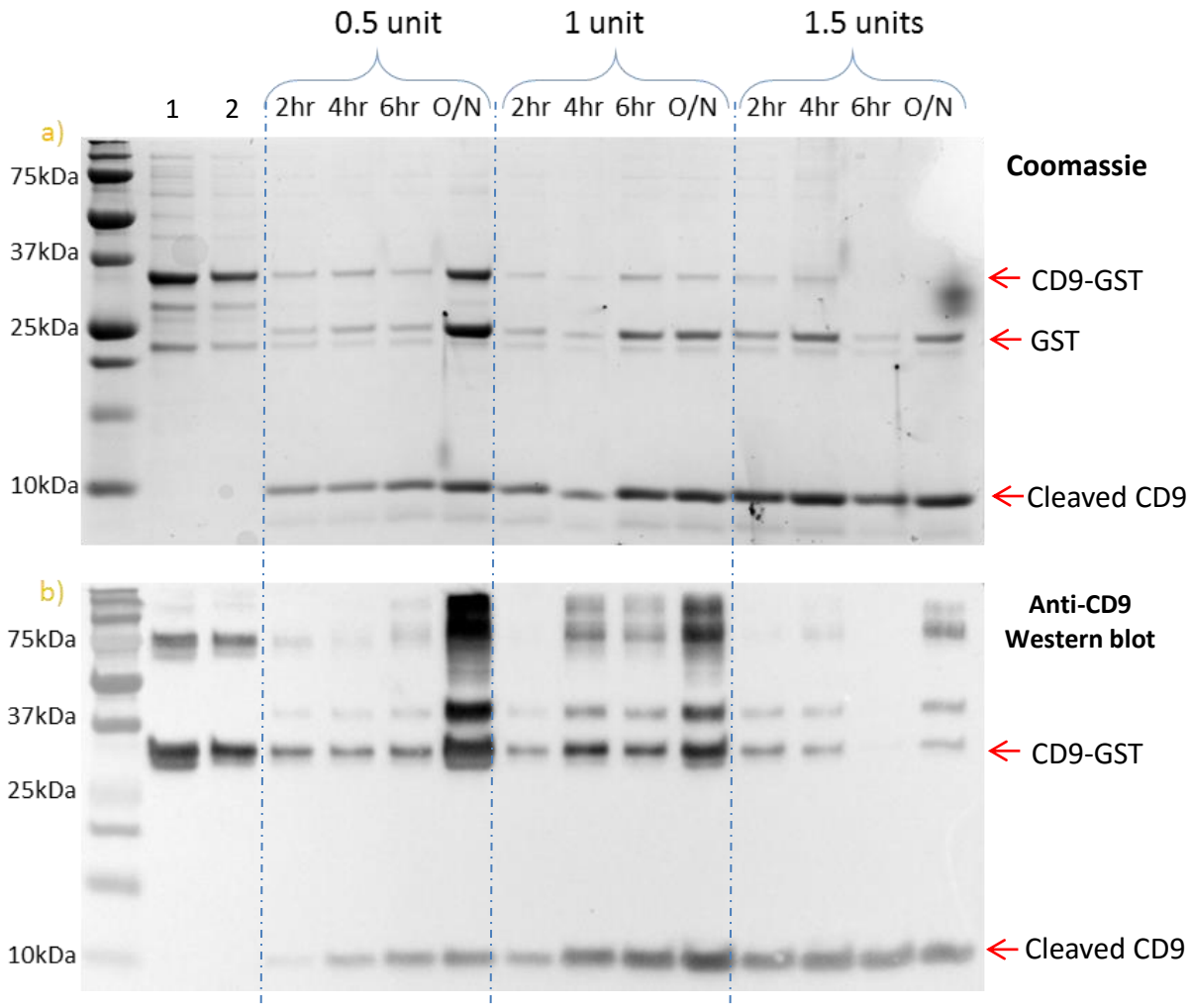

Figure 5.8: Optimisation of EC2-GST cleavage using a batch method. CD9-EC2 GST fusion protein was cleaved using three different concentration of thrombin and four different incubation times according to the batch cleavage method (Section 2.2.3.13). Lanes one and two show the original uncleaved sample and the protein removed from the beads following an initial wash respectively. **(a)** Coomassie stain of the resultant cleaved proteins **(b)** Western blot probed with an anti-CD9 monoclonal antibody.

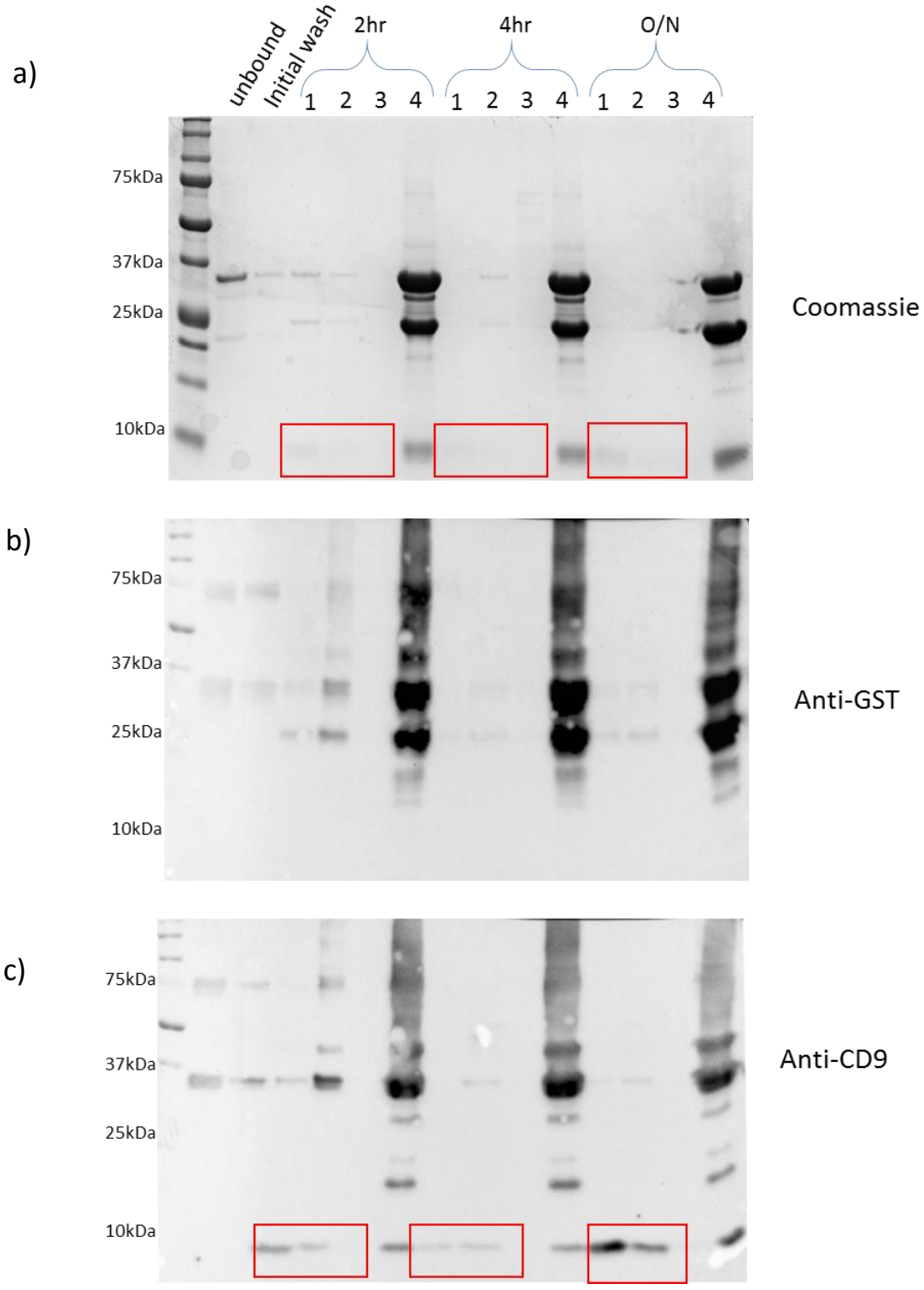

Figure 5.9: Effect of incubation time for EC2-GST cleavage using the column method. On column cleavage of CD9-EC2-GST fusion proteins was carried out (section 2.2.3.14) using one unit of thrombin with varied incubation times as indicated. Lanes one and two show the proteins which did not bind to the beads and the initial wash before cleavage. **(a)** Coomassie stain following cleavage **(b)** anti-GST Western blot following cleavage **(c)** anti-CD9 Western blot following cleavage. 1 = Cleavage fraction one, 2 = Cleavage fraction two, 3 = Wash following cleavage, 4 = Protein remaining on Glutathione sepharose beads.

Figures 5.9a and 5.9c (Lane 4) indicate that some of the cleaved protein remains attached to the glutathione Sepharose beads so in an attempt reduce the non-specific associations between the proteins and beads, a higher concentration of NaCl was used, along with 0.1% Triton X-100. A higher quantity of thrombin was also used (1.5 units) to see if this improved protein yields. When comparing the first cleavage fraction of Figure 5.10 (Lane 3) a thicker band can be observed when using 1.5 units of thrombin as opposed 1 unit, with densitometry analysis indicating around a three-fold improvement. Interestingly, almost no protein is visible in the cleaved fraction when using a higher amount of NaCl and Triton X-100 (Figure 5.10c), perhaps due to the protein precipitating out of solution due to the higher salt concentration.

5.2.3.2 CD spectroscopy

Once the optimum cleavage conditions had been established (16 hour incubation with 1.5 units of thrombin and standard PBS salt concentration (137 mM)), the purified tetraspanin EC2-GST fusion proteins were cleaved prior to CD spectroscopy analysis. Each of the cleaved proteins were quantified by Bradford assays (Section 2.2.3.10) and analysed by Coomassie staining and Western blotting using anti-tetraspanin antibodies (Figure 5.11). Coomassie staining indicates no contaminating protein in the cleavage fraction and similarly no GST was detected in cleaved fractions of CD9 and CD81 by Western blot analysis. Bands are present at ~10 kDa in anti-CD9, anti-CD81 and anti-CD151 Western blots, however there are no such bands displayed in the anti-CD63 Western blots. Spectra attained for CD9 and CD81 are displayed in Figure 5.12; readings were deconvoluted using the online software DICHROWEB using the SELCON3 and CONTIN algorithms. Secondary structure predictions were averaged from the two algorithms, however relatively high NRMSD values indicate that secondary predictions may not be as accurate as desired (perhaps resulting from difficulty in accurately estimating protein concentrations at such low values). However, an estimated 52% α-helical content of CD81 is comparable to the 58% previously reported (Rajesh et al., 2012) and the spectra for both CD9 and CD81 have a characteristic α-helical shape with minima at 208 nm and 222 nm which are expected for these proteins, suggesting that the estimated readings are somewhat reliable. Despite optimising cleavage and repeated cleavage attempts, quantities of cleaved CD63 and CD151 were still poor and not sufficiently concentrated to give acceptable spectra. After optimisation, cleavage efficiency of CD9-EC2 was ~50%, a tenfold increase over that reported by previous lab members. However CD63-EC2 exhibited a cleavage efficiency of ~20% and its UV absorbance readings, and that of CD151 displayed light scattering which indicates protein aggregates. It is possible that removal of the GST tag reduced the solubility of the proteins and in the 6-cys containing EC2 domains this has a more pronounced effect which could lead to them precipitating out of solution (Terpe, 2003).

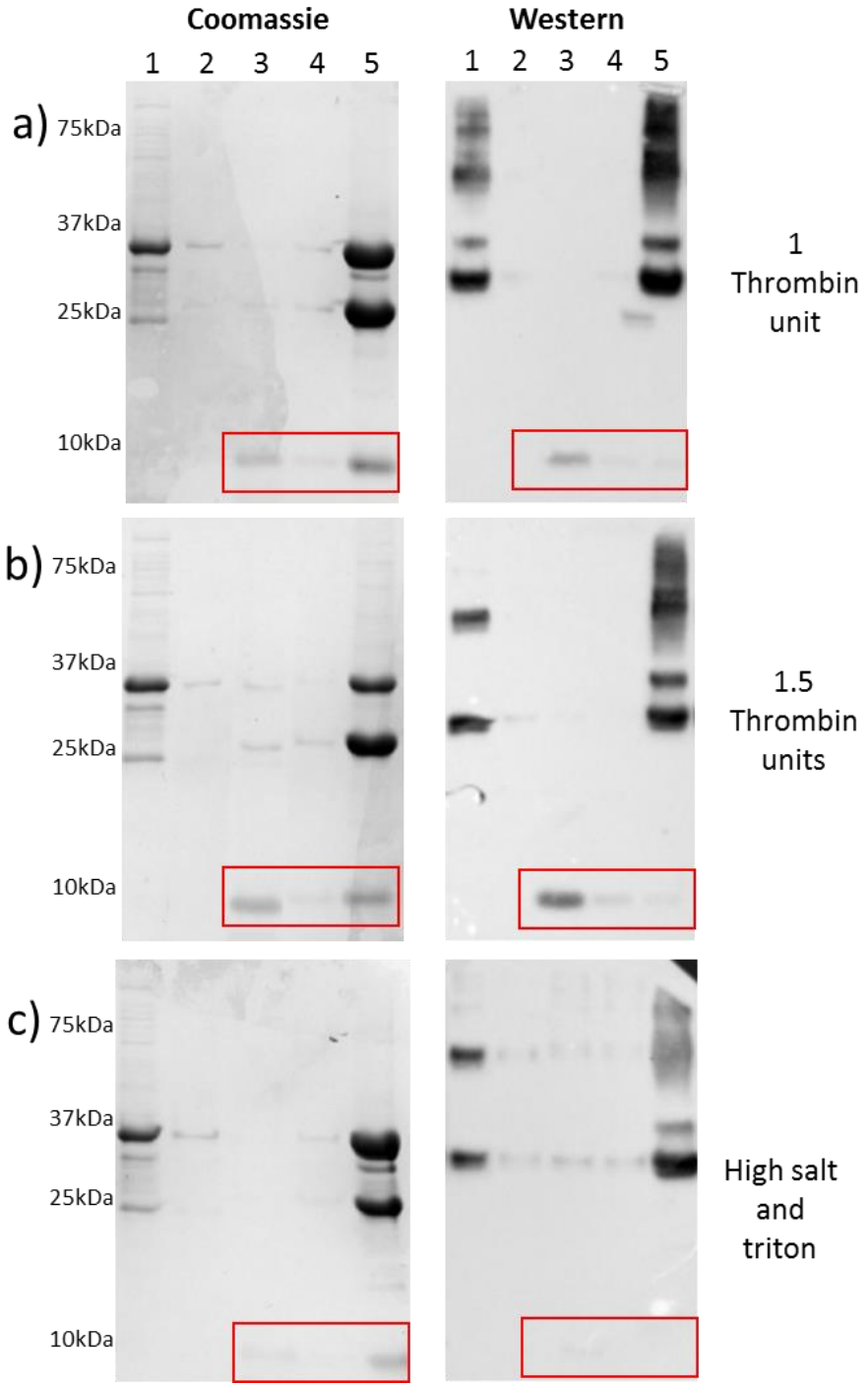

Figure 5.10: Effect of increased thrombin and increased NaCl on EC2-GST cleavage. On column cleavage (2.2.3.14) of CD9-EC2-GST fusion protein was carried out overnight using 1 or 1.5 units of thrombin or 1 unit of thrombin with 0.5M NaCl and 0.1% Triton X-100. 1= Protein not bound to beads, 2= Wash prior to cleavage, 3= Cleavage fraction one, 4= Cleavage fraction two, 5= Protein remaining on beads after cleavage.

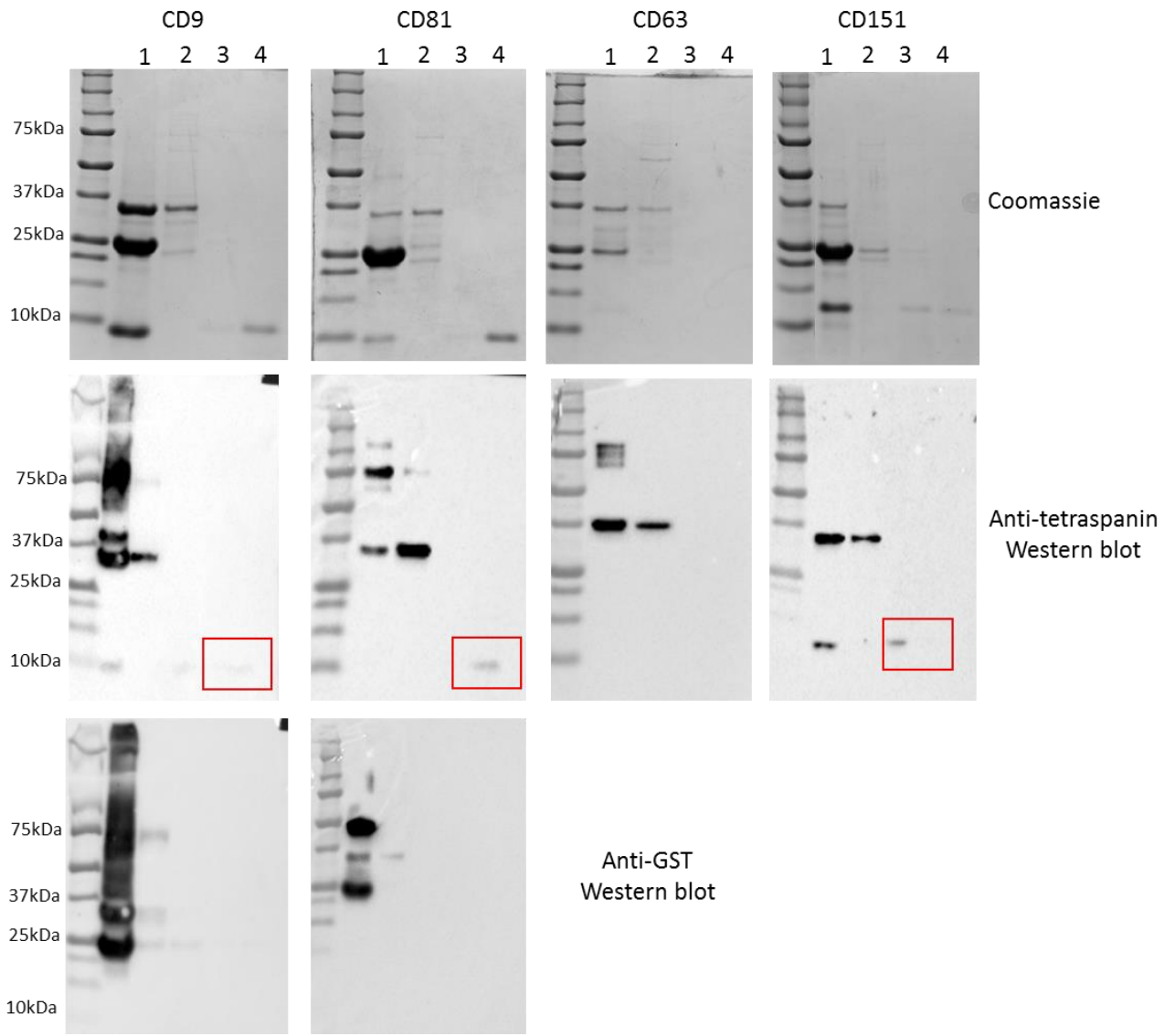

Figure 5.11: On column cleavage of several recombinant EC2-GST fusion proteins. On column cleavage (2.2.3.14) of CD9, CD63 and CD81 and CD151 EC2 GST fusion proteins was carried out overnight using 1.5 units of thrombin. Samples following cleavage were analysed by SDS-PAGE followed by Coomassie staining or Western blotting using relevant anti-tetraspanin monoclonal antibodies or an anti-GST antibody (as CD spectra could not be attained for CD63 and CD151, anti-GST blots were not carried out on them). 1= Protein remaining on beads following cleavage, 2= Protein not bound to beads, 3= Cleavage fraction one, 4= Cleavage fraction two.

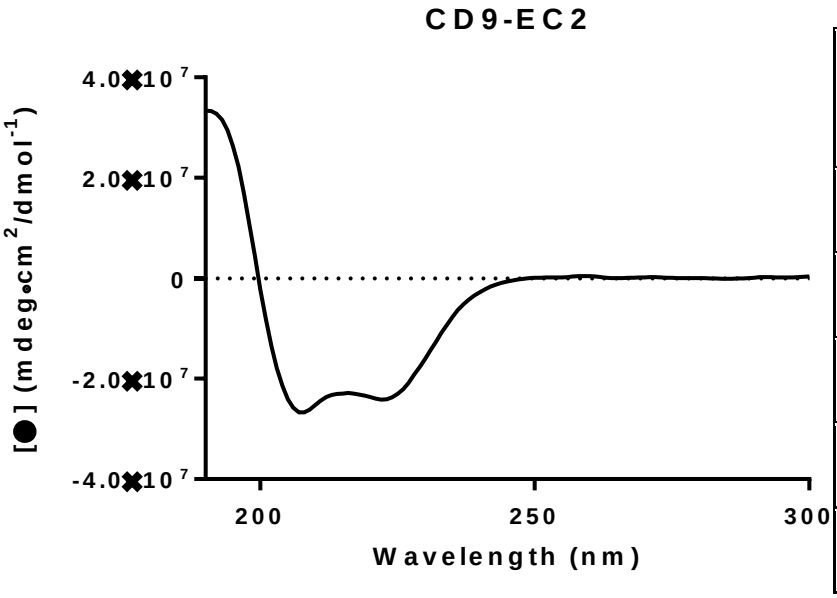

Structural Feature	Estimated Percentage
α-helix	50
B-sheet	7
Turns	13
Unordered	28
Total	98

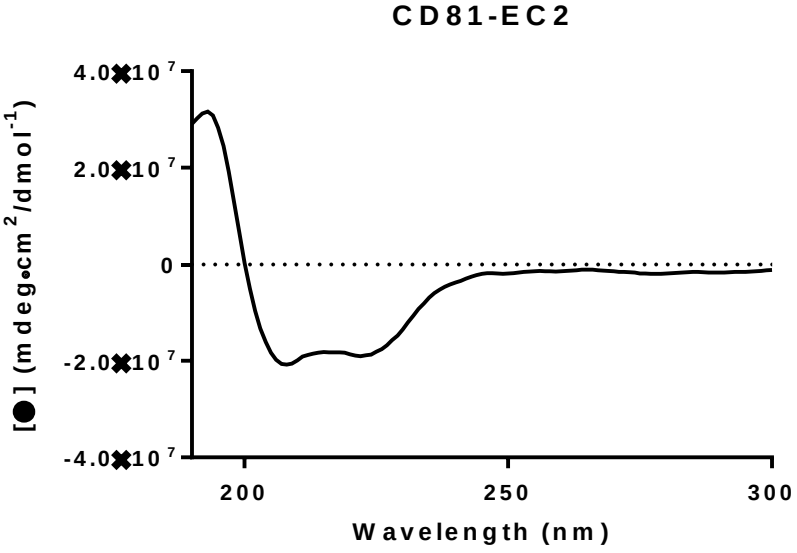

Structural Feature	Estimated Percentage
α-helix	52
B-sheet	5
Turns	18
Unordered	25
Total	100

Figure 5.12: Far UV CD spectra for CD9-EC2 and CD81-EC2. CD spectroscopy was carried out on CD9 and CD81 EC2 according to section 2.2.3.15. Estimated secondary structure percentages are an average of those given by SELCON3 and CONTIN analysis programs used by DICHOWEB with average RMSD values of 0.115 for CD9 estimations and 0.179 for CD81. Graphs are representative of two repeats.

5.3 Discussion

5.3.1 Recombinant EC2 binding

Following on from previous results which demonstrated that the recombinant EC2 domains do not affect degranulation (Chapter 4), it was considered that the EC2 proteins may not be able to bind to RBL-2H3 cells. The binding of recombinant EC2 domains to specific cell types but not others was demonstrated by Kelić *et al.* (2001) who showed that CD81 EC2 bound to neurons, but not astrocytes, despite the latter expressing endogenous CD81 also. Furthermore, Parthasarathy *et al.* (2009) demonstrated that recombinant CD63 EC2 binding to monocytes only took place once the cells were stimulated with ConA. In this chapter the binding of EC2 domains to two cell lines, HEC-1B and RBL-2H3 cells, was compared. In chapter 4 it was considered that EC2 domains may disrupt TEMs on the RBL-2H3 surface and in doing so disrupt IgE signalling; however this was shown not be the case. On the other hand, recombinant CD9, CD63 and CD81 EC2 domains did affect bacterial adhesion to Hec-1B cells, where they are suggested to function, through disruption of TEMs acting as "adhesion platforms" containing receptors for meningococcal attachment (Green et al., 2011).

Initial experiments monitored binding to RBL-2H3 cells indirectly using a fluorescent anti-GST antibody; however, non-specific antibody binding was high and accounted for a large proportion of the detected signal. The majority of recombinant EC2 binding was similar to that of the GST control, with the exception of CD81, which was significantly higher. However, there were concerns that the high levels of binding exhibited by the anti-GST antibody itself may have been masking a large proportion of the interaction so directly labelled EC2 proteins were utilised in later experiments. In these assays, the higher concentrations of each EC2 domain bound to both cell types significantly more than the corresponding GST control, with the exception of CD151 to HEC-1B cells. As previously reported (Kelić et al., 2001), homotypic interactions do not seem to be required for recombinant EC2 binding to a specific cell, as evidenced by recombinant CD9 EC2 binding to RBL-2H3 cells which do not express CD9. In contrast, CD151 exhibits poor binding to HEC-1B cells (which do not express CD151) suggesting homotypic interactions may be involved in some circumstances. Moreover, the amount EC2 binding to RBL-2H3 cells does not correlate to the homology displayed between the rat and human orthologous; for instance CD151 has the highest homology (86.8% identity) and yet the lowest degree of binding. Direct comparisons of EC2 binding to the different cell types is difficult due to higher level of GST binding seen with the HEC-1B cells. However, the low binding values for CD151 EC2 on HEC-1b cells are surprising, as recombinant CD151 EC2 was previously shown to significantly decrease bacterial adhesion to these cells (albeit with a

different recombinant protein preparation). This could mean that binding is not required for modulation of cellular activity, alternatively the interaction is such that it cannot be identified in this fashion, for example if it is more transient. Moreover, CD81 shows high binding to HEC-1b cells and yet does not alter bacterial adhesion, perhaps suggesting a different manner of interaction to the other EC2 domains.

Competitive binding experiments were undertaken using an excess of unlabelled GST-EC2 protein in an attempt to determine the specificity of EC2 interaction with the cells. Labelled CD9 and CD63 EC2 binding to RBL-2H3 cells diminishes slightly with increasing concentrations of unlabelled EC2 protein which may indicate binding to a specific saturable "receptor". However, it has yet to be determined if the same response is seen when using an excess of control protein such as GST. Competitive binding experiments using HEC-1B cells exhibited much higher variation, which may have arisen from inaccuracies when using small volumes of labelled protein, or prolonged storage of the labelled proteins, leading to their deterioration (e.g. possible aggregate formation or the label dissociating from the proteins). Interestingly the binding of the labelled GST protein to HEC-1B cells does not show as much variation, perhaps suggesting an intrinsic property of the EC2 domains which is contributing to the varied nature of the results. For example, if the EC2 domains are intercalating into TEMs then this type of cellular binding may not be easily saturated and therefore MFI values would not decrease when higher concentrations of unlabelled proteins are applied to the cells. Moreover, it is possible that the EC2 domains form dimers or even multimers which may impact upon the binding values. After further refinement it would be desirable to determine if binding of labelled protein could be reduced using an excess of the same protein. It would also be necessary to use an excess of control protein (GST for example) to show that any inhibition in binding was due to binding sites being occupied. It would also be possible to use an excess of other tetraspanin EC2 domains to see if the binding of one tetraspanin can be inhibited using another member.

5.3.2 LPS contamination of recombinant EC2 domains

Many recombinant proteins are produced in *E. coli* because of its relative simplicity, high yields and established methods. However the end product inherently contains a number of contaminating bacterial components such as LPS. Under normal *in vivo* conditions, when an immune cell encounters LPS, it is a signal of infection and the cell responds by producing cytokines and inflammatory mediators. In an *in vitro* setting, immune cells respond similarly, and depending on the process under investigation these changes can have a pronounced effect on cellular behaviour. In certain instances the effect of endotoxin contamination has

been confused with that of a recombinant protein under investigation. For instance, recombinant heat shock protein 70 (HSP70) was thought to induce TNFα production but this property was later attributed to the contaminating endotoxin (Gao and Tsan, 2003). A number of methods have been described to reduce the levels of LPS within a sample, however none are able to completely remove it (Wakelin et al., 2006). Alternatively, agents can be added to neutralise the endotoxin such as PMB (Polymyxin B) which binds to the lipid A portion, however this can also stimulate cytokine production (Damais et al., 1987).

Tetraspanins have been implicated in a number of cellular fusion events including; viral induced syncytium formation (Weng et al., 2009), sperm-egg fusion (Rubinstein et al., 2006; Zhu et al., 2002), muscle cell fusion (Tachibana and Hemler, 1999) and monocyte fusion (Parthasarathy et al., 2009; Takeda et al., 2003). In several of these scenarios it is thought that tetraspanins function by regulating associated fusogenic proteins, for example, restricting the access of viral fusion proteins to cell-cell junctions (Singethan et al., 2008). Recombinant EC2 domains have displayed activity in a number of fusion events and as such have been used to investigate tetraspanin involvement. However, LPS contamination of the recombinant EC2 domains has recently been shown to affect ConA and RankL induced fusion of monocytes cells (Fanaei, 2013) and as the mode of action of EC2 domains is yet to be determined, it is important to show that LPS is not the active component in each functional assay that they are used. More recently recombinant EC2 domains have been shown to modulate levels of macrophage fusion induced by *B. thailandensis.* Reduction of fusion in this manner is not a result of reduced bacterial adhesion (A. Elgawidi, unpublished data) and the mechanism of action of the EC2 proteins is instead suggested to be due to interference with tetraspanin regulation of fusogenic proteins. Although control experiments using pure LPS showed no effects (Atiga Elgawidi, personal communication), it was deemed important to correlate the levels of LPS within the proteins to their effect on this kind of fusion (Figure 5.6). Importantly there was no trend between the amount of LPS within the sample and the resultant MNGC size or fusion index, and there was similarly no correlation with their effects on bacterial adhesion thus indicating that endotoxin was not the contributing factor. However, it is important to note that this can only be considered the case within these particular experiments as others assays may be more sensitive to the endotoxin contaminant. It is interesting that some previous work indicated that LPS had an effect on ConA induced fusion of primary monocytes whilst it does not affect *B. thailandensis* induced fusion of the mouse macrophage cell line. It is possible that the use of a cell lines rather than primary cells was responsible for the difference in LPS sensitivity, alternatively (and perhaps more likely), the bacterial induced cell fusion may not be sensitive to the presence of LPS because LPS is

inherently in the system due to the incubation with bacteria. Interestingly, the same EC2 domain produced from different rounds of expression and purification had differing levels of LPS, suggesting that the amount of LPS within a sample is not dependent on an inherent property of the EC2 domain but rather slight differences in its expression and purification. Additionally, previous work (Chapter 3, Figure 3.17) displayed no difference in endotoxin levels between CD9 EC2 purified by batch or column method suggesting that LPS levels are more influenced by slight differences growth, harvesting and lysis of the bacterial cultures rather than downstream purification. This result also emphasises the importance of separate LPS quantifications for EC2 domains produced from different rounds of purification. In future it may be desirable to utilise an *E. coli* system such as ClearColi® which expresses a modified version of LPS (Lipid IV_A) which does not illicit an immune response in human cells (Mamat et al., 2015). This however would not be appropriate for experiments such as these, where mouse cells are utilised and as of yet there is no stain available which contains the modification found in Rosetta-gami which makes them appropriate for EC2 expression. Alternatively there are methods of LPS removal or reduction which could be implemented when lower levels or no LPS is required (Reichelt et al., 2006).

The functional effects described for the EC2 domains in this chapter (both on bacterial adhesion to HEC-1B cells and fusion events in J774.2 cells) show that the recombinant proteins produced during the present work do have biological activity in some systems despite them not affecting RBL-2H3 degranulation. Furthermore, their ability to modulate events in the mouse macrophage cell line demonstrates that homology between tetraspanin ortholgues is such that the human EC2 domains are active on rodent cells.

5.3.3 CD spectroscopy of recombinant EC2 domains

CD spectroscopy has been used by Rajesh *et al.* (2012) to show that the CD81-EC2 which they produced had 58% α-helical content, similar to that reported from the CD81 crystal structure. Properties of EC2 proteins produced by one group are not readily transferred to those produced by another due to changes in the expression procedure. Indeed EC2 domains from different groups can have different efficacy, for example recombinant CD9 EC2 used by Zhu *et al.* (2002) shows inhibitory effect on sperm egg fusion at 250 µg/ml whereas Higginbottom *et al.* (2003) showed an effect at 0.1µg/ml which the authors suggest is due to different folding states of the recombinant proteins. Thus far our group has solely used antibody-based methods (e.g. Western blots) to confirm correct folding of the EC2 domains; however, this only confirms that the antibody binding region is correctly folded and a band on a Western blot could be displayed from only a small proportion of the sample having the correct folding

pattern. It was therefore desirable to undertake CD spectroscopy on our proteins to investigate their secondary structure characteristics; however the GST tag had to first be removed. Previous lab members reported low cleavage efficiencies (5%) and unstable products when attempting to remove the GST tag from CD9 (Hulme, 2010) so initial efforts went into optimising cleavage and focused on a batch method which would enable recovery of cleaved proteins in a small sample volume and therefore potentially higher concentrations. The resulting cleavage products contained both uncleaved EC2-GST fusion proteins and free GST, presumably from transfer of some glutathione Sepharose beads into the cleavage fraction; moreover, these contaminants were present in subsequent cleavage attempts and could not be removed by repeated glutathione incubation. In an effort to prevent these proteins being introduced into the cleaved fraction, on-column cleavage was next used. Fortunately this method resulted in much cleaner cleavage products with none of the undesired protein bands apparent in Coomassie stained gels and no GST containing proteins in the cleaved proteins (as determined by Western blot). Length of incubation with thrombin and the amounts of thrombin used were altered and a cleavage efficiency of ~50% was attained for CD9 EC2. On the other hand, cleavage of CD63 was around 20% efficient and the resulting concentrations of both CD63 and CD151 were low. It is possible that these proteins were more susceptible to non-specific degradation by thrombin; alternatively, their solubility could have been adversely affected by the removal of GST leading to aggregation (which might explain the high light scattering following cleavage). In future experiments, higher initial concentrations could be used to attain more cleavage protein or further optimisation could be undertaken, for example altering buffer conditions to aid with protein solubility. Inclusion of a His tag at the 3' end of EC2 constructs may also be beneficial as it would enable efficient purification of EC2 domain following cleavage.

Unfortunately the low recovery of CD63 and CD151 following cleavage meant that spectra for these two proteins could not be gathered. CD spectra were attained for CD9 and CD81, however, and the online program DichroWeb was used to estimate the percentage secondary structure for each protein. Relatively high NRMSD values (>0.1) suggest that the secondary structure predictions may not be reliable (Whitmore and Wallace, 2008), however 52% predicated α-helical content of CD81-EC2 is comparable to the 58% reported elsewhere (Rajesh et al., 2012) and the spectra do have a characteristic α-helical shape giving confidence in the correct folding of the CD9 and CD81 EC2 domains. Given that CD63 and CD151 contain six di-sulphide bonds and potentially a more complex structure it would useful to attain spectra for these EC2 domains too as there is theoretically a greater incidence of misfolding.

Spectra of CD63 would also enable comparisons to be made between the human rat-CD63 EC2 domains produced previously to see if the predicted secondary structure differences.

Chapter 6: General discussion

6.1 General discussion

It has been reiterated throughout this thesis that the tetraspanin family of proteins are important in a multitude of processes and yet our understanding of the functions of individual members is limited. The EC2 domains in the form of recombinant proteins have already proven useful tools in assessing tetraspanin function (Barreiro et al., 2008; Green et al., 2011; Ho et al., 2006; Parthasarathy et al., 2009; Zhu et al., 2002). Initial work in this study involved the attempted expression of EC2s from selected tetraspanins in mammalian and insect cells, with the aim of producing reagents which would more closely resemble the corresponding region of native tetraspanin proteins. Difficulties were encountered in producing the proteins in eukaryotic cells so later work focused on expression and optimisation of expression in bacteria. The effects of the EC2 proteins on IgE mediated degranulation were then investigated using the RBL-2H3 cell line as a model system. Although a number of studies have linked tetraspanins to IgE mediated degranulation (Fleming et al., 1997; Kitani et al., 1991; Köberle et al., 2012; Kraft et al., 2005, 2013; Peng et al., 2011; Smith et al., 1995), their role within this process remains unknown and this is the first time the recombinant EC2 domains have been used to assess their involvement. Finally, efforts were made to characterise the protein in terms of LPS content, folding and cellular binding capacity.

Chapter 3 focused primarily on EC2 expression in eukaryotic systems (specifically CHO, HEK-293 and SF9 cells). The desire for these eukaryotic recombinant EC2 domains stemmed from the inherent downsides found in the bacterially expressed EC2 domains which include:

A. Suggestions of incorrect protein folding due to antibodies which were raised against these proteins not recognizing the native tetraspanins (Jiraviriyakul, 2010) (Azorsa et al., 1999).
B. Lack of glycosylation, a modification which is required for some tetraspanin function (Ono et al., 2000; Ranjan et al., 2014).
C. LPS contamination resulting from the use of *E. coli* as a host for expression rendering the proteins unsuitable for some functional assays.

Not only would eukaryotic expression of the EC2 domains overcome these issues but it would also enable comparisons to be made between EC2 domains produced in different hosts. For instance, the functional relevance of glycosylation could be examined by carrying out functional assays in paralleled with glycosylated and de-glycosylated proteins. The structural

differences could also be inspected, perhaps by CD spectroscopy experiments similar to those carried out previously to compare CD81 expressed in prokaryotic and eukaryotic systems (Rajesh et al., 2012). Moreover, comparisons between the structures of tetraspanins with higher cysteine numbers would give an indication as to how well bacterial systems cope with the folding of these proteins. Some tetraspanin EC2 domains which contain six to eight cysteines (e.g. Tspan-4, Tspan-5, Tspan-8 and Tspan-31) and therefore have 3-4 potential di-sulphide bonds and more complex folding structures, give extremely low yields when expressed in bacteria. This is suggested to arise from aggregation caused by misfolding within the reducing environment of the *E. coli* cytoplasm (Fanei, 2013). This limits the tools available to study these particular family members, which is compounded in some cases by the lack of monoclonal antibodies towards the native proteins. Furthermore, tetraspanins which contain 8 cysteine residues within the EC2 are becoming increasingly appreciated as a subdivision of the tetraspanin family with some conserved properties (Dornier et al., 2012), making reagents for assessing their function ever more desirable. The improved folding associated with eukaryotes means they are more likely to be able to produce the required recombinant EC2 domains, which are not only useful functional tools in themselves but may also be used as antigens to produce monoclonal antibodies which recognise the native proteins.

Although there are benefits to eukaryotic expression, multiple attempts at producing the recombinant EC2 domains in these systems did not yield the desired product. It is difficult to define where the problem in mammalian expression arose, but PCR experiments showed that the DNA was integrated into the host genome and that the cells were producing EC2 encoding mRNA. it is possible that the issue was with the coding RNA itself; for example if the RNA product was poorly processed due to its short size (Ntini et al., 2013). Alternatively, problems may have arisen if overexpression of the EC2 domains was toxic to the host cells. Indeed only one other group have expressed the EC2 domains in a mammalian host and a transient form of expression was used (Rajesh et al., 2012), which may suggest an inherent property of the EC2 domains that makes them difficult to express.

With regards to bacterial expression, each of the investigated tetraspanins (CD9, CD63, CD81 and CD151) were expressed and recognised by their respective antibodies and efforts were made to optimise the amount of soluble protein recovered by altering IPTG levels and length of time temperature used for induction. The four tetraspanins were selected based on their involvement in IgE mediated signalling, with at least two of these (CD9 and CD81) being co-immunoprecipitated with the high affinity IgE receptor itself (Abdala-Valencia et al., 2015; Fleming et al., 1997; Higginbottom et al., 2000a; Kraft et al., 2005; Peng et al., 2011). Since several tetraspanins have been implicated in IgE mediated degranulation, it was theorised that

they might regulate FcεRI activity due to its presence within a TEM. Recombinant EC2 domains have been suggested to affect various processes through disruption of TEMs (Barreiro et al., 2008; Green et al., 2011; Parthasarathy et al., 2009). Therefore, as described in **Chapter 4,** the recombinant EC2 domains were utilised in in an effort to further understand tetraspanin involvement in degranulation and as an initial investigation into any therapeutic application.

After extensive investigation, it was shown that EC2 domains do not affect IgE mediated degranulation in RBL-2H3 cells. Several hypotheses were suggested as to why these results were seen, with focus on (a) our understanding of tetraspanins involvement in IgE signalling, and (b) the mechanism of recombinant EC2 domain activity. Firstly, it was proposed that although FcεRI interacts with tetraspanins, the receptor may not be found within a TEM. The possible involvement of lipid-rafts in IgE mediated signalling may also indicate this as the microdomains are often seen as distinct regions. However, this could be a rare instance of coalescence between the microdomains. Alternatively, as tetraspanins are dynamic in the membrane and are not restricted to TEMs (Espenel et al., 2008), the association with FcεRI could be outside of a TEM environment. Moreover, the reports of tetraspanin association (Peng et al., 2011) with FcεRI may not indicate direct, primary associations and may instead allude to more distal interactions through a common partner protein. It is possible that the inhibitory effects on IgE degranulation observed using anti-tetraspanin monoclonal antibodies are due to higher affinity for their target proteins whereas the recombinant EC2 proteins may require interactions with clustered partners in the context of a TEM to illicit a response.

If it is assumed that FcεRI is within a TEM then either recombinant EC2 domains do not disrupt the TEM as initially speculated (Figure 6,1b), or they do not disrupt the TEM to a high enough extent to affect FcεRI signalling. Evidence that recombinant EC2 domains disrupt TEMs includes their ability to modulate TEM involving process (Ho et al., 2006; Takeda et al., 2003; Zhu et al., 2002) and increased spacing and diffusion rates of TEM associated component when treating cells with recombinant EC2 domains. Also, treatment with CD9-EC2 not only affects the diffusion of endogenous CD9 but also endogenous CD151 suggesting a broader effect on TEMs dynamics (Barreiro et al., 2005). With this limited information it is conceivable that the recombinant proteins could function in other ways, for instance it has also been suggested that they may compete for binding with tetraspanin partner proteins which may have more specific outcomes (Figure 6.1c) (Higginbottom et al., 2003; Parthasarathy et al., 2009; Zhu et al., 2002).

In **Chapter 5,** several properties of recombinant EC2 domains were examined in an effort to shed more light on how they function. Firstly the binding of recombinant EC2 domains to two

cell lines was examined (RBL-2H3 and HEC-1B). In both instances the binding of the recombinant EC2 domains was greater than that of the GST control protein (with the exception of CD151 to HEC-1B cells), indicating that the labelled recombinant proteins do indeed bind to the cells. The binding patterns did not correlate with degree of labelling of the recombinant proteins and, in the case of binding to RBL-2H3 cells, there was no relationship between the binding and homology between human and rat orthologues, suggesting that the differences in binding were an inherent property of the EC2 proteins. The overall level of binding of the recombinant proteins (indicated by the total MFI values) were greater for HEC-1B cells than those displayed by RBL-2H3; however GST binding was also higher, so it is likely that there is some contribution from non-specific association making direct comparisons difficult. In competitive binding assays, the binding of labelled CD9 and CD63 to RBL-2H3 cells diminished with increasing concentrations of unlabelled protein, indicating that the binding was to a saturable binding partner at the cells surface. On the other hand, labelled CD9 and CD63 binding to HEC-1B cells did not decrease in the same way. The HEC-1B MFI values also show a higher degree of variation between experiments compared to the GST control, which could be due to technical issues; however it is possible that the increased variation and lack of inhibition of binding are a result of different binding properties (for instance intercalation into the TEM).

LPS levels in the recombinant proteins were later measured and were then correlated to their effects on monocyte fusion induced by the bacterium B*. thailandensis*. The lack of relation between activity and LPS content confirmed that LPS was not the active component in recombinant protein preparations in this instance, although this cannot be said definitively for each assay in which they are used. It was also noted that the amount of LPS within the recombinant proteins varied between rounds of purification suggesting that levels of LPS are not dictated by the particular recombinant protein being expressed but are determined by variations in expression and purification procedures.

Finally, the secondary structures of the tetraspanins were investigated using CD spectroscopy. This attributed both CD9 and CD81 with a predominantly α-helical structure which is as expected from these proteins (Kitadokoro et al., 2001) suggesting they are correctly folded in the most part. Unfortunately, spectra for CD63 and CD151 could not be attained due to insufficient protein yields following cleavage.

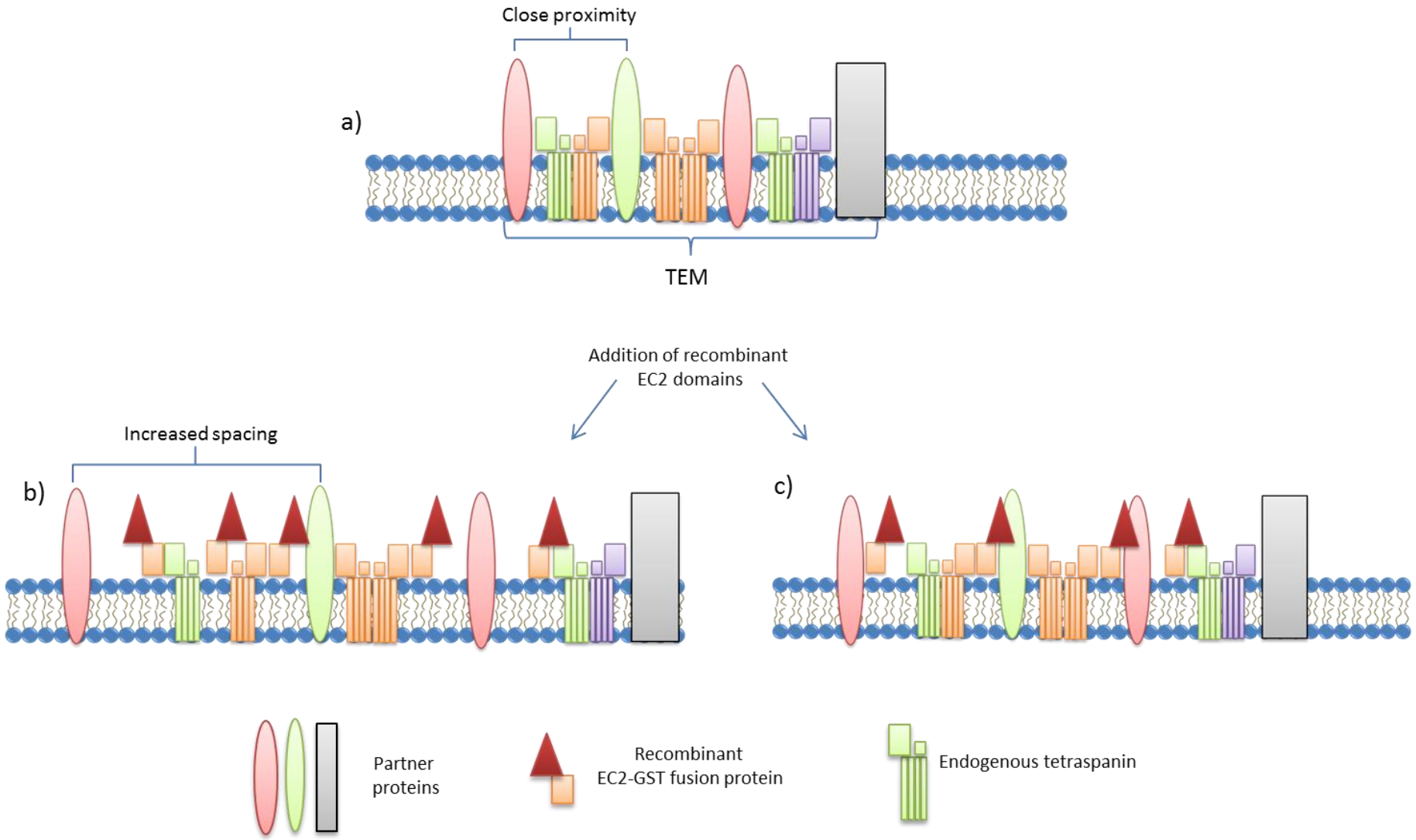

Figure 6.1: Diagrammatic representation of the proposed mechanisms of EC2 action. (a) Under normal circumstances Partner proteins are normally held in an ordered fashion in close proximity within a TEM. **(b)** Recombinant EC2 domains added exogenously bind and intercalate between tetraspanins on the cell surface which leads to general disruption of the ordered TEM structure and decreased partner protein clustering, resulting in downstream physiological effects. **(c)** Recombinant EC2 domains added exogenously bind to partner proteins therefore preventing the binding of exogenous tetraspanins and stopping any specific effects which result from these interactions.

6.2 Future directions

6.2.1 Improved expression systems

Production of mammalian EC2 domains is still a desirable prospect despite time constraints meaning that attempts to attain these proteins had to be halted. Future efforts could be made accounting for the issues which have been suggested here. For example, a tightly regulated inducible mammalian promoter or transient gene expression could be utilised to circumvent issues with potential toxic effects of EC2 domain overexpression (Wurm, 2004). On the other hand, being as yeast do not express endogenous tetraspanins, these may be resistant to the potential cytotoxic effects of the EC2 domains and may therefore be an attractive alternative host which is able to glycosylate the proteins they produce. Indeed, *Pishia pastoris* has previously been used for the expression of full length CD81 (Jamshad et al., 2008). To prevent the possible issues with shorter RNA products new expression constructs including an epitope tag and cleavage site could be generated (similar to those previously used successfully for CD63 expression (Jiraviriyakul, 2010).

In chapter 3 some elements of the bacterial expression were altered to favour higher recombinant EC2 yields, but there are numerous other changes which could be implemented to enable easier downstream processing and potentially give higher protein yields. Firstly, (as previously suggested) the inclusion of both a GST and His tag would enable two step purification which would aid in the removal of lower molecular weight (presumably truncated) proteins from the initial preparations. A second affinity tag would also allow for purification following cleavage of the bulky GST tag, moreover, because a His tag is not reliant on tertiary structure for affinity purification, it would enable purification following denaturation of inclusion bodies if this was considered in future. Other protein tags could be utilised which are suggested to aid in fusion protein solubility to a greater extent than GST, for instance maltose binding protein (MBP) which can also function as an affinity tag (Esposito and Chatterjee, 2006). Alternatively, a leader sequence could be included to enable periplasmic expression with the hopes of producing more soluble proteins in the non-reducing environment of the pariplasmic space.

The choice of bacterial host might also be altered. Rosetta-gami cells do contain modifications which are beneficial for expression of tetraspanin EC2 domains, however there may be other commercial strains of *E. coli* which offer distinct advantages. For instance, SHuffle cells which have similar modifications to Rosetta-gami but have the added benefit of the disulphide bond isomerase DsbC being constitutively expressed and retained in the cytoplasm, which aids in the folding of the disulphide containing proteins (Kurokawa et al., 2000). Yields of recombinant

EC2 proteins from Rosetta-gami and Shuffle cells were previously compared (Fanei, 2013) and SHuffle cells were found to give higher yields; however the amount of LPS in the preparations was consistently higher also. That being said, in LPS sensitive assays, even a small amount of protein can modulate cellular activity (Gao and Tsan, 2003) so unless LPS can be completely removed from the preparations the cost of increased LPS contamination may be worthwhile for higher protein yields. When considering experiments which would be altered by the inclusion of LPS, it may be favourable to utilise the ClearColi® strain of E. coli. These cells do not have the adaptations found in Rosetta-gami so would presumably give a lower proportion of soluble protein; however they have modified LPS which does not illicit a response in human immune cells which may enable the recombinant proteins to be used in more assays (Mamat et al., 2015). It seems that one could make a selection of bacterial strain based on the application of the resultant protein, for example a different systems could be used when a higher quantity of protein is required or when LPS is a concern.

6.2.2 Tetraspanin involvement in IgE signalling

Since little is known about tetraspanin involvement in degranulation and the mode of action of EC2 domains is ambiguous, it is difficult to speculate on the implications of the results obtained here. However, improved understanding of one unknown will enable greater interpretation of the data herein. For example, if the EC2 domains are proven more definitively to disrupt TEMs, than one could say with more conviction that the IgE receptor is not located within a tetraspanin enriched microdomain. Alternatively, if further studies did show that FcεRI partitioned into tetraspanin enriched microdomain, then it is likely that the recombinant EC2 do not disrupt TEMS. Mast cell lysis with different strengths of detergent followed by co-immunoprecipitation using anti-tetraspanin antibodies may help to determine the extent of tetraspanins FcεRI interaction (i.e. if they are primary direct interactions or not). It may also be desirable to study the association of tetraspanins with the high affinity IgE receptor during different phases of mast cell activation, to determine if they associate with one another following RBL-2H3 activation for example. FcεRI is thought to partition into lipid rafts following activation (Field et al., 1995) so association of the receptor with tetraspanins at this point may indicate an overlap between the two types of microdomain (which could be examined further by sucrose density centrifugation).

Deletion of specific genes may prove a more direct method of determining what effects disruption of the TEM has on degranulation. Although single deletions show mild phenotypes, multiple genes could be knocked down via RNAi of removed through CRISPR. Future work could also focus on other steps in the degranulation pathway, for instance effects on calcium

influx and alteration in cytokine production rather than focusing on the extent of granule release. Indeed CD151-/- ex-vivo mast cells shows enhanced expression of proinflamatory cytokines despite no changes in degranulation (Abdala-Valencia et al., 2015). With this in mind, tetraspanin gene disruption followed by cytokine profiling may be advantageous. This more general approach would be useful in characterising the family as a whole, not just its specific involvement in IgE mediated degranulation. For example micro-array analysis could display which processes specific tetraspanins are required for, it is possible that a tetraspanin database could allow tetraspanins functional properties to be related to their physical structure more readily.

6.2.3 EC2 mode of action

Further analysis of EC2 mode of action would allow results to be deciphered more readily. CD spectroscopy is useful for analysing the proteins secondary structure but further physical characterisation may be helpful also. For example, CD81 EC2 crystallised as a dimer (Kitadokoro et al., 2001), and it would be interesting to determine if the other EC2 domains exist in a dimerised state and may inform more about how they function. This could be achieved using native PAGE or size exclusion chromatography (although the GST tag would have to be removed first at this dimerises naturally). As previously mentioned, Barreiro *et al.* used “nearest neighbour analysis” to show that the EC2 domains were able to affect the spacing or diffusion of two TEM associated proteins. If the same technique were applied to other instances where EC2 domains modulate cell function (for instance bacterial adhesion or cell fusion) it may be possible to say that the EC2 domains routinely affect TEM associated proteins. Alternatively, high resolution microscopy could be used to analyse the distribution of GFP labelled/ antibody stained partner proteins (e.g. FcεRI) before and after recombinant EC2 treatment to determine if the proteins alter distribution or diffusion of partner proteins.

Initial attempts were made to examine the binding of recombinant EC2 domains to cells and now the methods for EC2 labelling and binding have been established it may be possible to look at this further. Firstly the nature of binding could be established i.e. whether it can be inhibited by the corresponding unlabelled tetraspanins and/or by other tetraspanin proteins which may be competing for the same site. It may then be possible to establish what is required for binding to the cell surface. It has been indicated here and elsewhere (Kelić et al., 2001) that homotypic interactions are not required; it would be useful to determine if association with other tetraspanin family members is necessary. Visualisation of binding may be useful also and initial attempts were made at analysing binding microscopically; perhaps in future endeavours expression of fluorescently-tagged tetraspanin proteins at the cell surface

followed by binding assays may give an indication as to any co-localisation between endogenous and exogenous tetraspanins. Co-immunoprecipitation or GST pull downs might help identify interacting proteins, however previous pull-down experiments were unsuccessful (our group, unpublished data). Cell-free methods maybe more sensitive in identifying specific tetraspanin binding partners, for example, Biacore could be used to generate dissociation constants which may provide a more accurate read as to whether a binding partner is primary secondary or tertiary (Phizicky and Fields, 1995).

Although targeting of tetraspanins using EC2 domains may not be applicable in the context of reduction of degranulation they may be a viable target for other therapeutic areas. It has been proposed that TEMs enable the formation of adhesion platforms which in turn allow microbial infection (Green et al., 2011). Disruption of TEMs using recombinant EC2 domains reduced bacterial adhesion to endothelial cells and has been proposed as an antimicrobial treatment which offers the advantage of not targeting the microbe itself, therefore resistance is less likely to arise due to selection pressure (Green et al., 2011; Hassuna et al., 2009). Instances of direct pathogen–tetraspanin association may not be as readily disrupted by EC2 treatment however, as CD81 EC2s were unable to reduce HCV infection where as anti-CD81 mAbs and siRNA knockdown of CD81 did (Molina et al., 2008) therefore disruption of TEM function by siRNA may be beneficial when targeting specific tetraspanins which are known to take place in disease. The involvement of various tetraspanins in tumour progression also raises the possibility of targeting tetraspanins for treatment of cancer. For example high levels of CD151 expression are linked with a poor prognosis in lung and prostate cancer and mouse xenograft models with mutated CD151 show reduced tumour growth (Yang et al., 2008). Anti-CD151 mAbs have also been shown to reduce tumour cell metasitasis (Kohno et al., 2002) and recently an anti-CD37 antibody called Otlertuzumab has entered clinical trials for treatment of non-hodgkin lymphoma (NHL). Otlertuzumab induces apoptosis in the bound cell by signalling through CD37 which increases the levels of the pro-apoptotic protein BIM (Pagel et al., 2014). Due to CD37s restricted expression in B-cells this offers a directed approach to treat B-cell malignancies. Other mAbs have shown promise in in-vivo models for instance and CD81 mAbs results in increased recovery from spinal injury and an anti-CD9 mAb reduced colon carcinoma growth (Ovalle et al., 2007). It is possible that the antibodies have a stronger more directed effect than the EC2 domains due to their specific and high affinity binding towards one tetraspanin, however EC2 domains may prove to be a valuable therapeutic with a more general disputing effect (Hemler, 2008).

Although EC2 domains have proven useful in determining tetraspanin function several instances, they do have a number of limitations. In addition to effects seen due to bacterial

contaminants in the final preparations, they are also difficult to produce in high quantities due to a propensity to stick to plastic ware and the amount of miss folding due to large numbers of disulphide bonds. Another concern is their unknown mode of action making elucidation of results challenging, furthermore, EC2 domains represent only one form of tetraspanin EC2 domain whereas native tetraspanins may be more homogenous, for instance CD9 has 13 splice variants and CD63 has 16.

Bibliography

Abdala-Valencia, H., Bryce, P.J., Schleimer, R.P., Wechsler, J.B., Loffredo, L.F., Cook-Mills, J.M., Hsu, C.-L., and Berdnikovs, S. (2015). Tetraspanin CD151 Is a Negative Regulator of FcεRI-Mediated Mast Cell Activation. J. Immunol.

Abidi, F.E. (2002). A novel 2 bp deletion in the TM4SF2 gene is associated with MRX58. J. Med. Genet. *39*, 430–433.

Abraham, S.N., and Malaviya, R. (1997). Mast cells in infection and immunity. Infect. Immun. *65*, 3501–3508.

Abraham, S.N., and St John, A.L. (2010). Mast cell-orchestrated immunity to pathogens. Nat. Rev. Immunol. *10*, 440–452.

Altmann, F., Staudacher, E., Wilson, I.B.H., and März, L. (1999). Insect cells as hosts for the expression of recombinant glycoproteins. Glycoconj. J. *16*, 109–123.

Andrews, P.W., Knowles, B.B., and Goodfellow, P.N. (1981). A human cell-surface antigen defined by a monoclonal antibody and controlled by a gene on chromosome 12. Somatic Cell Genet. *7*, 435–443.

Apgar, J.R. (1997). Increased degranulation and phospholipase A 2 , C , and D activity in RBL cells stimulated through FcεR1 is due to spreading and not simply adhesion. J. Cell Sci. *110*, 771–780.

Arpin, M., Chirivino, D., Naba, A., and Zwaenepoel, I. (2011). Emerging role for ERM proteins in cell adhesion and migration. Cell Adh. Migr. *5*, 199–206.

Asai, K., Kitaura, J., Kawakami, Y., Yamagata, N., Tsai, M., Carbone, D.P., Liu, F.T., Galli, S.J., and Kawakami, T. (2001). Regulation of mast cell survival by IgE. Immunity *14*, 791–800.

Azorsa, D.O., Hyman, J. a, and Hildreth, J.E. (1991). CD63/Pltgp40: a platelet activation antigen identical to the stage-specific, melanoma-associated antigen ME491. Blood *78*, 280–284.

Azorsa, D.O., Moog, S., Cazenave, J.P., and Lanza, F. (1999). A general approach to the generation of monoclonal antibodies against members of the tetraspanin superfamily using recombinant GST fusion proteins. J. Immunol. Methods *229*, 35–48.

Balbás, P. (2001). Understanding the art of producing protein and nonprotein molecules in Escherichia coli. Mol. Biotechnol. *19*, 251–267.

Baneyx, F. (1999). Recombinant protein expression in Escherichia coli. Curr. Opin. Biotechnol. *10*, 411–421.

Baneyx, F., and Mujacic, M. (2004). Recombinant protein folding and misfolding in Escherichia coli. Nat. Biotechnol. *22*, 1399–1408.

Bari, R., Zhang, Y.H., Zhang, F., Wang, N.X., Stipp, C.S., Zheng, J.J., and Zhang, X. a (2009). Transmembrane interactions are needed for KAI1/CD82-mediated suppression of cancer invasion and metastasis. Am. J. Pathol. *174*, 647–660.

Barnes, L.M., Bentley, C.M., and Dickson, A.J. (2003). Stability of protein production from recombinant mammalian cells. Biotechnol. Bioeng. *81*, 631–639.

Barreiro, O., Yáñez-Mó, M., Sala-Valdés, M., Gutiérrez-López, M.D., Ovalle, S., Higginbottom, A., Monk, P.N., Cabañas, C., and Sánchez-Madrid, F. (2005). Endothelial tetraspanin microdomains regulate leukocyte firm adhesion during extravasation. Blood *105*, 2852–2861.

Barreiro, O., Zamai, M., Yáñez-Mó, M., Tejera, E., López-Romero, P., Monk, P.N., Gratton, E., Caiolfa, V.R., and Sánchez-Madrid, F. (2008). Endothelial adhesion receptors are recruited to

adherent leukocytes by inclusion in preformed tetraspanin nanoplatforms. J. Cell Biol. *183*, 527–542.

Bausinger, H., Lipsker, D., Ziylan, U., Manié, S., Briand, J.P., Cazenave, J.P., Muller, S., Haeuw, J.F., Ravanat, C., de la Salle, H., et al. (2002). Endotoxin-free heat-shock protein 70 fails to induce APC activation. Eur. J. Immunol. *32*, 3708–3713.

Beaven, M. a. (2009). Our perception of the mast cell from Paul Ehrlich to now. Eur. J. Immunol. *39*, 11–25.

Beckwith, K. a., Byrd, J.C., and Muthusamy, N. (2015). Tetraspanins as therapeutic targets in hematological malignancy: a concise review. Front. Physiol. *6*, 1–13.

Berditchevski, F., and Odintsova, E. (2007). Tetraspanins as regulators of protein trafficking. Traffic *8*, 89–96.

Berditchevski, F., Bazzoni, G., and Hemler, M.E. (1995). Specific association of CD63 with the VLA-3 and VLA-6 integrins. J. Biol. Chem. *270*, 17784–17790.

Berditchevski, F., Gilbert, E., Griffiths, M.R., Fitter, S., Ashman, L., and Jenner, S.J. (2001). Analysis of the CD151·α3β1 Integrin and CD151·Tetraspanin Interactions by Mutagenesis. J. Biol. Chem. *276*, 41165–41174.

Berditchevski, F., Odintsova, E., Sawada, S., and Gilbert, E. (2002). Expression of the palmitoylation-deficient CD151 weakens the association of alpha 3 beta 1 integrin with the tetraspanin-enriched microdomains and affects integrin-dependent signaling. J. Biol. Chem. *277*, 36991–37000.

Bessette, P.H., Aslund, F., Beckwith, J., and Georgiou, G. (1999). Efficient folding of proteins with multiple disulfide bonds in the Escherichia coli cytoplasm. Proc. Natl. Acad. Sci. U. S. A. *96*, 13703–13708.

Bieneman, A.P., Chichester, K.L., Chen, Y.H., and Schroeder, J.T. (2005). Toll-like receptor 2 ligands activate human basophils for both IgE-dependent and IgE-independent secretion. J. Allergy Clin. Immunol. *115*, 295–301.

Blank, U., Falcone, F.H., and Nilsson, G. (2013). The history of mast cell and basophil research - Some lessons learnt from the last century. Allergy Eur. J. Allergy Clin. Immunol. *68*, 1093–1101.

Boddey, J. a., Day, C.J., Flegg, C.P., Ulrich, R.L., Stephens, S.R., Beacham, I.R., Morrison, N. a., and Peak, I.R. a (2007). The bacterial gene lfpA influences the potent induction of calcitonin receptor and osteoclast-related genes in Burkholderia pseudomallei-induced TRAP-positive multinucleated giant cells. Cell. Microbiol. *9*, 514–531.

Boesze-Battaglia, K., Goldberg, A.F.X., Dispoto, J., Katragadda, M., Cesarone, G., and Albert, A.D. (2003). A soluble peripherin/Rds C-terminal polypeptide promotes membrane fusion and changes conformation upon membrane association. Exp. Eye Res. *77*, 505–514.

Boon, C.J.F., den Hollander, A.I., Hoyng, C.B., Cremers, F.P.M., Klevering, B.J., and Keunen, J.E.E. (2008). The spectrum of retinal dystrophies caused by mutations in the peripherin/RDS gene. Prog. Retin. Eye Res. *27*, 213–235.

Borriello, F., Granata, F., Varricchi, G., Genovese, A., Triggiani, M., and Marone, G. (2014). Immunopharmacological modulation of mast cells. Curr. Opin. Pharmacol. *17C*, 45–57.

Boucheix, C., and Rubinstein, E. (2001). Tetraspanins. C. Cell. Mol. Life Sci. *58*, 1189–1205.

Boucheix, C., Benoit, P., Frachet, P., Billard, M., Worthington, R.E., Gagnon, J., and Uzan, G. (1991). Molecular cloning of the CD9 antigen: A new family of cell surface proteins. J. Biol. Chem. *266*, 117–122.

Bradford, M.M. (1976). A rapid and sensitive method for the quantitation of microgram quantities of protein utilizing the principle of protein-dye binding. Anal. Biochem. *72*, 248–254.

Brandt, E.B., Strait, R.T., Hershko, D., Wang, Q., Muntel, E.E., Scribner, T. a, Zimmermann, N.,

Finkelman, F.D., and Rothenberg, M.E. (2003). Mast cells are required for experimental oral allergen – induced diarrhea. J. Clin. Invest. *112*.

Brinkmann, U., Mattes, R.E., and Buckel, P. (1989). High-level expression of recombinant genes in Escherichia coli is dependent on the availability of the dnaY gene product. Gene *85*, 109–114.

Britain, G., Reserved, A.R., and Press, P. (1991). Production Scale Insect Cell Culture. Biotechnol. Adv. *9*, 51–58.

Brown, M. a, Pierce, J.H., Watson, C.J., Falco, J., Ihle, J.N., and Paul, W.E. (1987). B cell stimulatory factor-1/interleukin-4 mRNA is expressed by normal and transformed mast cells. Cell *50*, 809–818.

Buchner, J., and Rudolph, R. (1991). Routes to active proteins from transformed microorganisms. Curr. Opin. Biotechnol. *2*, 532–538.

Cannon, K.S., and Cresswell, P. (2001). Quality control of transmembrane domain assembly in the tetraspanin CD82. EMBO J. *20*, 2443–2453.

Cao, S.S., and Kaufman, R.J. (2012). Unfolded protein response. Curr. Biol. *22*, R622–R626.

Carrió, M.M., and Villaverde, a. (2002). Construction and deconstruction of bacterial inclusion bodies. J. Biotechnol. *96*, 3–12.

Caughey, G.H. (2007). Mast cell tryptases and chymases in inflammation and host defense. Immunol. Rev. *217*, 141–154.

Chang, T.W. (2000). The pharmacological basis of anti-IgE therapy. Nat. Biotechnol. *18*, 157–162.

Charrin, S., Manié, S., Oualid, M., Billard, M., Boucheix, C., and Rubinstein, E. (2002). Differential stability of tetraspanin/tetraspanin interactions: role of palmitoylation. FEBS Lett. *516*, 139–144.

Charrin, S., Manié, S., Billard, M., Ashman, L., Gerlier, D., Boucheix, C., and Rubinstein, E. (2003a). Multiple levels of interactions within the tetraspanin web. Biochem. Biophys. Res. Commun. *304*, 107–112.

Charrin, S., Manié, S., Thiele, C., Billard, M., Gerlier, D., Boucheix, C., and Rubinstein, E. (2003b). A physical and functional link between cholesterol and tetraspanins. Eur. J. Immunol. *33*, 2479–2489.

Charrin, S., le Naour, F., Silvie, O., Milhiet, P.-E., Boucheix, C., and Rubinstein, E. (2009). Lateral organization of membrane proteins: tetraspanins spin their web. Biochem. J. *420*, 133–154.

Charrin, S., Jouannet, S., Boucheix, C., and Rubinstein, E. (2014). Tetraspanins at a glance. J. Cell Sci. 1–8.

Chen, E.H., Grote, E., Mohler, W., and Vignery, A. (2007). Cell-cell fusion. FEBS Lett. *581*, 2181–2193.

Choi, J.H., and Lee, S.Y. (2004). Secretory and extracellular production of recombinant proteins using Escherichia coli. Appl. Microbiol. Biotechnol. *64*, 625–635.

Claas, C., Stipp, C.S., and Hemler, M.E. (2001). Evaluation of Prototype Transmembrane 4 Superfamily Protein Complexes and Their Relation to Lipid Rafts. J. Biol. Chem. *276*, 7974–7984.

Clarke, G., Goldberg, a F., Vidgen, D., Collins, L., Ploder, L., Schwarz, L., Molday, L.L., Rossant, J., Szél, a, Molday, R.S., et al. (2000). Rom-1 is required for rod photoreceptor viability and the regulation of disk morphogenesis. Nat. Genet. *25*, 67–73.

Crew, V.K., Burton, N., Kagan, A., Green, C. a., Levene, C., Flinter, F., Brady, R.L., Daniels, G., and Anstee, D.J. (2004). CD151, the first member of the tetraspanin (TM4) superfamily

detected on erythrocytes, is essential for the correct assembly of human basement membranes in kidney and skin. Blood *104*, 2217–2223.

Curti, E., Kwityn, C., Zhan, B., Gillespie, P., Brelsford, J., Deumic, V., Plieskatt, J., Rezende, W.C., Tsao, E., Kalampanayil, B., et al. (2013). Expression at a 20L scale and purification of the extracellular domain of the Schistosoma mansoni TSP-2 recombinant protein: A vaccine candidate for human intestinal schistosomiasis. Hum. Vaccines Immunother. *9*, 2342–2350.

Dalton, A.C., and Barton, W. a (2014). Over-expression of secreted proteins from mammalian cell lines. Protein Sci. *23*, 517–525.

Damais, C., Jupin, C., Parant, M., and Chedid, L. (1987). Induction of human interleukin-1 production by polymyxin B. J Immunol Methods *101*, 51–56.

Demain, A.L., and Vaishnav, P. (2009). Production of recombinant proteins by microbes and higher organisms. Biotechnol. Adv. *27*, 297–306.

Deng, J., Yeung, V.P., Tsitoura, D., DeKruyff, R.H., Umetsu, D.T., and Levy, S. (2000). Allergen-induced airway hyperreactivity is diminished in CD81-deficient mice. J. Immunol. *165*, 5054–5061.

DeSalle, R., Mares, R., and Garcia-España, A. (2010). Evolution of cysteine patterns in the large extracellular loop of tetraspanins from animals, fungi, plants and single-celled eukaryotes. Mol. Phylogenet. Evol. *56*, 486–491.

Dombrowicz, D., Flamand, V., Brigman, K.K., Koller, B.H., and Kinet, J.P. (1993). Abolition of anaphylaxis by targeted disruption of the high affinity immunoglobulin E receptor alpha chain gene. Cell *75*, 969–976.

Don, R.H., Cox, P.T., Wainwright, B.J., Baker, K., and Mattick, J.S. (1991). "Touchdown" PCR to circumvent spurious priming during gene amplification. Nucleic Acids Res. *19*, 4008.

Dornier, E., Coumailleau, F., Ottavi, J.-F., Moretti, J., Boucheix, C., Mauduit, P., Schweisguth, F., and Rubinstein, E. (2012). TspanC8 tetraspanins regulate ADAM10/Kuzbanian trafficking and promote Notch activation in flies and mammals. J. Cell Biol. *199*, 481–496.

Draber, P., Halova, I., Levi-Schaffer, F., and Draberova, L. (2012). Transmembrane adaptor proteins in the high-affinity IgE receptor signaling. Front. Immunol. *2*, 1–11.

Ehrlich, P. (1879). Uber die specifischen granulationen des Blutes.

El-Agamy, D.S. (2012). Targeting c-kit in the therapy of mast cell disorders: Current update. Eur. J. Pharmacol. *690*, 1–3.

Ellerman, D.A., Ha, C., Primakoff, P., Myles, D.G., and Dveksler, G.S. (2003). Direct binding of the ligand PSG17 to CD9 requires a CD9 site essential for sperm-egg fusion. Mol. Biol. Cell *14*, 5098–5103.

Eshhar, Z., Ofarim, M., and Waks, T. (1980). Generation of hybridomas secreting murine reaginic antibodies of anti-DNP specificity. J. Immunol. *124*, 775–780.

Espenel, C., Margeat, E., Dosset, P., Arduise, C., Le Grimellec, C., Royer, C.A., Boucheix, C., Rubinstein, E., and Milhiet, P.-E. (2008). Single-molecule analysis of CD9 dynamics and partitioning reveals multiple modes of interaction in the tetraspanin web. J. Cell Biol. *182*, 765–776.

Esposito, D., and Chatterjee, D.K. (2006). Enhancement of soluble protein expression through the use of fusion tags. Curr. Opin. Biotechnol. *17*, 353–358.

Fanaei, M., Monk, P.N., and Partridge, L.J. (2011). The role of tetraspanins in fusion. Biochem. Soc. Trans. *39*, 524–528.

Feigelson, S.W., Grabovsky, V., Shamri, R., Levy, S., and Alon, R. (2003). The CD81 Tetraspanin Facilitates Instantaneous Leukocyte VLA-4 Adhesion Strengthening to Vascular Cell Adhesion Molecule 1 (VCAM-1) under Shear Flow. J. Biol. Chem. *278*, 51203–51212.

Ferrer, M., Chernikova, T.N., Timmis, K.N., and Golyshin, P.N. (2004). Expression of a Temperature-Sensitive Esterase in a Novel Chaperone-Based Escherichia coli Strain Expression of a Temperature-Sensitive Esterase in a Novel Chaperone-Based Escherichia coli Strain. *70*, 4499–4504.

Field, K.A., Holowka, D., and Baird, B. (1995). Fc epsilon RI-mediated recruitment of p53/56lyn to detergent-resistant membrane domains accompanies cellular signaling. Proc. Natl. Acad. Sci. *92*, 9201–9205.

Finn, G.K., Kurz, B.W., Cheng, R.Z., and Shmookler Reis, R.J. (1989). Homologous plasmid recombination is elevated in immortally transformed cells. Mol. Cell. Biol. *9*, 4009–4017.

Fleming, T.J., Donnadieu, E., Song, C.H., Laethem, F. Van, Galli, S.J., and Kinet, J.-P. (1997). Negative Regulation of FcεRI-mediated Degranulation by CD81. J. Exp. Med. *186*, 1307–1314.

Flint, M., von Hahn, T., Zhang, J., Farquhar, M., Jones, C.T., Balfe, P., Rice, C.M., and McKeating, J. a (2006). Diverse CD81 proteins support hepatitis C virus infection. J. Virol. *80*, 11331–11342.

Foster, L.J., De Hoog, C.L., and Mann, M. (2003). Unbiased quantitative proteomics of lipid rafts reveals high specificity for signaling factors. Proc. Natl. Acad. Sci. U. S. A. *100*, 5813–5818.

Galli, S.J., Nakae, S., and Tsai, M. (2005). Mast cells in the development of adaptive immune responses. Nat. Immunol. *6*, 135–142.

Gao, B., and Tsan, M.-F. (2003). Endotoxin contamination in recombinant human heat shock protein 70 (Hsp70) preparation is responsible for the induction of tumor necrosis factor alpha release by murine macrophages. J. Biol. Chem. *278*, 174–179.

Garman, S.C., Kinet, J.P., and Jardetzky, T.S. (1998). Crystal structure of the human high-affinity IgE receptor. Cell *95*, 951–961.

Gartlan, K.H., Wee, J.L., Demaria, M.C., Nastovska, R., Chang, T.M., Jones, E.L., Apostolopoulos, V., Pietersz, G. a, Hickey, M.J., van Spriel, A.B., et al. (2013). Tetraspanin CD37 contributes to the initiation of cellular immunity by promoting dendritic cell migration. Eur. J. Immunol. *43*, 1208–1219.

Genovese, a., Bouvet, J.P., Florio, G., Lamparter-Schummert, B., Bjorck, L., and Marone, G. (2000). Bacterial immunoglobulin superantigen proteins A and L activate human heart mast cells by interacting with immunoglobulin E. Infect. Immun. *68*, 5517–5524.

Ghildyal, N., Mcneil, H.P., Gurish, M.F., Austen, K.F., and Stevens, R.L. (1992). Transcriptional Regulation of the Mucosal Mast Cell-specific Protease Gene, MMCP-8,. Mol. Biol. *267*, 8473–8477.

Gorman, C.M., Howard, B.H., and Reeves, R. (1983). Expression of recombinant plasmids in mammalian cells is enhanced by sodium butyrate. Nucleic Res. *1*, 7631–7648.

Green, L.R., Monk, P.N., Partridge, L.J., Morris, P., Gorringe, A.R., and Read, R.C. (2011). Cooperative role for tetraspanins in adhesin-mediated attachment of bacterial species to human epithelial cells. Infect. Immun. *79*, 2241–2249.

Greenfield, N. (2007). Using circular dichroism spectra to estimate protein secondary structure. Nat. Protoc. *1*, 2876–2890.

Guan, K.L., and Dixon, J.E. (1991). Eukaryotic proteins expressed in Escherichia coli: an improved thrombin cleavage and purification procedure of fusion proteins with glutathione S-transferase. Anal. Biochem. *192*, 262–267.

Gurish, M.F., and Boyce, J. a. (2006). Mast cells: Ontogeny, homing, and recruitment of a unique innate effector cell. J. Allergy Clin. Immunol. *117*, 1285–1291.

Guruprasad, K., Reddy, B. V, and Pandit, M.W. (1990). Correlation between stability of a protein and its dipeptide composition: a novel approach for predicting in vivo stability of a protein from its primary sequence. Protein Eng. *4*, 155–161.

Hamawy, M.M., Oliver, C., Mergenhagen, S.E., and Siraganian, R.P. (1992). Adherence of rat basophilic leukemia (RBL-2H3) cells to fibronectin-coated surfaces enhances secretion. J. Immunol. *149*, 615–621.

Harvima, I.T., Levi-Schaffer, F., Draber, P., Friedman, S., Polakovicova, I., Gibbs, B.F., Blank, U., Nilsson, G., and Maurer, M. (2014). Molecular targets on mast cells and basophils for novel therapies. J. Allergy Clin. Immunol. *134*, 530–544.

Hassuna, N., Monk, P.N., Moseley, G.W., and Partridge, L.J. (2009). Strategies for targeting tetraspanin proteins: potential therapeutic applications in microbial infections. BioDrugs *23*, 341–359.

Hemler, M.E. (1990). VLA proteins in the integrin family: structures, functions, and their role on leukocytes. Annu. Rev. Immunol. *8*, 365–400.

Hemler, M.E. (2001). Specific tetraspanin functions. J. Cell Biol. *155*, 1103–1107.

Hemler, M.E. (2003). Tetraspanin proteins mediate cellular penetration, invasion, and fusion events and define a novel type of membrane microdomain. Annu. Rev. Cell Dev. Biol. *19*, 397–422.

Hemler, M.E. (2005). Tetraspanin functions and associated microdomains. Nat. Rev. Mol. Cell Biol. *6*, 801–811.

Hemler, M.E. (2008). Targeting of tetraspanin proteins--potential benefits and strategies. Nat. Rev. Drug Discov. *7*, 747–758.

Hemler, M.E. (2013). Tetraspanin proteins promote multiple cancer stages. Nat. Rev. Cancer *14*, 49–60.

Henz, B.M., Maurer, M., Lippert, U., Worm, M., and Babina, M. (2001). Mast cells as initiators of immunity and host defense. Exp. Dermatol. *10*, 1–10.

Higginbottom, a, Wilkinson, I., McCullough, B., Lanza, F., Azorsa, D.O., Partridge, L.J., and Monk, P.N. (2000a). Antibody cross-linking of human CD9 and the high-affinity immunoglobulin E receptor stimulates secretion from transfected rat basophilic leukaemia cells. Immunology *99*, 546–552.

Higginbottom, A., Quinn, E.R., Kuo, C.C., Flint, M., Wilson, L.H., Bianchi, E., Nicosia, A., Monk, P.N., McKeating, J. a, and Levy, S. (2000b). Identification of amino acid residues in CD81 critical for interaction with hepatitis C virus envelope glycoprotein E2. J. Virol. *74*, 3642–3649.

Higginbottom, A., Takahashi, Y., Bolling, L., Coonrod, S. a., White, J.M., Partridge, L.J., and Monk, P.N. (2003). Structural requirements for the inhibitory action of the CD9 large extracellular domain in sperm/oocyte binding and fusion. Biochem. Biophys. Res. Commun. *311*, 208–214.

Ho, S.-H., Martin, F., Higginbottom, A., Partridge, L.J., Parthasarathy, V., Moseley, G.W., Lopez, P., Cheng-Mayer, C., and Monk, P.N. (2006). Recombinant extracellular domains of tetraspanin proteins are potent inhibitors of the infection of macrophages by human immunodeficiency virus type 1. J. Virol. *80*, 6487–6496.

Ho, S.N., Hunt, H.D., Horton, R.M., Pullen, J.K., and Pease, L.R. (1989). Site-directed mutagenesis by overlap extension using the polymerase chain reaction. Gene *77*, 51–59.

Hogue, I.B., Grover, J.R., Soheilian, F., Nagashima, K., and Ono, A. (2011). Gag Induces the Coalescence of Clustered Lipid Rafts and Tetraspanin-Enriched Microdomains at HIV-1 Assembly Sites on the Plasma Membrane. J. Virol. *85*, 9749–9766.

Hong, H., Kitaura, J., Xiao, W., Horejsi, V., Ra, C., Lowell, C. a, Kawakami, Y., and Kawakami, T. (2007). The Src family kinase Hck regulates mast cell activation by suppressing an inhibitory Src family kinase Lyn. Blood *110*, 2511–2519.

Hotta, H., Ross, A.H., Huebner, K., Isobe, M., Wendeborn, S., Chao, M. V, Ricciardi, R.P.,

Tsujimoto, Y., Croce, C.M., and Koprowski, H. (1988). Molecular Cloning and Characterization of an Antigen Associated with Early Stages of Melanoma Tumor Progression. Cancer Reseach *48*, 2955–2962.

Huang, M.M., Indik, Z., Brass, L.F., Hoxie, J. a, Schreiber, a D., and Brugge, J.S. (1992). Activation of Fc gamma RII induces tyrosine phosphorylation of multiple proteins including Fc gamma RII. J. Biol. Chem. *267*, 5467–5473.

Huang, S., Yuan, S., Dong, M., Su, J., Yu, C., Shen, Y., Xie, X., Yu, Y., Yu, X., Chen, S., et al. (2005). The phylogenetic analysis of tetraspanins projects the evolution of cell-cell interactions from unicellular to multicellular organisms. Genomics *86*, 674–684.

Huang, S., Tian, H., Chen, Z., Yu, T., and Xu, A. (2010). The evolution of vertebrate tetraspanins: gene loss, retention, and massive positive selection after whole genome duplications. BMC Evol. Biol. *10*, 306.

Hulme, R.S., Higginbottom, A., Palmer, J., Partridge, L.J., and Monk, P.N. (2014). Distinct Regions of the Large Extracellular Domain of Tetraspanin CD9 Are Involved in the Control of Human Multinucleated Giant Cell Formation. PLoS One *9*, e116289.

Hynes, R.O. (1992). Integrins: versatility, modulation, and signaling in cell adhesion. Cell *69*, 11–25.

Irani, a a, Schechter, N.M., Craig, S.S., DeBlois, G., and Schwartz, L.B. (1986). Two types of human mast cells that have distinct neutral protease compositions. Proc. Natl. Acad. Sci. U. S. A. *83*, 4464–4468.

Ishizaka, K., Ishizaka, T., and Alerts, E. (1967). Identification of γ E-Antibodies as a Carrier of Reaginic Activity. J. Immunol. *99*, 1187–1198.

Ishizaka, K., Tomioka, H., and Ishizaka, T. (1970). Mechanisms of passive sensitization. I. Presence of IgE and IgG molecules on human leukocytes. J. Immunol. *105*, 1459–1467.

Iwai, K., Ishii, M., Ohshima, S., Miyatake, K., and Saeki, Y. (2007). Expression and function of transmembrane-4 superfamily (tetraspanin) proteins in osteoclasts: reciprocal roles of Tspan-5 and NET-6 during osteoclastogenesis. Allergol. Int. *56*, 457–463.

Jamshad, M., Rajesh, S., Stamataki, Z., McKeating, J. a, Dafforn, T., Overduin, M., and Bill, R.M. (2008). Structural characterization of recombinant human CD81 produced in Pichia pastoris. Protein Expr. Purif. *57*, 206–216.

Jankowski, S.A., Mitchell, D.S., Smith, S.H., Trent, J.M., and Meltzer, P.S. (1994). SAS, a gene amplified in human sarcomas, encodes a new member of the transmembrane 4 superfamily of proteins. Oncogene *9*, 1205–1211.

Jayapal, K., Wlaschin, K., Hu, W., and Yap, G. (2007). Recombinant protein therapeutics from CHO cells-20 years and counting. Chem. Eng. Prog. *103*, 40–47.

Jegou, A., Ziyyat, A., Barraud-Lange, V., Perez, E., Wolf, J.P., Pincet, F., and Gourier, C. (2011). CD9 tetraspanin generates fusion competent sites on the egg membrane for mammalian fertilization. Proc. Natl. Acad. Sci. *108*, 10946–10951.

Jenkins, N., and Curling, E.M. a (1994). Glycosylation of recombinant proteins: Problems and prospects. Enzyme Microb. Technol. *16*, 354–364.

Joly, J.C., and Swartz, J.R. (1994). Protein folding activities of Escherichia coli protein disulfide isomerase. Biochemistry *33*, 4231–4236.

Jung, K.-K., Liu, X.-W., Chirco, R., Fridman, R., and Kim, H.-R.C. (2006). Identification of CD63 as a tissue inhibitor of metalloproteinase-1 interacting cell surface protein. EMBO J. *25*, 3934–3942.

Junge, H.J., Yang, S., Burton, J.B., Paes, K., Shu, X., French, D.M., Costa, M., Rice, D.S., and Ye, W. (2009). TSPAN12 Regulates Retinal Vascular Development by Promoting Norrin- but Not

Wnt-Induced FZD4/??-Catenin Signaling. Cell *139*, 299–311.

Kaji, K., Oda, S., Shikano, T., Ohnuki, T., Uematsu, Y., Sakagami, J., Tada, N., Miyazaki, S., and Kudo, a (2000). The gamete fusion process is defective in eggs of Cd9-deficient mice. Nat. Genet. *24*, 279–282.

Kalesnikoff, J., Huber, M., Lam, V., Damen, J.E., Zhang, J., Siraganian, R.P., and Krystal, G. (2001). Pathways in Mast Cells that Lead to Cytokine Production and Cell Survival. *14*, 801–811.

Kaplan, W., Hüsler, P., Klump, H., Erhardt, J., Sluis-Cremer, N., and Dirr, H. (1997). Conformational stability of pGEX-expressed Schistosoma japonicum glutathione S-transferase: a detoxification enzyme and fusion-protein affinity tag. Protein Sci. *6*, 399–406.

Kato, N., Nakanishi, M., and Hirashima, N. (2003). Cholesterol depletion inhibits store-operated calcium currents and exocytotic membrane fusion in RBL-2H3 cells. Biochemistry *42*, 11808–11814.

Kawakami, T., and Galli, S.J. (2002). Regulation of mast-cell and basophil function and survival by IgE. Nat. Rev. Immunol. *2*, 773–786.

Kazarov, A.R., Yang, X., Stipp, C.S., Sehgal, B., and Hemler, M.E. (2002). An extracellular site on tetraspanin CD151 determines α3 and α6 integrin-dependent cellular morphology. J. Cell Biol. *158*, 1299–1309.

Kelić, S., Levy, S., Suarez, C., and Weinstein, D.E. (2001). CD81 regulates neuron-induced astrocyte cell-cycle exit. Mol. Cell. Neurosci. *17*, 551–560.

Kelly, S.M., Jess, T.J., and Price, N.C. (2005). How to study proteins by circular dichroism. Biochim. Biophys. Acta *1751*, 119–139.

Kespichayawattana, W., Rattanachetkul, S., Wanun, T., Utaisincharoen, P., and Sirisinha, S. (2000). Burkholderia pseudomallei induces cell fusion and actin-associated membrane protrusion: A possible mechanism for cell-to-cell spreading. Infect. Immun. *68*, 5377–5384.

Kim, J., Cleich, G.J., and Kita, H. (1997). Roles of CD9 Molecules in Survival and Activation of Human Eosinophils. Culture *7*.

Kim, J.Y., Kim, Y.G., and Lee, G.M. (2012). CHO cells in biotechnology for production of recombinant proteins: Current state and further potential. Appl. Microbiol. Biotechnol. *93*, 917–930.

Kitadokoro, K., Bordo, D., Galli, G., Petracca, R., Falugi, F., Abrignani, S., Grandi, G., and Bolognesi, M. (2001). CD81 extracellular domain 3D structure: insight into the tetraspanin superfamily structural motifs. EMBO J. *20*, 12–18.

Kitani, S., Berenstein, E., Mergenhagen, S., Tempstg, P., and Siraganian, R.P. (1991). A Cell Surface Glycoprotein of Rat Basophilic Leukemia Cells Close to the High Affinity IgE Receptor (FcrRI). J. Biol. Chem. *266*, 1903–1909.

Knol, E.F., Mul, F.P., Jansen, H., Calafat, J., and Roos, D. (1991). Monitoring human basophil activation via CD63 monoclonal antibody 435. J. Allergy Clin. Immunol. *88*, 328–338.

Köberle, M., Kaesler, S., Kempf, W., Wölbing, F., and Biedermann, T. (2012). Tetraspanins in mast cells. Front. Immunol. *3*, 106.

Kohno, M., Hasegawa, H., Miyake, M., Yamamoto, T., and Fujita, S. (2002). CD151 enhances cell motility and metastasis of cancer cells in the presence of focal adhesion kinase. Int. J. Cancer *97*, 336–343.

Kopito, R.R. (2000). Aggresomes, inclusion bodies and protein aggregation. Trends Cell Biol. *10*, 524–530.

Kovalenko, O. V, Yang, X., Kolesnikova, T. V, and Hemler, M.E. (2004). Evidence for specific tetraspanin homodimers: inhibition of palmitoylation makes cysteine residues available for

cross-linking. Biochem. J. *377*, 407–417.

Kovalenko, O. V, Metcalf, D.G., DeGrado, W.F., and Hemler, M.E. (2005). Structural organization and interactions of transmembrane domains in tetraspanin proteins. BMC Struct. Biol. *5*, 11.

Kraft, S., Fleming, T., Billingsley, J.M., Lin, S.-Y., Jouvin, M.-H., Storz, P., and Kinet, J.-P. (2005). Anti-CD63 antibodies suppress IgE-dependent allergic reactions in vitro and in vivo. J. Exp. Med. *201*, 385–396.

Kraft, S., Jouvin, M.-H., Kulkarni, N., Kissing, S., Morgan, E.S., Dvorak, A.M., Schröder, B., Saftig, P., and Kinet, J.-P. (2013). The Tetraspanin CD63 Is Required for Efficient IgE-Mediated Mast Cell Degranulation and Anaphylaxis. J. Immunol.

Krämer, B., Schulte, D., Körner, C., Zwank, C., Hartmann, A., Michalk, M., Söhne, J., Langhans, B., Nischalke, H.-D., Coenen, M., et al. (2009). Regulation of NK cell trafficking by CD81. Eur. J. Immunol. *39*, 3447–3458.

Kropshofer, H., Spindeldreher, S., Röhn, T. a, Platania, N., Grygar, C., Daniel, N., Wölpl, a, Langen, H., Horejsi, V., and Vogt, a B. (2002). Tetraspan microdomains distinct from lipid rafts enrich select peptide-MHC class II complexes. Nat. Immunol. *3*, 61–68.

Kulczycki, A., Isersky, C., and Metzger, H. (1974). The interaction of IgE with rat basophilic leukemia cells. I. Evidence for specific binding of IgE. J. Exp. Med. *139*, 600–616.

Kulka, M., Sheen, C.H., Tancowny, B.P., Grammer, L.C., and Schleimer, R.P. (2008). Neuropeptides activate human mast cell degranulation and chemokine production. Immunology *123*, 398–410.

Kunder, C. a, St John, A.L., Li, G., Leong, K.W., Berwin, B., Staats, H.F., and Abraham, S.N. (2009). Mast cell-derived particles deliver peripheral signals to remote lymph nodes. J. Exp. Med. *206*, 2455–2467.

Kurokawa, Y., Yanagi, H., and Yura, T. (2000). Overexpression of protein disulfide isomerase DsbC stabilizes multiple-disulfide-bonded recombinant protein produced and transported to the periplasm in Escherichia coli. Appl. Environ. Microbiol. *66*, 3960–3965.

Lammerding, J., Kazarov, A.R., Huang, H., Lee, R.T., and Hemler, M.E. (2003). Tetraspanin CD151 regulates 6 1 integrin adhesion strengthening. Proc. Natl. Acad. Sci. *100*, 7616–7621.

Larrick, J.W., and Thomas, D.W. (2001). Producing proteins in transgenic plants and animals. Curr. Opin. Biotechnol. *12*, 411–418.

Latysheva, N., Muratov, G., Rajesh, S., Padgett, M., Hotchin, N. a, Overduin, M., and Berditchevski, F. (2006). Syntenin-1 is a new component of tetraspanin-enriched microdomains: mechanisms and consequences of the interaction of syntenin-1 with CD63. Mol. Cell. Biol. *26*, 7707–7718.

Lee, J.H., Kim, J.W., Kim, D.K., Kim, H.S., Park, H.J., Park, D.K., Kim, A.-R., Kim, B., Beaven, M. a, Park, K.L., et al. (2011). The Src family kinase Fgr is critical for activation of mast cells and IgE-mediated anaphylaxis in mice. J. Immunol. *187*, 1807–1815.

Levy, R., Weiss, R., Chen, G., Iverson, B.L., and Georgiou, G. (2001). Production of correctly folded Fab antibody fragment in the cytoplasm of Escherichia coli trxB gor mutants via the coexpression of molecular chaperones. Protein Expr. Purif. *23*, 338–347.

Lin, S., Cicala, C., Scharenberg, A.M., and Kinet, J.P. (1996). The FceRI beta subunit functions as an amplifier of FceRI gamma-mediated cell activation signals. Cell *85*, 985–995.

von Lindern, J.J., Rojo, D., Grovit-Ferbas, K., Yeramian, C., Deng, C., Herbein, G., Ferguson, M.R., Pappas, T.C., Decker, J.M., Singh, A., et al. (2003). Potential Role for CD63 in CCR5-Mediated Human Immunodeficiency Virus Type 1 Infection of Macrophages. J. Virol. *77*, 3624–3633.

Lineberry, N., Su, L., Soares, L., and Fathman, C.G. (2008). The single subunit transmembrane E3 ligase gene related to anergy in lymphocytes (GRAIL) captures and then ubiquitinates transmembrane proteins across the cell membrane. J. Biol. Chem. *283*, 28497–28505.

Lipski, S., Grabbe, J., and Henz, B.M. (1996). Absence of MHC class II antigen on mast cells at sites of inflammation in human skin. Exp. Dermatol. *5*, 120–124.

Liu, L., He, B., Liu, W.M., Zhou, D., Cox, J. V, and Zhang, X. a (2007). Tetraspanin CD151 promotes cell migration by regulating integrin trafficking. J. Biol. Chem. *282*, 31631–31642.

Loewen, C.J.R., and Molday, R.S. (2000). Disulfide-mediated Oligomerization of Peripherin / Rds and Rom-1 in Photoreceptor Disk Membranes. J. Biol. Chem. *275*, 5370–5378.

Macauley-Patrick, S., Fazenda, M.L., McNeil, B., and Harvey, L.M. (2005). Heterologous protein production using the Pichia pastoris expression system. Yeast *22*, 249–270.

Maecker, H.T., Todd, S.C., and Levy, S. (1997). The tetraspanin superfamily: molecular facilitators. FASEB J. *11*, 428–442.

Malaviya, R., Twesten, N.J., Ross, E. a, Abraham, S.N., and Pfeifer, J.D. (1996). Mast cells process bacterial Ags through a phagocytic route for class I MHC presentation to T cells. J. Immunol. *156*, 1490–1496.

Malaviya, R., Gao, Z., Thankavel, K., van der Merwe, P. a, and Abraham, S.N. (1999). The mast cell tumor necrosis factor alpha response to FimH-expressing Escherichia coli is mediated by the glycosylphosphatidylinositol-anchored molecule CD48. Proc. Natl. Acad. Sci. U. S. A. *96*, 8110–8115.

Mamat, U., Wilke, K., Bramhill, D., Schromm, A.B., Lindner, B., Kohl, T.A., Corchero, J.L., Villaverde, A., Schaffer, L., Head, S.R., et al. (2015). Detoxifying Escherichia coli for endotoxin-free production of recombinant proteins. Microb. Cell Fact. *14*, 1–15.

Marbach, A., and Bettenbrock, K. (2012). Lac operon induction in Escherichia coli: Systematic comparison of IPTG and TMG induction and influence of the transacetylase LacA. J. Biotechnol. *157*, 82–88.

Martin, F., Roth, D.M., Jans, D.A., Pouton, C.W., Monk, P.N., Moseley, G.W., and Partridge, L.J. (2005). Tetraspanins in Viral Infections : a Fundamental Role in Viral Biology ? J. Virol. *79*, 10839–10851.

Masciopinto, F., Campagnoli, S., Abrignani, S., Uematsu, Y., and Pileri, P. (2001). The small extracellular loop of CD81 is necessary for optimal surface expression of the large loop, a putative HCV receptor. Virus Res. *80*, 1–10.

Masciopinto, F., Giovani, C., Campagnoli, S., Galli-Stampino, L., Colombatto, P., Brunetto, M., Yen, T.S.B., Houghton, M., Pileri, P., and Abrignani, S. (2004). Association of hepatitis C virus envelope proteins with exosomes. Eur. J. Immunol. *34*, 2834–2842.

Metcalfe, D.D. (2008). Mast cells and mastocytosis. Blood *112*, 946–956.

Metcalfe, D., Baram, D., and Mekori, Y. (1997). Mast cells. Physiol. Rev. *77*, 1033–1079.

Metcalfe, D.D., Peavy, R.D., and Gilfillan, A.M. (2009). Mechanisms of mast cell signaling in anaphylaxis. J. Allergy Clin. Immunol. *124*, 639–646.

Metz, M., Piliponsky, A.M., Chen, C.-C., Lammel, V., Abrink, M., Pejler, G., Tsai, M., and Galli, S.J. (2006). Mast cells can enhance resistance to snake and honeybee venoms. Science *313*, 526–530.

Miller, B.J., Georges-Labouesse, E., Primakoff, P., and Myles, D.G. (2000). Normal fertilization occurs with eggs lacking the integrin ??6??1 and is CD9-dependent. J. Cell Biol. *149*, 1289–1295.

Min, G., Stolz, M., Zhou, G., Liang, F., Sebbel, P., Stoffler, D., Glockshuber, R., Sun, T.-T., Aebi, U., and Kong, X.-P. (2002). Localization of uroplakin Ia, the urothelial receptor for bacterial

adhesin FimH, on the six inner domains of the 16 nm urothelial plaque particle. J. Mol. Biol. *317*, 697–706.

Min, G., Wang, H., Sun, T.-T., and Kong, X.-P. (2006). Structural basis for tetraspanin functions as revealed by the cryo-EM structure of uroplakin complexes at 6-A resolution. J. Cell Biol. *173*, 975–983.

Mol, C.D., Dougan, D.R., Schneider, T.R., Skene, R.J., Kraus, M.L., Scheibe, D.N., Snell, G.P., Zou, H., Sang, B.C., and Wilson, K.P. (2004). Structural basis for the autoinhibition and STI-571 inhibition of c-Kit tyrosine kinase. J. Biol. Chem. *279*, 31655–31663.

Molina, S., Castet, V., Pichard-Garcia, L., Wychowski, C., Meurs, E., Pascussi, J.M., Sureau, C., Fabre, J.M., Sacunha, A., Larrey, D., et al. (2008). Serum-derived hepatitis C virus infection of primary human hepatocytes is tetraspanin CD81 dependent. J Virol *82*, 569–574.

Monk, P.N., and Partridge, L.J. (2012). Tetraspanins: gateways for infection. Infect. Disord. Drug Targets *12*, 4–17.

Moseley, G.W.G. (2005). Tetraspanin-Fc receptor interactions. Platelets *48*, 40.

Moseley, G.W., Elliott, J., Wright, M.D., Partridge, L.J., and Monk, P.N. (2003). Interspecies contamination of the KM3 cell line: implications for CD63 function in melanoma metastasis. Int. J. Cancer *105*, 613–616.

Muranova, T.A., Ruzheinikov, S.N., Higginbottom, A., Clipson, J.A., Blackburn, G.M., Wentworth, P., Datta, A., Rice, D.W., and Partridge, L.J. (2003). Crystallization of a carbamatase catalytic antibody Fab fragment and its complex with a transition-state analogue. Acta Crystallogr. Sect. D Biol. Crystallogr. *60*, 172–174.

Le Naour, F., Rubinstein, E., Jasmin, C., Prenant, M., and Boucheix, C. (2000). Severely reduced female fertility in CD9-deficient mice. Science *287*, 319–321.

Le Naour, F., André, M., Boucheix, C., and Rubinstein, E. (2006). Membrane microdomains and proteomics: lessons from tetraspanin microdomains and comparison with lipid rafts. Proteomics *6*, 6447–6454.

Di Nardo, A., Vitiello, A., and Gallo, R.L. (2003). Cutting edge: mast cell antimicrobial activity is mediated by expression of cathelicidin antimicrobial peptide. J. Immunol. *170*, 2274–2278.

Di Nardo, A., Yamasaki, K., Dorschner, R. a, Lai, Y., and Gallo, R.L. (2008). Mast cell cathelicidin antimicrobial peptide prevents invasive group A Streptococcus infection of the skin. J. Immunol. *180*, 7565–7573.

Nilsson, G., Johnell, M., Hammer, C.H., Tiffany, H.L., Nilsson, K., Metcalfe, D.D., Siegbahn, a, and Murphy, P.M. (1996). C3a and C5a are chemotaxins for human mast cells and act through distinct receptors via a pertussis toxin-sensitive signal transduction pathway. J. Immunol. *157*, 1693–1698.

Nishikata, H., Oliver, C., Mergenhagen, S.E., and Siraganian, R.P. (1992). The rat mast cell antigen AD1 (homologue to human CD63 or melanoma antigen ME491) is expressed in other cells in culture. J. Immunol. *149*, 862–870.

Nishizumi, H., and Yamamoto, T. (1997). Impaired tyrosine phosphorylation and Ca2+ mobilization, but not degranulation, in lyn-deficient bone marrow-derived mast cells. J. Immunol. *158*, 2350–2355.

Ntini, E., Järvelin, A.I., Bornholdt, J., Chen, Y., Boyd, M., Jørgensen, M., Andersson, R., Hoof, I., Schein, A., Andersen, P.R., et al. (2013). Polyadenylation site-induced decay of upstream transcripts enforces promoter directionality. Nat. Struct. Mol. Biol. *20*, 923–928.

O'Gorman, S., Fox, D.T., and Wahl, G.M. (1991). Recombinase-mediated gene activation and site-specific integration in mammalian cells. Science *251*, 1351–1355.

O'Mahony, L., Akdis, M., and Akdis, C. a. (2011). Regulation of the immune response and

inflammation by histamine and histamine receptors. J. Allergy Clin. Immunol. *128*, 1153–1162.

Oba, M., and Tanaka, M. (2012). Intracellular Internalization Mechanism of Protein Transfection Reagents. Biol. Pharm. Bull. *35*, 1064–1068.

Ono, M., Handa, K., Withers, D. a., and Hakomori, S.I. (1999). Motility inhibition and apoptosis are induced by metastasis-suppressing gene product CD82 and its analogue CD9, with concurrent glycosylation. Cancer Res. *59*, 2335–2339.

Ono, M., Handa, K., Withers, D. a, and Hakomori, S. (2000). Glycosylation effect on membrane domain (GEM) involved in cell adhesion and motility: a preliminary note on functional alpha3, alpha5-CD82 glycosylation complex in ldlD 14 cells. Biochem. Biophys. Res. Commun. *279*, 744–750.

Oren, R., Takahashi, S., Doss, C., Levy, R., and Levy, S. (1990). TAPA-1, the target of an antiproliferative antibody, defines a new family of transmembrane proteins. Mol. Cell. Biol. *10*, 4007–4015.

Ortega, E., Schweitzer-Stenner, R., and Pecht, I. (1991). Kinetics of ligand binding to the type 1 Fc epsilon receptor on mast cells. Biochemistry *30*, 3473–3483.

Ovalle, S., Guti??rrez-L??pez, M.D., Olmo, N., Turnay, J., Lizarbe, M.A., Majano, P., Molina-Jim??nez, F., L??pez-Cabrera, M., Y????ez-M??, M., S??nchez-Madrid, F., et al. (2007). The tetraspanin CD9 inhibits the proliferation and tumorigenicity of human colon carcinoma cells. Int. J. Cancer *121*, 2140–2152.

Pagel, J.M., Spurgeon, S.E., Byrd, J.C., Awan, F.T., Flinn, I.W., Lanasa, M.C., Eisenfeld, A.J., Stromatt, S.C., and Gopal, A.K. (2014). Otlertuzumab (TRU-016), an anti-CD37 monospecific ADAPTIR™ therapeutic protein, for relapsed or refractory NHL patients. Br. J. Haematol. 1–8.

Pan, Y., Brown, C., Wang, X., and Geisert, E.E. (2007). The developmental regulation of CD81 in the rat retina. Mol. Vis. *13*, 181–189.

Parravicini, V., Gadina, M., Kovarova, M., Odom, S., Gonzalez-Espinosa, C., Furumoto, Y., Saitoh, S., Samelson, L.E., O'Shea, J.J., and Rivera, J. (2002). Fyn kinase initiates complementary signals required for IgE-dependent mast cell degranulation. Nat. Immunol. *3*, 741–748.

Parthasarathy, V., Martin, F., Higginbottom, A., Murray, H., Moseley, G.W., Read, R.C., Mal, G., Hulme, R., Monk, P.N., and Partridge, L.J. (2009). Distinct roles for tetraspanins CD9, CD63 and CD81 in the formation of multinucleated giant cells. Immunology *127*, 237–248.

Passante, E., and Frankish, N. (2009). The RBL-2H3 cell line: Its provenance and suitability as a model for the mast cell. Inflamm. Res. *58*, 737–745.

Passante, E., Ehrhardt, C., Sheridan, H., and Frankish, N. (2009). RBL-2H3 cells are an imprecise model for mast cell mediator release. Inflamm. Res. *58*, 611–618.

Peng, W.M., Yu, C.F., Kolanus, W., Mazzocca, a, Bieber, T., Kraft, S., and Novak, N. (2011). Tetraspanins CD9 and CD81 are molecular partners of trimeric FcεRI on human antigen-presenting cells. Allergy *66*, 605–611.

Petracca, R., Falugi, F., Galli, G., Norais, N., Rosa, D., Campagnoli, S., Burgio, V., Di Stasio, E., Giardina, B., Houghton, M., et al. (2000). Structure-function analysis of hepatitis C virus envelope-CD81 binding. J. Virol. *74*, 4824–4830.

Phizicky, E.M., and Fields, S. (1995). Protein-protein interactions: Methods for detection and analysis. Microbiological.Reviews *59*, 94–123.

Pileri, P., Uematsu, Y., Campagnoli, S., Galli, G., Falugi, F., Petracca, R., Weiner, a J., Houghton, M., Rosa, D., Grandi, G., et al. (1998). Binding of hepatitis C virus to CD81. Science *282*, 938–941.

Piliponsky, A.M., Chen, C.-C., Nishimura, T., Metz, M., Rios, E.J., Dobner, P.R., Wada, E., Wada, K., Zacharias, S., Mohanasundaram, U.M., et al. (2008). Neurotensin increases mortality and

mast cells reduce neurotensin levels in a mouse model of sepsis. Nat. Med. *14*, 392–398.

Plaut, M., Pierce, J.H., Watson, C.J., Hanley-Hyde, J., Nordan, R.P., and Paul, W.E. (1989). Mast cell lines produce lymphokines in response to cross-linkage of Fc epsilon RI or to calcium ionophores. Nature *339*, 64–67.

Powner, D., Kopp, P.M., Monkley, S.J., Critchley, D.R., and Berditchevski, F. (2011). Tetraspanin CD9 in cell migration. Biochem. Soc. Trans. *39*, 563–567.

Pribluda, V.S., Pribluda, C., and Metzger, H. (1994). Transphosphorylation as the mechanism by which the high-affinity receptor for IgE is phosphorylated upon aggregation. Proc. Natl. Acad. Sci. U. S. A. *91*, 11246–11250.

Protty, M.B., Watkins, N. a, Colombo, D., Thomas, S.G., Heath, V.L., Herbert, J.M.J., Bicknell, R., Senis, Y. a, Ashman, L.K., Berditchevski, F., et al. (2009). Identification of Tspan9 as a novel platelet tetraspanin and the collagen receptor GPVI as a component of tetraspanin microdomains. Biochem. J. *417*, 391–400.

Qi, J.C., Wang, J., Mandadi, S., Tanaka, K., Roufogalis, B.D., Madigan, M.C., Lai, K., Yan, F., Chong, B.H., Stevens, R.L., et al. (2006). Human and mouse mast cells use the tetraspanin CD9 as an alternate interleukin-16 receptor. Blood *107*, 135–142.

Qi, R., Ozaki, Y., Kuroda, K., Asazuma, N., Yatomi, Y., Satoh, K., Nomura, S., and Kume, S. (1996). Differential activation of human platelets induced by Fc gamma receptor II cross-linking and by anti-CD9 monoclonal antibody. J. Immunol. *157*, 5638–5645.

Qiu, J., Swartz, J.R., and Georgiou, G. (1998). Expression of active human tissue-type plasminogen activator in Escherichia coli. Appl. Environ. Microbiol. *64*, 4891–4896.

Rajan, T. V. (2003). The Gell-Coombs classification of hypersensitivity reactions: A re-interpretation. Trends Immunol. *24*, 376–379.

Rajesh, S., Sridhar, P., Tews, B.A., Fénéant, L., Cocquerel, L., Ward, D.G., Berditchevski, F., and Overduin, M. (2012). Structural basis of ligand interactions of the large extracellular domain of tetraspanin CD81. J. Virol. *86*, 9606–9616.

Ranjan, A., Bane, S.M., and Kalraiya, R.D. (2014). Glycosylation of the laminin receptor (α3β1) regulates its association with tetraspanin CD151: Impact on cell spreading, motility, degradation and invasion of basement membrane by tumor cells. Exp. Cell Res. *322*, 249–264.

Reber, L.L., and Frossard, N. (2014). Targeting mast cells in inflammatory diseases. Pharmacol. Ther. *142*, 416–435.

Reichelt, P., Schwarz, C., and Donzeau, M. (2006). Single step protocol to purify recombinant proteins with low endotoxin contents. Protein Expr. Purif. *46*, 483–488.

Riley, J.F., and West, G.B. (1953). The presence of histamine in tissue mast cells. J. Physiol. *120*, 528–537.

Robb, L., Tarrant, J., Groom, J., Ibrahim, M., Li, R., Borobakas, B., and Wright, M.D. (2001). Molecular characterisation of mouse and human TSSC6: evidence that TSSC6 is a genuine member of the tetraspanin superfamily and is expressed specifically in haematopoietic organs. Biochim. Biophys. Acta *1522*, 31–41.

Roberts, L.J., Lewis, R.A., Oates, J.A., and Austen, K.F. (1979). Prostaglandin thromboxane, and 12-hydroxy-5,8,10,14-eicosatetraenoic acid production by ionophore-stimulated rat serosal mast cells. Biochim. Biophys. Acta *575*, 185–192.

Rous, B.A.B., Reaves, B.B.J., Ihrke, G., Briggs, J.A.G., Gray, S.R., Stephens, D.J., Banting, G., and Luzio, J.P. (2002). Role of adaptor complex AP-3 in targeting wild-type and mutated CD63 to lysosomes. Mol. Biol. Cell *13*, 1071–1082.

Rubinstein, E., Naour, F. Le, Lagaudrière-Gesbert, C., Billard, M., Conjeaud, H., and Boucheix, C. (1996). CD9, CD63, CD81, and CD82 are components of a surface tetraspan network connected

to HLA-DR and VLA integrins. Eur. J. Immunol. *26*, 2657–2665.

Rubinstein, E., Ziyyat, A., Wolf, J.P., Le Naour, F., and Boucheix, C. (2006). The molecular players of sperm-egg fusion in mammals. Semin. Cell Dev. Biol. *17*, 254–263.

Russell, D., Oldham, N.J., and Davis, B.G. (2009). Site-selective chemical protein glycosylation protects from autolysis and proteolytic degradation. Carbohydr. Res. *344*, 1508–1514.

Sala-Valdés, M., Ursa, Á., Charrin, S., Rubinstein, E., Hemler, M.E., Sánchez-Madrid, F., and Yáñez-Mó, M. (2006). EWI-2 and EWI-F link the tetraspanin web to the actin cytoskeleton through their direct association with ezrin-radixin-moesin proteins. J. Biol. Chem. *281*, 19665–19675.

Sanyal, S., and Hawkins, R.K. (1981). Genetic interaction in the retinal degeneration of mice. Exp. Eye Res. *33*, 213–222.

Schäfer, T., Starkl, P., Allard, C., Wolf, R.M., and Schweighoffer, T. (2010). A granular variant of CD63 is a regulator of repeated human mast cell degranulation. Allergy *65*, 1242–1255.

Scholz, C.-J., Kurzeder, C., Koretz, K., Windisch, J., Kreienberg, R., Sauer, G., and Deissler, H. (2009). Tspan-1 is a tetraspanin preferentially expressed by mucinous and endometrioid subtypes of human ovarian carcinomas. Cancer Lett. *275*, 198–203.

Schwartz, L.B., Riedel, C., Caulfield, J.P., Wasserman, S.I., and Austen, K.F. (1981). Cell association of complexes of chymase, heparin proteoglycan, and protein after degranulation by rat mast cells. J. Immunol. *126*, 2071–2078.

Seigneuret, M. (2006). Complete predicted three-dimensional structure of the facilitator transmembrane protein and hepatitis C virus receptor CD81: conserved and variable structural domains in the tetraspanin superfamily. Biophys. J. *90*, 212–227.

Seigneuret, M., Delaguillaumie, a, Lagaudrière-Gesbert, C., and Conjeaud, H. (2001). Structure of the tetraspanin main extracellular domain. A partially conserved fold with a structurally variable domain insertion. J. Biol. Chem. *276*, 40055–40064.

Seldin, D.C., Adelman, S., Austen, K.F., Stevens, R.L., Hein, a, Caulfield, J.P., and Woodbury, R.G. (1985). Homology of the rat basophilic leukemia cell and the rat mucosal mast cell. Proc. Natl. Acad. Sci. U. S. A. *82*, 3871–3875.

Sheets, E.D., Holowka, D., and Baird, B. (1999). Critical role for cholesterol in Lyn-mediated tyrosine phosphorylation of FcepsilonRI and their association with detergent-resistant membranes. J. Cell Biol. *145*, 877–887.

Sheng, K.C., van Spriel, A.B., Gartlan, K.H., Sofi, M., Apostolopoulos, V., Ashman, L., and Wright, M.D. (2009). Tetraspanins CD37 and CD151 differentially regulate Ag presentation and T-cell co-stimulation by DC. Eur. J. Immunol. *39*, 50–55.

Shih, Y.-P., Kung, W.-M., Chen, J.-C., Yeh, C.-H., Wang, A.H.-J., and Wang, T.-F. (2002). High-throughput screening of soluble recombinant proteins. Protein Sci. *11*, 1714–1719.

Shoham, T., Rajapaksa, R., Boucheix, C., Rubinstein, E., Poe, J.C., Tedder, T.F., and Levy, S. (2003). The tetraspanin CD81 regulates the expression of CD19 during B cell development in a postendoplasmic reticulum compartment. J. Immunol. *171*, 4062–4072.

Shoham, T., Rajapaksa, R., Kuo, C., Levy, S., and Haimovich, J. (2006). Building of the tetraspanin web: distinct structural domains of CD81 function in different cellular compartments. Mol. Cell. Biol. *26*, 1373–1385.

Shokri, a, Sandén, a M., and Larsson, G. (2003). Cell and process design for targeting of recombinant protein into the culture medium of Escherichia coli. Appl. Microbiol. Biotechnol. *60*, 654–664.

Sibilano, R., Frossi, B., and Pucillo, C. (2014). Mast cell activation: A complex interplay of positive and negative signaling pathways. Eur. J. … 1–27.

Siebenhaar, F., Falcone, F.H., Tiligada, E., Hammel, I., Maurer, M., Sagi-Eisenberg, R., and Levi-Schaffer, F. (2014). The search for Mast Cell and Basophil models - Are we getting closer to pathophysiological relevance? Allergy n/a – n/a.

Simons, F.E.R., and Simons, K.J. (2011). Histamine and H1-antihistamines: Celebrating a century of progress. J. Allergy Clin. Immunol. *128*, 1139–1150.e4.

Simons, K., and Ikonen, E. (1997). Functional rafts in cell membranes. Nature *387*, 569–572.

Singethan, K., Müller, N., Schubert, S., Lüttge, D., Krementsov, D.N., Khurana, S.R., Krohne, G., Schneider-Schaulies, S., Thali, M., and Schneider-schaulies, J. (2008). CD9 clustering and formation of microvilli zippers between contacting cells regulates virus-induced cell fusion. Traffic *9*, 924–935.

Skehan, P., Storeng, R., Scudiero, D., Monks, a, McMahon, J., Vistica, D., Warren, J.T., Bokesch, H., Kenney, S., and Boyd, M.R. (1990). New colorimetric cytotoxicity assay for anticancer-drug screening. J. Natl. Cancer Inst. *82*, 1107–1112.

Smith, D.A., Monk, P.N., and Partridge, L.J. (1995). Antibodies against human CD63 activate transfected rat basophilic leukemia (RBL-2H3) cells. Mol. Immunol. *32*, 1339–1344.

van Spriel, A.B., and Figdor, C.G. (2010). The role of tetraspanins in the pathogenesis of infectious diseases. Microbes Infect. *12*, 106–112.

Stelekati, E., Bahri, R., D'Orlando, O., Orinska, Z., Mittrücker, H.W., Langenhaun, R., Glatzel, M., Bollinger, A., Paus, R., and Bulfone-Paus, S. (2009). Mast Cell-Mediated Antigen Presentation Regulates CD8+ T Cell Effector Functions. Immunity *31*, 665–676.

Stipp, C.S., Kolesnikova, T. V, and Hemler, M.E. (2003). Functional domains in tetraspanin proteins. Trends Biochem. Sci. *28*, 106–112.

Südhof, T.C., and Rothman, J.E. (2009). Membrane fusion: grappling with SNARE and SM proteins. Science *323*, 474–477.

Supajatura, V., Ushio, H., Nakao, a, Akira, S., Okumura, K., Ra, C., and Ogawa, H. (2002). Differential responses of mast cell Toll-like receptors 2 and 4 in allergy and innate immunity. J.Clin.Invest. *109*, 1351 – .

Szöllósi, J., Horejsí, V., Bene, L., Angelisová, P., and Damjanovich, S. (1996). Supramolecular complexes of MHC class I, MHC class II, CD20, and tetraspan molecules (CD53, CD81, and CD82) at the surface of a B cell line JY. J. Immunol. *157*, 2939–2946.

Tachibana, I., and Hemler, M.E. (1999). Role of Transmembrane 4 Superfamily (TM4SF) Proteins CD9 and CD81 in Muscle Cell Fusion and Myotube Maintenance Isao. Cell *146*, 893–904.

Takahashi, Y., Bigler, D., Ito, Y., and White, J.M. (2001). Sequence-specific interaction between the disintegrin domain of mouse ADAM 3 and murine eggs: role of beta1 integrin-associated proteins CD9, CD81, and CD98. Mol. Biol. Cell *12*, 809–820.

Takashima, T., Ohnishi, K., Tsuyuguchi, I., and Kishimoto, S. (1993). Differential regulation of formation of multinucleated giant cells from concanavalin A-stimulated human blood monocytes by IFN-gamma and IL-4. J. Immunol. *150*, 3002–3010.

Takeda, Y., Tachibana, I., Miyado, K., Kobayashi, M., Miyazaki, T., Funakoshi, T., Kimura, H., Yamane, H., Saito, Y., Goto, H., et al. (2003). Tetraspanins CD9 and CD81 function to prevent the fusion of mononuclear phagocytes. J. Cell Biol. *161*, 945–956.

Takeda, Y., Kazarov, A.R., Butterfield, C.E., Hopkins, B.D., Benjamin, L.E., Kaipainen, A., and Hemler, M.E. (2007). Deletion of tetraspanin Cd151 results in decreased pathologic angiogenesis in vivo and in vitro. Blood *109*, 1524–1532.

Tejera, E., Rocha-Perugini, V., López-Martín, S., Pérez-Hernández, D., Bachir, A.I., Horwitz, A.R., Vázquez, J., Sánchez-Madrid, F., and Yáñez-Mo, M. (2013). CD81 regulates cell migration

through its association with Rac GTPase. Mol. Biol. Cell *24*, 261–273.

Terpe, K. (2003). Overview of tag protein fusions: from molecular and biochemical fundamentals to commercial systems. Appl. Microbiol. Biotechnol. *60*, 523–533.

Terpe, K. (2006). Overview of bacterial expression systems for heterologous protein production: From molecular and biochemical fundamentals to commercial systems. Appl. Microbiol. Biotechnol. *72*, 211–222.

Tham, T.N., Gouin, E., Rubinstein, E., Boucheix, C., Cossart, P., and Pizarro-Cerda, J. (2010). Tetraspanin CD81 is required for Listeria monocytogenes invasion. Infect. Immun. *78*, 204–209.

Thomsen, P., Roepstorff, K., and Stahlhut, M. (2002). Caveolae Are Highly Immobile Plasma Membrane Microdomains, Which Are not Involved in Constitutive Endocytic Trafficking. Mol. Biol. Cell *13*, 238–250.

Todd, S.C., Doctor, V.S., and Levy, S. (1998). Sequences and expression of six new members of the tetraspanin/TM4SF family. Biochim. Biophys. Acta *1399*, 101–104.

Toru, H., Eguchi, M., Matsumoto, R., Yanagida, M., Yata, J., and Nakahata, T. (1998). Interleukin-4 promotes the development of tryptase and chymase double-positive human mast cells accompanied by cell maturation. Blood *91*, 187–195.

Trinchieri, G., and Sher, A. (2007). Cooperation of Toll-like receptor signals in innate immune defence. Nat. Rev. Immunol. *7*, 179–190.

Tsai, Y.C., Mendoza, A., Mariano, J.M., Zhou, M., Kostova, Z., Chen, B., Veenstra, T., Hewitt, S.M., Helman, L.J., Khanna, C., et al. (2007). The ubiquitin ligase gp78 promotes sarcoma metastasis by targeting KAI1 for degradation. Nat. Med. *13*, 1504–1509.

Tsitsikov, E.N., Gutierrez-Ramos, J.C., and Geha, R.S. (1997). Impaired CD19 expression and signaling, enhanced antibody response to type II T independent antigen and reduction of B-1 cells in CD81-deficient mice. Proc. Natl. Acad. Sci. U. S. A. *94*, 10844–10849.

Unternaehrer, J.J., Chow, A., Pypaert, M., Inaba, K., and Mellman, I. (2007). The tetraspanin CD9 mediates lateral association of MHC class II molecules on the dendritic cell surface. Proc. Natl. Acad. Sci. U. S. A. *104*, 234–239.

Vichai, V., and Kirtikara, K. (2006). Sulforhodamine B colorimetric assay for cytotoxicity screening. Nat. Protoc. *1*, 1112–1116.

Wakelin, S.J., Sabroe, I., Gregory, C.D., Poxton, I.R., Forsythe, J.L.R., Garden, O.J., and Howie, S.E.M. (2006). "Dirty little secrets"-Endotoxin contamination of recombinant proteins. Immunol. Lett. *106*, 1–7.

Wang, H., Min, G., Glockshuber, R., Sun, T.T., and Kong, X.P. (2009). Uropathogenic E. coli Adhesin-Induced Host Cell Receptor Conformational Changes: Implications in Transmembrane Signaling Transduction. J. Mol. Biol. *392*, 352–361.

Wang, H.W., Tedla, N., Lloyd, a R., Wakefield, D., and McNeil, P.H. (1998). Mast cell activation and migration to lymph nodes during induction of an immune response in mice. J. Clin. Invest. *102*, 1617–1626.

Wang, H.-X., Kolesnikova, T. V, Denison, C., Gygi, S.P., and Hemler, M.E. (2011). The C-terminal tail of tetraspanin protein CD9 contributes to its function and molecular organization. J. Cell Sci. *124*, 2702–2710.

Wang, Y., Tong, X., Omoregie, E.S., Liu, W., Meng, S., and Ye, X. (2012). Tetraspanin 6 (TSPAN6) negatively regulates retinoic acid-inducible gene I-like receptor-mediated immune signaling in a ubiquitination-dependent manner. J. Biol. Chem. *287*, 34626–34634.

Waterhouse, R., Ha, C., and Dveksler, G.S. (2002). Murine CD9 is the receptor for pregnancy-specific glycoprotein 17. J. Exp. Med. *195*, 277–282.

Weng, J., Krementsov, D.N., Khurana, S., Roy, N.H., and Thali, M. (2009). Formation of syncytia is repressed by tetraspanins in human immunodeficiency virus type 1-producing cells. J. Virol. *83*, 7467–7474.

Westers, L., Westers, H., and Quax, W.J. (2004). Bacillus subtilis as cell factory for pharmaceutical proteins: A biotechnological approach to optimize the host organism. Biochim. Biophys. Acta - Mol. Cell Res. *1694*, 299–310.

Whitmore, L., and Wallace, B. a. (2008). Protein secondary structure analyses from circular dichroism spectroscopy: Methods and reference databases. Biopolymers *89*, 392–400.

Whitmore, L., and Wallace, B.A. (2004). DICHROWEB, an online server for protein secondary structure analyses from circular dichroism spectroscopic data. Nucleic Acids Res. *32*, W668–W673.

Wildt, S., and Gerngross, T.U. (2005). The humanization of N-glycosylation pathways in yeast. Nat. Rev. Microbiol. *3*, 119–128.

Winterwood, N.E., Varzavand, A., Meland, M.N., Ashman, L.K., and Stipp, C.S. (2006). A critical role for tetraspanin CD151 in alpha3beta1 and alpha6beta4 integrin-dependent tumor cell functions on laminin-5. Mol. Biol. Cell *17*, 2707–2721.

Witherden, D. a, Boismenu, R., and Havran, W.L. (2000). CD81 and CD28 costimulate T cells through distinct pathways. J. Immunol. *165*, 1902–1909.

Woodbury, R.G., Miller, H.R., Huntley, J.F., Newlands, G.F., Palliser, a C., and Wakelin, D. (1984). Mucosal mast cells are functionally active during spontaneous expulsion of intestinal nematode infections in rat. Nature *312*, 450–452.

Wright, M.D., Henkle, K.J., and Mitchell, G.F. (1990). An immunogenic Mr 23,000 integral membrane protein of Schistosoma mansoni worms that closely resembles a human tumor-associated antigen. J. Immunol. *144*, 3195–3200.

Wright, M.D., Ni, J., and Rudy, G.B. (2000). The L6 membrane proteins--a new four-transmembrane superfamily. Protein Sci. *9*, 1594–1600.

Wright, M.D., Moseley, G.W., and van Spriel, a B. (2004). Tetraspanin microdomains in immune cell signalling and malignant disease. Tissue Antigens *64*, 533–542.

Wu, X.C., Lee, W., Tran, L., and Wong, S.L. (1991). Engineering a Bacillus subtilis expression-secretion system with a strain deficient in six extracellular proteases. J. Bacteriol. *173*, 4952–4958.

Wu, X.R., Medina, J.J., and Sun, T.T. (1995). Selective interactions of UPIa and UPIb, two members of the transmembrane 4 superfamily, with distinct single transmembrane-domained proteins in differentiated urothelial cells. J. Biol. Chem. *270*, 29752–29759.

Wu, X.R., Sun, T.T., and Medina, J.J. (1996). In vitro binding of type 1-fimbriated Escherichia coli to uroplakins Ia and Ib: relation to urinary tract infections. Proc. Natl. Acad. Sci. U. S. A. *93*, 9630–9635.

Wu, X.-R., Kong, X.-P., Pellicer, A., Kreibich, G., and Sun, T.-T. (2009). Uroplakins in urothelial biology, function, and disease. Kidney Int. *75*, 1153–1165.

Wurm, F.M. (2004). Production of recombinant protein therapeutics in cultivated mammalian cells. Nat. Biotechnol. *22*, 1393–1398.

Xie, B., Zhou, G., Chan, S.Y., Shapiro, E., Kong, X.P., Wu, X.R., Sun, T.T., and Costello, C.E. (2006). Distinct glycan structures of uroplakins Ia and Ib: Structural basis for the selective binding of FimH adhesin to uroplakin Ia. J. Biol. Chem. *281*, 14644–14653.

Yadav, S., Shi, Y., and Wang, H. (2010). IL-16 effects on A549 lung epithelial cells: dependence on CD9 as an IL-16 receptor? J. Immunotoxicol. *7*, 183–193.

Yanez-Mó, M., Barreiro, O., Gonzalo, P., Batista, A., Megías, D., Genís, L., Sachs, N., Sala-Valdés,

M., Alonso, M. a., Montoya, M.C., et al. (2008). MT1-MMP collagenolytic activity is regulated through association with tetraspanin CD151 in primary endothelial cells. Blood *112*, 3217–3226.

Yáñez-Mó, M., Barreiro, O., Gordon-Alonso, M., Sala-Valdés, M., and Sánchez-Madrid, F. (2009). Tetraspanin-enriched microdomains: a functional unit in cell plasma membranes. Trends Cell Biol. *19*, 434–446.

Yang, H., Xiao, X., Li, S., Mai, G., and Zhang, Q. (2011). Novel TSPAN12 mutations in patients with familial exudative vitreoretinopathy and their associated phenotypes. Mol. Vis. *17*, 1128–1135.

Yang, X., Claas, C., Kraeft, S.-K., Chen, L.B., Wang, Z., Kreidberg, J.A., and Hemler, M.E. (2002). Palmitoylation of tetraspanin proteins: modulation of CD151 lateral interactions, subcellular distribution, and integrin-dependent cell morphology. Mol. Biol. Cell *13*, 767–781.

Yang, X., Kovalenko, O. V, Tang, W., Claas, C., Stipp, C.S., and Hemler, M.E. (2004). Palmitoylation supports assembly and function of integrin-tetraspanin complexes. J. Cell Biol. *167*, 1231–1240.

Yang, X.H., Richardson, A.L., Torres-Arzayus, M.I., Zhou, P., Sharma, C., Kazarov, A.R., Andzelm, M.M., Strominger, J.L., Brown, M., and Hemler, M.E. (2008). CD151 accelerates breast cancer by regulating α6 integrin function, signaling, and molecular organization. Cancer Res. *68*, 3204–3213.

Yauch, R.L., Berditchevski, F., Harler, M.B., Reichner, J., and Hemler, M.E. (1998). Highly stoichiometric, stable, and specific association of integrin alpha3beta1 with CD151 provides a major link to phosphatidylinositol 4-kinase, and may regulate cell migration. Mol. Biol. Cell *9*, 2751–2765.

Yaucht, R.L., Kazarov, A.R., Desai, B., Lee, R.T., and Hemler, M.E. (2000). Direct extracellular contact between integrin α3β1 and TM4SF protein CD151. J. Biol. Chem. *275*, 9230–9238.

Yoshida, T., Kawano, Y., Sato, K., Ando, Y., Aoki, J., Miura, Y., Komano, J., Tanaka, Y., and Koyanagi, Y. (2008). A CD63 mutant inhibits T-cell tropic human immunodeficiency virus type 1 entry by disrupting CXCR4 trafficking to the plasma membrane. Traffic *9*, 540–558.

Young, R.J., Owens, R.J., Mackay, G. a, Chan, C.M., Shi, J., Hide, M., Francis, D.M., Henry, a J., Sutton, B.J., and Gould, H.J. (1995). Secretion of recombinant human IgE-Fc by mammalian cells and biological activity of glycosylation site mutants. Protein Eng. *8*, 193–199.

Young, R.M., Holowka, D., and Baird, B. (2003). A lipid raft environment enhances Lyn kinase activity by protecting the active site tyrosine from dephosphorylation. J. Biol. Chem. *278*, 20746–20752.

Zahn-Zabal, M., Kobr, M., Girod, P. a, Imhof, M., Chatellard, P., de Jesus, M., Wurm, F., and Mermod, N. (2001). Development of stable cell lines for production or regulated expression using matrix attachment regions. J. Biotechnol. *87*, 29–42.

Van Zelm, M.C., Smet, J., Adams, B., Mascart, F., Schandené, L., Janssen, F., Ferster, A., Kuo, C.C., Levy, S., Van Dongen, J.J.M., et al. (2010). CD81 gene defect in humans disrupts CD19 complex formation and leads to antibody deficiency. J. Clin. Invest. *120*, 1265–1274.

Zemni, R., Bienvenu, T., Vinet, M.C., Sefiani, a, Carrié, a, Billuart, P., McDonell, N., Couvert, P., Francis, F., Chafey, P., et al. (2000). A new gene involved in X-linked mental retardation identified by analysis of an X;2 balanced translocation. Nat. Genet. *24*, 167–170.

Zhang, X. a, Kazarov, A.R., Yang, X., Bontrager, A.L., Stipp, C.S., and Hemler, M.E. (2002). Function of the tetraspanin CD151-alpha6beta1 integrin complex during cellular morphogenesis. Mol. Biol. Cell *13*, 1–11.

Zhou, G., Mo, W.J., Sebbel, P., Min, G., Neubert, T. a, Glockshuber, R., Wu, X.R., Sun, T.T., and Kong, X.P. (2001). Uroplakin Ia is the urothelial receptor for uropathogenic Escherichia coli:

evidence from in vitro FimH binding. J. Cell Sci. *114*, 4095–4103.

Zhu, G.-Z., Miller, B.J., Boucheix, C., Rubinstein, E., Liu, C.C., Hynes, R.O., Myles, D.G., and Primakoff, P. (2002). Residues SFQ (173-175) in the large extracellular loop of CD9 are required for gamete fusion. Development *129*, 1995–2002.

Zhu, Y.Z., Luo, Y., Cao, M.M., Liu, Y., Liu, X.Q., Wang, W., Wu, D.G., Guan, M., Xu, Q.Q., Ren, H., et al. (2012). Significance of palmitoylation of CD81 on its association with tetraspanin-enriched microdomains and mediating hepatitis C virus cell entry. Virology *429*, 112–123.

Zöller, M. (2009). Tetraspanins: push and pull in suppressing and promoting metastasis. Nat. Rev. Cancer *9*, 40–55.

Appendix

Figure 7.1: Vector maps, Created in Snapgene

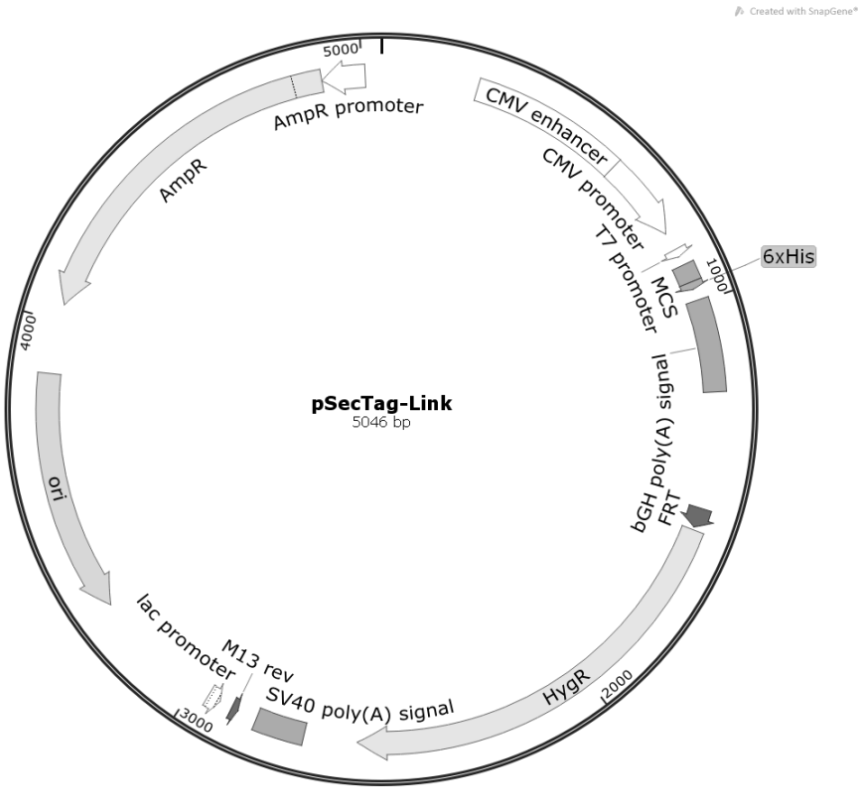

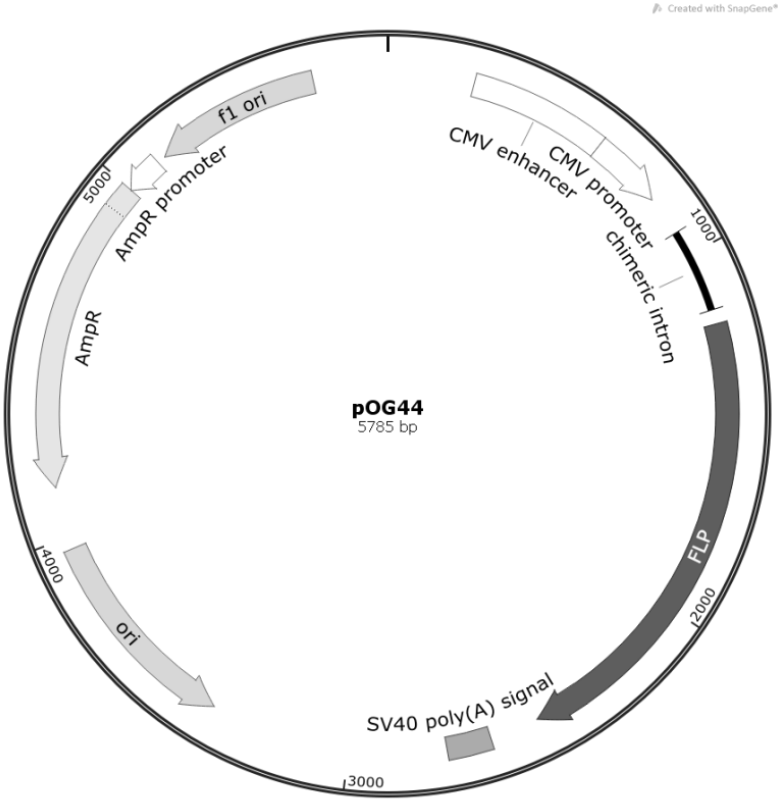

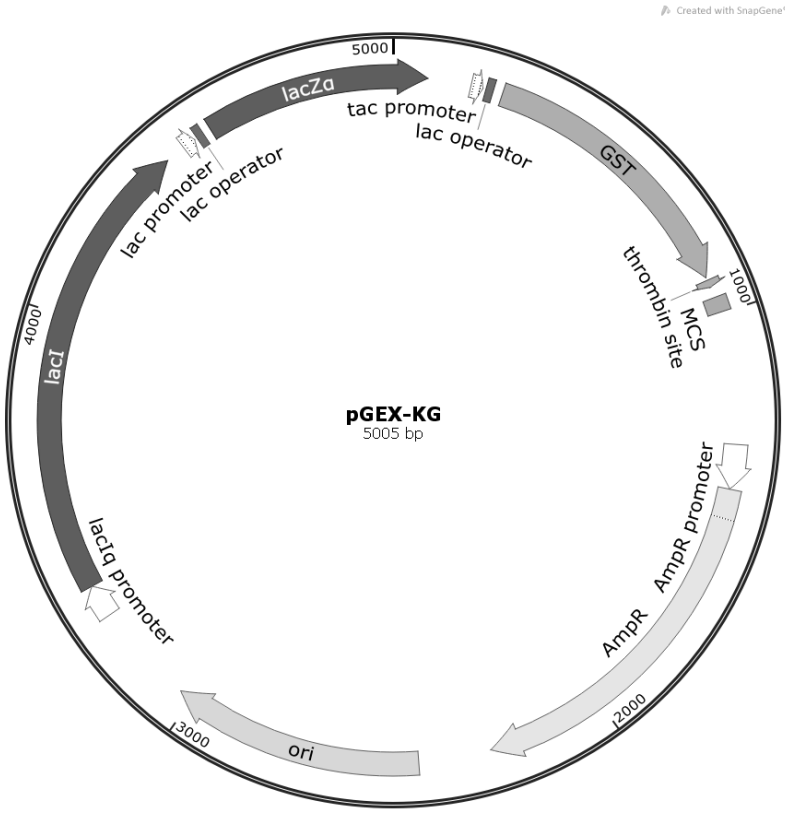
Created with SnapGene®
5000
lacZα
tac promoter
lac operator
GST
thrombin site
MCS
1000
lac promoter
lac operator
4000
lacI
pGEX-KG
5005 bp
AmpR promoter
AmpR
lacIq promoter
2000
3000
ori

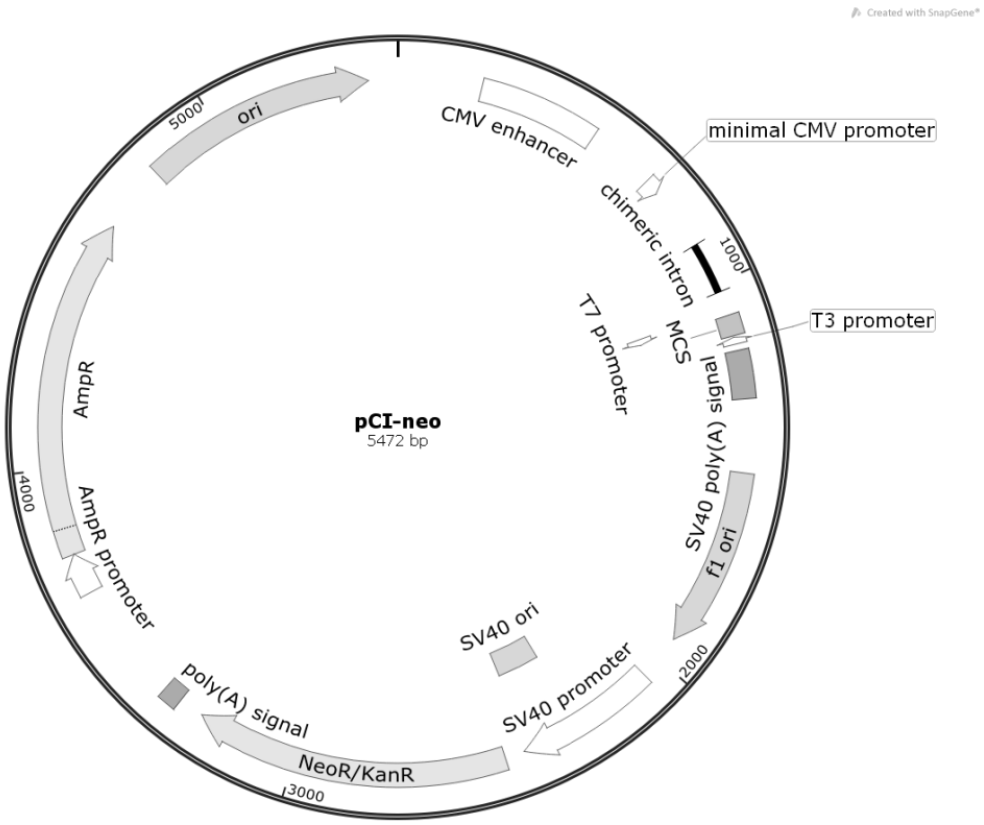
Created with SnapGene®
5000
ori
CMV enhancer
minimal CMV promoter
chimeric intron
1000
T3 promoter
T7 promoter
MCS
SV40 poly(A) signal
f1 ori
pCI-neo
5472 bp
AmpR
4000
AmpR promoter
SV40 ori
2000
poly(A) signal
SV40 promoter
NeoR/KanR
3000

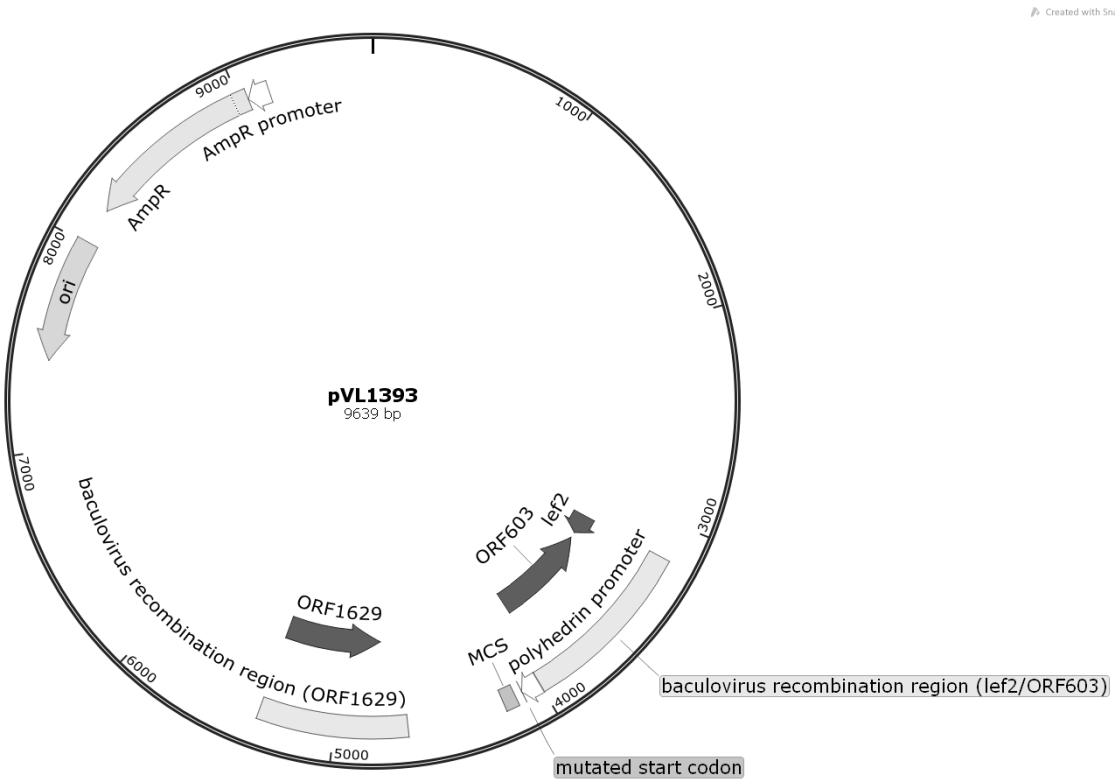
Created with SnapGene®
pVL1393
9639 bp
1000
2000
3000
4000
5000
6000
7000
8000
9000
AmpR promoter
AmpR
ori
baculovirus recombination region (ORF1629)
ORF1629
ORF603
lef2
polyhedrin promoter
MCS
baculovirus recombination region (lef2/ORF603)
mutated start codon

Primer Name	Sequence	Used in
Hamster actin forward	5’ CCTCTATGCCAACACAGTGC 3’	CHO RT-PCR control
Hamster actin reverse	5’ CCTGCTTGCTGATCCACATC 3’	CHO RT-PCR control
Human actin forward	5’ TGACAGGATCGAGAAGGAGA 3’	HEK-293 RT-PCR control
Human actin reverse	5’ CGCTCAGGAGGAGCAATG 3’	HEK-293 RT-PCR control
Leader sequence forward	5’ TTGCGCGCTAGCCACCATGGAGACAGACACAC 3’	Flp-in cloning
Leader sequence reverse 9	5’ CATCCTTGTGGTCACCAGTGGAACCTGGA 3’	Flp-in cloning
Leader sequence reverse 151	5’ GCTGGTAGTAGTCACCAGTGGAACCTGGA 3’	Flp-in cloning
Leader sequence reverseTspan5	5’ AGTCTTTGAAGTCACCAGTGGAACCTGGA 3’	Flp-in cloning
CD9 forward	5’ CACTGGTGACCACAAGGATGAGGTGATTAAG 3’	Flp-in cloning
CD9 reverse AgeI (CD9R1)	5’ TTGCGCACCGGTTTTATTGTCGAAGACCTCTTTG 3’	Flp-in cloning
CD9 Reverse HindIII (CD9R2)	5’ TTGCGCAAGCTTCTATTTATTGTCGAAGACCTCTTTG 3’	Flp-in cloning
CD151 Forward	5’ CACTGGTGACTACTACCAGCAGCTGAACAC 3’	Flp-in cloning
CD151 reverse AgeI (CD151R1)	5’ TTGCGCACCGGTGTGCTCCTGGATGAAGGTC 3’	Flp-in cloning
CD151 reverse HindIII (CD151R2)	5’ TTGCGCAAGCTTCTAGTGCTCCTGGATGAAGGTC 3’	Flp-in cloning
Tspan5 Forward	5’ CACTGGTGACTTCAAAGACTGGATCAAAGACC 3’	Flp-in cloning
Tspan5 Reverse AgeI (Tspan5R1)	5’ TTGCGCACCGGTATTGTCCTGCAACCACTTCTC 3’	Flp-in cloning
Tspan5 Reverse HindIII (Tspan5R2)	5’ TTGCGCAAGCTTCTAATTGTCCTGCAACCACTTCTC 3’	Flp-in cloning
CD9 Forward	5’ GCGCGCGATATCCACAAGGATGAGGTGATTAAG 3’	pCINEO cloning
CD9 reverse	5’ GGGCCCTCTAGATCATTTATTGTCGAAGACCTCTTTG 3’	pCINEO cloning
CD151 Forward	5’ GGGCCCGATATCTACTACCAGCAGCTGAACAC 3’	pCINEO cloning

CD151 Reverse	5’ GCGCGCTCTAGATCAGTGCTCCTGGATGAAGGTCTC 3’	pCINEO cloning
CD9 EC2 forward	5’ GGATCCCACAAGGATGAGGTGATTAAG 3’	Insect expression
CD9 EC2 forward HIS tag	5’ GGATCCCACCACCACCACCACCACCACAAGGATGAGGTGATTAAG 3’	Insect expression
CD9 EC2 reverse	5’ GCGGCCGCTTTATTGTCGAAGACCTCTTTG 3’	Insect expression
CD9 EC2 reverse His tag	5’ GCGGCCGCCACCACCACCACCACCACTTTATTGTCGAAGACCTCTTTG 3’	Insect expression
CD9 full length forward	5’ GGATCCATGCCGGTCAAAGGAG 3’	Insect expression
CD9 full length forward HIS tag	5’ GGATCCCACCACCACCACCACCACATGCCGGTCAAAGGAG 3’	Insect expression
CD9 full length reverse	5’ GCGGCCGCCTAGACCATCTCGCGG 3’	Insect expression
CD9 full length reverse His tag	5’ GCGGCCGCCACCACCACCACCACCACCTAGACCATCTCGCGG 3’	Insect expression
Tspan5 EC2 forward	5’ GGATCCTTCAAAGACTGGATCAAAGAC 3’	Insect expression
Tspan5 EC2 forward HIS tag	5’ GGATCCCACCACCACCACCACCACTTCAAAGACTGGATCAAAGAC 3’	Insect expression
Tspan5 EC2 reverse	5’ GCGGCCGCATTGTCCTGCAACCACTTC 3’	Insect expression
Tspan5 EC2 reverse His tag	5’ GCGGCCGCCACCACCACCACCACCACATTGTCCTGCAACCAC 3’	Insect expression
Tspan5 full length forward	5’ GGATCCATGTCCGGGAAGC 3’	Insect expression
Tspan5 full length forward HIS tag	5’ GGATCCCACCACCACCACCACCACATGTCCGGGAAGCAC 3’	Insect expression
Tspan5 full length reverse	5’ GCGGCCGCCTACCAGCTCGCCCTG 3’	Insect expression
Tspan5 full length reverse His tag	5’ GCGGCCGCCACCACCACCACCACCACCTACCAGCTCGCCCTG 3’	Insect expression
Rat CD63 Forward	5’ ATTATTGAATTCTATTTAGAGACCAGGTGAAGTC 3’	Bacteria expression of Rat CD63
Rat CD63 Reverse	5’ ATTATTAAGCTTTCAGTTCTTCCTCAGCCATGC 3’	Bacteria expression of Rat CD63
CMV forward primer	5’ CGCAAATGGGCGGTAGGCGTG 3’	Sequencing primer
BGH reverse primer	5’ TAGAAGGCACAGTCGAGG 3’	Sequencing primer

pGEX forward sequencing primer	5’ GAGCTGTTGACAATTAATCATCGG 3’	Sequencing primer
pGEX reverse sequencing primer	5’ CCGGGAGCTGCATGTGTCAGAGG 3’	Sequencing primer

Table 7.1: Primer sequences and there application

Figure 7.2 Rat and human EC2 alignment. Sequences aligned with ClustalW and highlighted using BoxShade.

CD9

```
Human     1 HKDEVIKEVQEFYKDTYNKLKTKDEPQRETLKAIHYALNCCGLAGGVEQFISDICPKKDVLETFTVKSCPDAIKEVFDNK 80
Rat       1 HKDEVIKETQEFYKDTYQKLRNKDEPQRETLKAIHMALNCCGIAGGVEQFISDICPKKQVLESFQVKSCPDAIDEVFHSK 80
```

85% identity

CD63

```
Human     1 FRDKVMSEFNNNFRQQMENYPKNNHTASILDRMQADFKCCGAANYTDWEKIPSMSKNRVPDSCCINVTVGCGINFNEKAIHKEGCVEKIGGWLRKN 96
Rat       1 FRDQVKSEFSKSFQKQMQNYLTDNKTATILDKLQKFNKCCGASNYTDWERIPGMAKDRVPDSCCINITVGCGNDFKESTIHTQGCVETIAAWLRKN 96
```

64.6% identity

CD81

```
Human     1 NKDQIAKDVKQFYDQALQQAVVDDDANNAKAVVKTFHETLDCCGSSTLTALTTSVLKNNLCPSGSNIISNLFKEDCHQKIDDLFSGKLY 89
Rat       1 NKDQIAKDVKQFYDQALQQAVMDDDANNAKAVVKTFHETLNCCGSNTLTTLTTAVLRNSLCPSSSNSFTQLLKEDCHQKIDELFSGKLY 89
```

84.3% identity

CD151

```
Human     1
YYQQLNTELKENLKDTMTKRYHQPGHEAVTSAVDQLQQEFHCCGSNNSQDWRDSEWIRSQEAGGRVVPDSCCKTVVALCGQRDHASNIYKVEGGCITKLETFIQEH 106
Rat       1
YYQQLNTELKENLKDTMIKRYHQSGHEGVTNAVDKLQQEFHCCGSNNSRDWRDSEWIRSGEADSRVVPDSCCKTVVTGCGKREHASNIYKVEGGCITKLESFIQEH 106
```

86.8% identity

Figure 7.3: Mouse and human EC2 alignment. Sequences aligned with ClustalW and highlighted using BoxShade

CD9

```
Human     1 HKDEVIKEVQEFYKDTYNKLKTKDEPQRETLKAIHYALNCCGLAGGVEQFISDICPKKDVLETFTVKSCPDAIKEVFDNK 80
mouse     1 HKDEVIKELQEFYKDTYQKLRSKDEPQRETLKAIHMALDCCGIAGPLEQFISDTCPKKQILESFQVKPCPEAISEVFNNK 80
```

77.5% identity

CD63

```
Human     1 FRDKVMSEFNNNFRQQMENYPKNNHTASILDRMQADFKCCGAANYTDWEKIPSMSKNRVP DSCCINVTVGCGINFNEKAIHKEGCVEKICGWLRKN 96
Mouse     1 FRDQVKSEFNKSFQQQMQNYLKDNKTATILDKLQKENNCCGASNYTDWENIPGMAKDRVP DSCCINITVGCGNDFKESTIHTQGCVETIAIWLRKN 96
```

66.8% identity

CD81

```
Human     1 NKDQIAKDVKQFYDQALQQAVVDDDANNAKAVVKTFHETLDCCGSSTLTALTTSVLKNNLCPSGSNIISNLFKEDCHQKIDDLFSGKLY
Mouse     1 NKDQIAKDVKQFYDQALQQAVMDDDANNAKAVVKTFHETLNCCGSNALTTLTTTILRNSLCPSGGNILTPLLQQDCHQKIDELFSGKLY
```

80.9% identity

CD151

```
human     1
YYQQLNTELKENLKDTMTKRYHQPGHEAVTSAVDQLQQEFHCCGSNNSQDWRDSEWIRSQEAGGRVVPDSCCKTVVALCGQRDHASNIYKVEGGCITKLETFIQEH
mouse     1
YYQQLNTELKENLKDTMVKRYHQSGHEGVSSAVDKLQQEFHCCGSNNSQDWQDSEWIRSGEADSRVVPDSCCKTMVAGCGKRDHASNIYKVEGGCITKLETFIQEH
```

88.7% identity

Figre 7.4 Sequence and region of CD9 EC2 peptides. Three letter amino acid sequences of the relevant CD9 peptides are displayed in the table whilst their positions are depicted in the schematic tetraspanin representation.

Peptide name	**Peptide sequence**
8001:	Ser Lys His Asp Glu Val Ile Lys Glu Val Gln Glu Phe Tyr
8001 Scrambled:	Glu Glu Val Lys Lys Phe Glu Ser Gln His Asp Ile Tyr Val
8003:	Gly Leu Ala Gly Gly Val Glu Gln Phe Ile Ser Asp Ile Ser
8003 Scrambled:	Ile Asp Ser Gly Phe Val Gly Gln Ile Ala Ser Gly Leu Glu

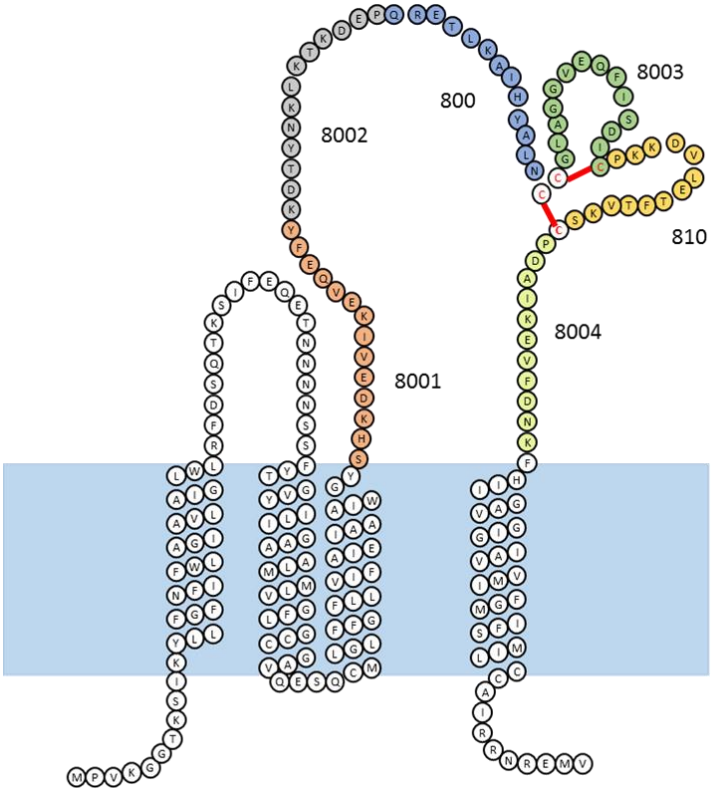

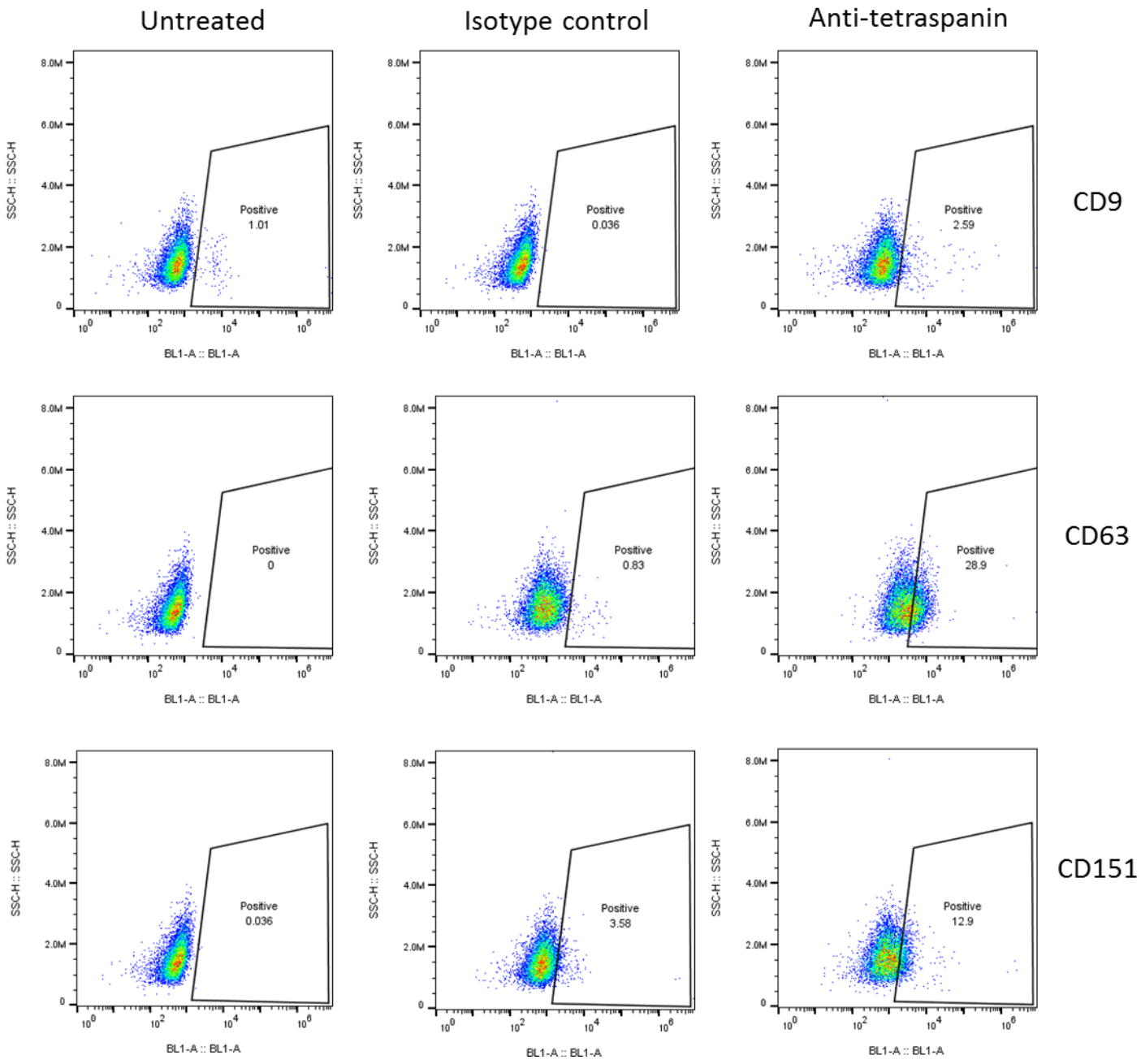

Figure 7.5 Example isotype gating used for checking tetraspanin expression on RBL-2H3 cells. For each anti-tetraspanin antibody gates were established based on the relevant isotype control antibody, MFI reading are also shown in figure 4.1

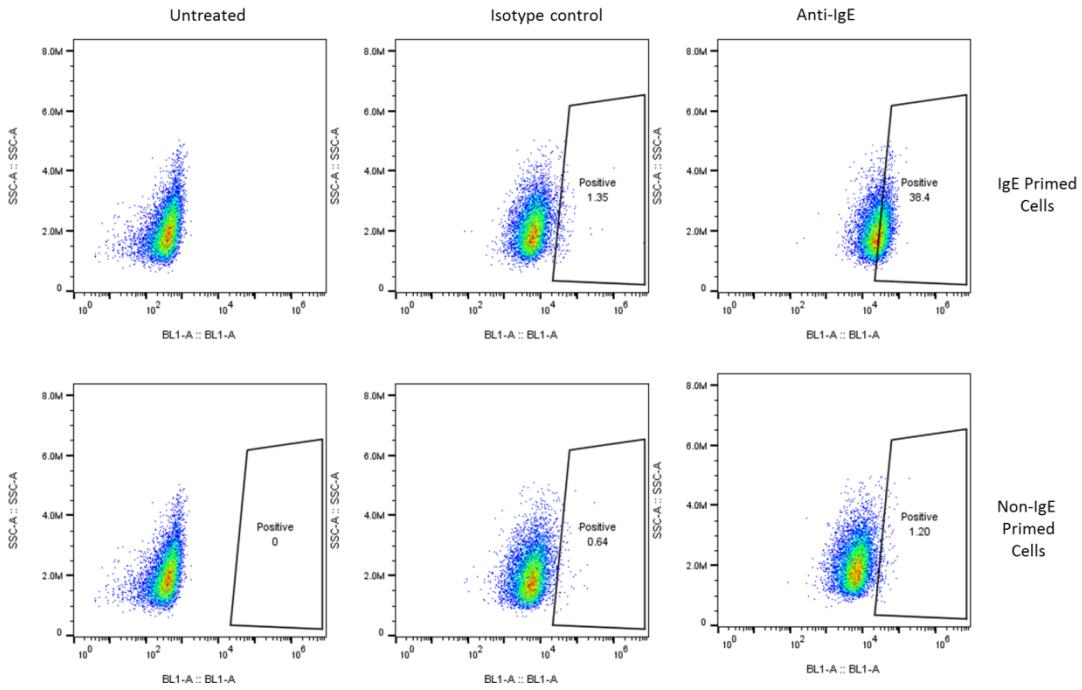

Figure 7.6 Scatter graphs showing percentage positive of IgE primed and Non-IgE primed RBL-2H3 cells probed with an anti-IgE antibody. For each anti-tetraspanin antibody gates were established based on the relevant isotype control antibody, MFI reading are also shown in figure 4.1